DISSERTATIONES PHYSICAE UNIVERSITATIS TARTUENSIS
28

NUCLEAR RESONANCE STUDIES OF LOCAL STRUCTURE IN $RBa_2Cu_3O_{6+x}$ COMPOUNDS

IVO HEINMAA

TARTU 1999

DISSERTATIONES PHYSICAE UNIVERSITATIS TARTUENSIS

28

DISSERTATIONES PHYSICAE UNIVERSITATIS TARTUENSIS
28

NUCLEAR RESONANCE STUDIES OF LOCAL STRUCTURE IN $RBa_2Cu_3O_{6+x}$ COMPOUNDS

IVO HEINMAA

TARTU UNIVERSITY
PRESS

The study was carried out at the Institute of Chemical Physics and Biophysics Tallinn, Estonian, and at the Institut für Festkörperforschung, Forschungszentrum Jülich, Germany.

The Dissertation was admitted on April 21, 1999, in partial fulfillment of the requirements for the degree of Doctor of Philosophy in physics (solid state physics), and allowed for defence by the Council of the Department of Physics, University of Tartu.

Supervisor: Prof. Endel Lippmaa, Institute of Chemical Physics and Biophysics, Estonia.

Opponents: Prof. Vladimir Hiznjakov, University of Tartu, Estonia
Dr. Erkki Lähderanta, University of Turku, Finland

Defence: June 7, 1999, at University of Tartu, Tartu, Estonia.

Tartu Ülikooli Kirjastuse trükikoda
Tiigi 78, Tartu 50410
Tellimus nr. 348

CONTENTS

LIST OF ORIGINAL PAPERS

This thesis is based on the following papers, which will be referred to in the text by their Roman numerals:

I. **I. Heinmaa**, H. Lütgemeier, S. Pekker, G. Krabbes, and M. Buchgeister, Copper NMR and NQR in $YBa_2Cu_3O_x$ and $GdBa_2Cu_3O_x$ with x between 6 and 7. A study of the oxygen ordering, Appl. Magn. Reson. **3**, pp. 689–709 (1992).

II. H. Lütgemeier and **I. Heinmaa**, Oxygen Order and Spin Structure in $YBa_2Cu_3O_x$ deduced from Copper NMR and NQR, in: Proceedings of the Workshop on Phase Separation in Cuprate Superconductors, Erice, Italy, 6–12 May 1992, eds. K. A. Müller and G. Benedek, (World Scientific, 1993), pp. 243–261.

III. H. Lütgemeier, **I. Heinmaa**, and A. V. Egorov, Study of Oxygen Ordering in HT_c Superconductors by Magnetic Resonance of Different Nuclei, Physica Scripta, **T49**, pp. 137–142 (1993).

IV. H. Lütgemeier, **I. Heinmaa**, D. Wagener, and S. M. Hosseini, Superconductivity Versus Oxygen Concentration in 123 Compounds: Influence of RE Ionic Radii Studied by Cu NQR, in: Phase Separation in Cuprate Superconductors, eds. E. Sigmund and K. A. Müller, (Springer-Verlag, Berlin, 1994), pp. 225–235.

V. H. Lütgemeier, S. Schmenn, and **I. Heinmaa**, A microscopic Model for the different Tc(x) dependence in $REBa_2Cu_3O_{6+x}$ HT_c _ Superconductors containing different RE-ions, J. Low Temp. Phys. **105**, pp. 693–698 (1996).

VI. H. Lütgemeier, S. Schmenn, P. Meuffels, O. Storz, R. Schöllhorn, Ch. Niedemayer, **I. Heinmaa**, and Yu. Baikov, A different type of oxygen order in $REBa_2Cu_3O_{6+x}$ HT_c superconductors with different RE ionic radii, Physica C **267**, pp. 191–203 (1996).

VII. R. Stern, **I. Heinmaa**, H. Lütgemeier, M. Mali, J. Roos, and D. Brinkmann, $^{63,65}Cu$ NQR Studies in Oxygen Deficient $Y_2Ba_4Cu_7O_{15-x}$ ($0 \leq x \leq 0.6$), Physica C **235–240**, pp. 1655–1656 (1994).

VIII. H. Lütgemeier and **I. Heinmaa**, Investigation of the Antiferromagnetic Order in the 123 Compounds $REBa_2Cu_3O_y$ by NQR and NMR, in: Condensed matter studies by nuclear methods, eds. J. Stanek and A. T. Pedziwiatr, (World Scientific, Singapore, 1991) pp. 264–276.

IX. E. Lippmaa, E. Joon, **I. Heinmaa**, V. Miidel, A. Miller, and R. Stern, Radio-Spectroscopic Studies of Magnetic Properties of High Temperature Superconductors, Z. Naturforsch., **45a**, pp. 401–404 (1990).

1. INTRODUCTION

The discovery of high-temperature superconductivity in the copper oxide based compound $La_{2-x}Ba_xCuO_4$ ($T_c \approx 35$ K) in 1986 by J. G. Bednorz and K. A. Müller [1], for which they were awarded the 1987 Nobel Prize, gave solid state physics one of its most exciting problems. Historical significance of high temperature superconductors (HTSC) is illustrated in Fig. 1.1. The steep breakthrough of critical temperatures after 1986 explains why this remarkable discovery caused an unprecedented outburst of research activity among the solid state physicists and chemists. In early 1987 was discovered $YBa_2Cu_3O_7$ compound with T_c=93K [2], thus exceeding the boiling point of liquid nitrogen (77.4 K). At present time T_c of the cuprate superconductors has reported to be as high as 134 K in $HgBa_2Ca_2Cu_3O_{8+x}$ [3] and under external pressure of 150 kbar even 153K can be reached [4].

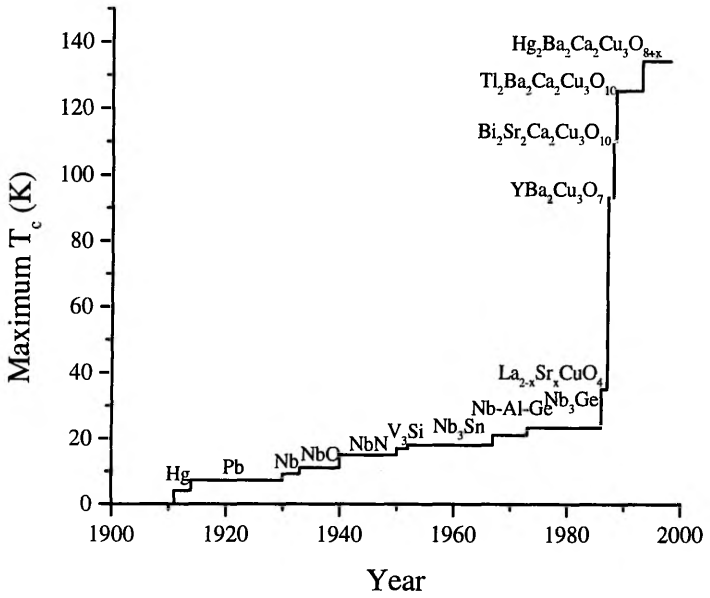

Fig. 1.1. Development of the highest critical temperatures of superconductors after discovery of the phenomenon in 1911 by Kammerlingh Onnes.

Despite of a large amount of experimental and theoretical work done with the aim to understand the mechanism of high temperature superconductivity, there is not yet agreement on a complete theory of high temperature superconductivity. By now a consensus has formed that the strong electron repulsion and the quasi-two-dimensional layered nature of these materials are responsible for their anomalous physical properties and high T_c. The repulsive electron interaction in the cuprates is the reason of a strong antiferromagnetic (AF) exchange interaction between the electronic spins at neighbouring copper sites. This AF interaction induces an antiferromagnetic long range ordering (Néel state) and it is believed [5–7] that it causes the formation of the singlet pairs.

The best studied family of the HTSC is of the type $RBa_2Cu_3O_{6+x}$ ($0 \leq x \leq 1$), often cited as "123" compounds, where R can be Y, La, or majority of rare earth elements — Nd, Sm, Eu, Gd, Dy, Ho, Er, Tm, Yb or Lu. The Pr compound with the same structure is a semiconducting antiferromagnet for any oxygen content x, and Ce and Tb do not form the 123 structure. The structure of R123 consists of a sequence of block layers, either insulating or charge reservoirs, and conducting CuO_2 planes to which superconductivity is mainly confined (see Fig. 1.2).

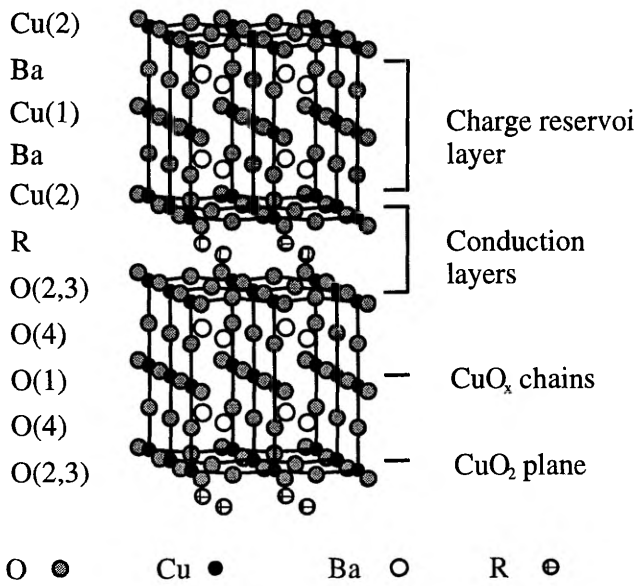

Fig. 1.2. Crystal structure of $RBa_2Cu_3O_{6+x}$.

According to the present understanding the main properties of HTSC depend on the doping level of CuO_2 planes. Four characteristic doping level regions have been distinguished in the phase diagram. *Undoped* CuO_2 plane is an antiferromagnetic insulator with the Néel temperature about 400K for R123. At

certain doping level the Néel temperature vanishes and the system becomes to so called *underdoped* superconductor. In this region the critical temperature grows linearly with carrier concentration [8]. The highest T_c is achieved at *optimally doped* CuO_2 plane. At higher doping the T_c decreases. This region is called *overdoped* superconductor. Here the properties become similar to that of the normal metals.

It is believed that especially underdoped cuprates hide the key properties of the high temperature superconductivity. Recent high resolution photoemission study of the density of states in $La_{2-x}Sr_xCuO_4$ shows [9] that in the underdoped region the system cannot be regarded as a normal Fermi liquid which is weakly perturbed by AF correlation, but rather an AF state perturbed by the motion of doped holes. The normal state properties like the Knight shift [10, 11], heat capacity [12], infrared [13], and transport [14] behaviour reflect the presence of d-wave-like pseudogap in the electron spectrum. Originally nuclear magnetic resonance relaxation and inelastic neutron scattering data [15] were interpreted [16] as opening of the pseudogap well above T_c in the spin excitation spectrum only. Later angle resolved photoemission spectroscopy (ARPES) measurements [9, 17] showed that this pseudogap is a real gap in the density of states having the same *d*-wave type symmetry as the superconducting gap. Microscopic origin of this pseudogap is yet to be established. The pseudogap has been associated with the development of AF correlations or short-range AF order [18], with short range metallic/AF stripe order [19] or with the preformed pairs, which lose their coherence above T_c but still keep local pairing [10, 20–22]. The major problem is that there is not yet theoretical agreement about the excitation produced by a hole in the AF CuO_2 plane (see e.g. Dagotto [23]). For example, in *t*-J model it is considered that a doped hole is located in the oxygen orbitals and forms with the adjacent Cu $3d^9$ hole a singlet state, so called Zhang-Rice singlet [24]. In alternative scenario the calculations show that a hole doped into the AF plane creates a spin-polarized cluster, magnetic polaron, with 5–8 parallel copper spins [25].

In the 123 structure the doping of the CuO_2 layer is determined by the number of oxygen ions in the CuO_x layer and by particular oxygen arrangement in this layer. Depending on the oxygen content, x, the system goes from antiferromagnetic insulator at x=0 to slightly overdoped superconductor at x=1.

The detailed phase diagram of oxygen doped R123 (Fig. 1.3) appears to be different for small and large R^{3+} compounds [26, 27]. The compounds with a small R^{3+} (Yb, Tm, Er, Gd, Y) show the well known for $YBa_2Cu_3O_{6+x}$ phase diagram [28]. Here the antiferromagnetic phase is maintained with high Néel temperature for oxygen concentrations $0 \le x \le 0.3$ and the superconductivity starts at $x \ge 0.4$ showing two plateaus in T_c vs x curve, namely "60K plateau" at $0.45 \le x \le 0.65$ and "90K plateau" at $0.85 \le x \le 1$. The two plateaus were attributed to the two orthorhombic structures termed Ortho-I and Ortho-II observed in

these compounds, where Ortho-I is the ordinary structure of fully oxygenated R123 with oxygens ordered into Cu-O chains along the *b*-axis and Ortho-II is the structure at x=0.5 where the oxygens of every other chain are missing (Fig. 1.4). At *x* around 0.5 other ordered superstructures can be constructed. Among these the "herringbone structure" minimizing Coulombic repulsion in the structure of single oxygen ions [29] has been found by x-ray diffraction in a single crystal of Y123 with x=0.35 [30], a result which could not be confirmed in a later experiment [31]. The compounds with a large R^{3+} (Sm, Nd, La) show AF phase for $0 \leq x \leq 0.6$ and the superconductivity appears at $x \geq 0.7$ with rapid increase of T_c as x increases. It is remarkable that in oxygen doped R123 the transition from antiferromagnetic to superconducting phase occurs without any detectable gap between the phases.

The T_c value of optimally doped R123 increases with increasing ionic radius of R^{3+} from 92 K for Yb1237 to 95.5 K for Nd1237 [32] whereas the Néel temperature T_N of undoped R1236 decreases with increasing ionic radius of R^{3+} (T_N=412 K and 385 K for Y1236 [33] and Nd1236 [34], respectively).

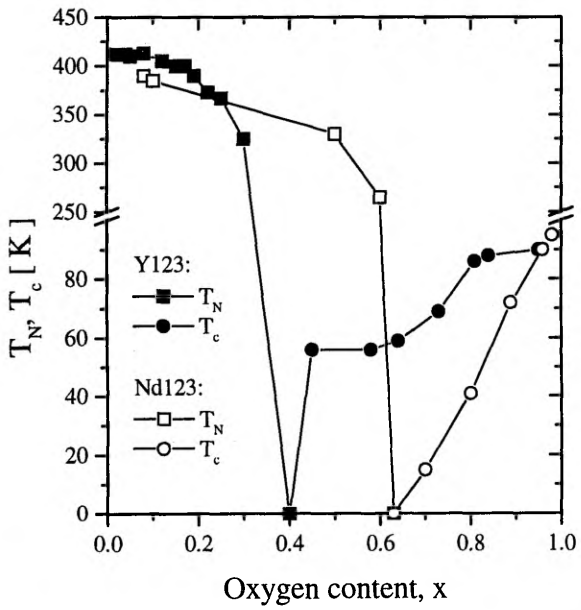

Fig. 1.3. The phase diagram of Y123 and Nd123. Y123 data: T_N from ^{89}Y NMR line width [33], T_c from resistivity [28]. Nd123 data: T_N from μSR and T_c from resistivity [VI].

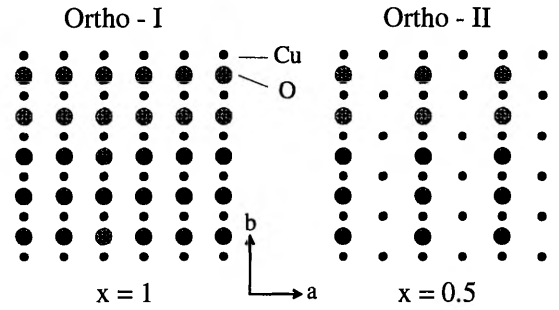

Fig. 1.4. Oxygen arrangements in the Cu(1) plane of the Y123 compound at oxygen content x=1 and x=0.5.

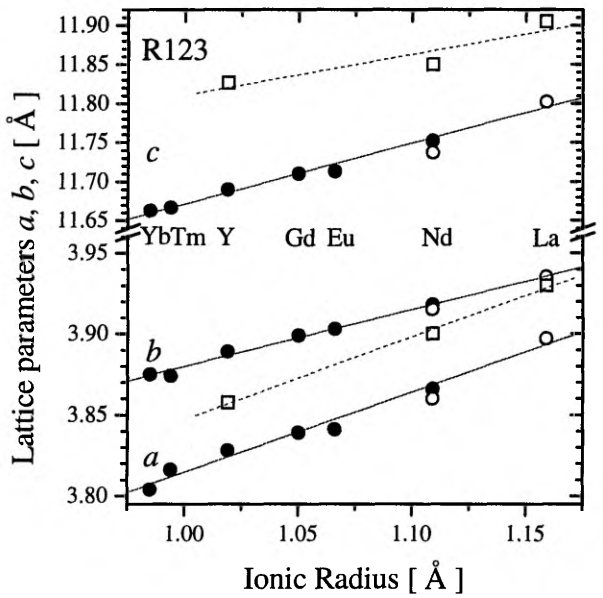

Fig. 1.5. Lattice parameters of orthorhombic R1237 (circles) and tetragonal R1236 (squares) as a function of R^{3+} ionic radius; full symbols from Ref. [32], open symbols from [VI].

The lattice parameters of fully oxygenated orthorhombic R1237 and tetragonal R1236 compounds show linear dependence on the ionic radius of R^{3+} (Fig. 1.5).

It is interesing to note that the doping of the planes in Y123 can be achieved also by substituting three-valent Y^{3+} by two-valent Ca^{2+} in tetragonal compound $Y_{1-y}Ca_yBa_2Cu_3O_6$ (YCa236). In this case the concentration of holes per Cu(2) in the planes is controlled by Ca content and is exactly n_h=y/2. The phase diagram of YCa236 [35, 36] is found to be different from that in oxygen doped R123,

but very similar to the case observed in $La_{2-x}Sr_xCuO_4$. In fact, the YCa236 system varies from AF insulating state at $y<0.06$, through an intermediate spin-glass state at $0.07<y<0.18$ to a superconducting state at $0.18<y<0.3$ with T_c up to 40 K. This difference in phase diagram of Ca doped and oxygen doped Y123 is not yet understood.

Thus the problem of local order in the R123 compounds has attracted considerable scientific interest because it provides additional information about the atomic arrangements responsible for the charge transfer which destroys the AF ordering in the CuO_2 layers and turns on the superconductivity. Since in HTSC the coherence length (or superconducting pair size) hardly exceeds a few lattice spacings, which probably means that the pairing force is made up by local interactions, the information about the local order in R123 is extremely valuable. Furthermore, several models of high temperature superconductivity assume a phase separation in the conducting CuO_2 plane into hole-rich metallic and hole-poor AF regions [19, 37, 38], indication of which might be found in the study of the local structure in CuO_2 layer.

In addition, the R123 structure appears to be an ideal system for studies of two-dimensional ordering phenomena. Many theoretical models describing the oxygen ordering and charge transfer in Y123 have been put forward [39–46] most of which are based on the assumption that only in-plane oxygen interactions are of importance. One of the most popular models is the two-dimensional asymmetric next-nearest-neighbour Ising (ASYNNNI) lattice gas model originally proposed by de Fontaine *et al.* [39], where the ordering of oxygen is determined by three effective interactions: a large repulsive interaction V_1 between oxygens in the sites O(1) and the always vacant site O(5), attractive interaction V_2 between nearest oxygens along the chain direction and small repulsive interaction V_3 between oxygens in neighbouring chains. The calculations based on this model have successfully described the structural phase diagram and kinetics of oxygen ordering [42] and the T_c dependence on the oxygen content in Y123 [43].

Due to the lack of long range order in the most interesting region of doping levels of R123 the local structure cannot be studied by usual diffraction methods. Therefore several local probe techniques have been applied. Among them Gd^{3+} EPR [47, 48], and inelastic neutron scattering on R^{3+} [49, 50] have been very informative techniques for probing the crystal field effects at R^{3+} sites due to oxygen ordering in the CuO_x layer.

The main aim 0of this work is to use the NMR and NQR techniques to study, on a microscopic scale, the structural changes in the CuO_x layer and related changes of the electronic and magnetic properties of CuO_2 planes of the R123 compounds.

We have shown [I, II] that the oxygen arrangement in CuO_x layer can be studied by Cu(1) NQR spectra of Y123 and Gd123. Later we applied the same technique to study the ordering in Tm123 [III], Nd123 [IV], and La123 [V–VI]

compounds. In paper [VII] we studied the oxygen ordering in the structure of $Y_2Ba_4Cu_7O_{15-x}$ where the doping level is depending on the oxygen content in Cu-O chains of the so called 123 block of the structure. In papers [II and VIII] several aspects of the magnetic structure in R123 are studied. In paper [IX] we have shown the anomalous behaviour of relaxation and the Knight shift of ^{63}Cu and ^{17}O in underdoped Y123 associated with the pseudogap phenomenon.

In the following we will review the main results of these studies while concentrating on the aspects of the doping-induced changes of the local structure in different R123.

The work is organised as follows. In the next chapter we will give the basic concept of the NMR/NQR technique. In the third chapter we briefly characterise the samples and the measurement procedure. In the 4-th chapter we present the main results concerning oxygen ordering in the CuO_x layer. The 5-th chapter is devoted to the effects seen by the copper nuclear resonance in the antiferromagnetic and superconducting CuO_2 plane. In the discussion given in chapter 6 we will argue on the oxygen ordering parameters obtained by NQR technique and propose a simple microscopic mechanism of chain to plane charge transfer by oxygen doping and its consequences to the R123 phase diagram.

2. THEORETICAL BACKGROUND

2.1. The Nuclear Spin Hamiltonian of Copper

Both copper isotopes ^{63}Cu and ^{65}Cu have a nuclear spin I=3/2 and a electric quadrupole moment Q, arising from a nonspherical nuclear charge distribution (Table 2.1).

Table 2.1. Gyromagnetic ratios γ_n, quadrupole moments Q, and natural abundance of the two copper isotopes

	γ_n (MHz/T)	Q (b)	Nat. abundance (%)
^{63}Cu	11.285	–0.211	69
^{65}Cu	12.089	–0.195	31

In the presence of external or internal magnetic field H_0 and local electric field gradients (EFG), the nuclear spin system can be described by the Hamiltonian [51, 52]:

$$\mathcal{H} = \mathcal{H}_{\text{Zeeman}} + \mathcal{H}_{\text{quadrupole}} \tag{2.1}$$

with the Zeeman term

$$\begin{aligned}\mathcal{H}_{\text{Zeeman}} = -\gamma_n \hbar H_0 \big[& I_Z (1+K_{ZZ}) \cos\vartheta + I_Y (1+K_{YY}) \sin\vartheta \sin\varphi \\ & + I_Y (1+K_{XX}) \sin\vartheta \cos\varphi \big]\end{aligned} \tag{2.2}$$

and the quadrupolar term

$$\mathcal{H}_{\text{quadrupole}} = \frac{eQV_{zz}}{4I(2I+1)} \left[3I_z - I(I+1) + \frac{1}{2}\eta \left(I_+^2 + I_-^2 \right) \right]. \tag{2.3}$$

The principal axis coordinate system (PAS) of the EFG tensor **V** is chosen in a way that the diagonal elements are related as $|V_{xx}| \le |V_{yy}| \le |V_{zz}|$. In this case the asymmetry parameter can be defined as $\eta = \left(V_{xx} - V_{yy}\right) / V_{zz}$, $\eta = 0 \div 1$. **K** is the magnetic hyperfine shift tensor. Due to the symmetry of the crystal, **K** is also diagonal in the PAS of the EFG tensor. In Eq. (2.2) ϑ and φ are the polar

and azimuth angles of the magnetic field direction in the PAS of the EFG tensor.

In the absence of the magnetic field we have an NQR experiment, described by the quadrupolar term of the Hamiltonian. In this case the energy levels $\pm m$ of I=3/2 nuclei are degenerate and the only resonance frequency is given by:

$$\omega_{NQR} = \frac{eQV_{ZZ}}{2h}\sqrt{1+\frac{1}{3}\eta^2}\ . \tag{2.4}$$

When both terms in the Hamiltonian contribute to the spectrum, the correct transition frequencies should be determined by numerical diagonalization of the Hamiltonian. Using the definitions

$$\omega_0 = \gamma_n H_0,$$

$$\omega_Q = \frac{eQV_{ZZ}}{2h},$$

$$A = \omega_0\left(1+K_{ZZ}\right)\cos\vartheta,$$

$$B = -\left[i\left(1+K_{YY}\right)\sin\varphi + \left(1+K_{XX}\right)\cos\varphi\right]\sin\vartheta,$$

$$C = \frac{\eta}{\sqrt{3}}$$

the matrix presentation of $\mathcal{H}$ is relatively simple:

$$\mathcal{H} = \frac{1}{2}\begin{bmatrix} \omega_Q - 3A & \sqrt{3}\omega_0 B^* & \omega_Q C & 0 \\ \sqrt{3}\omega_0 B & -\omega_Q - A & 2\omega_0 B^* & \omega_Q C \\ \omega_Q C & 2\omega_0 B & -\omega_Q + A & \sqrt{3}\omega_0 B^* \\ 0 & \omega_Q C & \sqrt{3}\omega_0 B & \omega_Q + 3A \end{bmatrix}. \tag{2.5}$$

An example of ^{63}Cu and ^{65}Cu resonance frequencies as a function of magnetic field H_0 obtained by exact diagonalization of the Hamiltonian (2.5) is given in Figure 2.1. At this H_0 is directed along the main principal axis of EFG and for clarity the asymmetry parameter has been taken η=0. The figure shows different experiments which provide quadrupolar coupling and magnetic shift

parameters. At zero field the NQR spectrum consists of two lines at frequencies given by Eqn. (2.4), corresponding to the transition between degenerate eigenstates $m = \pm 3/2 \leftrightarrow \pm 1/2$ of the two copper isotopes denoted by long (^{63}Cu) and short (^{65}Cu) arrows. A small magnetic field splits the resonance lines. Observation of such splitting unambiguously refers to the presence of static magnetic field.

At high magnetic fields the NMR spectrum can be obtained either by sweeping magnetic field at fixed frequency or by seeping frequency at fixed magnetic field. In both cases the spectrum of each copper isotope consists of three lines corresponding to three allowed transitions of *I=3/2* nuclei ($m = -3/2 \leftrightarrow -1/2, -1/2 \leftrightarrow 1/2$, and $1/2 \leftrightarrow 3/2$).

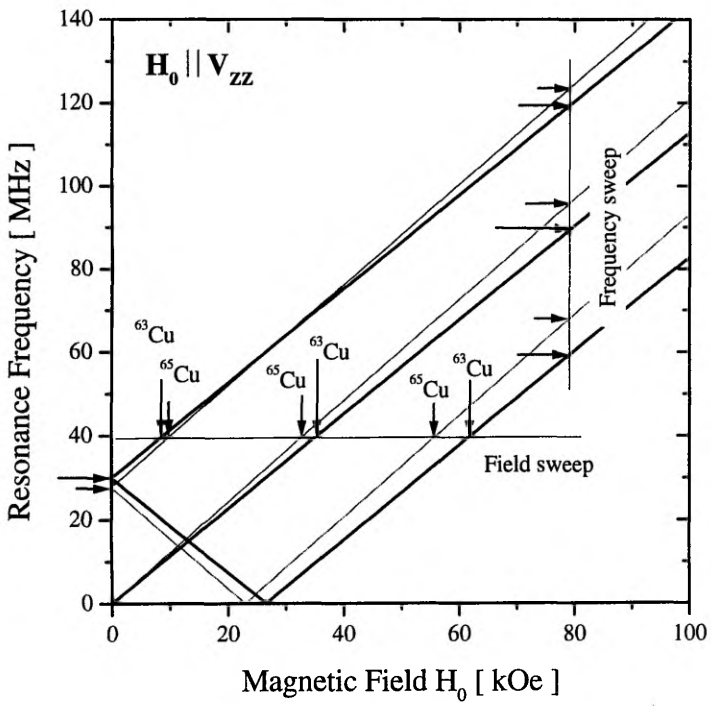

Fig. 2.1. ^{63}Cu and ^{65}Cu resonance frequencies as a function of magnetic field H_0.

2.2. The Electric Field Gradient

The EFG is a ground-state property of a material providing detailed information about the charge distribution at a nucleus site in the crystal.

In the traditional approach the EFG tensor is a sum of a lattice contribution ($\mathbf{V}^{LAT}$) and a valence contribution ($\mathbf{V}^{VAL}$):

$$\mathbf{V} = \mathbf{V}^{VAL} + \mathbf{V}^{LAT}. \tag{2.7}$$

The lattice contribution is caused by the ionic charges in the crystal and can be calculated as

$$V_{\alpha\beta}^{LAT} = (1-\gamma_\infty)\sum_k q_k \left(\frac{3x_\alpha^k x_\beta^k - \delta_{\alpha\beta} r_k^2}{r_k^5} \right), \tag{2.8}$$

where the parameter γ_∞ is known as Sternheimer antishielding factor [53], q_k x_α^k and r_k are the charge, coordinate and distance of the ion k. Summation is usually done within a sphere of sufficiently large radius r>50Å [54].

The valence contribution to the EFG is caused by the electrons in a partially filled Cu-*3d* orbitals and can be expressed as [55]:

$$\begin{aligned} V_{ZZ}^{VAL} &= -C\frac{4}{7}e\langle r^{-3}\rangle \left[n_{3d(x^2-y^2)} - n_{3d(3z^2-r^2)} + n_{3d(xy)} - \frac{1}{2}n_{3d(xz)} + \frac{1}{2}n_{3d(yz)} \right], \\ &= -2V_{XX}^{VAL} = -2V_{YY}^{VAL} \end{aligned} \tag{2.9}$$

where $n_{3d(x,y,z)}$ are the number of holes in noted *3d* orbitals. The coefficient C describes the covalency or effective hole number in *3d* orbital. For free Cu^{2+} ion C=1.

As far as we measure the EFG by quadrupolar interaction, it is more convenient to express the EFG components in frequency units

$$\nu_{\alpha\alpha} = \frac{eQ}{2h} V_{\alpha\alpha}, \tag{2.10}$$

where $\frac{eQ}{2h} = -7.647 \cdot 10^{-9}$ Hz / esu for ^{63}Cu. For the free Cu^{2+} ion with the hole in $3d(x^2-y^2)$ orbital one obtain the valence contribution for ^{63}Cu ν_{ZZ}^{VAL}=73 MHz [54]. Similarly, if the hole is in $3d(3z^2-r^2)$ orbital, the valence contribution is equal to –73 MHz.

3. EXPERIMENTAL

3.1. Samples

The samples of $RBa_2Cu_3O_{6+x}$ which are studied in the present work have been prepared at different laboratories noted in the Table 3.1.

The details of the samples are described in the denoted papers

Table 3.1. Origin of the samples studied in this work

Samples	Ref.	Details	Synthesized at
Y123	I, II	oriented powder	Central Research Institute for Physics, Budapest (A. Janossy, S. Pekker)
Y123	I, II	powder	Zentralinstitut für Festkörperphysik, Dresden (G. Krabbes)
Gd123	I, II	powder	Institut für Strahlen- und Kernphysik, Univ. Bonn (M. Buchgeister)
Tm123	II, III	powder	Institut für Strahlen- und Kernphysik, Univ. Bonn (S. M. Hosseini, D. Wagener)
Nd123	IV–V	powder	Institut für Strahlen- und Kernphysik, Univ. Bonn (S. M. Hosseini, D. Wagener)
La123	VI	powder	Technical University of Berlin, (R. Schöllhorn, O. Storz), Oxygen treated by Yu. Baikov, Joffe Institute, St. Petersburg
Y123	IX	oriented powder ^{17}O enriched	Institute of Chemical Physics and Biophysics, Tallinn (E. Joon, S. Vija)

The oxygen concentration was usually determined by the weight change. The typical procedure of the preparation of the series of samples with different oxygen content was the following [VI]. The initial pellets of R-123 with a total mass of about 10 g were divided into 10 pieces and have been treated without grinding. The first step was vacuum treatment at 10^{-6} Torr and 690°C for 4 hours. For loading with oxygen a calibrated volume of 103 cm^3 was used and the amount of oxygen absorbed was determined from the pressure difference and controlled by the weight increase. The oxygen was absorbed at 200 to 400°C. To avoid nonuniform oxygen distribution, the samples were heated to 700°C and then cooled at 10°C/min rate. After this procedure the oxygen pressure was below 0.1 Torr.

It appeared that the quality of the initial R123 material can be effectively tested by the linewidth of the Cu(1) NQR resonance in completely deoxygenated compounds R1236. Considerable broadening of the resonance line occurs in the case of defective cation lattice. Furthermore, considerable substitution of Ba^{2+} by La^{3+} or Nd^{3+}, which usually occurs in La123 and Nd123, manifests itself in the NQR spectrum by additional splitting of the Cu(1) resonance line

due to the induced magnetic field at Cu(1) site within the AF-II structure (see below section 5.2).

3.2. NQR/NMR Measurements

The NMR/NQR experiments were typically carried out at liquid He temperatures 4.2K or 1.3K on home-built pulse spectrometers. The NMR spectra were obtained by collecting the echo signal at fixed frequency and scanning automatically the external magnetic field in discrete steps. The NQR spectra were obtained at zero external field by scanning the frequency in discrete steps and integrating the spin echo amplitude. In order to reduce the contribution to the signal due to the rf pulse tail, we have used the phase alternation techniques. The rf amplitude of the pulses was chosen to obtain the maximum echo intensity at a duration of about 5 μs for the 180° pulse. Since under these conditions the bandwidth of excitation is below the linewidth of all components in the spectrum, the echo amplitude normalized by the square of the excitation frequency is proportional to the number of nuclei at resonance. Thus the intensities of different resonances in the NQR spectra measure the amount of copper at the corresponding sites.

In order to get comparable intensity data from the spectra, we have made a computer fit to the experimental resonance lines. The spectra were fitted to the sum of suitable number of pairs of Lorentzian lines corresponding to the ^{63}Cu/^{65}Cu resonances. The ratio of the frequencies, amplitudes and widths within the pair were taken as $^{65}f/^{63}f=^{65}Q/^{63}Q=0.924$, $^{65}I/^{63}I=^{65}n/^{63}n$ kept constant.

4. OXYGEN ORDER IN THE CuO_x LAYER OF R123

In the following chapter we will give the main experimental results about the oxygen ordering in the CuO_x plane as seen by copper nuclear resonance.
We will show that

- the EFG values at Cu(1) sites with different oxygen coordination can be well described within the point charge model,
- different intensity distribution of the Cu(1) NQR lines in different R123 compounds yields different oxygen ordering: in Y-, Tm- and Gd123 oxygen ions in the basal plane are clustered preferentially in long chain fragments, while in La123 the oxygens tend to be single and in Nd123 almost random distribution of oxygens is found,
- the average chain length in the region of 60K plateau is about 10 oxygen ions.

4.1. The NQR Frequencies of Cu(1) Sites

In R123 structure the oxygen ions in the basal plane are organized into linear chains [28, 56], therefore only three different Cu(1) sites can be found in the CuO_x layer of oxygen deficient R123 structure given in Fig. 4.1, where we have labelled these sites as $Cu(1)_2$, $Cu(1)_3$, and $Cu(1)_4$. The index refers to the number of the nearest oxygen neighbours.

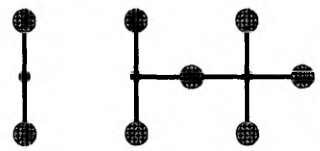

$Cu(1)_2$ $Cu(1)_3$ $Cu(1)_4$

Fig. 4.1. Possible Cu(1) configurations in the oxygen deficient CuO_x layer.

It is straightforward that the two-coordinated copper site $Cu(1)_2$ is the only Cu(1) site in the tetragonal $RBa_2Cu_3O_6$ compound, whereas the four-coordinated site $Cu(1)_4$ is the only one in the fully oxygenated orthorhombic compound $RBa_2Cu_3O_7$. At intermediate oxygen concentrations all three possible copper configurations exist — the $Cu(1)_2$ sites in empty fragments,

$Cu(1)_4$ sites constitute intact chains and $Cu(1)_3$ sites are situated at the ends of the chains.

The NQR spectra of oxygen deficient Y123 show a number of lines in the frequency region of 20 to 31.5 MHz belonging to different copper sites in the CuO_x layer and also to Cu(2) sites in the CuO_2 plane [57–59]. We have made unambiguous site assignment using discrimination of the Cu(2) signal in Gd123, where the copper in Cu(2) sites has very fast relaxation due to neighbouring magnetic Gd^{3+} ion [I]. As a result we were able to assign the lines in the NQR spectra of oxygen deficient R123, belonging to the three basic Cu(1) configurations. The NQR frequencies of Y123 at different oxygen contents are given in Fig. 4.2. The figure shows that comparatively narrow $Cu(1)_3$ resonance appears at the same frequency (24 MHz) in the broad region of oxygen contents ($0.3<x<0.8$).

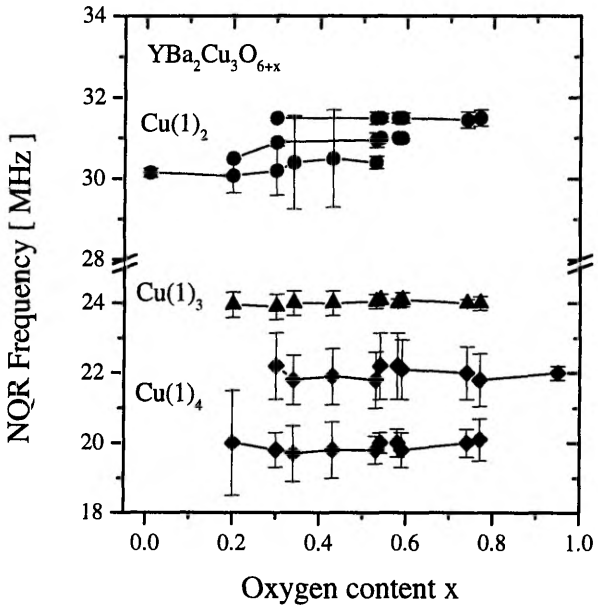

Fig. 4.2. ^{63}Cu NQR frequencies of Cu(1) configurations in Y123 samples at different oxygen contents. The error bars express the widths of the lines.

The two resonance lines belonging to $Cu(1)_4$ sites are broad except of the samples of high oxygen content, reflecting a distribution of the O-Cu-O fragment lengths. We have assigned the resonance at 20 MHz to the sites in the short chains, whereas the line at 22 MHz corresponds to the sites in long chains. The behaviour of comparatively narrow lines belonging to $Cu(1)_2$ sites is particularly interesting. In the spectra of samples of tetragonal phase it has a resonance frequency 30.1 MHz, while at higher oxygen content in addition to

that line two distinct lines at 31.0 MHz and 31.5 MHz appear in the spectrum (see Fig. 4 in [I]). With further increase of oxygen content the lines at 30.1 and 31.0 MHz disappear whereas the line at 31.5 MHz can be observed up to the oxygen contents x~0.8. Such behaviour can be explained in a rather simple way. At high oxygen content the $Cu(1)_2$ sites can be found only in the empty fragments between two intact chains. Therefore these sites contribute to the NQR line at 31.5 MHz. Similarly, the line at 31 MHz corresponds to the sites in empty fragment between an intact and another empty fragment. The third line close to the frequency of the sites in tetragonal samples belongs to the sites in empty fragments between two other empty fragments. All experimental data [57–59] show that superconductivity disappears in the samples where the $Cu(1)_2$ line at 31.5 MHz is missing. This fact with the interpretation above allows to make a conclusion about the relation between local order and superconductivity: superconductivity does not occur in R123 samples where the oxygen filled chain fragments in the CuO_x layer are separated along the a-direction by more than one empty fragment.

Similar NQR lines corresponding to Cu(1) sites can be found in the NQR spectra of Gd123 samples and of the other R123 as well. In Fig. 4.3 we show the NQR frequencies of the three basic Cu(1) configurations determined from the NQR spectra of different R123 as a function of the ionic radius of R^{3+}.

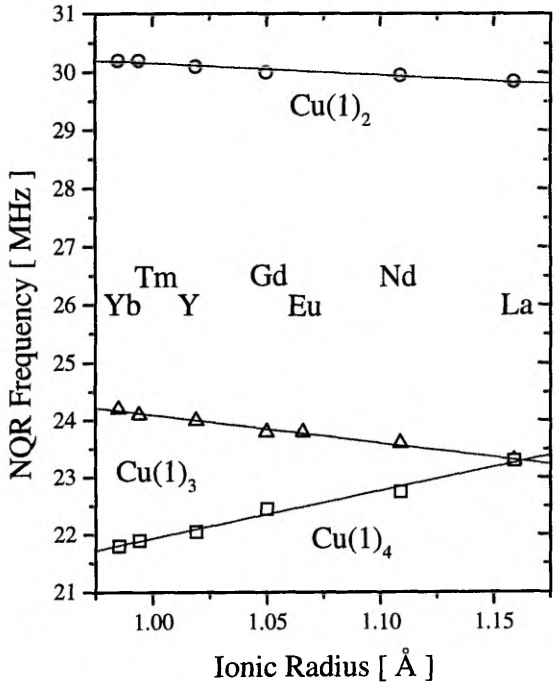

Fig. 4.3. NQR frequencies of $Cu(1)_2$, $Cu(1)_3$ and $Cu(1)_4$ sites in R-123 structure at different radii of R^{3+} ions [VI].

Here the $Cu(1)_2$ site is the site in R1236 compound and the $Cu(1)_4$ site is the site in R1237 compound. It is seen that the NQR frequency of all three Cu(1) configurations show almost linear dependence on the ionic radius of R^{3+}. Since the lattice parameters of R123 show similar linear dependence on the ionic radius of R^{3+} (see Fig. 1.5), we believe the difference in NQR frequencies of different R123 is related to the change of the lattice parameters.

In order to clarify this point we have performed EFG calculations within the point charge model for three basic Cu(1) configurations in Y-, Nd- and La123 structures. As described above (see section 2.2), the EFG at a given copper site arises from the valence and lattice contributions. Calculating the lattice sum for that copper site, one can evaluate two unknown parameters, the Sternheimer antishielding factor γ_∞ and the valence contribution, from experimentally determined quadrupolar coupling tensor. Such procedure yields in most cases only one reasonable set of parameters despite of the fact that the sign of the EFG tensor cannot be determined from NMR/NQR experiment.

The results of the calculation are give in Table 4.1. It shows that the calculated EFG values reproduce well the observed NQR frequencies of all three Cu(1) configurations in different R123 structures. It proves that the dependence of the NQR frequencies of Cu(1) sites on R^{3+} shown in Fig. 4.3 is due to the differences of the lattice parameters of R123 compounds. Furthermore, the parameters obtained from the calculation can be used in the analysis of doping induced structural changes.

The calculation procedure was as follows. First we calculated the lattice sum for all three Cu(1) configurations using well established crystallographic data for Y1236 and Y1237 [60]. The local environment of $Cu(1)_3$ site was constructed by adding a O^{2-} ion between two neighbouring $Cu(1)_2$ sites in the Y1236 structure. The ionic charges in the Y1236 structure are straightforward. In Y1237 structure the charge of the ions is not that clear. It is commonly accepted that an extra hole in this structure is located on oxygen ions. Although the distribution of the hole among the oxygens is a matter of discussions, we found that the effective oxygen charges given by Zimmermann [61] as –1.62, –1.885 and –1.92 at O(1), O(2,3) and O(4), respectively, give the best description of the EFG at $Cu(1)_4$ site. Then we found γ_∞ and the valence contribution, ν^{VAL}, from the experimental EFG tensor. At the end, using the same deduced parameters we found the EFG and NQR frequencies for Cu(1) sites in Nd123 and La123 structures. The lattice sum for Nd and La123 compounds was obtained taking the lattice parameters *a*, *b* and *c* as determined for our samples [VI], where we detected only minor substitution of Nd/La in Ba position, assuming the same as in Y123 structure ionic coordinates. Concerning the simulation parameters we must add the following comments. In $Cu(1)_2$ site, the copper is in Cu^{+1} state and the EFG value for copper with a closed *d*-shell is determined purely by the lattice contribution. The value of Sternheimer

antishielding factor for Cu^{1+} ion γ_∞=–5.32 deduced in this study, fits well with the literature values (see *e.g.* γ_∞=–5.5 in Ref. [62], γ_∞=–5.2 in Ref. [54]). For two-valent copper we found the Sternheimer antishielding factor γ_∞=–10.1 and –10.4 for three- and four-coordinated copper, respectively.

Interesting information emerges from the comparison of the valence contributions for three and four-coordinated copper. In order to achieve experimentally determined symmetry of the EFG tensor at $Cu(1)_3$ site [63], one has to use a negative valence contribution –57.6 MHz with the main axis along the *c*-axis of the crystal, whereas for $Cu(1)_4$ site the valence contribution of +59.4 MHz along the *a*-axis gives best match to the experimental EFG. This means formally that in $Cu(1)_3$ site the copper has about 0.79 holes in its $3d(3z^2–r^2)$ orbital while in the $Cu(1)_4$ sites 0.81 holes occupy, as expected, the $3d(x^2–y^2)$ orbital. Burdett *et al.* [56] have noted that for copper the so called T-shape geometry like that in $Cu(1)_3$ sites is abnormal and very exotic. Nevertheless, according to their calculation the highest energy orbital for copper in the T-shape configuration is $3d(x^2–y^2)$, in contradiction with our analysis. On the other hand, the highest energy orbital $3d(3z^2–r^2)$ is characteristic for copper in the linear coordination [56], therefore our analysis indicates that in $Cu(1)_3$ sites the two-valent copper having a hole in its $3d(3z^2–r^2)$ orbital is mainly bonded to the nearest apex oxygens and only weakly bonded to the oxygen along the chain direction. This can be the reason why the width and frequency of the corresponding NQR resonance line is almost insensitive to the changes of oxygen arrangement in the Cu-O chains.

Using parameters in Table 4.1 one can show that the above mentioned change of the NQR frequency of $Cu(1)_2$ line in Y123 must be ascribed to the change of the distance between Cu(1) and the apex oxygen O(4). Calculating the distance from the $Cu(1)_2$ resonance at 31.5 MHz in orthorhombic Y123 we obtained 1.78 Å which is much shorter than that of $Cu(1)_4$-O(4) (1.85 Å in Y1237 [60]). This result confirms the model drawn by Cava *et al.* [28] from the analysis of neutron diffraction data, and the results of the x-ray diffraction data by Grybos *et al.* [64] on Y123 single crystal of ortho-II phase, stating that in the CuO_x layer the copper site primarily consists of a mixture of $Cu(1)_2$ and $Cu(1)_4$ with twofold copper having shorter bond lengths than the fourfold copper.

Table 4.1. Experimental and calculated NQR frequencies of $Cu(1)_2$, $Cu(1)_3$ and $Cu(1)_4$ sites in Y-, Nd- and La123 structures

Site	Structure		ν_{aa}	ν_{bb}	ν_{cc}	η	ν_{NQR} (MHz)
$Cu(1)_2$		γ_∞=–5.32					
		ν^{VAL}=0					
	Y1236	ν^{LAT}	–15.05	–15.05	30.10	0	**30.1**
		EXP			±30.1	0	**30.1**
	Nd1236	ν^{LAT}	–14.99	–14.99	29.98	0	**29.98**
		EXP					**29.95**
	La1236	ν^{LAT}	–14.79	–14.79	29.58	0	**29.58**
		EXP					**29.83**
$Cu(1)_3$		γ_∞=–10.1					
		ν^{VAL}	28.79	28.79	–57.58		
	Y1236	ν^{LAT}	–37.11	–5.14	42.25		
	$+O^{2-}$	$\nu^{LAT+VAL}$	–8.32	23.65	–15.33	0.30	**24.0**
		EXP			±15.3	0.3	**24.0**
	Nd1236	ν^{LAT}	–36.65	–5.71	42.36		
	$+O^{2-}$	$\nu^{LAT+VAL}$	–7.86	23.08	–15.22	0.32	**23.5**
		EXP					**23.6**
	La1236	ν^{LAT}	–36.04	–5.82	41.86		
	$+O^{2-}$	$\nu^{LAT+VAL}$	–7.25	22.97	–15.72	0.37	**23.5**
		EXP					**23.3**
$Cu(1)_4$		γ_∞=–10.4					
		ν^{VAL}	59.44	–29.72	–29.72		
		ν^{LAT}	–40.60	10.40	30.20		
	Y1237	$\nu^{LAT+VAL}$	18.84	–19.32	0.48	0.95	**22.04**
		EXP			±0.48	0.95	**22.05**
		ν^{LAT}	–40.05	9.98	30.07		
	Nd1237	$\nu^{LAT+VAL}$	19.39	–19.74	0.35	0.96	**22.6**
		EXP					**22.7**
		ν^{LAT}	–39.44	9.89	29.55		
	La1237	$\nu^{LAT+VAL}$	20.00	–19.83	–0.17	0.98	**23.0**
		EXP	–	–	–		**23.3**

4.2. Intensity Distribution of Cu(1) Lines

In order to provide qualitative and quantitative characterisation of oxygen ordering in the CuO_x layer, we have studied the intensity distribution of the Cu(1) NQR lines. Different relative intensity of the Cu(1) lines of different R123 is most evident at oxygen content x about 0.5 as shown in Fig. 4.4.

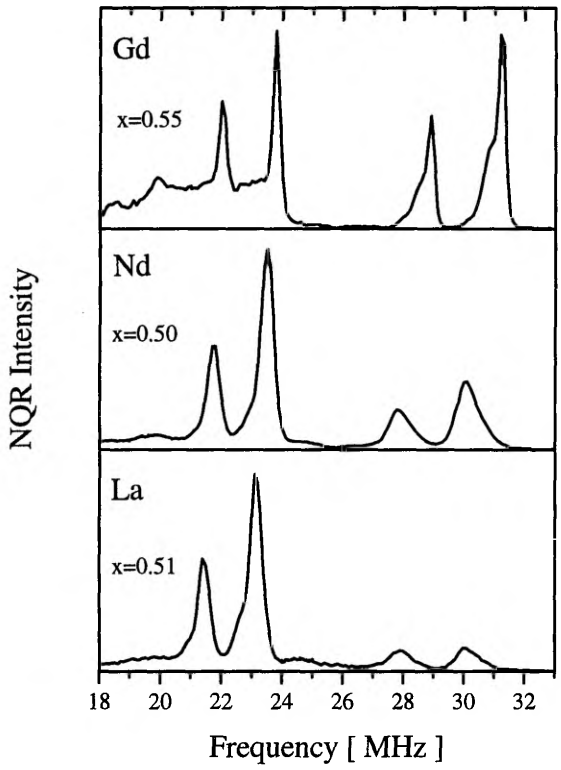

Fig. 4.4. NQR spectra of Cu(1) sites in Gd123, Nd123 and La123 with oxygen content x around 0.5.

Here the spectrum of Gd123 shows the $^{63}Cu/^{65}Cu$ doublet at 31.2/28.9 MHz corresponding to $Cu(1)_2$ sites, the other doublet at 23.8/22.0 MHz corresponds to the $Cu(1)_3$ sites, the broad background under this doublet plus doublet at 19.9/18.4 MHz is assigned to the copper in $Cu(1)_4$ sites. One can see that the intensity of the line corresponding to $Cu(1)_2$ sites is remarkably smaller in Nd123 and almost missing in the spectrum of La123, which mainly show only the doublet at 23.1/21.4 MHz corresponding to the $Cu(1)_3$ sites. While at this oxygen content half of the oxygen sites in the CuO_x layer are occupied, this means that in La compound most of the oxygen ions in the layer remain single converting two neighbouring copper ions from Cu^+ to Cu^{2+} in $Cu(1)_3$ geometry, whereas in Gd123 with similar oxygen content the oxygen ions are clustered in longer fragments leaving a comparable amount of copper in $Cu(1)_2$ sites of empty fragments.

Further evidence of different oxygen ordering in different R123 can be found looking at the dependence of the relative intensities of NQR lines on

oxygen content x, shown in Fig. 4.5. Here I_2, I_3 and I_4 note relative intensities of the lines corresponding to $Cu(1)_2$, $Cu(1)_3$ and $Cu(1)_4$ sites, respectively.

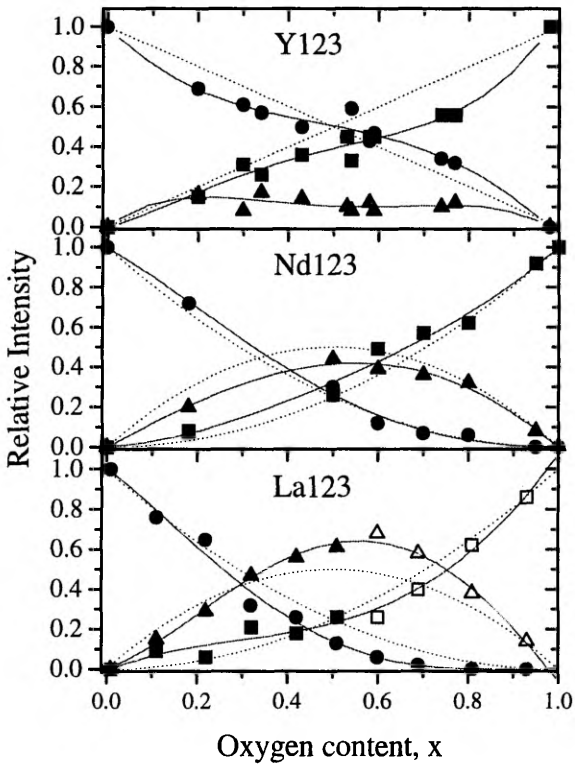

Fig. 4.5. Relative intensities of the three Cu(1) configurations in the Y123, Nd123 and La123 compounds: circles — I_2, triangles — I_3, squares — I_4. Full symbols determined directly from NQR spectra, open symbols (for La123) are calculated from relative intensity of $Cu(1)_2$ line, the full lines are for guiding the eye, the dotted lines are intensity distributions according to the models given in the text.

In La123 I_3 and I_4 cannot be separately obtained directly from the NQR spectrum, since the frequencies of $Cu(1)_3$ and $Cu(1)_4$ are not separated. Here the intensities I_3 and I_4 are calculated from the relative intensity of $Cu(1)_2$ line at given oxygen concentration x using following the simple and obvious expressions

$$I_3 = 2\left(1 - x - I_2\right), \qquad I_4 = I_2 + 2x - 1. \tag{4.1}$$

These intensity distributions can be compared with some asymptotic models of oxygen arrangements in the CuO_x layer.

First, a complete oxygen ordering into the long chains leaving the rest of the layer empty would lead to

$$I_2 = 1 - x, \quad I_3 = 0, \quad I_4 = x. \tag{4.2}$$

Evidently this case (illustrated by dotted lines for Y123 in Fig. 4.5) is not followed in the experimental distributions. In Y123 the I_3 intensity hardly exceeds 0.2 and the nearly linear part of I_2 and I_4 curves in the range $0.2<x<0.8$ manifests that comparatively long oxygen fragments are present.

Second, completely random distribution of oxygen on all allowed oxygen sites in the chains gives

$$I_2 = (1-x)^2, \quad I_3 = 2x(1-x), \quad I_4 = x^2. \tag{4.3}$$

Dotted lines for Nd123 in Fig. 4.5 demonstrate that the NQR intensities of Nd123 can be well described by this model. Comparison of the intensity distribution in La123 with the random case (dotted lines for La123) shows that at intermediate oxygen concentrations the I_3 intensity is larger and I_2 intensity is smaller than expected for the random case. This tells us that the oxygen ions tend to repel each other. Indeed, repulsive interaction between oxygen ions keeping them as far from each other as possible leads to the intensity distribution:

$$\begin{aligned} &I_2 = 1-2x, \quad I_3 = 2x, \quad I_4 = 0, \\ &\text{for } 0 \le x \le 0.5, \text{ and} \\ &I_2 = 0, \quad I_3 = 2(1-x), \quad I_4 = 2x-1 \\ &\text{for } 0.5 \le x \le 1. \end{aligned} \tag{4.4}$$

This ideal case would lead at oxygen concentration x=0.5 to the relative intensities $I_2=I_4=0$, $I_3=1$. Although this ideal case is not observed in the experimental spectra of La123, such comparison gives clear indication that in La123 the oxygen ions tend to repel each other.

In the lattice gas picture [39] the long chains in the CuO_x layer of Y123 are formed due to the effective attractive interaction between the oxygen ions in neighbouring sites along the chain direction. Thus, the intensity distribution of Cu(1) lines in different R123 show that with growing ionic radius of R^{3+} (or with growing lattice parameters of R123) this attractive interaction decreases to zero in Nd123 and changes to slightly repulsive in La123 case.

4.3. Length of Copper-Oxygen Chains

Assuming all oxygen ions are arranged in fragments of the type $(Cu\text{-}O)_n\text{-}Cu$ we can use the NQR intensities of Cu(1) sites and determine the average length of the fragments, which is given as

$$\overline{n} = 1 + 2\,I_4 / I_3\,, \tag{4.5}$$

In Figure 4.6 we have plotted the average chain length for different R123 as a function of oxygen content. One can see in the figure that the average chain length at a given oxygen content decreases with increasing radius of the R^{3+}. For Y123 the growth of the average chain length with oxygen content is almost exponential (straight dotted line in the figure), at low oxygen content $x < 0.5$, in the region of "60K plateau" ($0.5 < x < 0.8$) the average chain length of Y123 is around 10 oxygen ions.

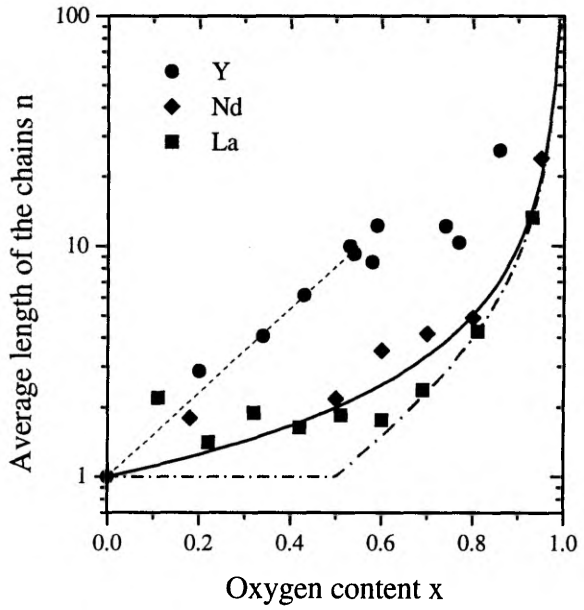

Fig. 4.6. Average length of the (Cu-O)n chains versus oxygen content for different R123 compounds, the dashed line is a guide to the eye, the full line represent the case of random distribution of oxygen ions in the CuO_x layer (Eq. 4.6), and dash-dotted line the case of effective repulsion (Eq. 4.7).

At higher oxygen concentration the sample Y1236.86 shows already substantially longer chains with $\overline{n} = 26$ similar to the case in Tm123, where we

found [III, IV] that the average chain length increases rapidly exceeding 100 in the region of "90K plateau" at 0.85<x<1.

For Nd123, as expected from the intensity distribution of Cu(1) lines, the growth of the chain length follows reasonably well the case of random distribution of oxygen ions in the CuO_x layer. According to the Eqs. (4.3) and (4.5) the average chain length in random case can be expressed as

$$\overline{n} = 1/(1-x), \tag{4.6}$$

which is illustrated by full line in Fig. 4.6.

In the model of repulsive interaction between the oxygen ions (Eq. 4.4) the growth of the chain length can be evaluated as

$$\begin{aligned} \overline{n} &= 1 && \text{for } x \le 0.5 \\ \overline{n} &= x/(1-x) && \text{for } x \ge 0.5. \end{aligned} \tag{4.7}$$

The dash-dotted line in Fig. 4.6 represent this case of the growth of the average chain length.

5. LOCAL ORDER IN THE CuO_2 PLANE

In this chapter we review the experimental findings concerning the changes in the antiferromagnetic CuO_2 plane at oxygen doping of R123 as seen by copper Cu(2) nuclear resonance. We will show that

- the antiferromagnetic state in La123 and Nd123 is extended up to the oxygen content $x \cong 0.6$, after which the systems become superconductive,
- in La123 slightly different magnetic sites can be found in the antiferromagnetic CuO_2 plane,
- the hyperfine magnetic field and EFG at the magnetic copper sites in R123 depend linearly on the ionic radius of R^{3+},
- a few percent of impurities like Fe, Al, Ga, V substituting Cu(1) cause ferromagnetic coupling between adjacent CuO_2 bilayers.

5.1. Magnetic Cu(2) Sites in Antiferromagnetic CuO_2 plane

In the antiferromagnetic state a local magnetic moment creates hyperfine magnetic field B_{hf} on Cu(2) nuclei. In the presence of this local field one can record a NMR spectrum without applying external magnetic field, the so called zero field NMR (ZFNMR). It has been shown that copper ZFNMR is a versatile tool for studying the local order in antiferromagnetic cuprates [65–69]. Using this technique Mendels *et al.* [68] have shown that in Y123 the breakdown of the antiferromagnetic order occurs at oxygen concentration x about 0.3, furthermore, it was shown that no considerable intensity loss and frequency shift of the ZFNMR occurs in the region $0 \leq x \leq 0.2$ which means that within this doping level region all copper ions in the CuO_2 plane carry equal magnetic moments.

We have carried out similar experiments on a series of Nd123 and La123 samples [see VI] and found that here the ZFNMR spectra can be detected up to the oxygen content $x=0.6$ which means that antiferromagnetic order persists in the doping region $0 \leq x \leq 0.6$. Abrupt intensity loss in the ZFNMR spectra occurs at $0.5 < x \leq 0.6$. where also the Néel temperature starts to decrease. As far as the samples of Nd123 and La123 with oxygen content $x=0.7$ show superconductivity we can conclude that antiferromagnetic CuO_2 planes become superconducting at oxygen content $0.6 < x < 0.7$ without overlap or gap in the phase diagram. Similar proximity of the AF and superconducting phases is characteristic to all members of oxygen doped R123.

In Fig. 5.1. ZFNMR spectra of Cu(2) of a set of La123 samples with different oxygen content are shown. As described in section 2.1 the NMR spectrum of one copper isotope with spin I=3/2 consists of three lines corresponding to the central transition (m=+1/2↔–1/2) and the two satellite transitions (m=±3/2↔±1/2). Thus, the spectrum of copper in a given site consists of 6 lines, three of which belong to ^{63}Cu and the other three to ^{65}Cu isotope. The spectrum of 6 lines can be readily seen in La123 at x=0.11. From the position of the lines in the spectrum one can get by exact diagonalization of the Hamiltonian (2.5) the hyperfine local field B_{hf}, the EFG tensor parameters ν_Q and η, and the polar and azimuth angles ϑ and φ. For La123 (x=0.11) we obtained B_{hf} =6.76 T, ν_Q=30.04 MHz, η=0, ϑ=90 degrees. Since the main axis of the EFG tensor at Cu(2) is along crystallographic c-axis, the magnetic moment lies in the CuO_2 plane, similarly to the case in antiferromagnetic Y123 compound [65, 66, 68].

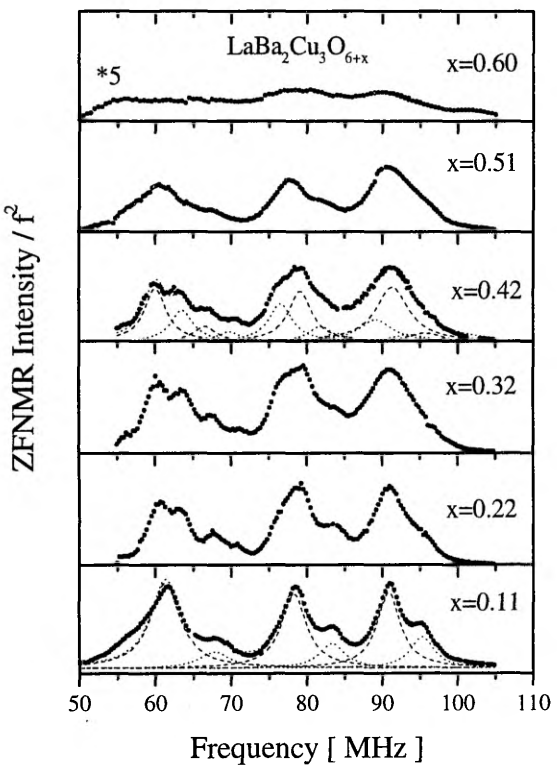

Fig. 5.1. ZFNMR spectra at 4.2K of Cu(2) sites in La123 at different oxygen content x. The intensity of the x=0.60 sample is multiplied by 5. For two spectra individual components of the spectrum are illustrated by dotted lines: one lattice site contributes six lines to the spectrum — three lines (central transition and two satellites) for ^{63}Cu and three lines for ^{65}Cu isotope.

The intensity of the ZFNMR resonance in samples with oxygen content $x \leq 0.51$ is found to be unchanged within 10% accuracy of our experiment. In the x=0.60 sample the overall intensity is about 0.1 from that of the other samples (the Néel temperature for this sample was 290K as measured by μSR technique [VI]). This means that the number of magnetic copper sites in the CuO_2 planes is not changed at oxygen content $x \leq 0.51$. Similar behaviour was observed in Nd123. Thus one can see in Nd123 and La123 the same behaviour as established for antiferromagnetic Y123 [68] where the number of magnetic copper sites was found to be constant up to the oxygen concentrations where the Néel temperature was less than 90% from initial value.

A closer look at the ZFNMR spectra of La123 with oxygen content $0.22 \leq x \leq 0.42$ indicates existence of different Cu(2) sites (or a superstructure) in the antiferromagnetic plane. Such behaviour was not observed in antiferromagnetic Y123 [68] where with oxygen doping only broadening of the lines in ZFNMR spectra occurs. Unfortunately, the individual lines are not resolved enough at the high frequency part of the spectra which does not allow unambiguous determination of the parameters of the different sites. A reasonable fit of the spectra can be achieved assuming two magnetic Cu(2) sites with slightly different symmetric (η=0) quadrupolar coupling tensors and B_{hf} directed at ϑ=90 degrees with respect the main axis of EFG tensor ($\vec{B}_{hf} \perp c$). The results of such simulation are given in Fig. 5.2. One can see that the mean value of B_{hf} is almost constant in the region ($0.11 < x < 0.5$). The parameters of the two different sites detected in the range $0.22 \leq x \leq 0.42$ show a correlation such that the site having larger B_{hf} has smaller ν_Q and *vice versa*, the site having smaller B_{hf} has a larger quadrupolar coupling constant. Similar correlation has been deduced from the analysis of the line widths in the ZFNMR spectra of Y123 [68].

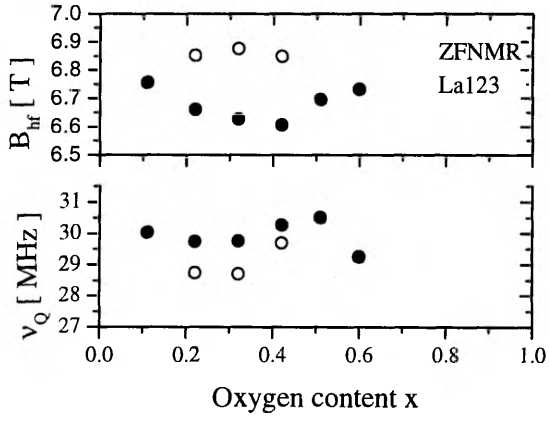

Fig. 5.2. Quadrupolar coupling constant ν_Q and the hyperfine field B_{hf} at Cu(2) in antiferromagnetic La123 at 4.2K at different oxygen contents x; the open and solid symbols denote respectively the parameters of two different copper sites.

Since the splitting of the ZFNMR lines occurs at low oxygen concentrations where the hole number doped to the AF planes is shown to be close to zero even in Y123 [68], and since the same type of correlation between B_{hf} and ν_Q is obtained also by plotting the parameters of different antiferromagnetic R123 compounds as a function of the ionic radius of R^{3+} (Fig. 5.3), we believe that the two slightly different Cu(2) sites in antiferromagnetic La123 result from structural changes and not from the doped holes in the AF plane. Most probably, the microscopic origin of the observed splitting of the ZFNMR lines is that the doped oxygen ions cause a change of the adjacent apex oxygen position resulting in changes in the quadrupolar coupling at the Cu(2) (see section 5.3). Here we must admit that information obtained from the ZFNMR spectra is not sufficient to evaluate specific (super)structure of oxygen doped La123 in the antiferromagnetic planes. Therefore we cannot answer which of the number of proposed single-oxygen local arrangements [29] in the basal plane is present in AF La123.

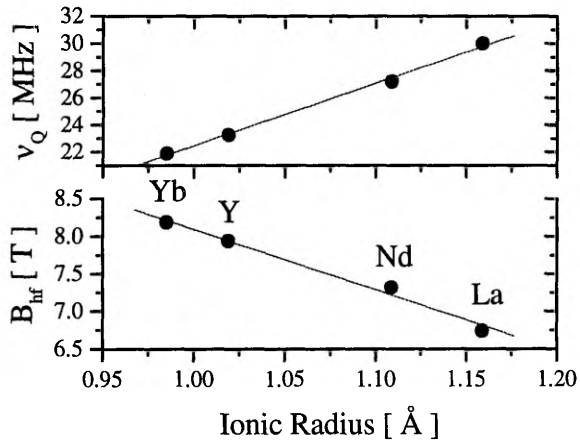

Fig. 5.3. Quadrupolar coupling constant ν_Q and the hyperfine field B_{hf} at Cu(2) in different antiferromagnetic R123 ($x\approx 0$) as a function of the ionic radius of R^{3+}. The straight lines are for guiding the eye.

Comparison of the experimental B_{hf} data in different R123 shows that the average static magnetic moment at Cu(2) in antiferromagnetic La123 and Nd123 is considerably smaller than that in Y123. $\langle S \rangle = 0.56\mu_B$, $0.61\mu_B$ and $0.66\mu_B$ for La-, Nd- and Y123, respectively, if hyperfine coupling constant for Cu $12T/\mu_B$ is assumed.

We have found that the ZFNMR intensity of the antiferromagnetic La123 sample with the highest oxygen content x=0.6 (T_N=290K) is only 0.1 of the intensity for the samples with lower oxygen content. This sudden change of the intensity has to be attributed to holes injected into the CuO_2 layers. Following

discussion by Mendels *et al.* [68], one can calculate the hole number in the plane assuming that in the framework of the *t-J* model one local hole should affect five Cu(2) sites. Taking into account also the next-nearest sites, one would expect that the hole will wipe out from the spectrum at least 13 Cu(2) sites. Then the hole number can be calculated from $\left(1-n_h\right)^{13}=0.1$ giving n_h=0.16. This result is well above the 3% maximum doping for which the Néel state disappears in the other HTSC compounds with known hole concentration. Therefore one must admit that the number z of Cu sites in the AF plane affected by single hole must be much larger than 13. Taking realistic value of n_h=0.02 one obtains that z~100 from $\left(1-n_h\right)^{z}=0.1$. Such large number of Cu sites in the AF plane affected by single hole may be taken as evidence that the injected holes are itinerant.

5.2. Influence of Trivalent Ions at Cu(1) Site to the Magnetic Structure of R123

The antiferromagnetic structure (AFI) of Y123 was solved by Tranquada *et al.* [70] using magnetic neutron diffraction. In this structure the magnetic moments at Cu(2) sites are oriented perpendicular to the tetragonal *c* axis and alternate antiferromagnetically within the CuO_2 planes and along the *c* axis (see Fig. 5.4). Kadowaki *et al.* [71] and later Shamoto *et al.* [72] reported for undoped Y123 single crystals a reordering to a second antiferromagnetic phase AFII at low temperature with a transition temperature T_{N2} of about 40K and 15K, respectively. The AFII phase has a similar antiferromagnetic arrangement of the spins in the CuO_2 layer as that in the AFI structure, but due to ferromagnetic coupling between bilayers through the Cu(1) layer a different stacking of the spins along the *c* axis occurs, which results in a doubling of the unit cell along *c*.

The structure at AFI↔AFII reordering was shown to be an interesting homogeneous magnetic structure [69, 70] where the spin axis of one bilayer is rotated by an angle α from original direction in AFI and that of the neighbouring bilayers is rotated by the same angle in opposite direction. As a result of such turn of the spins in neighbouring bilayers a magnetic field at Cu(1) is induced magnitude of which is depending on the turn angle. Thus, the structure AFI+AFII can be described by turning angle α.

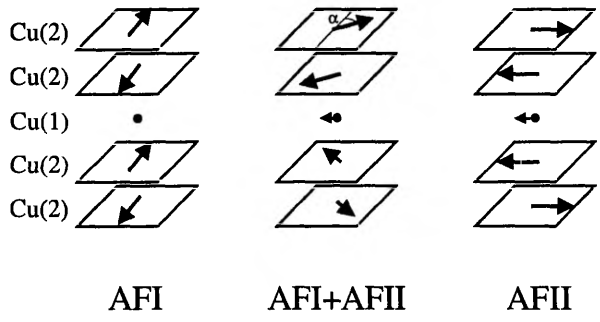

Fig. 5.4. Different stacking of antiferromagnetic planes detected in R123 where AFI denote the ordinary structure with antiferromagnetic coupling between bilayers, AFII is the low temperature structure with ferromagnetic coupling between bilayers, AFI+AFII is the intermediate structure were the magnetic moments in adjacent bilayers are turned in the Cu(2) layer by certain angle $\pm\alpha$; the latter two structures result an induced magnetic field at Cu(1).

The origin of the ferromagnetic coupling between the bilayers is not yet clear. Originally it was proposed [71] that magnetic Cu^{2+} in $Cu(1)_3$ sites created by oxygen doping causes the ferromagnetic coupling. This explanation does not work because the AFII structure was not detected in pure polycrystalline Y123 at any oxygen content x. Lütgemeier [67], and Lütgemeier and Rupp [73] showed that Fe impurities in antiferromagnetic $YBa_2Cu_{3-y}Fe_yO_{6+x}$ cause a Zeeman splitting of $Cu(1)_2$ NQR line due to the induced magnetic field at $Cu(1)_2$ in AFII structure. It was shown that the transition temperature T_{N2} increases with Fe concentration y and increasing the oxygen content x leads to depression of the AFII phase. Also, it was found that the size of the Zeeman splitting depends roughly linearly on temperature. From this it was concluded that magnetic Fe^{3+} impurities mediate an effective ferromagnetic coupling between the bilayers. In favor of this explanation one can add that the AFII phase has been observed in $Nd_{1+y}Ba_{2-y}Cu_3O_{6+x}$ [74, 75], containing magnetic rare earth Nd^{3+} in Ba sites. We found by NQR [VIII, II] that not only magnetic impurities but also the other, nonmagnetic impurities like Al^{3+}, Ga^{3+} and V^{3+} substituting Cu(1) cause low temperature ordering into the AFII structure.

In Fig. 5.5 we have shown two samples of $Cu(1)_2$ Zeeman-split NQR spectra in $YBa_2(Cu_{1-y}M_y)_3O_{6.0}$, with y=0.025, M=Ga or V. The spectra demonstrate different influence of the dopants to the AF structure: The Ga-doped sample shows typical spectrum in the case of ferromagnetically aligned bilayers with T_{N2}>4.2K, while the same amount of V impurities does not induce reordering of the structure into an AFII structure at 4.2K (bottom spectrum). A turning angle in the AFI+AFII phase with a small hyperfine field B_{hf}=25mT at Cu(1) can be observed at 1.2K. The hyperfine field 25mT would correspond to a

turning angle α=7 degrees, if for fully ordered AFII structure Bhf=190mT at Cu(1) is assumed. The small splitting in V-doped sample at 1.2K demonstrates that turning of the bilayers is homogeneous, which means that the effect of impurities is a long range effect and not local. A possible reason why V impurities have less influence on the magnetic structure than Ga or Al could be that V in a valence state V^{2+} can substitute copper in Cu(2) sites.

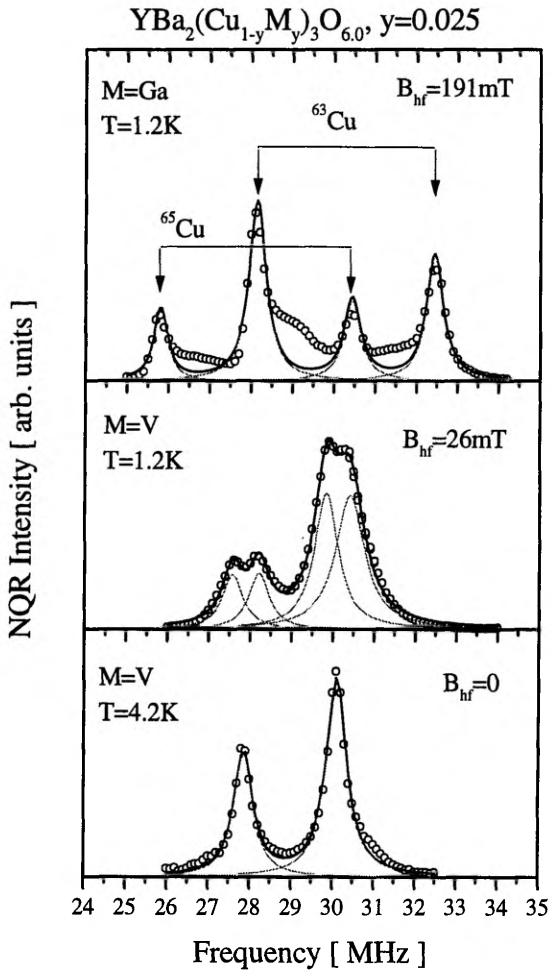

Fig. 5.5. $Cu(1)_2$ NQR line in $YBa_2(Cu_{1-y}M_y)_3O_{6.0}$ with y=0.025, M=Ga or V. In Ga-doped sample the Zeeman splitting corresponds to transferred hyperfine field at $Cu(1)_2$ B_{hf}=191mT; in V-doped sample a small hyperfine field B_{hf}=26mT is observed at 1.2K, whereas at 4.2K no splitting is observed.

While Y123 single crystals grown in Al_2O_3 crucibles are always contaminated by some amount of Al, our finding explains why neutron diffraction carried out

on single crystals may show at low temperatures the reordering into AFII phase. Later this statement was verified by neutron diffraction technique [76] showing that no low temperature AFII was found in oxygen-lean Y123 single crystal grown in an yttrium stabilized zirconia crucible.

The fact that nonmagnetic impurities at Cu(1) cause low temperature reordering of the magnetic structure tells us that the magnetic mechanism of ferromagnetic coupling between two bilayers may have to be revised. Furthermore, we have observed the AFII structure also in La1236 samples where nonmagnetic La^{3+} substitutes for Ba.

Recently Brecht et al [77] proposed for the origin of the AFI-AFII transition a mechanism where Al impurities give rise to Al^{3+}-O^{2-}-Cu^{2+} fragments with free Cu^{2+} spins within Cu(1) layer. Polarization of these free spins in the Cu(1) layer mediates an effective ferromagnetic coupling between bilayers.

Further studies of this interesting reordering phenomenon are needed. Samples of well defined oxygen content would help to clarify whether this explanation is the final one or not.

5.3. Cu(2) Sites in Metallic State

Despite of the fact that the Cu(2) sites in the CuO_2 plane of R123 have always five next nearest oxygen neighbours in pyramidal configuration, the EFG at Cu(2) in superconducting samples is strongly different from that in the antiferromagnetic samples. In Y123 the EFG value ν_Q at Cu(2) changes from 23.2 MHz in undoped Y1236 to 31.5 MHz in Y1237. In Ortho-II region two different Cu(2) NQR lines at 27.7 and 30.8 MHz [78, 79, I] have been observed. These lines were attributed to the Cu(2) sites neighbouring the sites $Cu(1)_2$ and $Cu(1)_4$, respectively. Different EFG value at these Cu(2) sites arises mainly from different distance between Cu(2) and the apex oxygen O(4) in the Ortho-II structure. It is interesting to note that the two different Cu(2) sites in Ortho-II have the same Knight shift and almost identical spin lattice relaxation T_1, [78] which indicates uniform spin-density and dynamics in the conducting CuO_2 layer.

In Fig. 5.6 we give the EFG values at Cu(2) in different fully oxygen doped R1237 in comparison with that in the undoped R1236. One can see that different R123 show different change of ν_Q at doping from R1236 to R1237.

The increase of the EFG value with doping is observed also in $La_{2-x}Sr_xCuO_4$, where ν_Q increases linearly with Sr doping from 33 MHz at x=0 to 36.2 MHz for x=0.15 [80] and is ascribed to the change of the hole density in the CuO_2 plane. From the frequency shift a phenomenological relation between

the hole density in CuO_2 plane and the NQR frequency as dv_Q/dn=21 MHz/hole has been derived. Similar relation with dv_Q/dn=23.4 MHz/hole was used for estimation of the hole concentration in different blocks of $Y_2Ba_4Cu_7O_{15}$ system [81].

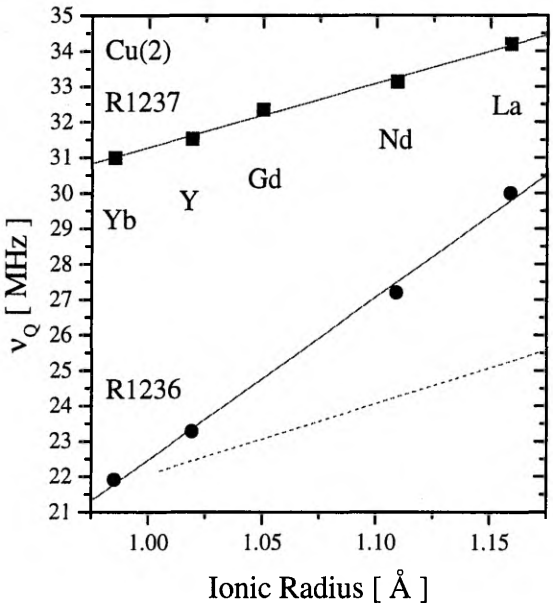

Fig. 5.6. The EFG at 4.2K of Cu(2) sites in superconducting R1237 and antiferromagnetic R1236 as a function of R^{3+} ionic radius. Solid lines: linear fit to the experimental data; dashed line — change of the ν_Q of R1236 due to lattice expansion.

Qualitatively the increasing of ν_Q at Cu(2) with increasing hole concentration can be well understood within the point charge model (see section 2.2) as decreasing of the lattice contribution ν_Q^{LAT} to the EFG due to a more positive charge (hole) on oxygen ions. Since the valence contribution ν_Q^{VAL} of Cu(2) has opposite sign, the decreasing of ν_Q^{LAT} results in higher ν_Q at Cu(2) if ν_Q^{VAL} at given site is unchanged. Similar arguments explain the increase of ν_Q at Cu(2) with increasing R^{3+} size in R1237 and R1236 where the lattice contribution decreases due to expansion of the lattice. The calculation within the point charge model shows that the change of ν_Q in R1236 is too large to be accounted for solely by lattice expansion. Unfortunately, the same symmetry of the EFG tensor due to the lattice ions at Cu(2) and that due to the *d*-hole does not allow determination of the two contribution ν_Q^{LAT} and ν_Q^{VAL} from the single experimental value of ν_Q. For an estimate of the change of the ν_Q in R1236 due to the lattice expansion we have used an average literature value of the Sternheimer factor $1-\gamma_\infty = 15$ for Cu^{2+} in pyramidal configuration [54, 61]. The result of

such estimate (given by dashed line in Fig. 5.6) shows that about half of the change of the ν_Q in R1236 can be ascribed to the lattice expansion. The other half of the change must be ascribed to the increase of ν_Q^{VAL} with increasing ionic radius of R^{3+}. The latter change can be explained by different occupation of the $3d(3z^2-r^2)$ orbital. In pyramidal surrounding of copper a nonzero hole density in that orbital has been suggested [56]. According to theory (see Eq. 2.9) a certain hole density transferred from the $3d(x^2-y^2)$ orbital into $3d(3z^2-r^2)$ orbital decreases the value of the valence EFG. Since the lattice parameter c and the distance between the Cu(2) and apical oxygen O(4) increases with increasing ionic radius of R^{3+}, it is likely that the hole density in $3d(3z^2-r^2)$ orbital of Cu(2) in La1236 is smaller than that in Y1236, resulting in larger valence EFG of Cu(2) in La1236 compared to that in Y1236. Assuming the change of the EFG due to the lattice contribution as given in the Fig. 5.6, it is sufficient to transfer in La1236 about 0.03 holes from the $3d(3z^2-r^2)$ orbital into $3d(x^2-y^2)$ orbital compared to the charge distribution in Cu(2) orbitals in Y1236. The analysis shows the sensitivity of the EFG value with respect to charge distribution in copper *d*-shell.

Unlike the case of undoped R1236, the change of the quadrupolar frequencies in fully oxygenated R1237 can be described by the change of the EFG due to lattice expansion, which means that the charge distribution in Cu(2) orbitals of different R1237 is not much different. Besides, the data in Fig. 5.6 clearly show that the difference between the EFG value at Cu(2) site in fully oxygenated R1237 and that in undoped R1236 decreases with increasing size of R^{3+}. Assuming nearly equal hole concentration in the CuO_2 plane of different R1237 this means that there is no universal scaling between the hole count and Cu(2) quadrupolar frequency change in the R123 system.

At the end of this chapter we briefly discuss the Cu(2) relaxation. Unusual temperature behaviour of the nuclear spin lattice relaxation rate T_1^{-1} of Cu(2) in metallic CuO_2 plane is a much discussed topic in the problem of HTSC (see *e.g.* [23, 82, 83]).

In ordinary metals and usual BCS superconductors the relaxation rate shows the Korringa behaviour in the normal state $T_1^{-1} \propto K^2T$ where K is the Knight shift; just below T_c the enhancement of the relaxation rate, so called Hebel-Slichter peak, due to the increase of the density of states at the edge of superconducting gap, and finally in the superconducting state an activation type decay according to the size of the gap. In cuprate superconductors the situation is completely different and in underdoped cuprates the temperature behaviour is like that in Fig. 5.7 [IX]. At high temperatures the relaxation is only weakly temperature dependent, a characteristic of relaxation in paramagnetic compounds; below T<120K (well above T_c) with decreasing temperature the relaxation rate decreases smoothly as $T_1^{-1} \propto T^3$ down to the lowest temperatures without any significant change in the behaviour at T_c. The T^3 dependence is

associated with the d-wave model with gap zeros of lines [84]. It is interesting to note that similar relaxation behaviour is observed in heavy fermion compounds (e.g. $CeCu_2Si_2$), where the correlation gap opens at $T^*>T_c$ and in superconducting phase the nuclear spin-lattice relaxation rate T_1^{-1} follows the T^3 law [85].

After the discovery of the spin-gap effect in Y123 by neutron scattering [15] several NMR groups have regarded the spin-gap effect to be responsible for the peculiar temperature variation of the relaxation rate, at least in the normal conducting state [16].

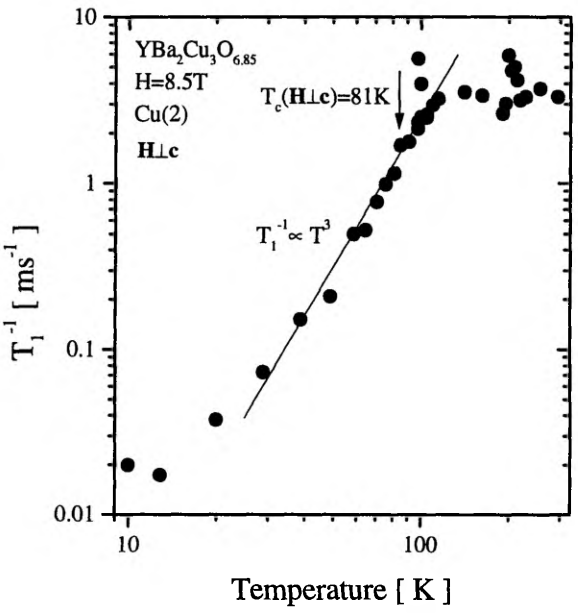

Fig. 5.7. The temperature dependence of T_1^{-1} of ^{63}Cu at the Cu(2) site in slightly underdoped Y123 (from Ref. [IX]) at orientation $H \perp c$.

Without going into details we mention that the relaxation behaviour of Cu(2) has been accounted successfully in many other scenarios. For example, Emery and Kivelson [86] calculated the relaxation in the model, where a system of holes in the antiferromagnetic plane tends to separate into hole-rich stripes and hole-poor antiferromagnetic regions, frustrated by long-range Coulomb interaction. Alexandrov [87] calculated the relaxation in a completely different model, where triplet bosons, bipolarons, are responsible for the relaxation. Mukhin and de Jongh [88] calculated the NMR behaviour in the model where real-space-pairs (bosons) move through the 2D AF lattice.

6. DISCUSSION

In this section we will discuss the possible reasons for the different oxygen ordering patterns in different R123. Using the experimentally established random oxygen distribution in Nd123 we find that chain to plane charge transfer destroying the continuous AF order in the CuO_2 plane and evoking superconductivity in R123, occurs at surprisingly long $[Cu\text{-}O]_n\text{-}Cu$ lengths ($n \geq 7$) only.

6.1. Oxygen Ordering in R123

The main results of this study are obtained from intensity distribution of the Cu(1) lines. Since it is the first time when such analysis of the spectrum is applied to R123 it is reasonable to ask how reliable are these data. The question is justified because Cu^{2+} in $Cu(1)_3$ and $Cu(1)_4$ sites can carry a steady magnetic moment which shifts the resonance line out of the NQR spectrum. The straight answer to that question could be obtained from the comparison of the total absolute intensities of Cu(1) lines. In a series of semiconducting La123 samples we found that within 10% accuracy, the total intensity in the Cu(1) NQR spectrum was constant without systematic loss of the intensity. Unfortunately, uncertainties in the absolute intensity due to relaxation effects and sensitivity of the measuring coil are hard to eliminate especially in comparison of the spectra of superconducting and insulating samples. In paper [I] we calculated the oxygen content from Cu(1) relative intensities. The differences between these so calculated and determined by weight uptake oxygen content did not exceed ± 0.1, which we believe is a strong argument that the intensity distribution of Cu(1) NQR lines adequately reflects the site distribution in Cu(1) layer. The average chain lengths determined by us in Y- and Gd123 were found to be in good agreement with the calculation performed within lattice gas (ASYNNNI) model by Tornau *et al.* [89] if the effective intrachain attractive interaction between the nearest neighbour oxygens was taken $|V_2|=1090$ K, which is (only) 30% lower than the first-principles theoretical value 1520 K [90].

The very argument in favour of the NQR method is the finding that different R123 produce different intensity distribution of the Cu(1) NQR lines. Therefore we can conclude that overwhelming majority of the copper sites in Cu(1) layer contribute to the NQR spectrum. The only possibility for that is the case when the magnetic Cu^{2+} ions in Cu(1) layer are either in frustrated or in singlet state.

We have unambiguously shown that in contrast to the oxygen ordering in Tm-, Y- or Gd123 where oxygen ions form preferably long chain fragments, in R123 with large R^{3+} ions the oxygen ions are distributed randomly (Nd) or tend to repel each other (La). In the language of 2-dimensional lattice gas model [39] it would mean that the effective intrachain interaction between oxygens (V_2) changes with ionic radius of R^{3+} from attractive through zero to repulsive. This behaviour is not yet theoretically explained. As given by de Fontaine *et al.* [91] an effective intrachain attractive interaction in the ASYNNNI model results from strong O-Cu interaction, brought about by Cu d-orbital and O p-orbital coupling which always favours O-Cu-O configurations. In order to get repulsive interaction one has to involve repulsive Coulombic interaction between the oxygens as proposed by Aligia et al [92] which cancels effectively the attractive interaction or turn it to repulsive. Unfortunately, this explanation gives an opposite tendency, because the repulsive Coulombic interaction should be the smallest in La123 where the distance between the nearest oxygens is the largest. In a recent theoretical work Gawiec *et al.* [93] pointed out that the intrachain interaction depends also on the energy level of the oxygen hole band of the CuO_2 layer which can be different in Y123 compared to that in Nd123 and La123. We have shown above (see section 5.3) by the analysis of the change of the EFG value in R1236 compounds, slightly smaller hole density in the $3d(3z^2-r^2)$ orbital of Cu(2) in La1236 compared to the situation in Y1236 may be taken as an indication of a smaller coupling between the CuO_x chains and CuO_2 planes in La123.

We found that the average chain length in the Ortho-II phase region of Y123 and Gd123 is about 10 oxygen ions. This value was found to be in accordance with the estimates to the cluster length in the Ortho-II phase estimated by inelastic neutron scattering in Er123 [50]. On the other hand, X-ray and neutron scattering line shape analysis [94] show that the highest correlation lengths found in a very slowly cooled single crystal with x=0.55 are 240, 17 and 9 Å in *b*, *a* and *c* direction, respectively. Even longer chain lengths in the Ortho-II region are derived from from anisotropic optical reflectivity [95]. The main reason for such difference seems to be the fact that in the NQR spectrum we count all the copper ions, those which are part of the long chains and also those which constitute the "chain" of a single oxygen ion, the latter "chains", probably, will not be counted in the intensity of diffraction peak and certainly not in the optical conductivity. Therefore we believe that the above techniques estimate the average of the long chains whereas the NQR provides the bulk average chain length.

6.2. T_c *vs* Oxygen Arrangement in the CuO_x Layer

Using information about the distribution of oxygen in the basal plane it is tempting to find out which microscopic oxygen arrangements in R123 structure are responsible for the superconductivity. From μ-SR experiments Uemura *et al.* [8] found that in underdoped HTSC compounds a linear dependence between T_c and the number of carriers (holes) in CuO_2 plane exists. Basing on the statistics obtained from the Monte Carlo simulations within the lattice gas model Poulsen *et al.* [43] found that the experimental T_c *vs* x dependence of Y123 perfectly scales with the number of oxygen atoms in minimum size Ortho-I and Ortho-II type square clusters. They found that the minimum size Ortho-I clusters include 8 oxygen sites in CuO_x layer of which at least 7 must be occupied, their minimum size Ortho-II clusters include 16 oxygen sites of which at least 15 must be occupied.

In the case of random oxygen distribution which we showed is a good approximation for Nd123 we can easily evaluate the number of oxygens, *i.e* a probability to find an oxygen in the noted Ortho-I clusters having 8 sites, occupied by at least 7 oxygens. Assuming that each of these oxygens donate about 0.3 holes per one Cu(2) in the plane [46, 93], one gets the number of holes per Cu(2) as a function of oxygen content as

$$n_h = 0.3\left(7x^7 - 6x^8\right), \tag{6.1}$$

where x is the oxygen content.

Figure 6.1 shows an excellent scaling between $T_c(x)$ of Nd123 and hole density $n_h(x)$ calculated in the above manner. It is interesting to point out that Nd123 system becomes superconducting when about 0.05 holes per Cu(2) are transferred to the plane. The same hole number in the CuO_2 plane is needed for superconducting $La_{2-x}Sr_xCuO_4$ as well.

Although the model proposed by Poulsen *et al.* gives a good description of $T_c(x)$, we do see some weak sides of the square cluster model. First, depending on the position of the vacancy, the cluster may include also single oxygen fragments, which certainly do not contribute to the charge carriers. Second, it is hard to explain why the chain fragments in Ortho-II clusters contributing to charge transfer must be two times longer than those in Ortho-II clusters. According to theoretical studies by Zaanen *et al.* [40], Uimin *et al.* [96], the $[Cu\text{-}O]_n$-Cu fragments being shorter than some critical length k do not take part in the charge transfer. Therefore it seems physically more meaningful to find out the minimum chain length which contributes to superconducting charge carriers.

Again, in case of random oxygen distribution in the CuO_x layer it is possible to show that the number of oxygens in the chains of the length n≥k is given by expression

$$p_{n\geq k} = kx^k - (k-1)x^{(k+1)}. \qquad (6.2)$$

Taking k=7 one get exactly (incidentally) the same hole count $n_h(x)$ given by Eq. (6.1) which we have seen scales well with $T_c(x)$.

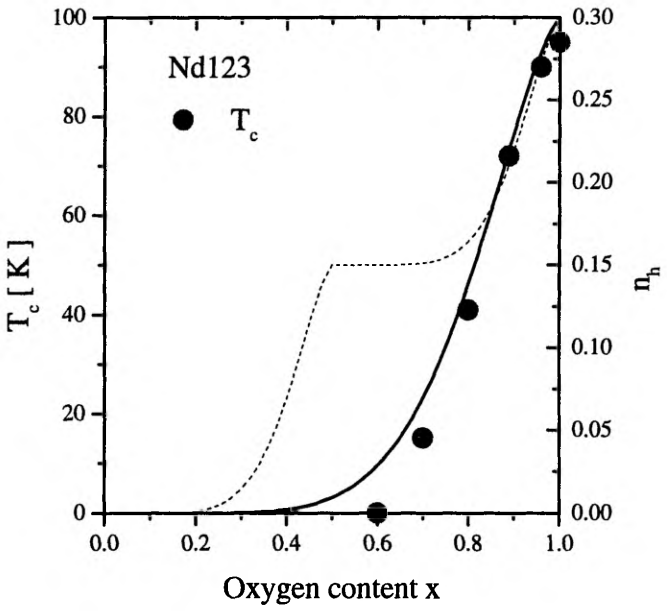

Fig. 6.1. Variation of superconducting transition temperature Tc(x) with oxygen content x in $NdBa_2Cu_3O_{6+x}$ (circles); full line presents calculated by Eq. (4.8) number of transferred holes per Cu(2), n_h in the structure with random distribution of oxygens; dashed line gives the hole count in the structure where every other chain grows randomly (see text).

In Y123 the distribution of chain length cannot be determined solely from the intensity distribution of Cu(1) NQR lines, giving only the mean value of the chain lengths. In order to demonstrate that the same chain length dependent charge transfer model might work also in the ortho-II type structures we have approximated the oxygen arrangement in Y123 to the case where at 0<x<0.5 every second chain will be filled randomly leaving the other chains empty and at 0.5<x<1 the half of the chains are already filled, whereas the other half will be randomly filled. (Such approximation was found to describe reasonably well

the intensities of Gd^{3+} EPR spectra in slightly Gd-doped Y123 [48].) Applying Eq. (4.8) for this case will give the hole count depicted in Fig. 6.1 by dashed line. As one can see, this simple model of the charge transfer by linear clusters of oxygens, where only those clusters containing at least 7 oxygens contribute to superconducting carriers, can also describe the plateau behaviour of $T_c(x)$ of Y123.

6.3. Charge Transfer in R123

We have established that the intensity of the ZFNMR spectra of Cu(2) in antiferromagnetic La123 is unchanged up to oxygen concentrations $x \leq 0.5$, in close vicinity to the superconducting phase. This means that no considerable number of holes is transferred to the CuO_2 planes. Similar conclusion was made by ZFNMR study of AF Y123 [68]. Calculation of the hole concentration within the above model fits well this behaviour (see Fig. 6.1), giving for the hole number n_h=0.025 at the border of AF/SC phases at x=0.6, all in a good agreement with the concentration which destroys the Néel state in other cuprates. Thus the model, where only linear chains or clusters containing at least 7 oxygen ions donate the holes gives a good qualitative description of the charge transfer in R123. The question is why at least seven? It is known that theoretical calculations [40, 93, 96] predict a much shorter maximum length of non-doping fragments — between 1 and 3 oxygens, depending on the position of the energy band of the one-dimensional CuO_x chains, relative to that of CuO_2 plane. Unfortunately, the band structure of doped R123 is not well established. Important is that according to this theoretical picture the holes can reside in the CuO_x chains if it is energetically more favourable. As shown by many authors (see *e.g.* Dagotto [23], Kampf [82]) it is energetically more favourable to create in the AF plane a pairs of holes instead of two separate holes, where the gain in energy is due to partial restoration of the AF order. A natural condition for the creation of such hole pair is that $[Cu\text{-}O]_n$-Cu chain is long enough to provide the two holes. Taking that the charge transferred by one oxygen ion in the chain is 0.3e [46, 93] we get that the hole pair is transferred to the CuO_2 plane if $n \geq 7$. In other words, the proposed charge transfer model for R123 presumes creation of local hole pairs.

As an interesting example, we remind that doping of the planes in the R123 structure can be achieved also by substituting three-valent R^{3+} by two-valent Ca^{2+} in the tetragonal compound $Y_{1-y}Ca_yBa_2Cu_3O_6$ (YCa236). In this case the concentration of holes per Cu(2) in the planes is controlled by the Ca content and is exactly n_h=y/2. The phase diagram of YCa236 shows [35] that the Néel state disappears at y=0.06, when hole concentration in the CuO_2 plane n_h

exceeds 0.03. In variance of the case of oxygen doping, the superconducting phase in YCa236 appears after an intermediate disordered magnetic phase at $y \geq 0.18$ (see also [36]). Due to this intermediate magnetic phase the phase diagram of YCa236 is more like that of the well known $La_{2-x}Sr_xCuO_4$.

In proposed scenario of charge transfer the different phase diagram of YCa236 is straightforward. One must note the different doping mechanism of YCa236, where injected holes in the CuO_2 plane are the result of sample preparation at high temperature where the distribution of Ca ions is random. Here the Néel state is destroyed by 3% single holes whereas the hole pairs contributing to the superfluid density appear at considerably higher dopant concentration (9%) when the mean distance between the holes is less than 3–4 lattice constants.

Thus, present analysis of the charge transfer in R123 favours theories where preformed hole pairs in the antiferromagnetic CuO_2 plane contributing to the superfluid density are considered.

Concluding this section we want to discuss the concept where the hole doped into the AF plane creates in its vicinity a spin-polarised cluster, often denoted as magnetic polaron or ferron [25, 97]. Such heavy pseudoparticles are known to form in many magnetic semiconductors [98]. It is suggested [37, 38] that at higher doping concentrations the spin-polarised clusters start to build up a microscopic percolation network resulting in a transition from insulating to metallic and superconducting phase. In alternative scenarios the polarons get paired forming spin-bipolarons (see *e.g.* Mott [97]) resulting superconductivity at Bose-Einstein condensation temperature of bipolarons.

Since the static hyperfine field B_{hf} and the EFG at the copper in such magnetic polaron is different from that of Cu(2) in unperturbed antiferromagnet, the existence of such polarons would be seen in ZFNMR spectra of AF R123. Calculations [25] give that the spin density at the central copper in spin polarized cluster is about 25% smaller than at the rest of the coppers. The quadrupolar coupling ν_Q due to a hole at neighbouring oxygen can be estimated to be about 4 MHz larger. We have shown above that ZFNMR spectra in La123 do not show the existence of such sites in samples with oxygen content $x \leq 0.5$. Similar conclusion was made by ZFNMR study of antiferromagnetic Y123 [68]. Thus, ZFNMR spectra of R123 do not support percolation scenarios for single magnetic polarons since in this case a considerable amount (critical concentration for site percolation is 0.59) of copper must be included in ferromagnetic clusters.

The scenario by Mott [97] of magnetic bipolarons match better with the present nuclear resonance findings. First, such pseudoparticles, hole pairs, in AF layer fit to the proposed charge transfer model, second, the magnetic bipolarons have a property to move through the AF plane by flipping the spins at the periphery of the bipolaron. The latter process could be the reason of

abrupt intensity loss of the ZFNMR spectra in the AF samples close to the border of superconductivity (see section 5.1). The same arguments support the scenario by Emery and Kivelson [19, 21] of fluctuating stripes formed of hole pairs carrying supercurrent. Existence of incommensurate peaks in neutron scattering in optimally doped $La_{2-x}Sr_xCuO_4$ has been taken as strong evidence for fluctuating stripes in this compound [99]. Recently Mook *et al.* [100] found similar incommensurate peaks in superconducting Y1236.6.

SUMMARY

This dissertation concentrates on several aspects of local order in the $RBa_2Cu_3O_{6+x}$ family of high temperature superconductors which have been studied by copper nuclear resonance techniques. We have carried out systematic measurements on several members of R123 family (R=Y, Tm Gd, Nd, La) at different oxygen concentrations. Since the resonance frequency of copper nuclei is a function of the local electric field gradient and local magnetic field, the nuclear resonance can be effectively used to study the local order in these materials.

We found that the NQR spectrum of the copper in Cu(1) sites of the charge donating layer of R123 exhibits several resonance lines which were attributed to the sites $Cu(1)_2$, $Cu(1)_3$ and $Cu(1)_4$, with 2, 3 and 4 nearest neighbour oxygens, respectively. The analysis of the EFG tensors yields that in $Cu(1)_2$ sites the copper is in $3d^{10}$ state while in $Cu(1)_3$ and $Cu(1)_4$ sites the copper is in $3d^9$ state with the vacant $d(3z^2-r^2)$ and $d(x^2-y^2)$ orbital, respectively. Intensity distribution of the Cu(1) resonance lines allows characterize the oxygen ordering in the CuO_x layer *e.g.* to determine the average length n of the (Cu-O)n-Cu chains.

We have shown that at given oxygen content in different R123 the oxygen ordering into chains is different. The oxygen ions in R123 with smaller ionic radius of R^{3+} (Tm, Y, Gd) have tendency to form longer chains than in the compounds with larger rare earth (Nd, La). This explains the different phase diagram of these compounds. Furthermore, in Nd123 the growth of the chains in the charge reservoir layer can be well described by random distribution of oxygen in that plane. This case allows to calculate the chain lengths responsible for effective chain to plane charge transfer. We have proposed a simple charge transfer model where only the chains longer than 7 oxygen ions contribute to the charge carriers in the conducting planes which adequately describes the peculiarities of the phase diagrams of different R123 compounds and gives a reasonable scaling between T_c and the number of carriers doped into the CuO_2 planes.

The nuclear resonance spectra of copper Cu(2) in the antiferromagnetic CuO_2 show that in R123 (R=Nd, La) the antiferromagnetic order is extended up to the oxygen concentrations x=0.6. No considerable changes of the hyperfine field or the EFG value at Cu(2) manifesting the presence of doped holes in the antiferromagnetic plane in samples with high Néel temperature was found. Few percent of impurities like Fe, Al, Ga, V substituting Cu(1) cause at low temperature a different stacking of antiferromagnetic CuO_2 planes with double unit cell along *c*-axis due to the ferromagnetic alignment of adjacent CuO_2 bilayers.

The main arguments proposed:

- the intensities of Cu(1) nuclear resonance lines of two-, three- and fourfold oxygen coordinated sites reflect the oxygen distribution in CuO_x layer of R123 and allow to determine the mean length of $(Cu\text{-}O)_n$-Cu chains at given oxygen content,
- different intensity distribution of the Cu(1) NQR lines in different R123 compounds yields different oxygen ordering: in Y-, Tm- and Gd123 the oxygen ions in the basal plane are clustered preferentially in long chain fragments, while in La123 the oxygens tend to be single and in Nd123 an almost random distribution of oxygens is found,
- the average chain length in the region of the "60K plateau" is about 10 oxygen ions,
- the antiferromagnetic state in La123 and Nd123 is extended up to the oxygen content $x \cong 0.6$, after which the systems become superconductive,
- two slightly different magnetic sites found in the antiferromagnetic CuO_2 plane of La123 reflect possibly single oxygen structures in the CuO_x layer,
- the hyperfine magnetic field and EFG at the magnetic Cu(2) sites in R123 depend linearly on the ionic radius of R^{3+},
- few percent of impurities like Fe, Al, Ga, V substituting Cu(1) cause at low temperature a different stacking of antiferromagnetic CuO_2 planes showing a ferromagnetic coupling between adjacent CuO_2 bilayers,
- antiferromagnetic order in the CuO_2 planes can be locally driven and modified by charge transfer from the $(Cu\text{-}O)_n$-Cu chains if the chain length $n \geq 7$ is long enough to provide whole hole pair(s) to the CuO_2 planes.

REFERENCES

[1] J. G. Bednorz and K. A.Müller, Z. Phys. **B64**, 189 (1986).

[2] M. K. Wu, J. R. Asburn. C. J. Torng, P. H. Hor, R. L. Meng, L. Gao, Z. J. Huang, Y. Q. Wang and C. W. Chu, Phys. Rev. Lett. **58**, 908 (1987).

[3] A. Schilling, M. Cantoni, J. D. Guo, and H. R. Ott, Nature **362**, 56 (1993).

[4] C. W. Chu, L. Gao, F. Chen, Z. J. Huang, R. L. Meng, and Y. Y. Xue, Nature **365**, 323 (1993).

[5] S.-C. Zhang, Science, **275**, 1089 (1997).

[6] N. Nagaosa, Science, **275**, 1078 (1997).

[7] E. Fradkin, Nature **387**, 18 (1997).

[8] Y. J. Uemura *et al.*, Phys. Rev. Lett. **62**, 2317 (1989).

[9] A. Ino, T. Mizokawa, K. Kobayashi, A. Fujimori, T. Sasagawa, T. Kimura, K. Kishio, K. Tamasaku, H. Eisaki, and S. Uchida, Phys. Rev Lett., **81**, 2124 (1998).

[10] W. W. Warren, Jr., and R. E. Walstedt, Z. Naturforsch., **45a**, 385 (1990).

[11] G. V. Williams, J. L. Tallon, E. M. Haines, R. Michalak, and R. Dupree, Phys. Rev. Lett., **78**, 721 (1997).

[12] J. Loram, K. A. Mirza, J. R. Cooper, W. Y. Liang, Phys. Rev. Lett. **71**, 1740 (1993).

[13] D. N. Basov et al, Phys. Rev. B **50**, 3511 (1994).

[14] B. Batlogg, H. Y. Hwang, H. Takagi, R. J. Cava, H. L. Kao, and J. Kwo, Physica C **235–240**, 130 (1994).

[15] J. Rossat-Mignot, L. P. Regnault, C. Vettier, P. Bourges, P. Burlet, J. Bossy, J. H. Henry, and G. Laperot, Physica B **180–181**, 383 (1992).

[16] A. J. Millis, H. Monien, and D. Pines, Phys. Rev. B **42** 167 (1990).

[17] A. G. Loeser *et al.*, Science **273**, 325 (1996).

[18] J. Schmalian, D. Pines, and B. Stojkovic, Phys. Rev. Lett. **80**, 3839 (1998).

[19] V. J. Emery, S. A. Kivelson, and O. Zachar, Phys. Rev. B. **56**, 6120 (1997).

[20] S. Doniach and M. Inui, Phys. Rev. B **41**, 6668 (1990).

[21] V. J. Emery and S. A. Kivelson, Nature, **374**, 434 (1995).

[22] N. Trivedi and M. Randeria, Phys. Rev. Lett. **75** 312 (1995).

[23] E. Dagotto, Reviews of Modern Phyics, **66**, 763 (1994).

[24] F. C. Zhang and T. M. Rice, Phys. Rev. B **37**, 9423 (1988).

[25] D. Klemm, M. Letz, E. Sigmund, and G. V. Zavt, Phys. Rev. B **50**, 7046 (1994).

[26] M. Buchgeister, Thesis Universitaet Bonn (1991).

[27] T. Krekels, H. Zou, G. van Tendeloo, D. Wagener, M. Buchgeister, S. M. Hosseini, and P. Herzog, Physica C **196**, 363 (1992).

[28] R. J. Cava, A. W. Hewat, E. A. Hewat, B. Batlogg, M. Marezio, K. M. Rabe, J. J. Krajewski, W. F. Peck Jr., And L. W. Rupp Jr., Physica C **165**, 419 (1990).

[29] A. A. Aligia, J. Garces, and H. Bonadeo, Physica C **190**, 234 (1990).

[30] Th. Zeiske, D. Hohlwein, R. Sonntag, F. Kubanek, and G. Collin, Z. Phys. B **86**, 11 (1992).

[31] F. Yakhou, V. Plakhty, G. Burlet, B. Kviatkovsky, J. Y. Henry, J. P. Lauriat, E. Elkaim, and E. Resoouche, Solid State Commun., **94**, 695 (1995).

[32] B. Büchner, U. Calliess, H. D. Jostarndt, W. Schlabitz, and D. Wohlleben, Sol. State Comm. **73**, 357 (1990).
[33] H. Alloul, T. Ohno, H. Casalta, J. F. Marucco, P. Mendels, J. Arabski, and G. Collin, and M. Mehbod, Physica C **171**, 419 (1990).
[34] A. H. Moudden, G. Shirane, J. M. Tanquada, R. J. Birgeneau, Y. Endoh, K. Yamada, Y. Hidaka, and T. Murakami, Phys. Rev. B **38**, 8720 (1988).
[35] X. Labouze, H. Alloul, G. Collin, and J. F. Marucco, Physica C **235–240**, 1599 (1994).
[36] J. Hejtmánek, Z. Jirák, K. Knízek, M. Dlouhá, and S. Vratislav, Phys. Rev. B **54**, 16226 (1996).
[37] V. Hizhnjakov, E. Sigmund, Physica C **156**, 655 (1988).
[38] V. Hizhnjakov, E. Sigmund, and G. Seibold, in: Phase Separation in Cuprate Superconductors, eds. E. Sigmund and K. A. Müller, Springer-Verlag, Berlin, 1994.
[39] D. de Fontaine, L. T. Wille, and S. C. Moss, Phys. Rev. B **36**, 5709 (1987).
[40] J. Zaanen, A. T. Paxton, O. Jepsen, and O. K. Andersen, Phys. Rev. Lett. **60**, 2685 (1988).
[41] V. E. Zubkus, S. Lapinskas, and E. E. Tornau, Physica C **166**, 472 (1990).
[42] J. V. Andersen, H. Bohr, and O. G. Mouritsen, Phys. Rev. B, **42**, 283 (1990).
[43] H. F. Poulsen, N. H. Andersen, J. V. Andersen, H. Bohr, and O. G. Mouritsen, Nature, **349**, 594 (1991).
[44] G. Ceder, M. Asta, and D. de Fontaine, Physica C **177**, 106 (1991).
[45] A. Aligia, J. Garces, and H. Bonadeo, Physica C **190**, 234 (1992).
[46] W. Selke and G. V. Uimin, Physica C **214**, 37 (1993).
[47] A. Jánossy, A. Rockenbauer, S. Pekker, G. Oszlányi, G. Faigel, and L. Korecz, Physica C **171**, 457 (1990).
[48] S. Pekker, A. Jánossy, and A. Rockenbauer, Physica C **181**, 11 (1991).
[49] A. Furrer, J. Mesot, P. Allenspach, U. Staub, F. Fauth, and M. Guillaume, in: Phase Separation in Cuprate Superconductors, eds. E. Sigmund and K. A. Müller, Springer-Verlag, Berlin, 1994.
[50] A. Furrer, P. Allenspach, F. Fauth, M. Guillaume, W. Henggeler, J. Mesot, and S. Rosenkranz, Physica C **235–240**, 261 (1994).
[51] A. Abragam, Principiles of Nuclear Magnetism, Clarendon Press, Oxford, 1961.
[52] C. P. Slichter, Principles of Magnetic Resonance, 3-rd ed. Springer-Verlag 1990.
[53] R. M. Sternheimer, Phys. Rev. **84**, 244 (1951).
[54] T. Shimizu, J. Phys. Soc. Jap. **62**, 772 (1993).
[55] M. E. Garcia, and K. H. Bennemann, Phys. Rev. B **40**, 8809 (1989).
[56] J. K. Burdett and G. V. Kulkarni, Phys. Rev. B **40**, 8908 (1989).
[57] V. V. Serikov, A. M. Bogdanovich, S. V. Verkhovskii, Yu. I. Zhdanov, B. A. Alekshashin, K. N. Mikhalev, V. L. Kozhevnikov, and S. M. Chesnitskii, JETP Lett., **47**, 534 (1988).
[58] H. Yasuoka, T. Shimizu, T. Imai, and S. Sasaki, Hyperfine Int. **49**, 167 (1989).
[59] A. J. Vega, W. E. Farneth, E. M. McCarron, and R. K. Bordia, Phys. Rev. B **39**, 2322 (1989).

[60] D. C. Johnston, A. J. Jacobson, J. M. Newsam, J. T. Lewandowski, D. P. Goshorn, D. Xie, and W. B. Yelon, in: Chemistry of High-Temperature Superconductors, eds D. L. Nelson, M. S. Whittingham, and T. F. George, ACS Symposium Series **351**, (Amer. Chem. Soc., Washington, DC, 1987) p. 136.
[61] H. Zimmermann, Dissertation, Universität Zürich, 1991.
[62] K. Müller, M. Mali, J. Roos, and D. Brinkmann, Physica C **162–164**, 173 (1989).
[63] I. Heinmaa, H. Lütgemeier, A. Janossy, S. Pekker, G. Krabbes, and M. Buchgeister, 10-th Specialized Colloque AMPERE on NMR/NQR in High-Tc Superconductors, Zürich. August 26–30, 1991, p. 112–113.
[64] J. Grybos, D. Hohlwein, and F. Kubanek, Physica C **244**, 349 (1995).
[65] H. Yasuoka, T. Shimizu, Y. Ueda, and K. Kosuge, J. Phys. Soc. Jpn., **57**, 2659 (1988).
[66] Y. Yamada, K. Ishida, Y. Kitaoka, K. Asayama, H. Takagi, H. Iwabuchi, and S. Uchida, J. Phys. Soc. Jpn., **57**, 2663 (1988).
[67] H. Lütgemeier, Physica C **153–155**, 95 (1988).
[68] P. Mendels, H. Alloul, J. F. Marucco, J. Arabski, and G. Collin, Physica C **171**, 429 (1990).
[69] M. Abe, K. Kumagai, S. Awaji, and T. Fujita, Physica C **160**, 8 (1989).
[70] J. M. Tranquada, D. E. Cox, W. J. Kunnmann, H. Moudden, M. Suenaga, P. Zolliker, D. Vaknin, D. C. Johnston, S. K. Sinha, M. S. Alvarez, A. J. Jacobson, and D. C. Johnston, Phys. Rev. Lett. **60**, 156 (1988).
[71] H. Kadowaki, M. Nishi, Y. Yamada, H. Takeya, H. Takei, S. M. Shapiro, and G. Shirane, Phys. Rev. B **37**, 7932 (1988).
[72] S. Shamoto, M. Sato, J. M. Tranquada, B. J. Sternlieb, and G. Shirane, Phys. Rev. B **48**, 13817 (1993).
[73] H. Lütgemeier and B. Rupp, J. Phys. (Paris) **49**, C8–2147 (1988).
[74] A. H. Moudden, G. Shirane, J. M. Tanquada, R. J. Birgeneau, Y. Endoh, K. Yamada, Y. Hidaka, and T. Murakami, Phys. Rev. B **38**, 8720 (1988).
[75] W. H. Li, J. W. Lynn, and Z. Fisk, Phys. Rev. B **41**, 4801 (1990).
[76] H. Casalta, P. Schleger, E. Brecht, W. Montfrooij, N. H. Andersen, B. Lebech, W. W. Schmahl, H. Fuess, R. Liang, W. N. Hardy, and Th. Wolf, Physica C **235–240,** 1623 (1994).
[77] E. Brecht, W. W. Schmahl, H. Fuess, S. Schmenn, H. Lütgemeier N. H. Andersen, B. Lebech, and Th. Wolf, Phys. Rev. B **56**, 940 (1997).
[78] W. W. Warren, Jr., R. E. Walstedt, G. F. Brennert, R. F. Bell, G. P. Espinosa, and R. J. Cava, Physica C **162–164**, 179 (1989).
[79] T. Shimizu, H. Yasuoka, T. Tsuda, K. Koga, and Y. Ueda, Bull. Magn. Reson., **12**, 39 (1990).
[80] T. Imai, C. P. Slichter, K. Yoshimura, and K. Kosuge, Phys. Rev. Lett. **70**, 1002 (1993).
[81] R. Stern, M. Mali, I. Mangelschots, J. Roos, and D. Brinkman, Phys. Rev. B **50**, 426 (1994).
[82] A. Kampf, Physics Reports, **249**, 219 (1994).
[83] D. Brinkmann and M. Mali, in NMR — Basic Principle and Progress, edited by P. Diehl, E. Fluck, H. Günter, R. Kosfeld, and J. Seelig (Springer, Berlin 1994), vol. 31, p. 171.

[84] Y. Kitaoka, K. Ishida, S. Oshugi, K. Fujiwara, and K. Asayama, Physica C **185–189**, 98 (1991).
[85] Y. Kitaoka, K. Ueda, T. Kohara, and K. Asayama, Solid State Commun., **51**, 461 (1984).
[86] V. J. Emery and S. A. Kivelson, in Phase Separation in Cuprate Superconductors, edited by K. A. Müller and G. Benedek (World Scientific, Singapore, 1993).
[87] A. S. Alexandrov, Physica C **191**, 115 (1992).
[88] S. I. Mukhin and L. J. de Jongh, Physica C **211**, 77 (1993).
[89] E. E. Tornau, S. Lapinskas, A. Rosengren, and V. M. Matic, Phys. Rev. B **49**, 15952 (1994).
[90] P. E. Sterne and L. T. Wille, Physica C **162–164**, 223 (1989).
[91] D. de Fontaine, M. Asta, G. Ceder, R. McCormack, and G. van Tendeloo, Europhysics Lett. **19**, 229 (1992).
[92] A. A. Aligia, A. G. Rojo, and B. R. Alascio, Phys. Rev. B **38**, 6604 (1988).
[93] P. Gawiec, D. R. Grempel, G. Uimin, and J. Zittarz, Phys. Rev. B **53**, 5880 (1996).
[94] V. Plakhty, B. Kviatkovsky, A. Stratilanov, Yu. Chernenkov, P. Burlet, J. Y. Henry, C. Marin, E. Ressouche, J. Schweizer, F. Yakou, E. Elkaim, and J. P. Lauriat, Physica C **235–240**, 867 (1990).
[95] A. Zibold, K. Widder, H. P. Geserich, G. Bräuchle, H. Claus, H. v. Löhneysen, N. Nücker, A. Erb, and G. Müller-Vogt, Physica C **212**, 365 (1993).
[96] G. Uimin and J. Rossat-Mignod, Physica C **199**, 251 (1992).
[97] N. F. Mott, Physica C **205**, 191 (1993).
[98] E. L. Nagaev, Physics of Magnetic Semiconductors (Mir, Moscow, 1983).
[99] J. Tranquada *et al.*, Phys. Rev. B **54**, 7489 (1996).
[100] H. A. Mook, Pengcheng Dai, S. M. Hayden, G. Aeppli, T. G. Perring, and F. Dogan, Nature, **395**, 580 (1998).

ACKNOWLEDGEMENTS

During the past years I have had the priviledge of meeting and working with many great people working in the field of high temperature superconductivity. It is my pleasure to record acknowledgements to these people.

I am most grateful to my supervisor Prof. E. Lippmaa for initiating the study of the fascinating problem of high temperature superconductivity at the Institute of Chemical Physics and Biophysics, for his continuous interest and support.

I have benefited greatly from my colleagues in Tallinn NMR group — Dr. E. Kundla and Dr. M. Alla for teaching me the NMR secrets, Dr. A. Vainrub, Dr. R. Stern and Dr. E. Joon for a long cowork in this field, Dr. R. Teeäär, Dr. P. Sarv, Dr. A. Samoson, Dr. J. Past, A. Miller, V. Miidel, S. Vija, Prof. T. Pehk, T. Tuherm and many others for help and friendship.

I am deeply indebted to Dr. H. Lütgemeier and Prof. W. Zinn from the Institut für Festkörperforschung, at Forschungszentrum Jülich, who made it possible for me to carry out the NQR experiments during my several visits to Jülich. Unfortunately both of these great scientists have lately passed away. They both granted me great scientific freedom and always encouraged me to try out new ideas. I will always remember Dr. H. Lütgemeier not only as a scientist and organiser of fruitful scientific cooperation between different laboratories and people but also as a good friend and advisor.

I am grateful to many people and colleagues who I met during my work in Dr Lütgemeier's laboratory.

I am particularly thankful to Dr. A. Janossy for many fruitful ideas and stimulating discussions initiating systematic nuclear resonance study of oxygen deficient Y123.

I would like to thank all my NMR colleagues in Jülich, Dr. R. Michalak, Dr. A. Campos, Dr. A. Yakubovski, Dr. A. Egorov, Dr. K. Wagner, Dr. A. Gippius, Dr. Yu. Baikov, Dr. H. de Gronckel and Dr. S. Schmenn for their scientific help and the excellent scientific and social atmosphere.

Financial support by DAAD (Deutsche Akademischer Austauschdienst) during my visits to Jülich is greatly acknowledged.

The work is supported by Estonian Science Foundation (Grants no. 315, 604, 2506).

LÄHIKORRAPÄRA $RBa_2Cu_3O_{6+x}$ ÜHENDITES: TUUMARESONANTSI UURINGUD

Kokkuvõte

Kõrgtemperatuurseid ülijuhte iseloomustavad ülijuhtivate paaride väike mõõt (3–4 võrekaugust) ja lühikesed antiferromagnetilised korrelatsioonid. Osutatakse elektroonse faasiseparatsiooni võimalusele. Seetõttu on uutes ülijuhtides toimuvate protsesside mõistmiseks pööratud üha enam tähelepanu ainete lähikorrapära iseärasustele.

Vase tuumamagnetresonantsi (TMR) ja tuumakvadrupolresonantsi (TKR) katsetes avalduvad tuuma lokaalset ümbrust iseloomustavad parameetrid. Nendeks on elektriväljagradient (EVG), mis iseloomustab tuuma naabruses olevate ioonsete laengute jaotust ja vase 3d-orbitaalide asustatust; lokaliseeritud elektronide magnetmomendi põhjustatud peenstruktuurimagnetvälja tugevus tuuma asukohas (B_{hf}), mis iseloomustab vasel paiknevate magnetmomentide suurust ja suunda antiferromagnetiliselt korrastunud faasis; tuumaspinni relaksatsioon iseloomustab lokaalse välja fluktuatsioone. Seega on TMR ja TKR adekvaatsed ja otsesed lähikorrapära uurimise meetodid.

Käesolevas dissertatsioonis on uuritud vase TMR ja TKR meetoditega mitmesuguseid lähikorrapära iseärasusi $RBa_2Cu_3O_{6+x}$ (R123) tüüpi kõrgtemperatuursetes ülijuhtides. Töö raames on teostatud süstemaatilised tuumaresonantsiuuringud R123 ühendites (R=Y, Tm, Gd, Nd, La) sõltuvalt hapniku kontsentratsioonist.

Töö tulemusena selgitati välja järgmist.

- Laengukandjaid dopeeriva tasandi vase Cu(1) spektrijoonte intensiivsused kajastavad kahe, kolme ja nelja lähima hapnikunaabriga vase võrepunktide jaotust, mis võimaldab mõõta keskmist $(Cu\text{-}O)_n$-Cu ahelate pikkust n sõltuvalt hapniku kontsentratsioonist.
- Ühesuguse hapniku kontsentratsiooni juures on erinevates R123 ühendites erisugune hapniku lähikorrapära, kusjuures väiksema R^{3+} ioonraadiusega ühendites korrastuvad hapnikud pikematesse ahelatesse. Tm123, Y123, Gd123-s (ioonraadiuse kasvamise järjekorras) korrastuvad hapnikud eelistatult pikkadesse ahelatesse, mis seletab Ortho-II struktuuri olemasolu nendes ainetes, Nd123-s on ahelate pikkus kirjeldatav hapniku juhusliku jaotumisega dopeerivas tasandis, La123-s on ahela pikkused lühemad kui juhusliku jaotusega antud.
- Keskmine ahela pikkus Ortho-II struktuuris, millele vastab kriitilise temperatuuri kõvera "60K platoo", on 10 hapniku iooni.

- Oluliselt lühemate vask-hapnik-ahelate tõttu Nd123-s ja La123-s toimub nendes ühendites üleminek kõrge Néeli temperatuuriga antiferromagnetilisest faasist ülijuhtivasse faasi hapniku kontsentratsiooni vahemikus $0,6<x<0,7$.
- Väikese hapnikusisaldusega La123 antiferromagnetiliselt korrastunud CuO_2 tasandis on veidi erinevad vase magnetilised olekud, mis tõenäoliselt kajastavad üksikhapnike superstruktuure CuO_x tasandis.
- Lokaalne peenstruktuuri väli (lokaalne magnetmoment) ja EVG vase ioonidel antiferromagnetilises CuO_2 tasandis sõltub lineaarselt R123 võre parameetritest.
- Väike protsent lisandeid Fe, Al, Ga, V, mis asendavad võres Cu(1), põhjustavad madalatel temperatuuridel antiferromagnetiliste naaber-kaksiktasandite ferromagnetilise asetuse.
- Antiferromagnetiline kauge korrapära CuO_2 tasandis kaob ja asendub ülijuhtivusega laengu ülekandel $(Cu\text{-}O)_n\text{-}Cu$ ahelatest, kui ahelate pikkus $n\geq 7$ on piisavalt pikk, võimaldamaks laengupaari(de) ülekande CuO_2 tasandisse. Oleme seega pakkunud lihtsa ahel-tasand-laenguülekande mudeli, mis kirjeldab adekvaatselt R123 faasi diagramme, andes hea kooskõla T_c ja CuO_2 tasandisse legeeritud aukude arvu vahel.

PUBLICATIONS

I

Heinmaa, H. Lütgemeier, S. Pekker, G. Krabbes, and M. Buchgeister,
Copper NMR and NQR in $YBa_2Cu_3O_x$ and $GdBa_2Cu_3O_x$
with x between 6 and 7. A Study of Oxygen Ordering,
Appl. Magn. Reson. **3**, pp. 689–709.

Appl. Magn. Reson. 3, 689–709 (1992)

Applied Magnetic Resonance

Copper NMR and NQR in $YBa_2Cu_3O_x$ and $GdBa_2Cu_3O_x$ with x between 6 and 7. A Study of the Oxygen Ordering.

I. Heinmaa[1,2], H. Lütgemeier[1], S. Pekker[3], G. Krabbes[4] and M. Buchgeister[5]

[1] KFA, Forschungszentrum Jülich, IFF, Germany
[2] Institute of Chemical Physics and Biophysics, Tallinn, Estonia.
[3] Central Research Institute for Physics, Budapest, Hungary
[4] Zentralinstitut für Festkörperphysik und Werkstofforschung, Dresden, Germany
[5] Institut für Strahlen- und Kernphysik, Universität Bonn, Bonn, Germany

Received March 27, 1992

Abstract. The NQR and NMR spectra of copper in polycrystalline samples of $YBa_2Cu_3O_x$ and $GdBa_2Cu_3O_x$ with different oxygen concentration x have been measured at 4.2 and 1.2 K. The different influence of Gd spins on the Cu(1) and Cu(2) sites was used to separate the contributions of both sites in the spectra. The quantitative analysis of the spectra in the region $6.3 < x < 6.75$ allows the following conclusions about the ordering of the oxygen ions in the chains of the Cu(1) planes and about the magnetic state of the Cu(2) ions to be drawn. At about $x = 6.5$ oxygen orders in the ortho-II structure with every second chain filled. For higher x the coexistence of ortho-II and oxygen depleted ortho-I (all chains filled to about 80 %) gives the best description of the results. The average length of the Cu—O chains, n, is about 10 oxygen atoms per chain in the region of the 60 K plateau and decreases rapidly at lower x. The superconductivity disappears when $n < 6$. No signal of the Cu(2) sites is found in samples with T_c below the 60 K plateau due to the slowing down of the fluctuation rate of the electron spins of the Cu(2) ions. Magnetic order appears only in samples which do not become superconducting.

1. Introduction

The superconducting transition temperature, T_c, of the high-T_c superconductor $YBa_2Cu_3O_x$, $6.0 < x < 7.0$, ($YBCO_x$) is known to depend not only on the oxygen content, x, but also on the particular ordering of the oxygen atoms in the basal Cu(1)—O planes. Cava *et al.* [1,2] have shown the characteristic dependence of T_c on x with the onset of $T_c > 0$ for $x > 6.4$, the plateau of $T_c \approx 58$ K between $x > 6.45$ and $x > 6.65$, and the second plateau of $T_c \approx 93$ K for $6.85 < x < 7.0$. A similar dependence of T_c as a function of

x was found also in the isostructural compounds $REBa_2Cu_3O_x$ (RE = Gd, Yb, Er, Dy, Eu, Sm) [3]. The plateaus are generally ascribed to two orthorhombic structures, namely ortho-I and ortho-II for the 90 K and 60 K plateaus, respectively [2]. Ortho-I is the ordinary structure of the stoichiometric $x = 7$ compound with oxygen atoms O(1) situated between Cu(1) sites forming the Cu—O chains along the crystallographic b-axis; ortho-II is a structure with alternately filled and empty chains corresponding to a lattice parameter $2a$ and the ideal stoichiometry $x = 6.5$. The influence of the particular arrangement of the oxygen atoms in the Cu(1) plane was observed in many annealing experiments [1,2] and becomes most evident from quenching experiments on single crystals with $x < 6.6$ [4]. By quenching from 230° C, T_c may be reduced compared with well annealed samples by values up to 25 K and even annealing at room temperature leads to an increase of T_c. The local oxygen arrangement in the concentration region apart from the two well established structures is not yet experimentally clarified.

Different ordering schemes for the oxygen in the Cu(1) layer have been proposed [5—10]. The most simple one is the case where the oxygen ions and vacancies are randomly distributed in all Cu(1)—O(1)—Cu(1) chains. This randomly diluted ortho-I structure exists most probably for high and low x. In the models proposed by Alario-Franco *et al.* [6] and Zaanen *et al.* [7] which are explored also by Latge *et al.* [8], the alternation of one filled and one "diluted" chain for $x > 6.5$ and of a "diluted" and an empty chain for $x < 6.5$ is assumed. In the "diluted" chains the arrangement of the oxygen vacancies may be random [5] or ordered, e.g. with a maximum distance between the oxygen ions [7] or with special superstructures [6]. Ceder *et al.* [9] have calculated the local oxygen configuration for $6.5 < x < 7.0$ and predicted the possible existence of an ortho-III structure with a sequence of one empty and two filled chains. Poulsen *et al.* [10] calculated the T_c plateaus assuming only ortho-I and ortho-II type clusters in the structure. Unless the local order of oxygen is a long range order, the usual diffraction methods fail to confirm one of these models.

Since the electric field gradient (EFG) at the copper nuclei depends on the valence state of the ion itself and on the charge of the surrounding atoms, the copper NMR/NQR can be a straightforward method to study the ordering of oxygen in these materials. Unfortunately, the NQR spectra in oxygen deficient $YBCO_x$ change with x in a very complicated way [11—13]. Overlapping of the lines from the two copper isotopes (^{63}Cu, ^{65}Cu), from the Cu(1) and Cu(2) layers, and from the different configurations within the layers makes the analysis extremely difficult.

Recently Janossy *et al.* [14, 15] have studied the oxygen ordering by EPR of Gd^{3+} in slightly Gd-doped samples of $YBCO_x$. A series of fine structure lines in the EPR spectra was observed, which were assigned to various configurations of vacant and occupied first neighbour Cu(1)—O chains surrounding the Gd^{3+} ions.

In this paper we present the NQR and NMR spectra of copper in oxygen deficient $YBCO_x$ and $GdBCO_x$ with the aim to study the oxygen ordering in the lattice. We will use the advantage of $GdBCO_x$ system where separating of the Cu(1) and Cu(2) NQR lines is possible [16,17] and we will use the Gd^{3+} EPR spectra as an aid in the assignment of the lines to the particular copper sites in the lattice.

2. Experimental

The NQR and NMR experiments with oxygen deficient samples of YBCO and GdBCO have been performed over a long period with samples of different preparation and origin. For the quantitative analysis discussed below we used three series of samples presented in Table 1.

Table 1. Summary of samples investigated: oxygen concentration, x, T_c from susceptibility, relative intensities of the different components of the NQR signal of Cu(1), *I2*...*I4*, mean length of Cu–O chains, n (Eq.(3)), and oxygen concentration in the Cu(1) plane, z (Eq.(1)).

sample #	x	T_c K	*I4** %	*I4*** %	*I3* %	*I2* %	n	z
A1	6.0	—	—	—		100		0
A2	6.34	—	15	11	17	57	4.1	0.35
A3	6.43	—	27	9	14	50	6.2	0.43
A4	6.53	35	24	21	10	45	10.0	0.50
A5	6.59	56	8	37	8	47	12.3	0.49
A6	6.77	61	26	30	12	32	10.3	0.62
A7	7.0	90		100				1
B1	6.30	20	14	17	8	61	8.7	0.35
B2	6.54	56	7	26	8	59	9.2	0.37
B3	6.58	56	11	34	12	43	8.5	0.51
B4	6.74	70	8	48	10	34	12.2	0.61
C1	6.0	—				100		0
C2	6.35	—	7	12	36	45	2.1	0.37
C3	6.39		9	8	45	38	1.8	0.40
C4	6.50	20	9	35	19	37	5.6	0.53
C5	6.55	50	8	32	11	49	8.3	0.46
C6	6.65	52	10	36	12	42	8.7	0.52
C7	6.75	58	13	52	11	24	12.8	0.70
C8	7.0	92		100				1

A1...A7 $YBCO_x$ 0.1 % Gd slowly cooled from 650 °C [14]
B1,B2,B4 $YBCO_x$ annealed about 10 days 380 °C [18]
B3 $YBCO_x$ as-quenched [18]
C1...C8 $GdBCO_x$ slowly cooled from 800 °C [3]

The slightly Gd-doped samples of $Y_{0.999}Gd_{0.001}Ba_2Cu_3O_x$ (A1...A7) have been prepared by the equilibrium method as described earlier [14] and were already used for the EPR experiments. The appropriate amounts of fully oxidized ($x = 7.0$) and fully reduced ($x = 6.0$) materials were sealed in silica tubes at a pressure of 10^{-4} mbar. The tubes were heated to 650 °C and cooled to room temperature during 120 hours. The oxygen content has been checked by the change in weight. In order to get a useful information from the EPR and NMR spectra, these samples were uniaxially oriented in the magnetic field and fixed in epoxy as described in [14]. For comparison purposes and in order to investigate the influence of annealing, several $YBCO_x$ samples without Gd doping prepared by the quenching technique with subsequent annealing [18] were measured too (B1...B4). No difference in the spectra due to the small amount of Gd was detected.

The extraction of oxygen in the series of $GdBCO_x$ samples (C1...C8) has been done at higher temperature [3]. Here the reduction was performed in a vacuum oven equipped with temperature and pressure controllers. The weighted pellets of the compound with x about 7.0 were put into vacuum at room temperature and heated to 810 °C without pumping. The samples were held at that temperature for three hours and the desired amount of oxygen gas was removed. After the reduction process the samples were cooled down at 37 °C/h to room temperature. The oxygen content was calculated from the weight loss. The starting composition was determined by complete reduction to $x = 6.0$.

The accuracy of the oxygen concentration x given in Table 1 is difficult to estimate. Within each series of samples the increments of x are very reliable as was seen from the continuous development of all properties, especially from the x dependence of the EPR spectra which had been recorded at smaller steps of x [14,15]. As a result of the different preparation and calibration procedures, however, errors of x in the range of ± 0.1 must be admitted in comparison of results obtained for the different series of samples. The same holds for comparison with data from the literature.

The NMR/NQR measurements were carried out on a home-built pulse spectrometer. The spectra were recorded by accumulating the spin echo amplitude sweeping stepwise either the magnetic field at constant frequency (NMR) or the frequency at zero external field (NQR). To get comparable line intensities, each NQR spectrum was recorded using one coil tunable for the frequency range 17–35 MHz. As the intensity of the echo signal is proportional to the square of the resonance frequency, the spectra were normalized by dividing the echo intensities by the square of the frequency, as proposed by Vega *et al.* [13]. The measurements were performed at the temperatures 4.2 K or 1.2 K.

3. Copper NQR Spectra in $YBCO_x$

Simple copper NQR spectra are found in YBCO only for high and low oxygen concentration, x. In the stoichiometric compound with $x = 7$ the spectrum consists of two pairs of the $^{63}Cu/^{65}Cu$ lines at 31.5/29.1 MHz from the Cu(2) site and at 22.1/20.5 MHz assigned to the Cu(1) site with four oxygen neighbors, $Cu(1)_4$ [17,19,20]. In the following, we mention only the frequencies of the most abundant ^{63}Cu isotope. The lines of ^{65}Cu are shifted to lower frequency in correspondence to the ratio of the nuclear quadrupole moments, $(^{65}eQ/^{63}eQ) = 0.923$, and the intensities are smaller by the ratio of the natural abundances, 0.45. With decreasing x, $6.9 < x < 7.0$, the Cu(1) and Cu(2) lines become broader due to the creation of oxygen vacancies in the Cu(1)—O layer. The increase of the linewidth was found to be in agreement with a random distribution of the defects [21]. At $x < 6.9$, the spectra develop into a more complicated structure [11—13] which is the topic of our investigation.

In the antiferromagnetic compound with low oxygen concentration narrow lines are found again. For $x = 6.0$ only the line at 30.1 MHz of Cu(1) with two oxygen neighbours, $Cu(1)_2$, exists. At slightly increased x, a second NQR line at 24.0 MHz appears which has been attributed to the Cu(1) sites with one oxygen neighbour in the chain, $Cu(1)_3$ [17]. This line was observed in a very broad region of the oxygen concentration $6.1 < x < 6.8$ [12]. The NQR spectrum of the Cu(2) sites is missing in the antiferromagnetic phase since these sites carry the ordered magnetic moments which lead to the hyperfine field at the copper nucleus. From the antiferromagnetic NMR spectrum in the region of 90 MHz [22] a quadrupole frequency of 23.2 MHz is deduced which was found also above the Neel temperature by NMR in an external field only slightly shifted to 23.8 Mhz [23].

4. Site Assignment

From the NQR spectra published for intermediate x [11—13] and also from those shown below, it is evident that they cannot be described by a simple superposition of the Cu(2) line and the three Cu(1) lines for different oxygen coordination found in the limits of high and low x. It is even unclear which parts of the spectra correspond to the Cu(1) and Cu(2) sites and below which oxygen concentration the signal of the Cu(2) sites disappears by the development of an ordered or slowly fluctuating magnetic moment.

The separation of the Cu(2) and Cu(1) lines can be easily made in the $GdBCO_x$ compounds using the idea that the fluctuations of the rare earth moments above the Neel temperature $T_n = 2.2$ K induce significant relaxation effects at the nearby nuclei in the Cu(2) layer [17]. In the $x = 7$ com-

pound at $T = 4.2$ K the transverse relaxation time, T_2, of Cu(2) was found to be shorter by an order of magnitude compared to that of Cu(1) : $T_c = 16$ μs and 150 μs for Cu(2) and Cu(1), respectively [24]. Below T_n, the fluctuations are suppressed due to the AF ordering of the Gd moments, and the T_2 values increase. At 1.4 K we found $T_2 = 69$ μs and 255 μs for Cu(2) and Cu(1), respectively. Therefore the spin-echo amplitude of the nuclei in the Cu(2) sites at 4.2 K can be completely suppressed as shown in Fig.1. Here the NQR spectrum of $GdBCO_{6.75}$, recorded at 4.2 K consists only of Cu(1) lines, whereas the lines from both layers are present in the spectrum at 1.2 K.

The Cu(1) spectrum given in Fig.1 consists of the sharp ^{63}Cu lines at the frequencies 31.2 MHz and 23.8 MHz. Since they are situated near to the corresponding lines found at low x, we attributed these lines to the sites with two and three oxygen neighbours, $Cu(1)_2$ and $Cu(1)_3$, respectively. The broad spectrum around the maximum at 22.5 MHz is assigned to the ordinary $Cu(1)_4$. An additional peak can be seen at 20 MHz. This peak is present also in the spectra of the samples with lower x, but is not found in the spec-

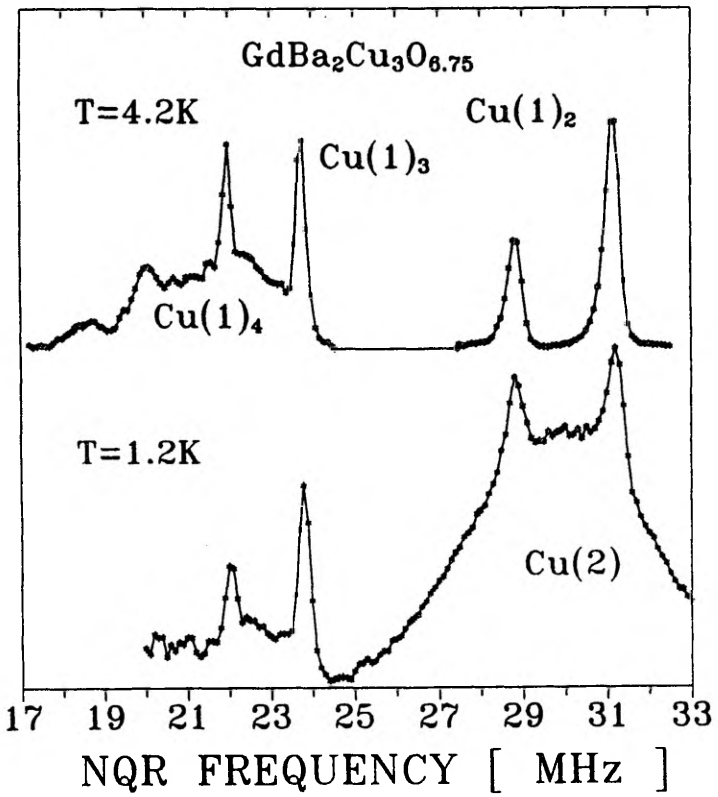

Fig.1. NQR spectrum of $GdBa_2Cu_3O_{6.75}$ (sample # C7) at 4.2 and 1.2 K.

trum of the $x = 7$ compound. To prove whether this line belongs to the Cu(1) layer, we measured T_2 at 4.2 K for all peaks and obtained the values $T_2 = 210$, 170, 280, and 260 μs at the frequencies 20.0, 22.5, 23.8 and 31.2 MHz, respectively. The close values of T_2 give a clear indication that all four lines belong to copper in the Cu(1) layer, the 20 MHz line belongs most likely to $Cu(1)_4$ in short fragments of filled chains. The linewidth of $Cu(1)_4$ is about ten times larger than the width of the $Cu(1)_2$ and $Cu(1)_3$ lines but is comparable to the width of the Cu(2) resonance seen in the spectrum at 1.2 K. The EFG at the Cu nuclei is determined by two contributions, namely, the lattice sum from the surrounding ions, and the distribution of the ionic charge itself. The broadening by lattice defects which alter the EFG via the lattice sum should be of the same order for all Cu(1) sites. Therefore the larger linewidth of the $Cu(1)_4$ and Cu(2) resonances cannot arise from the lattice defects but is mainly caused by the distribution of the ionic charge in these sites. The reason for this may be a different length of the chain fragments containing the $Cu(1)_4$ sites and the charge distribution within these fragments.

The comparison of the NQR spectra of $GdBCO_x$ recorded at $T = 4.2$ K and 1.2 K leads to the following results which will be used for the analysis of the spectra of $YBCO_x$ too: i) the spectra do not contain Cu(2) resonances at frequencies below $f < 25$ MHz, ii) the Cu(2) lines in 30 MHz region are very broad in comparison with the Cu(1) lines, and iii) there are no Cu(2) resonances seen in the NQR spectra of the samples with low oxygen concentration showing T_c values below the 60 K plateau ($x < 6.5$).

5. Cu(1) Spectra

The characteristic NQR spectra of $GdBCO_x$ at different oxygen concentrations x are given in Fig. 2. The spectra are recorded at 4.2 K and, consequently, present only the Cu(1) resonances. A small kink at 32.5 MHz belonging to the Cu(2) signal in the spectrum of the sample with $x = 7.0$ gives an estimate of the magnitude of possible Cu(2) contributions to the spectra. In Fig. 3 the corresponding spectra of $YBCO_x$ compounds are given which contain the broad Cu(2) signal besides the Cu(1) lines in the region between 26 and 32 MHz . Despite of some differences in the Cu(1) spectra of the two systems, namely, a stronger signal of $Cu(1)_3$ at 23.8 MHz and a weaker signal around 30 MHz in the $GdBCO_x$ system, the qualitative behavior is very similar. In the high frequency region the spectra in the samples with x between 6.6 and 6.8 consist of a single line of ^{63}Cu at the frequency 31.5 MHz in $YBCO_x$ and 31.2 MHz in $GdBCO_x$. At x below about 6.55 two more lines appear and the spectra exhibit three lines A, B, and C at the frequencies 31.5, 30.9 and 30.4 MHz, respectively, for YBCO (Fig.4) and at 31.2, 30.9 and 30.2 MHz in the case of GdBCO. With further decreasing x the spectra become broader and the fine structure disappears.

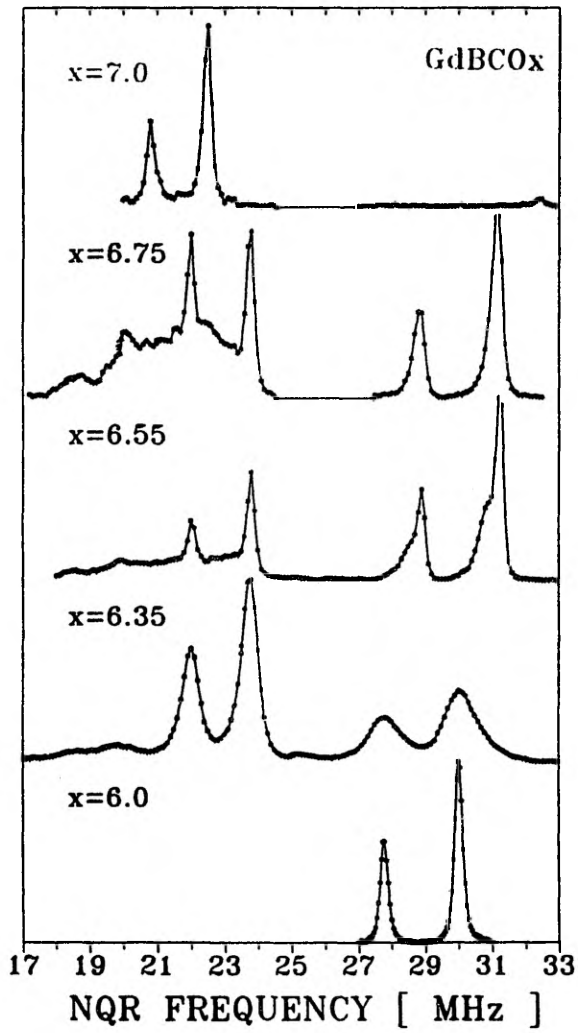

Fig.2. NQR spectra of the Cu(1) sites in $GdBa_2Cu_3O_x$ measured at 4.2 K for samples C1, C2, C5, and C7. The doublets of the ^{63}Cu line between 30 and 31.5 MHz belong to $Cu(1)_2$, those at 24 and 22.5 MHz to $Cu(1)_3$ and $Cu(1)_4$, respectively. Whereas the lines of $Cu(1)_3$ and $Cu(1)_2$ are relatively sharp for all x, $Cu(1)_4$ broadens severely for $x < 7$.

Different authors [11—13] have recorded similar data concerning the change of the NQR spectra around 30 MHz in this range of x, but with different explanations. The comparison of YBCO and GdBCO proves that all three lines belong to the Cu(1) sites. This type of spectrum has been found at different nominal values of the oxygen concentration x, e.g. in a sample with $x = 6.4$ and $T_c = 40$ K studied earlier by neutron diffraction [25]. In all cases the lines A, B, and C together were found only in superconducting samples with T_c below 50 K.

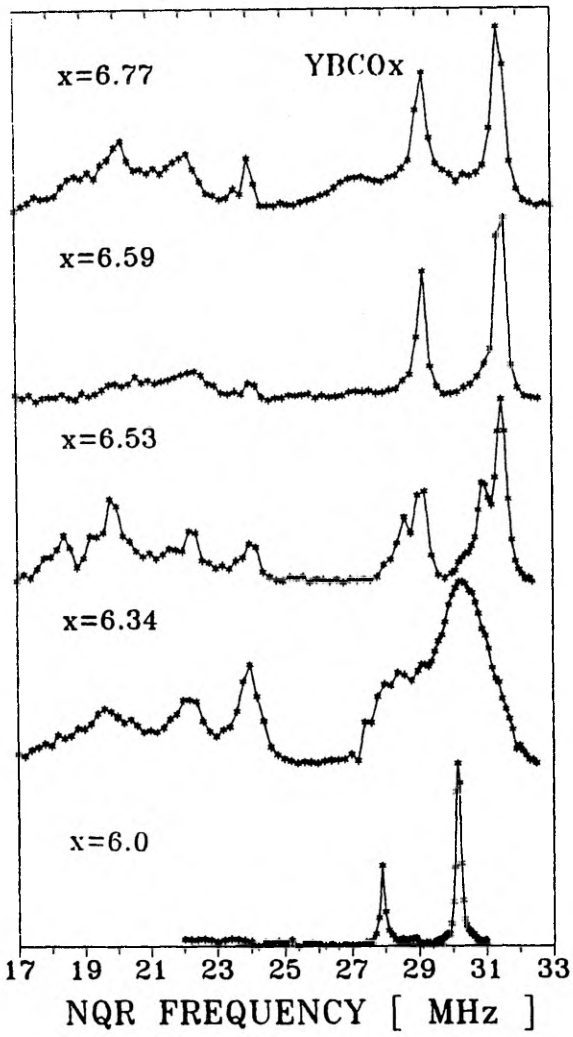

Fig.3. NQR spectra of $YBa_2Cu_3O_x$ (samples A1, A2, A4, A5, A6) measured at 1.2 K containing signals from the Cu(1) and Cu(2) sites. The Cu(2) intensity is reduced by the shorter T_2 values.

In order to solve the puzzle connected with the behavior of the NQR spectrum around 30 MHz in oxygen deficient samples, we recall the information gained by EPR of Gd^{3+} in oxygen deficient $YBCO_x$ [14,15]. These Gd^{3+} ions situated at the yttrium sites in the lattice between two Cu(2)—O layers are equally distant from four nearest Cu(1)—O chains. Therefore the crystal field at the Gd sites is influenced (via the charge distribution in Cu(2) planes) by the combination of two either "intact" or "empty" nearest chains in each plane. It was shown that the EPR spectra can be described within the model of the ortho-II structure where in the samples with oxygen con-

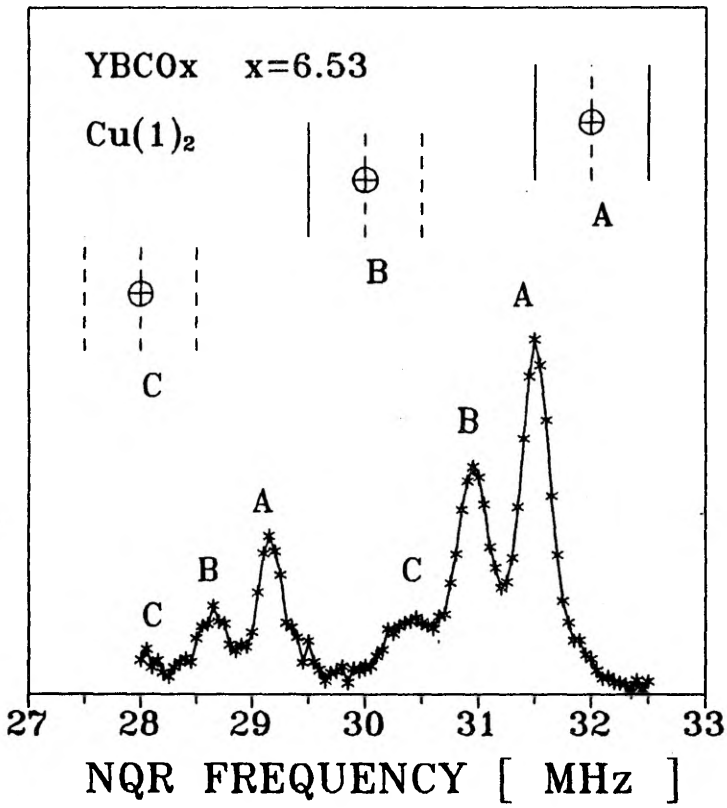

Fig.4. NQR spectrum of the Cu(1) sites with twofold oxygen coordination in $YBa_2Cu_3O_{6.53}$ (sample A4). The sites labeled A are embedded between two full chains, B and C between one or two neighbouring empty chains, respectively.

centration $x > 6.59$ every "empty" chain is situated between two intact chains, and in the samples with $x < 6.59$ two or more neighbouring chains appear to be empty [15].

The structure of the NQR spectra around 30 MHz can be explained in the same picture. We assign the single line A, seen in the spectra of the compounds with $x > 6.6$ to the $Cu(1)_2$ sites in between two intact chains as shown in Fig.4. Then the line B must be ascribed to the $Cu(1)_2$ sites between an intact chain and an empty one, and the line C to the $Cu(1)_2$ sites between two empty chains. The comparatively narrow lines of $Cu(1)_2$ show that the EFG values are determined only by the nearest coordination sphere and that the different lengths of the neighbouring intact chain fragments do not influence the resonance frequency. The frequency of line C is only 0.2 MHz above the $Cu(1)_2$ frequency found in fully deoxidized antiferromagnetic samples with $x = 6.0$. The close agreement of both frequencies is a further confirmation of our assignment of the line C to the $Cu(1)_2$ sites with empty neighbour chains.

The evolution of the NQR spectra at lower oxygen concentration is seen most clearly in the measurements at 77 K by Serikov *et al.* [11] where with decreasing x from 6.44 to 6.13 the main intensity moves from the line A through the line B to the line C. We attribute the broadening observed for $x < 6.5$ in our measurement at 4.2 K to the onset of the localization of the electronic spins at the Cu(2) sites. In the AF structure of pure YBCO with $x = 6.0$ the magnetic interactions of the Cu(1) sites with the two neighbouring Cu(2) planes are canceled exactly by symmetry [24]. If at increasing x the number of defects in the AF structure increases as is seen in the broadening of the AF NMR spectra at 90 MHz [26], the dipolar and transferred hyperfine fields are no longer canceled at the Cu(1) sites and cause the observed broadening of the NQR lines. This effect must disappear above the Neel temperature of the Cu(2) planes. Since T_n becomes small near $x = 6.4$, the spectra recorded at higher temperature [11,13] are not influenced by the disorder of the antiferromagnetic state.

The sequence of NQR spectra at decreasing x shows the development of the magnetic state at the Cu(2) sites in three steps: i) In the region of the 60 K plateau and at higher x the rate of the spin fluctuations is so large that the NQR lines at the Cu(1) and Cu(2) sites are not distorted. The influence of the fluctuations is important, however, for the spin-lattice relaxation. ii) The spin fluctuations become slower at the lower end of the 60 K plateau and cause the disappearing of the Cu(2) signal due to the fast nuclear relaxation, but do not yet distort the Cu(1) signal. iii) The onset of magnetic order in the Cu(2) layer becomes evident from the broadening of the Cu(1) NQR lines in samples with x reduced so much that they are no longer superconducting. Another indication of the onset of magnetism is found in the T_2 *measurements of* $GdBCO_x$, where the Cu(1) sites can be studied separately. Here we found a nonexponential magnetization decay for the Cu(1) lines with a superposition of fast and slow relaxation rates in the samples $x = 6.50$ and $x = 6.39$. This inhomogeneous relaxation at the Cu(1) sites can be explained assuming an additional relaxation path due to slowly fluctuating spins distributed inhomogeneously in the Cu(2) layers.

6. Intensity Distribution of the Cu(1) Lines

The best proof for the site assignment of the NQR lines in the systems $YBCO_x$ and $GdBCO_x$ can be a reasonable intensity distribution of the Cu(1) lines belonging to the sites with two, three, and four nearest oxygen neighbours. In order to get a quantitative estimate of the intensity distribution of the Cu(1) lines we simulated the normalized experimental spectra by pairs of the $^{63}Cu/^{65}Cu$ lines. In the frequency range $17 < f < 25$ MHz a reasonable agreement between the experimental spectrum and a simulation was established by fitting the width and the amplitude of three pairs of lines at the

nearly constant frequencies 23.8(1), 22.5(2) and 20.0(2) MHz in the case of $GdBCO_x$, and 24.0(1), 22.0(2) and 20.0(2) MHz for $YBCO_x$. In the region $25 < f < 33$ MHz the narrow $Cu(1)_2$ lines had to be separated from the broad background signal of Cu(2). As far as possible the intensities have been corrected according to the T_2 differences, but the appearance of a rapid component in the T_2 decay in the samples with x below 6.55 leads to rather large ambiguities. The relative intensities of $Cu(1)_2$ ($I2$), $Cu(1)_3$ ($I3$), and both components of $Cu(1)_4$ ($I4^*$ and $I4^{**}$) for all samples which have been evaluated are given in Table 1. The variation of the intensity for the three configurations at increasing x in the uniform series A of $YBCO_x$ and in the series C of $GdBCO_x$ reveal the general trend of increasing $I4 = I4^* + I4^{**}$ and decreasing $I2$ and $I3$. The reliability of the relative intensities can be checked by the oxygen concentration z in the Cu(1) layer which is determined by the relation

$$z = I4 + I3/2, \quad I4 = I4^* + I4^{**}. \tag{1}$$

The relation $z = x - 6$ is fulfilled in nearly all samples within the limit of accuracy (± 0.1) from which x and the intensities are determined (Table 1). However, the generally too small values of z show that the intensity $I2$ has been overestimated systematically at $x > 6.5$. The reason for this may be connected with problems of separating the $Cu(1)_2$ from the Cu(2) signal and with the correction for T_2. It is evident that the component at 20 MHz with the intensity $I4^*$ must belong really to the fourfold coordinated Cu(1), otherwise the value of z would be even smaller.

A random occupation of the O(1) sites in the Cu(1) chains by oxygen would lead to relative intensities depending on z as follows:

$$I2 = (1 - z)^2, \quad I3 = 2z(1 - z) \quad \text{and} \quad I4 = z^2. \tag{2}$$

This is evidently not the case in Table 1. The intensity $I3$ is too small by more than a factor of 2 at $x = 6.5$, which is a clear indication for the development of a non-random structure with longer chain fragments.

From the relative intensities we can estimate the average length of the chain fragments. The average number of oxygen atoms, n, in one chain fragment is simply determined by the ratio of the number of copper atoms within the chains, $I4$, and the number of the atoms terminating the chains, $I3$, by

$$n = 1 + 2\,I4/I3. \tag{3}$$

The values n increase with x in $GdBCO_x$ and $YBCO_x$ as shown in Table 1 and in Fig.5. The smaller values n in $GdBCO_x$ at the same x compared with

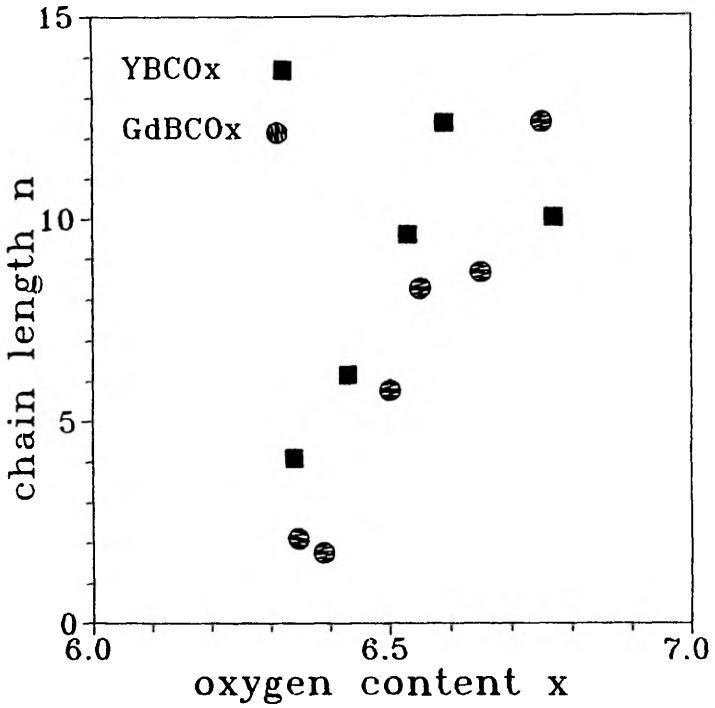

Fig.5. Mean length of oxygen chains in $YBa_2Cu_3O_x$ and $GdBa_2Cu_3O_x$ versus x.

$YBCO_x$ can be caused by the different preparation method in both systems, but in any case a strong increase of n is seen when x approaches 6.5. This is a clear evidence for the development of the ortho-II structure with filled and empty chains. Superconductivity appears in the samples with $n > 6$. The largest values of the chain length between 10 and 13 are found for $x > 6.5$.

7. Cu(2) Spectra

The NQR spectra consisting of the ^{63}Cu and ^{65}Cu lines appeared to be too complicated for the analysis of Cu(2) resonances. We found that the changes in the local environment of the Cu(2) sites in $YBCO_x$ due to the oxygen depletion can be followed better in the field sweep NMR spectra. We have measured these spectra of the uniaxially oriented samples with the crystallographic c-axis either parallel or perpendicular to the external magnetic field. The latter case is suitable also for the usual, previously not oriented powder samples which turn out to be perfectly oriented with the c-axis perpendicular to H in the superconducting state [17]. The spectrum given in Fig.6

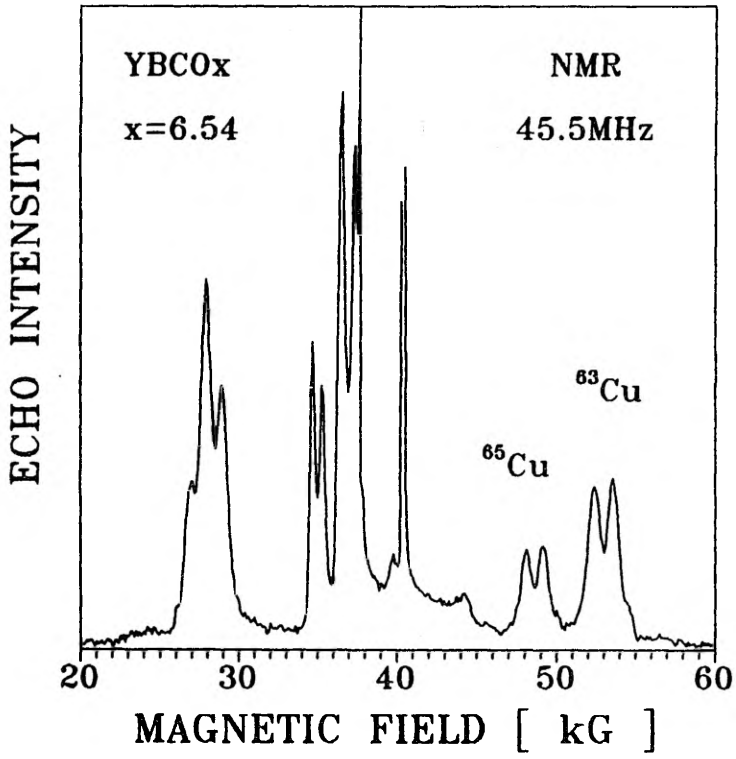

Fig.6. NMR spectrum of $YBa_2Cu_3O_{6.54}$ (sample B2) measured at 4.2 K and 45.5 MHz with the magnetic field applied perpendicular to the *c*-axis.

shows the full field sweep spectrum of the sample B2. Here the self-orientation of the superconducting grains in the magnetic field is seen from the well resolved lines. The spectrum shows the resonances from the two copper isotopes clearly separated in the high field satellite region as a result of the higher gamma value and a smaller quadrupolar shift of the isotope ^{65}Cu, but overlapping in the low field satellite. The most surprising result in this spectrum is the splitting of the Cu resonance into two lines of equal intensity and slightly different quadrupole coupling. Since in this particular sample the ortho-II structure was confirmed by electron diffraction [18], the splitting must be connected with the nonequivalent sites in this structure. In our NQR spectra the two lines are seen in the fit of the broad Cu(2) spectrum below the $Cu(1)_2$ signal with NQR frequencies of 30.8 and 27.7 MHz, in agreement with results of Warren *et al.* for a sample with a single Cu isotope [27] and Shimizu *et al.* [28]. From the Cu(1) sites only the $Cu(1)_2$ contribution is seen as a shoulder at the high field side of the doublet, whereas the resonances of $Cu(1)_4$ and $Cu(1)_3$ sites are smeared over a large region of the spectrum as expected due to the strong asymmetry of the EFG tensor of these sites [17].

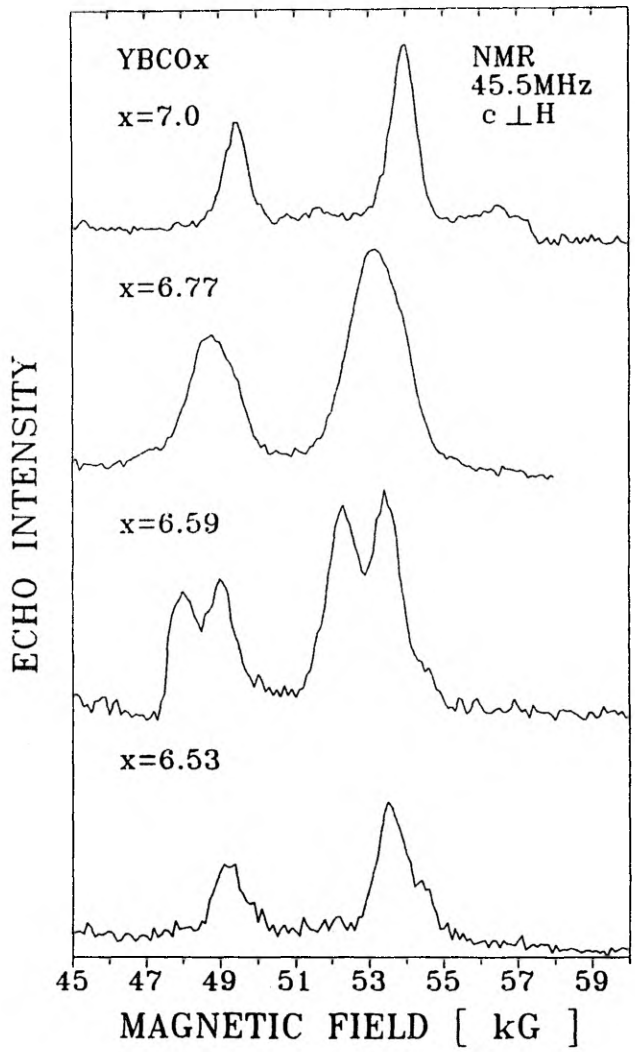

Fig.7. The high-field satellite in the NMR spectrum of $YBa_2Cu_3O_x$ for different x measured at 45.5 MHz with the magnetic field perpendicular to the c-axis (samples A4, A5, A6, A7).

The change of the NMR spectra in the region of the high-field satellite at decreasing x is shown for the magnetic field perpendicular and parallel to the c-axis in Figs.7 and 8, respectively. The spectra for the perpendicular field reveal a continuous shift of the Cu(2) resonances to lower fields corresponding tc lower NQR frequencies at x decreasing from 7.0 to 6.77 and the splitting around $x = 6.59$ into two lines of different EFG. The single line for $x = 6.53$ shifted also to higher field belongs to the Cu(1) resonances according to the interpretation of the spectra measured for the field parallel to

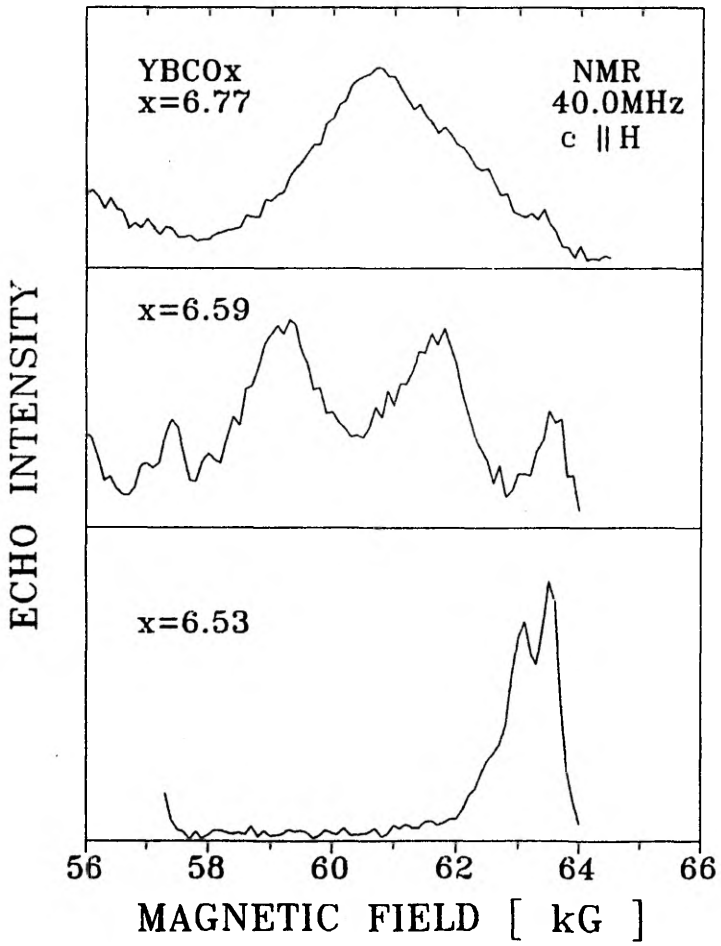

Fig.8. The high-field satellite in the NMR spectrum of $YBa_2Cu_3O_x$ for different x measured at 40 MHz with the magnetic field applied parallel to the c-axis (samples A4, A5, A6).

the c-axis (Fig.8). Here the spectrum of the $x = 6.59$ compound shows again the splitting of the Cu(2) resonance and the line belonging to the $Cu(1)_2$ sites at higher field. Only this latter component remains at $x = 6.53$. The splitting of this line into three components as in the NQR spectrum of Fig. 4 identifies these as the contributions of $Cu(1)_2$ (A,B,C). Thus this spectrum proves again that the resonance of the Cu(2) sites disappears in superconducting samples with small x and T_c below the 60 K plateau.

The comparison of the spectra for both orientations allows one to estimate the Knight shift and the symmetry of the EFG tensor. For all Cu(2) sites we arrive at a symmetric EFG along the c-axis and a positive orbital shift $K_{corb} = 1.4(2)$ % in c-direction independent of x. For the three $Cu(1)_2$

lines, on the other hand, a diamagnetic shift $K_{corb} = -0.2(1)$ % is the reason for the separation of the Cu(1) and Cu(2) spectra in Fig.8 [28]. The main axis of the EFG of these sites is along the c-axis too. The different shape of the Cu(1) spectrum at $x = 6.53$ for the field parallel or perpendicular to the c-axis can be caused either by a different orbital shift anisotropy of the three lines or, more probably, by a small asymmetry of the EFG by about 0.1.

The splitting of the Cu(2) line is found in all samples with $x < 6.7$ and disappears at larger x. The two components may be assigned to Cu(2) sites which are neighbours of full or empty Cu(1) chains [28]. Since the largest NQR frequency is found for $x = 7.0$, the larger of both frequencies should correspond to Cu(2) connected to a full chain. We did not find any sample with a significant difference in the intensities of both lines or with a shift of the frequencies or resonance fields.

It is interesting to point out that the center of gravity of the Cu(2) lines changes only little with x in the region of the 60 K plateau. Because the dominant contribution to the EFG at Cu(2) sites is due to the on-site holes [29], the nearly constant EFG in the plateau region means that the number of holes in the Cu(2) layer is nearly independent of x which may be the reason for the constant T_c.

8. Order of Oxygen in the Cu(1) Layers

The existence of the ortho-II structure is well proved by the spectra of Cu(1) and Cu(2). The two Cu(2) lines in the region $6.55 < x < 6.7$ show that two different Cu(2) sites exist at this concentration which are connected with full and empty chains, respectively. In the same region the spectrum of $Cu(1)_2$ contains only the line A corresponding to the sites in empty chains between full chains as expected in the case of ortho-II. The Cu(1) resonance reveals the details about the correlation length in this structure. The average length of the full chains is rather short, about 10 oxygen ions as shown by the large intensity $I3$ of the $Cu(1)_3$ ions at the chain ends.

Above $x = 6.5$ the filling of the Cu(1) layer with the oxygen ions can be modeled in different ways as mentioned in Section 1. The spectra presented above cannot confirm conclusively one particular model but we will discuss to what extent they support one of them. The most reliable quantity is the mean chain length n as defined by Eq.(3). In Fig.9 we plot n as a function of x for the models described above. In the case of a random filling of all O(1) sites $n < 5$ is valid for $x < 6.8$. In all models based on the ortho-II structure with full and diluted chains n diverges at $x = 6.5$ but becomes small again around $x = 6.7$ by the formation of the new chains. This effect is strongest for the condition of maximum distance between the oxygen ions [8], but also

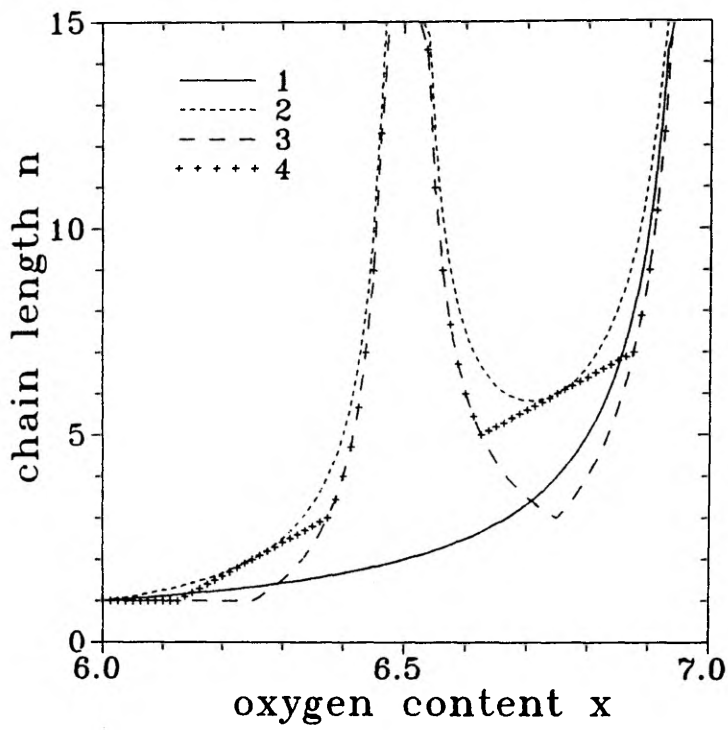

Fig.9. Mean length n of chains calculated for different models of the arrangement of the oxygen ions on the O(1) sites in the Cu(1) plane 1: random distribution (diluted ortho-I); 2: ortho-II with random filling of the diluted chains [5]; 3: ortho-II with maximal distance in the diluted chains [7]; 4: ordered structures based on ortho-II with larger unit cell [6].

for the other models [6,7] n decreases to at least 6. No decrease of n appears if the length in the diluted chains is the same as in the full ones. This implies either the coexistence of ortho-II and ortho-I clusters or the formation of sequences of filled and empty chains like the ortho-III structure.

The evaluation of our NQR spectra shows definitely no decrease of n to the values of about 6 at $x > 6.5$ (Fig.6). Therefore all models using the ortho-II structure with alternating full and diluted chains can be excluded. The randomly diluted ortho-I structure must be discarded for the same reason for $x < 6.8$. Further information is gained from the spectra of the Cu(2) sites. At $x > 6.7$ we have found only a broadening and a shift of the EFG distribution which means that in this range no pieces of empty chains exist which are long enough to induce new charged states with a well defined EFG in the Cu(2) planes. Thus the structure in this region must be considered as the diluted ortho-I structure. In the spectra for lower x the two narrower lines of equal intensity (Fig.8) show the appearance of the well ordered ortho-II structure with the same amount of empty and full chains.

Since we did not find an increase of the relative intensity of one of the two lines by changing x or annealing, the EFG of the Cu(2) sites gives strong evidence against the ortho-III structure for which to be present one of the lines should increase. The random filling of the empty chains, excluded already by the analysis of the Cu(1) spectra, is improbable also from this point of view. In this case the signal connected with the empty chains should decrease continuously with increasing x. Thus the best description of the x-dependence of the Cu(2) spectra is given by the model of a coexistence of clusters of diluted ortho-I with $x > 6.8$ and the pure ortho-II [10]. An example for this coexistance of both structures at $x = 6.63$ is given by Takigawa *et al.* [30, Fig.2b] where the line of ortho-I appears between the peaks of ortho-II.

In the range below the 60 K plateau only the Cu(1) signal can be observed, at least at the low temperatures of our experiment, 4.2 and 1.2 K. Here two features are evident: the decrease of the mean chain length n (Fig.5) calculated from the relative intensities of the $Cu(1)_3$ and $Cu(1)_4$ components in the spectrum, and the appearance of the lines B and C of $Cu(1)_2$ besides the line A (Fig.4). As found already by Serikov *et al.* [11], the superconductivity disappears in the samples where the line A is missing in the NQR spectrum. Assuming an ideal arrangement of the oxygen in full and empty chains, one can see that for a structure with every third chain occupied ($x = 6.33$) only the line B would be seen, for every fifth chain occupied ($x = 6.2$) the intensity of the lines B and C would be equal. In our non-superconducting samples A2 and C2 ($x = 6.35$), the intensity of the $Cu(1)_2$ resonances is already shifted to the line C. This means that the empty chains belong mainly to clusters with $x < 6.2$ and a considerable amount of oxygen is arranged in clusters of larger x. In contrast, the NQR spectrum of the weakly superconducting sample B1 produced by long annealing ($x = 6.3$, $T_c = 20$ K) shows 25% intensity of the $Cu(1)_2$ resonances in the line A and 60 % in B and, consistently with that, a large mean value of the fragment length n. Thus we find that the main effect of the annealing in this region of the oxygen concentration is to resolve the clusters with large x and to create long chains in the whole sample. According to this, the condition for the onset of superconductivity is that the filled chain fragments with a length of about six are attached to filled fragments at the next nearest chain, that means the existence of extended regions of the ortho-II structure.

9. Conclusion

The comparison of the Cu NQR spectra of $YBCO_x$ and $GdBCO_x$ and the Cu NMR spectra of $YBCO_x$ and their development as function of x has enabled us to determine the configurations in the Cu(1) and Cu(2) planes corresponding to the different peaks in the spectra. Without any quantitative

evaluation it is already evident that in all samples in the region of about $x = 6.5$ an ordered structure exists with a regular sequence of full and empty chains. The influence of different preparation and annealing procedures manifests itself only in the size of the ordered domains which may be so small that diffraction methods cannot detect the order. The disappearance of the NQR signal of the Cu(2) sites in the superconducting samples with T_c below the 60 K plateau shows the slowing down of the magnetic fluctuations of the Cu(2) spins. The sharp Cu(1) lines in these samples, however, prove that no magnetic order or spin glass state exists. Broad lines indicating the magnetic order are observed only in samples without superconductivity.

The quantitative analysis of the spectra has opened many possibilities for the investigation of the oxygen depleted $YBCO_x$. It allows one to determine the average length of the Cu—O chains. We find that in the region of the 60 K plateau this length saturates at about twelve oxygen atoms in a chain. It will be an interesting task to find out how this length increases at the transition to the 90 K plateau. As the condition for the onset of superconductivity we obtain about six oxygen atoms per chain arranged in domains of the ortho-II structure with every other chain filled. The coexistence of the pure ortho-II structure with an oxygen poor ortho-I structure at higher x follows from the Cu(2) spectra. Thus the systematic investigation of the Cu spectra in the region $6.6 < x < 7.0$ will be a valuable tool for further investigations of the ordering phenomena in these materials.

Acknowledgements

We are indebted to many colleagues who were engaged in the preparation and characterization of the samples used for this investigation, especially to J.M. Hosseini and D. Wagener, Bonn, and R.R. Arons, Jülich. A.J. Janossy, Budapest, contributed to this research by stimulating discussions. Financial support granted by the Bundesministerium für Forschung und Technologie through the DAAD and the international office of the Kernforschungszentrum Karlsruhe is gratefully acknowledged. I. Heinmaa would like to express his thanks to Prof. Zinn for the hospitality he received at the KFA Jülich.

References

[1] Cava R.J, Batlogg B., Chen C.H., Rietman E.A., Zahurak S.M., Werder D.: Phys. Rev. **B36**, 5719 (1987)

[2] Cava R,J., Hewat A.W., Hewat E.A., Batlogg B., Marezio M., Rabe K.M., Krajewski J.J., Peck W.F. Jr., Rupp L.M. Jr.: Physica C **165**, 419 (1990)

[3] Buchgeister M., Hiller W., Hosseini S.M., Kopitzki K., Wagener D. in: Proc. Int. Conf. on Transport Properties of Superconductors (Nikolsky R. ed), p. 511. Rio de Janeiro, Brazil 1990. Singapore: World Scientific 1990. Buchgeister M., Hiller, Hosseini S.M.,

Kopitski K., Wagener D.: Physics and Materials Science of High Temperature Superconductors, NATO ASI Series E 181, (Kossowski R., Methfessel S., Wohlleben D. eds), p.319. Dordrecht: Kluwer Academic Publishers, 1990.
[4] Claus H., Yang S., Paulikas A.P., Downey J.W., Veal B.W.: Physica C **171**, 205 (1990)
[5] Veal B.W., Paulikas A.: Physica C **184**, 329 (1991)
[6] Alario-Franko M.A., Chaillout C., Capponi J.J., Chenavas J., Marezio M.: Physica C **156**, 455 (1988)
[7] Zaanen J., Paxton A.T., Jepsen O., Andersen O.K.: Phys. Rev. Letters, **60**, 2685 (1988)
[8] Latge A., Anda E.V., Moran-Lopez J.L.: Phys. Rev. **B 42**, 4288 (1990)
[9] Ceder G., Asta M., de Fontaine D.: Physica C 177, 106 (1991)
[10] Poulsen C.F., Andersen N.H., Andersen J.V., Bohr H., Mouritsen O.G.: Nature **349**, 594 (1991)
[11] Serikov V.V., Bogdanovich A.M., Verkhovskii S.V., Zhdanov Yu.I., Alekshashin B.A., Mikhalev K.N., Kozhevnikov V.L., Chesnitskii S.M.: JETP Lett., **47**, 534 (1988)
[12] Yasuoka H., Shimizu T., Imai T., Sasaki S.: Hyperfine Int. **49**, 167 (1989)
[13] Vega A.J., Farneth W.E., McCarron E.M., Bordia R.K.: Phys. Rev. **B39**, 2322 (1989)
[14] Janossy A., Rockenbauer A., Pekker S., Oszlanyi G., Faigel G., Korecz L: Physica C **171**, 457 (1990)
[15] Pekker S., Janossy A., Rockenbauer A.: Physica C **181**, 11 (1991)
[16] Kohori Y., Shibai H., Oda Y., Kohara T., Kitaoka Y., Asayama K.: J. Phys. Soc. Japan **57**, 2912 (1988)
[17] Lütgemeier H.: Physica C **153–155**, 95 (1988)
[18] Krabbes G., Bieger W., Thomas J., Verges P., Lütgemeier H.: Physica C, (1991), to be published.
[19] Lütgemeier H., Pieper M.W.: Solid State Commun. **64**, 267 (1987)
[20] Mali M., Brinkmann D., Pauli L., Roos J., Zimmermann H.: Phys. Lett. **A124**, 112 (1987)
[21] Schiefer H., Mali M., Roos J., Zimmermann H., Brinkmann D., Rusiecki S., Kaldis E.: Physica C **162–164**, 171 (1989)
[22] Mendels P., Alloul H.: Physica C **156**, 355 (1988); Yasuoka H., Shimizu T., Ueda Y., Kosuge K.: J.Phys.Soc.Jpn 57, 2659 (1988); Yamada Y., Ishida K., Kitaoka Y., Asayama K., Takagi H., Iwabuchi H., Uchida S.: J.Phys.Soc.Jpn **57**, 2633 (1988)
[23] Mali M., Mangelschots I., Zimmermann H., Brinkmann D., Physica C **175**, 581 (1991)
[24] Lütgemeier H., Heinmaa I.: Proc. of XXVI Zakopane School on Physics (Stanek J., Pedziwiatr A.T. eds.), p.264, Zakopane, Poland 1991. Singapore: World Scientific 1991.
[25] Rupp B., Fischer P., Pörschke E., Arons R.R., Meuffels P.: Physica C **156**, 559, (1988)
[26] Matsamura M., Yamagata H., Yamada Y., Ishide K., Kitaoka Y., Asayuma K., Takagi H., Iwabuchi H., Uchida S.: J. Phys. Soc. Jpn. **57**, 3297 (1988); Mendels P., Alloul H., Marucco J.F., Arabski J., Collin G.: Physica C 171, 429 (1990)
[27] Warren W.W., Jr., Walstedt R.E., Brennert G.F., Bell R.F., Espinosa G.P., Cava R.J.: Physica C **162–164**, 179 (1989)
[28] Shimizu T., Yasuoka H., Tsuda T., Koga K., Ueda Y.: Bull. Magn. Res. **12**, 39 (1990)
[29] Hanzava K., Komatsu F., Yosida K.: J. Phys. Soc. Jpn **59**, 3345 (1990)
[30] Takigawa M., Reyes A.P., Hammel P.C., Thompson J.D., Heffner R.H., Fisk Z., Ott K.C.: Phys.Rev.B **43**, 247 (1991)

Author's address: Prof. Dr. H. Lütgemeier, Institut für Festkörperforschung, Forschungszentrum Jülich, Postfach 1913, W-5170 Jülich, Germany

II

H. Lütgemeier and I. Heinmaa,
Oxygen Order and Spin Structure in $YBa_2Cu_3O_x$ deduced from Copper NMR and NQR,
in: Proceedings of the Workshop on Phase Separation in Cuprate Superconductors,
Erice, Italy, 6–12 May 1992, eds. K. A. Müller and G. Benedek,
World Scientific, Singapore, etc, 1993, pp. 243–261.

OXYGEN ORDER AND SPIN STRUCTURE IN $YBa_2Cu_3O_x$ DEDUCED FROM COPPER NMR AND NQR

H. Lütgemeier*
IFF, Forschungszentrum Jülich, D–5170, Germany

I. Heinmaa
Institute of Chemical Physics and Biophysiscs, Tallinn, Estonia

ABSTRACT

The magnetic state and the arrangement of the oxygen ions in $YBa_2Cu_3O_x$, $6 < x < 7$, is investigated by analyzing the NQR spectra of copper. For this analysis it is important that the signals from the Cu(1) and Cu(2) sites can be distinguished in $GdBa_2Cu_3O_x$ due to the different influence of the magnetic Gd ions. At x near 6.5 the existence of the ortho–II structure with alternating filled and empty chains is evident, at higher x ortho–II and ortho–I with all chains filled coexist. The average chain length n is about 10 to 13 oxygen ions per chain in the region of the 60 K plateau and decreases fast at lower x. Superconductivity disappeares in samples with $n < 6$. No coexistence of magnetic order at the Cu(2) sites with superconductivity is found, but a slowing down of the magnetic fluctuations in samples with T_c below the 60 K plateau can be deduced from the disappearing Cu(2) NMR and NQR signals. In the antiferromagnetic region the spin structure is influenced by impurities like Fe, Al and Gd; but in any case the expectation value of the magnetic moments at the Cu(1) site in zero.

*The main part of this report has been presented at the Egyptian–German Workshop on HT_c Superconductivity at Fayonm and Shebin Al–Kome (1992) and will be published in Egyptian Journal of Solids.

1. Introduction

In $YBa_2Cu_3O_x$, $6 < x < 7$ (YBCO) and in most related compounds with Y replaced by rare earths like Gd, antiferromagnetic order of the copper ions in the Cu–O planes (Cu(2) sites) appears at an oxygen concentration x below about 6.4, with a Neel temperature which is about 400 K for $x = 6.0$. At x above 6.4 the samples become superconducting. The values of T_c increase with x showing a plateau in T_c of about 60 K in the region of $6.5 < x < 6.7$ and a second plateau with T_c of about 92 K for $x > 6.8$ [1]. Since in the structure of YBCO only the oxygen ions in the Cu(1) planes can be removed, these must be responsible for the transition from the antiferromagnetic insulator to the superconductor. Therefore the local arrangement of the oxygen ions in the Cu(1) planes is of great interest. A large amount of information about the structure has been obtained by diffraction methods, X–ray, neutron, and electron diffraction.

The structure of the antiferromagnet at $x = 6.0$ without oxygen in the Cu(1) plane is tetragonal. At a small increase of x the oxygen ions are distributed randomly on the sites between two Cu ions in this plane. At higher x, a transition to the orthorhombic structure of the superconductor at $x = 7$ appears, where only the O(1)–sites in b–direction, in the "chains", can be occupied. Since the value of Tc at intermediate x depends to a high degree on the thermal treatment of the samples it must be assumed that the arrangement of the oxygen ions on the O(1) sites is important for the superconductivity in oxygen depleted samples [1,2]. Different superstructures have been found by electron diffraction [1]. The structure at $x = 6.5$ with a unit cell of dimension 2a and every second chain either filled or empty is designated as ortho–II, and correspondingly the normal one at $x = 7.0$ as ortho–I. The problem of all diffraction methods is that local order can be detected only when the correlation length of the structure is long enough.

Since the electric field gradient (EFG) at a copper nucleus depends on the valence state of the ion itself and on the charge of the surrounding atoms, the copper NMR/NQR can be a direct method to study the surrounding of the Cu ions and by this the local order of oxygen in these materials. Unfortunately, the NQR spectra in oxygen deficient $YBCO_x$ change with x in a very complicated way [3,4,5]. Overlapping of the lines from the two copper isotopes (^{63}Cu, ^{65}Cu), from the Cu(1) and Cu(2) layers, and from the different configurations within the layers makes the analysis extremely difficult.

In this report we present the NQR and NMR spectra of copper in oxygen deficient $YBCO_x$ and $GdBCO_x$ with the aim to study the oxygen ordering in the lattice and the magnetic order of the Cu–ions in the antiferromagnetic state. We will use the advantage of the $GdBCO_x$ system where separating of the Cu(1) and Cu(2) NQR lines is possible [6,7]

2. NMR and NQR of copper

Natural copper contains two isotopes ^{63}Cu and ^{65}Cu, both with the nuclear spin $I = 3/2$. The magnetic dipole moments and the electric quadrupole moments differ by about 10%. Since the ^{63}Cu isotope of larger abundance (69%) reveals the smaller value of the gyromagnetic ratio, gamma, and the larger quadrupole moment, eQ, the origin of an interaction can be determined easily from the different behavior of both isotopes. The quadrupole moment couples to the electric field gradient tensor (EFG) determined by the charge distribution in the crystal, which can be

expressed by the largest eigenvalue, eQ, and the asymmetry parameter, η [8]. Without a magnetic field, the degeneracy of the +–m levels is retained and for I=3/2 only one "pure NQR" line $|\pm 1/2> \rightarrow |\pm 3/2>$ can be observed at the frequency $\nu_{NQR} = \nu_Q(1+\eta^2/3)^{1/2}$ with the quadrupole frequency $\nu_Q = e^2qQ/2h$. The asymmetry parameter cannot be determined from the pure NQR spectrum for I = 3/2 since only one transition exists. This is possible in an applied magnetic field which leads at low field to the Zeeman splitting of the NQR lines or at high field to the NMR spectrum with quadrupole splitting. Since in both cases the splitting depends on the orientation of the magnetic field relative to the main axes of the EFG tensor, the spectra of powder samples become broad. In metallic samples only the region of the penetration depth of the r.f. field contributes to the signal. For this reason powder samples are used in most experiments and the orientation of the grains is of great importance.

In the case of antiferromagnetic order, the hyperfine interaction leads to a local magnetic field, the hyperfine field, at those Cu ions which carry the magnetic moments. The Zeeman splitting of the nuclear levels by this hyperfine field determines the frequency of the antiferromagnetic nuclear magnetic resonance (AFNMR) which can be observed without an applied magnetic field. For copper the corresponding frequencies are much larger than the NQR frequencies.

3. Experimental

All experiments presented here have been performed by the standard spin-echo technique at 4.2 or 1.2 K either by sweeping the frequency at zero field (NQR and AFNMR) or the magnetic field at fixed frequency (NMR). As the intensity of the echo signal is proportional to the square of the resonance frequency, the NQR spectra were normalized by dividing the echo intensities by the square of the frequency.

The NQR and NMR experiments with oxygen deficient samples of YBCO and GdBCO have been performed over a long period with samples of different preparation and origin. For the quantitative analysis discussed below we used three series of samples presented in Tab.1.

Slightly Gd–doped samples $Y_{0.999}Gd_{0.001}Ba_2Cu_3O_x$ (A1..A7) have been prepared by the equilibrium method at 650°C as described in ref.[9] and had been already used for Gd EPR experiments [9]. In order to get useful information from the EPR and NMR spectra, these samples had been uniaxially oriented in the magnetic field and fixed in epoxy. For comparison purposes and in order to investigate the influence of annealing, several $YBCO_x$ samples without Gd doping prepared by the quenching technique with subsequent annealing [10] were investigated, too (B1..B4). The extraction of oxygen in the series of $GdBCO_x$ samples (C1...C8) has been done at 810°C at controlled pressure [11]. The oxygen concentration x given in Tab.1 has been determined in different ways and the accuracy is difficult to estimate. Within each series of samples the increments of x are very reliable as was seen from the continuous development of all properties, especially from the x dependence of the EPR spectra which had been recorded at smaller steps of x [9]. As a result of the different preparation and calibration procedures, however, errors of x in the range of +–0.1 must be admitted in the comparison of results obtained for the different series of samples. The same holds for the comparison with data from the literature.

Tab.1:

Summary of samples investigated: oxygen concentration, x, T_c from susceptibility, relative intensities of the different components of the NQR signal of Cu(1), I2..I4, mean length of Cu–O chains, n (eq.3), and oxygen concentration in the Cu(1) plane, z (eq.1).

sample #	x	T_c K	I4* %	I4** %	I3 %	I2 %	n	z
A1	.6.0					100		0
A2	6.34		15	11	17	57	4.1	0.35
A3	6.43		27	9	14	50	6.2	0.43
A4	6.53	35	24	21	10	45	10.0	0.50
A5	6.59	56	8	37	8	47	12.3	0.49
A6	6.77	61	26	30	12	32	10.3	0.62
A7	7.0	90		100				1
B1	6.30	20	14	17	8	61	8.7	0.35
B2	6.54	56	7	26	8	59	9.2	0.37
B3	6.58	56	11	34	12	43	8.5	0.51
B4	6.74	70	8	48	10	34	12.2	0.61
C1	6.0					100		0
C2	6.35		7	12	36	45	2.1	0.37
C3	6.39		9	8	45	38	1.8	0.40
C4	6.50	20	9	35	19	37	5.6	0.53
C5	6.55	50	8	32	11	49	8.3	0.46
C6	6.65	52	10	36	12	42	8.7	0.52
C7	6.75	58	13	52	11	24	12.8	0.70
C8	7.0	92		100				1

A1..A7 $YBCO_x$ 0.1% Gd slowly cooled from 650°C [9]
B1,B2,B4 $YBCO_x$ annealed about 10 days 380°C [10]
B3 $YBCO_x$ as–quenched [10]
C1..C8 $GdBCO_x$ slowly cooled from 800°C [11]

4. Copper NQR Spectra in $YBCO_x$

Simple NQR spectra of copper are found in YBCO only for high and low oxygen concentration, x. In the stoichiometric compound with x near 7 the spectrum consists of two pairs of the $^{63}Cu/^{65}Cu$ lines at 31.5/29.1 MHz from the Cu(2) site and at 22.1/20.5 MHz assigned to the Cu(1) site, Cu(1)4, with four oxygen neighbors [6,12]. In the following we mention only the frequencies of the most abundant ^{63}Cu isotope. The lines of ^{65}Cu are shifted to lower frequency by the ratio of the nuclear quadrupole moments, $(^{65}eQ/^{63}eQ) = 0.923$, and the intensities are smaller by the ratio of the natural abundances, 0.45.

The assignment of the lines to the different sites was determined from the intensity ratio of the lines [12] (since one formula unit contains one Cu(1) and two Cu(2) sites), by symmetry arguments since only the Cu(2) sites can reveal the nearly axial symmetry of the EFG along the c–axis found in the NMR spectra for the line at 31.5 MHz [6], and by the influence of Gd ions on both lines [6]. In $GdBa_2Cu_3O_x$ the electron spins of the Gd ions order antiferromagnetically at about 2.2 K. Above this temperature the fluctuations of the magnetic moments induce strong relaxation of the nearby Cu(2) nuclei but leave the Cu(1) sites undistorted. Below the Neel temperature, however, the ordered moments influence both sites only weakly [7].

With decreasing x, $6.9 < x < 7.0$ the Cu(1) and Cu(2) lines become broader due to the creation of oxygen vacancies in the Cu(1)–O layer. The increase of the linewidth was found to be in agreement with a random distribution of the defects [13]. At $x < 6.9$ the spectra develop into a more complicated structure [3,4,5] which is the topic of our investigation.

In the antiferromagnetic compound with low oxygen concentration the narrow lines are found again. For $x = 6.0$ only the NQR lines of Cu(1) with two oxygen neighbours, Cu(1)2, exist (30.1 MHz). At slightly increased x, a second NQR line at 24.0 MHz appears which has been attributed to the Cu(1) sites with one oxygen neighbour in the chain, $Cu(1)_3$ [6]. This line was observed in a very broad region of the oxygen concentration $6.1 < x < 6.8$ [4]. The NQR spectrum of the Cu(2) sites is missing in the antiferromagnetic region since these sites carry the ordered magnetic moments leading to the hyperfine field at the copper nucleus. From the AFNMR spectrum in the region of 90 MHz [14] a quadrupole splitting corresponding to a frequency of 23.2 MHz is deduced which was found also above the Neel temperature by NMR in an external field only slightly shifted to 23.8 MHz [15].

5. Cu(1) Spectra

We have used the $GdBCO_x$ samples in order to separate the signals of the Cu(1) sites from the Cu(2) site spectrum. At 4.2 K the NQR signal (Fig.1) contains only the Cu(1) signal since the Cu(2) nuclei are distorted severely by the fluctuations of the nearby magnetic moments of the Gd ions. At 1.2 K below the Neel temperature of the Gd spins, however, the full spectrum of both layers is observed. It is evident that the Cu(1) spectrum contains the sharp lines whereas ths Cu(2) spectrum is so broad, that the contributions of the two isotopes are not separated. The comparison of the spectra at both temperatures for lower x shows that no signal of the Cu(2) layers exists below 25 MHz and no Cu(2) resonance can be observed in samples with low x showing T_c values below the region of the 60 K plateau.

Fig. 1: NQR spectrum of $GdBa_2Cu_3O_{6.75}$ (sample # C7) at 4.2 and 1.2 K.

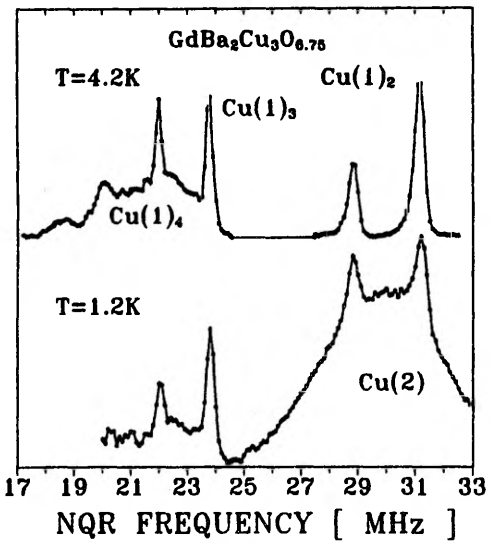

Fig. 2: NQR spectra of the Cu(1) sites in $GdBa_2Cu_3O_x$ measured at 4.2 K for samples C1, C2, C5, C7, and C8. Each value of the EFG leads to a doublet for the ^{63}Cu and the less abundant ^{65}Cu isotopes. The doublets with the ^{63}Cu line between 30 and 31.5 MHz belong to $Cu(1)_2$, those at 24 and 22.5 MHz to $Cu(1)_3$ and $Cu(1)_4$, respectively. Whereas the lines of $Cu(1)_3$ and $Cu(1)_2$ are relatively sharp at all x, $Cu(1)_4$ broadens severely for $x < 7$.

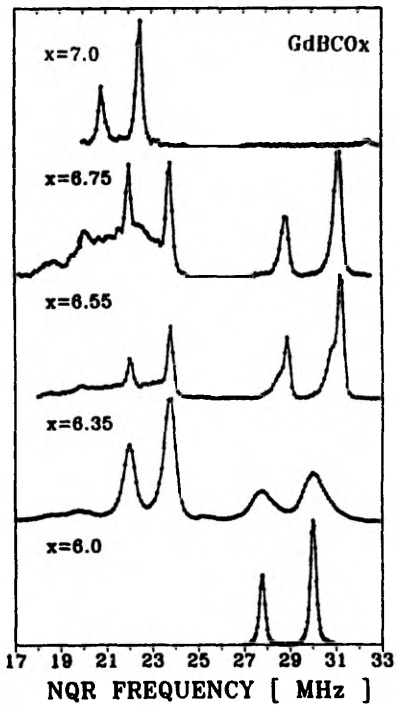

The Cu(1) spectrum in Fig.1 contains two narrow lines for ^{63}Cu at 31.2 and 23.8 MHz. Since they are near to the corresponding lines found at low x, we attribute these lines to the twofold and threefold coordinated Cu(1) sites, $Cu(1)_2$ and $Cu(1)_3$, respectively. Correspondingly, the broader structure below 22.5 MHz is assigned to the $Cu(1)_4$ site. In most samples we found also a line at about 20 MHz. Since the transverse ralaxation times of all these lines are similar (about 0.2 ms at 4.2 K) we assume that the structure at about 20 MHz must belong to the $Cu(1)_4$ site, too, most probably to sites in short chain segments.

The characteristic NQR spectra of Cu(1) in $GdBCO_x$ (Fig. 2.) show the change of the spectra with the oxygen concentrations x. The corresponding spectra of $YBCO_x$ compounds are quite similar with only a small shift of the frequencies, but mixed with the signal of the Cu(2) layers. In the high frequency region the spectra consist in the samples with x between 6.6 and 6.8 of a single line of ^{63}Cu at the frequency 31.2 MHz in $GdBCO_x$ and 31.5 MHz in $YBCO_x$. At x below about 6.55 two more lines appear and the spectra exhibit three lines A, B, and C at the frequencies 31.2, 30.9 and 30.2 MHz, respectively, in the case of GdBCO, and at 31.5, 30.9 and 30.4 MHz for YBCO (Fig. 3). With further decreasing x the spectra become broader and the fine structure disappears.

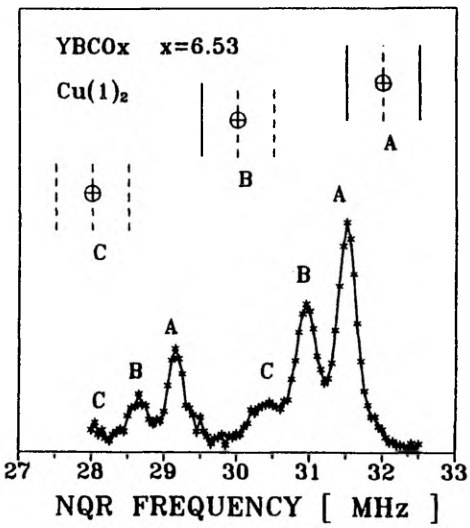

Fig. 3: NQR spectrum of the Cu(1) sites with twofold oxygen coordination in $YBa_2Cu_3O_{6.53}$ sample A4) with explanation of sites A between two full chains, B and C with one or two neigh bouring empty chains, respectively.

Different authors [3,4,5] have recorded similar data about the change of the NQR spectra around 30 MHz in this range of x, but with different explanations. The comparison of YBCO and GdBCO proves that all three lines belong to the Cu(1) sites. The threefold spectrum has been found at different nominal values of the oxygen concentration x, e.g. in a sample with x = 6.4 and T_c = 40 K studied earlier by neutron diffraction [16]. In all cases the lines A, B, and C were found together in one sample only if it was superconducting with T_c below 50 K.

Three different configurations of the twofold coordinated $Cu(1)_2$ site can be found easily in a model which assumes that the oxygen ions are ordered with either

filled or empty chains. We assign the single line A, the only one seen in the spectra of the compounds with $x > 6.6$, to the $Cu(1)_2$ sites between two intact chains as shown in Fig. 3. Then the line B must be ascribed to the $Cu(1)_2$ sites between an intact and an empty one, and the line C to the $Cu(1)_2$ sites between two empty chains. Since the frequency of line C is only 0.2 MHz larger than the frequency of $Cu(1)_2$ at $x = 6.0$, our assignment is confirmed.

The evolution of the NQR spectra at lower oxygen concentration is seen most clearly in the measurements at 77 K by Serikov et al. [3] where with decreasing x from 6.44 to 6.13 the main intensity moves from the line A through line B to the line C. We attribute the broadening observed at $x < 6.5$ in our measurement at 4.2 K to the onset of the localization of the electronic spins at the Cu(2) sites. In the AF structure of pure YBCO with $x = 6.0$ the magnetic interactions of the Cu(1) sites with the two neighbouring Cu(2) planes are canceled exactly by symmetry [7]. If at increasing x the number of defects in the AF structure increases as is seen in the broadening of the AFNMR spectra at 90 MHz [16], the dipolar and transferred hyperfine fields are no longer canceled at the Cu(1) sites and cause the observed broadening of the NQR lines. This effect must disappear above the Neel temperature of the Cu(2) planes. Since Tn becomes low near $x = 6.4$, the spectra recorded at higher temperature [3,5] are not influenced by the disorder of the antiferromagnetic state.

6. Correlation time of the Cu(2) spins

The sequence of NQR spectra at decreasing x shows the development of the magnetic state at the Cu(2) sites in three steps: i) In the region of the 60 K plateau of T_c and at higher x the rate of the spin fluctuations is so large that the NQR lines at the Cu(1) and Cu(2) sites are not distorted. The influence of the fluctuations is important, however, for the spin–lattice relaxation. ii) The spin fluctuations become slower at the lower end of the 60 K plateau and cause the disappearing of the Cu(2) signal due to the fast nuclear relaxation, but do not yet distort the Cu(1) signal. iii) The onset of magnetic order in the Cu(2) layer becomes evident from the broadening of the Cu(1) NQR lines in samples with x reduced so much that they are no longer superconducting. Another indication of the onset of magnetism is found in the T_2 measurements of $GdBCO_x$, where the Cu(1) sites can be studied separately. Here we found a nonexponential magnetization decay of the Cu(1) lines in the samples $x = 6.50$ and $x = 6.39$ with a superposition of fast and slow relaxation rates. This inhomogeneous relaxation at the Cu(1) sites can be explained assuming an additional relaxation path due to slowly fluctuating spins distributed inhomogeneously in the Cu(2) layers.

7. Intensity distribution of the Cu(1) lines

The best proof of the site assignment of the NQR lines in the systems $YBCO_x$ and $GdBCO_x$ can be a reasonable intensity distribution of the Cu(1) lines belonging to the sites with two, three, and four nearest oxygen neighbours. In order to get a quantitative estimate of the intensity distribution of the Cu(1) lines we simulated the normalized experimental spectra by pairs of the $^{63}Cu/^{65}Cu$ lines. The relative intensities of $Cu(1)_2$ (I2), $Cu(1)_3$ (I3), and both components of $Cu(1)_4$ (I4* and I4**, see section 5) for all samples evaluated are given in Tab.1.

The variation of the intensity for the three configurations at increasing x in the series A of $YBCO_x$ of uniform preparation and in series C of $GdBCO_x$ reveal the general trend of increasing I4 = I4* + I4** and decreasing I2 and I3. The reliability of the relative intensities can be checked by the oxygen concentration z in the Cu(1) layer which is determined by

$$z = I4 + I3/2, \quad I4 = I4^* + I4^{**}. \tag{1}$$

The relation z = x–6 is fulfilled in nearly all samples within the limit of accuracy (± 0.1) by which x and the intensities are determined (Tab.1), but the generally too small values of z show that the intensity I2 has been overestimated systematically at x > 6.5. The reason may be connected with problems of separating the $Cu(1)_2$ from the Cu(2) signal and with the correction for T_2. It is evident that the component at 20 MHz with the intensity I4* must belong really to the fourfold coordinated Cu(1), otherwise the value of z would be even smaller.

A random occupation of the O(1) sites in the Cu(1) chains by oxygen would lead to relative intensities depending on z as follows:

$$I2=(1-z)^2, \quad I3 = 2z(1-z) \quad \text{and} \quad I4 = z^2 . \tag{2}$$

This is evidently not the case in Tab.1. The intensity I3 is too small by more than a factor 2 for all samples with x near 6.5. This is a first clear indication for the development of a non–random structure with long chain fragments in the region x = 6.5.

From the relative intensities we can estimate the average length of the chain fragments. The average number of oxygen atoms, n, in one chain fragment is simply determined by the ratio of the number of copper atoms within the chains, I4, and the number of the atoms terminating the chains, I3, by

$$n = 1 + 2(I4/I3) \tag{3}$$

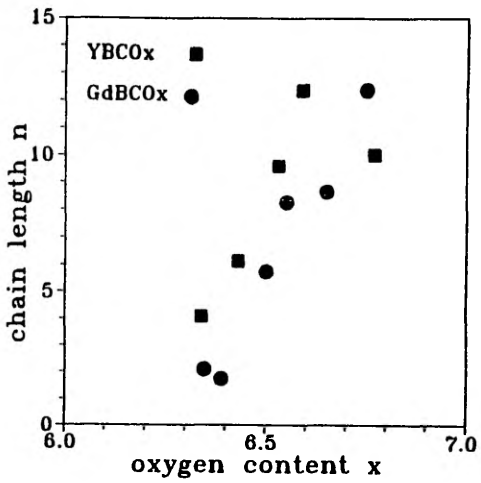

Fig. 4: Mean length of oxygen chains in $YBa_2Cu_3O_x$ and $GdBa_2Cu_3O_x$ versus x.

The values of n increase with x in $GdBCO_x$ and $YBCO_x$ as shown in Tab. 1 and in Fig. 4. The smaller values of n in $GdBCO_x$ at the same x compared with $YBCO_x$ can be caused by the different preparation method in the two systems, but in any case a strong increase of n is seen when x approaches 6.5. This is a clear evidence for the development of the ortho–II structure with filled and empty chains. Superconductivity appears in the samples with $n > 6$. The largest values of the chain length between 10 and 13 are found for $x > 6.5$.

8. Cu(2) spectra

The NQR spectra containing of the ^{63}Cu and ^{65}Cu lines of Cu(2) and $Cu(1)_2$ (Fig. 1 for 4.2 K) are too complicated for the analysis of the Cu(2) resonances. We found, that the changes in the local environment of the Cu(2) sites in $YBCO_x$ due to the oxygen depletion can be followed better in the field sweep NMR spectra. We have measured these spectra of the uniaxially oriented samples with the crystallographic c–axis either parallel or perpendicular to the external magnetic field. The latter case is suitable also for the usual, previously not oriented powder samples which turn out to be perfectly oriented with the c–axis perpendicular to H in the superconducting state [6]. The spectrum, given in Fig.5 shows the full field sweep

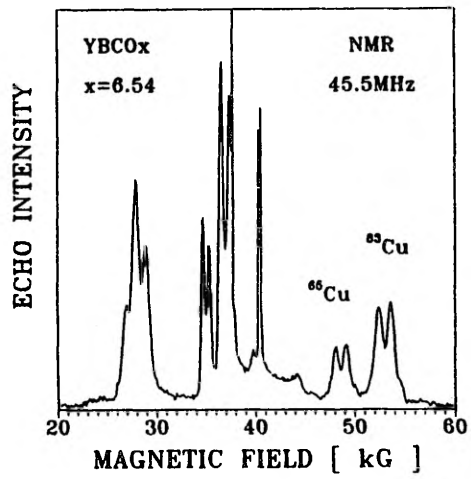

Fig. 5: NMR spectrum of $YBa_2Cu_3O_{6.54}$ (sample B2) at 4.2 K measured at 45.5 MHz, with the magnetic field applied perpendicular to the c–axis.

spectrum of the sample B2. Here the self–orientation of the superconducting grains in the magnetic field is seen from the well resolved lines. The spectrum shows the resonances from the two copper isotopes clearly separated in the high field satellite region as a result of the higher gamma value and a smaller quadrupolar shift of the isotope ^{65}Cu, but overlapping in the low field satellite. The most surprising result in this spectrum is the splitting of the Cu resonance with two lines of equal intensity and slightly different quadrupole coupling. In our NQR spectra the two lines are seen in the fit of the broad Cu(2) spectrum below the $Cu(1)_2$ signal with NQR frequencies of 30.8 and 27.7 MHz in agreement with results of Warren et al. for a

sample with a single Cu isotope [18] and Shimizu et al. [19]. From the Cu(1) sites only the $Cu(1)_2$ contribution is seen as a shoulder at the high field side of the doublet, whereas the resonances of $Cu(1)_4$ and $Cu(1)_3$ sites are smeared over a large region of the spectrum as expected due to the strong asymmetry of the EFG tensor of these sites [6].

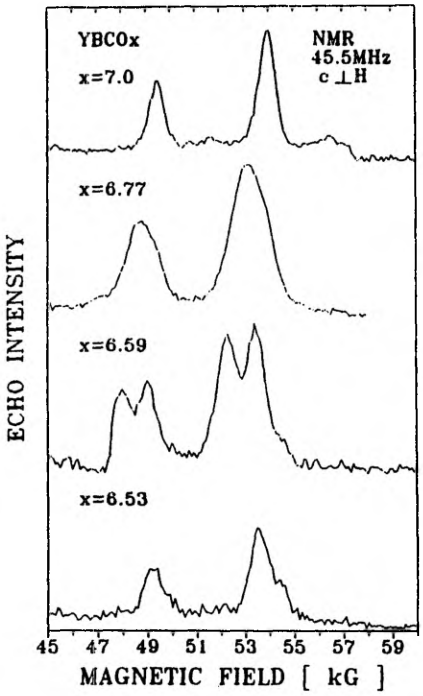

Fig. 6:The high–field satellite in the NMR spectrum of $YBa_2Cu_3O_x$ at different x measured at 40 MHz for the magnetic field perpendicular to the c–axis (samples A4, A5, A6, A7).

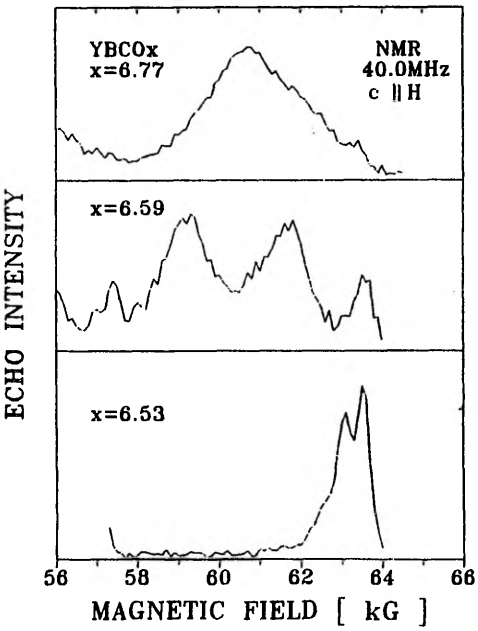

Fig. 7: The high–field satellite in the NMR spectrum of $YBa_2Cu_3O_x$ at different x measured at 40 MHz for the magnetic field applied parallel to the c–axis (samples A4, A5, A6)

The change of the NMR spectra in the region of the high–field satellite at decreasing x for grain oriented powder samples is shown for the magnetic field perpendicular and parallel to the c–axis in Figs. 6 and 7, respectively. The spectra for the perpendicular field reveal a continuous shift of the Cu(2) resonances to lower fields corresponding to lower NQR frequencies at x decreasing from 7.0 to 6.77 and the splitting around x = 6.59. The single line for x = 6.53 shifted again to higher field belongs to the Cu(1) resonances according to the interpretation of the spectra measured for the field parallel to the c–axis (Fig.7). Here the spectrum of the x = 6.59 compound shows again the splitting of the Cu(2) resonance. Another line is found at higher field which is the only component remaining at x = 6.53. The splitt-

ing of this line into three components in the NQR spectrum of Fig.3 identifies these as the contributions of $Cu(1)_2$ (A,B,C). Thus this spectrum proves again that the resonance of the Cu(2) sites disappears in superconducting samples of low x with T_c values below the 60 K plateau. The main advantage of the NMR spectra in this case is the separation of the Cu(2) and $Cu(1)_2$ contributions by different values of the orbital Knight shift at the two sites [19].

The splitting of the Cu(2) line is found in all samples with $x < 6.7$ but disappears at larger x. We did not find any indication for a continuous transition between these spectra like a change of the relative intensities of both peaks or a line shift, only the intensity between the peaks changes and is lower in the annealed sample B2 than in the quenched one B3. Thus it seems that the spectra at larger x consist of the superposition of the split ($x = 6.55$) and the unsplit ($x = 6.8$) components. This is most obvious in a spectrum published recently by Takigawa et al. for $x = 6.63$ [20].

9. Order of Oxygen in the Cu(1) Layers

The evaluation of the chain length n from the different components of the Cu(1) spectrum has already proved, that a random occupation of the O(1) sites in the Cu(1) plane does not exist in our samples. The spectra of the Cu(1) and Cu(2) sites in samples with x slightly higher than 6.5 can be described perfectly in the model of the ortho–II structure with every second chain filled: The two Cu(2) lines show two different Cu(2) sites to exist connected with "full" and "empty" chains, respectively. Here we assume that the line at higher field which means with the larger EFG, corresponds to the Cu(2) sites near the full chains, since it agrees nearly with the line for $x = 7$. In the same region the spectrum of $Cu(1)_2$ contains only the line A which we assigned to the sites in "empty chains" between "full" chains. As expected in the case of the pure ortho–II structure, this line represents nearly one half of all Cu(1) sites (Tab.1).

The Cu(1) resonance reveals the details about the correlation length in this structure. The average length of the "full" chains is rather short, about 10 oxygen ions per chain as shown by the large intensity I3 of the terminating $Cu(1)_3$ ions. This means that the number of defects in this structure is high and the coherence length can be small. Since all information we can gain from counting the different sites, concerns only the arrangement of the oxygen ions in the Cu(1) plane and not the sequence of the planes along the c–axis, we cannot prove the existence of a three dimensional order.

Above and below $x = 6.5$ the filling of the Cu(1) layer with the oxygen ions can be modeled in different ways. One group of models is based on the ortho–II structure with every other chain either empty or partly filled for $x < 6.5$ and either full or partly filled at $x > 6.5$. Within the partly filled chains different arrangements have been proposed, e.g. a random distribution [21], the condition of maximal distance between the oxygen ions [22], or ordered superstructures at multiples of $x–6 = 0.125$ [23]. These models show different dependence of the chain length on x (Fig.8). But they agree in the general behavior that after the divergence at $x = 6.5$, n becomes smaller again to about 6 at $x = 6.7$ by the formation of the new chains. At larger x, n does not differ much from the values expected for the random distribution.

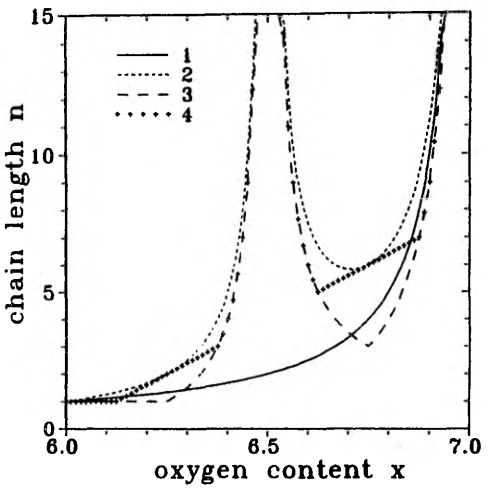

Fig. 8: Mean length n of chains calculated for different models of the arrangement of the oxygen ions on the O(1) sites in the Cu(1) plane
1: random distribution (diluted ortho–I)
2: ortho–II with random filling of the "diluted" chains [21]
3: ortho–II with maximal distance in the "diluted" chains [22]
4: ordered structures based on ortho–II with larger unit cell [23].

The experimental data in Tab.1 and Fig. 4 show no decrease of n for $x > 6.5$ which means that the oxygen ions entering the ortho–II structure form chains of the same length as in pure ortho–II. This may happen in two ways: the first is the formation of domains of ortho–I in coexistance with ortho–II [24], the second means ordered sequences of full and empty chains like ortho–III with one empty and two filled chains [25]. This second model can be excluded from the Cu(2) spectra since in this case the intensity of the line corresponding to the filled chains should increase at the cost of the other line. The spectra, however, show the ortho–II lines together with the broadened ortho–I line corresponding to the coexistence of the pure ortho–II structure with the oxygen depleted ortho–I of about $x = 6.8$.

In the range below the "60 K plateau" only the Cu(1) signal can be observed at least at the low temperatures of our experiment, 4.2 and 1.2 K. Here two features are evident: the decrease of the mean chain length n (Fig.4) calculated from the relative intensities of the $Cu(1)_3$ and $Cu(1)_4$ components in the spectrum, and the appearance of the lines B and C of $Cu(1)_2$ besides line A (Fig.3). As found already by Serikov et al. [3] the superconductivity disappears in the samples where the line A is missing in the NQR spectrum. Assuming an ideal arrangement of the oxygen in full and empty chains, one can see that for a structure with every third chain occupied ($x = 6.33$) only the line B would be seen, for every fifth chain occupied ($x = 6.2$) the lines B and C with equal intensities. In our not superconducting samples A2 and C2 ($x = 6.35$), the intensity of the $Cu(1)_2$ resonances is already shifted to the line C. This means, that the empty chains belong mainly to clusters with $x < 6.2$ and a considerable amount of the oxygen is arranged in clusters of larger x. In contrast, the NQR spectrum of the weakly superconducting sample B1 produced by long annealing ($x = 6.3$, $T_c = 20$ K) shows 25% intensity of the $Cu(1)_2$ resonances in the line A and 60% in B and, consistent with that, a large mean value of the chain length n. Thus we find that the main effect of the annealing in this region of the oxygen concentration is to resolve the clusters with large x, and to create long chains in the whole sample. Accordingly the condition for the onset of superconductivity is that the filled chain fragments with a length of about 6 are attached to filled fragments at the next nearest chain, that means the existence of

extended regions of the ortho–II structure. In agreement with this result, domains of the ortho–II structure have been found also by neutron scattering in a superconducting single crystal with $T_c = 38$ K and $x = 6.4$ [26].

In a non superconducting crystal with $x = 6.35$ a different oxygen structure containing only isolated oxygen ions has been found by neutron [27] and X–ray [28] diffraction. This structure would lead to an intensity for the $Cu(1)_3$ sites, I3, of 70 %. As we found maximal values for I3 of only 45 % (Tab.1), this arrangement cannot be the dominant part in any of our samples. The intensity of the superstructure reflexes in both diffraction experiments, however, is small and corresponds to only 12 % of the total crystal[28]. Therefore the results from diffraction and NQR are not really contradictory.

10. The Antiferromagnetic State of $YBa_2Cu_3O_x$

In the antiferromagnetic state the hyperfine field of 7.95 T at the Cu(2) sites [14] is an indication of the magnetic order at these sites. It is independent of the oxygen concentration [17]; but above $x = 6.2$ the intensity of the AFNMR spectrum decreases due to the distortion of the antiferromagnetic coherence. The antiferromagnetic spin structure of pure YBCO is determined by three AF exchange

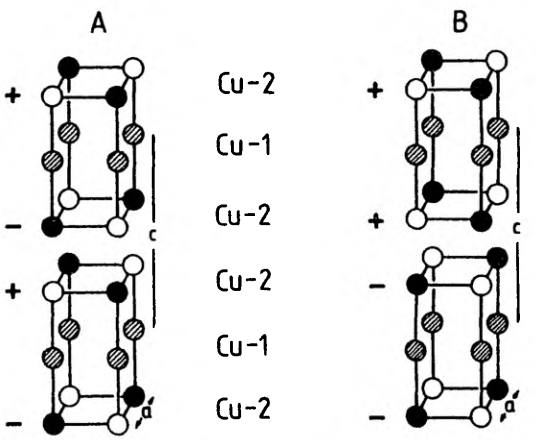

Fig. 9: The two different AF structures of Cu in 123 compounds with different stacking sequences of the magnetic Cu(2) layers.
A: structure of pure samples without a local magnetic field at Cu(1) sites.
B: structure in Fe doped samples allowing a dipolar and transferred hyperfine field at Cu(1).

coupling constants [29]: the coupling of the nearest neighbor Cu(2) spin within the layers, $J = 1700$ K, between the two planes of a bilayer, $J_b > 10^{-2}J$, and a very weak one between the bilayers, $J' = 10^{-5}J$. By this symmetry (Fig. 9a) the local fields from the Cu(2) ions, either the dipolar or the transferred hyperfine fields, disappear at the Cu(1) sites as is seen from the narrow NQR lines of Cu(1) with two or three oxygen neighbors, $Cu(1)_2$ and $Cu(1)_3$, respectively (Fig. 2). From the

linewidth follows an upper limit for a local field of less than 0.05 T at x = 6.3 which decreases to 0.02 T at x = 6.0.

The magnetic structure becomes different at low temperature, if the material is doped by about 1% of Fe. In this case a splitting of the $Cu(1)_2$ line [30] appears at 4.2 K caused by a field of 0.16 T perpendicular to the c–axis (Fig. 10). We have found the same splitting also for other trivalent ions, Al and Ga [7] which mainly enter the Cu(1) sites, but not for the divalent ions Zn and Ni, which probably occupy only the Cu(2) sites. Kumagai et al. [31] reported a different influence of impurities: split lines for magnetic Fe, Co, and Ni ions and unsplit lines for Al and Zn.

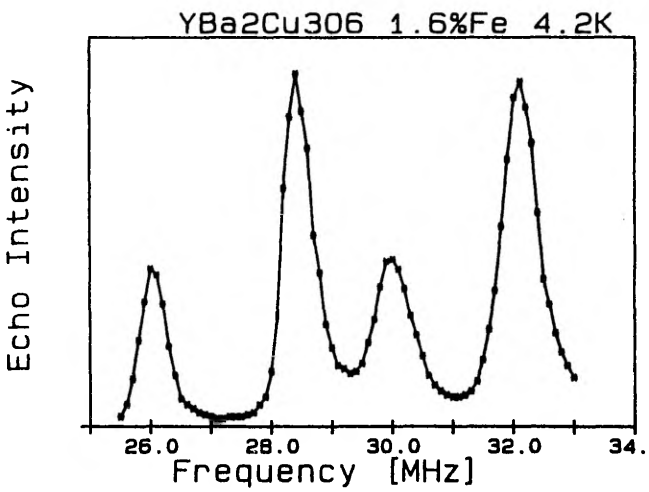

Fig. 10:
NQR spectrum of the Cu(1) site in $YBa_2(Cu_{1-x}Fe_x)_3O_6$ with x = 0.016 Fe at 4.2 K showing the Zeeman splitting by a field of 0.16 T.

The reason of the local field at the Cu(1) ions is a changed stacking sequence of the AF Cu(2) layers which has been found also by neutron diffraction in single crystals of YBCO [32] and NdBCO [33]. In the new structure the magnetic moments of the two Cu(2) ions neighboring a Cu(1) ion are directed parallel (Fig. 9b) that means the stacking sequence is changed from +o–+o– to +o+–o–, where "+" and "–" represent the directions of the Cu(2) spins and "o" the zero moment of Cu(1). In this way the AF unit cell is doubled in c–direction as seen by neutron diffraction, and the field contributions from the Cu(2) moments do no longer cancel each other at the Cu(1) sites. The ordered Cu(2) magnetic moment of 0.7 μ_B leads to the dipolar field of only 0.02 T (the earlier estimate [7,30] was too large) and the main contribution to the local field must be a transferred hyperfine field of about 0.1 T mediated by each apex oxygen ion. The transferred hyperfine field by the interaction of two Cu(2) neighbors in the layer has been estimated to about 2 T [19]. This means, that the hyperfine interaction Cu(1)–O–Cu(2) is only one order of magnitude smaller than the in plane Cu(2)–O–Cu(2) interaction. The ratio of interlayer to intralayer hyperfine interaction is asthonishingly large compared with the small ratio of the corresponding components of the exchange interaction [29].

The comparison of the AFNMR spectra of the two structures shows the same hyperfine field [34] which means that the change of the stacking sequence has no influence on the ordered magnetic moments of the Cu(2) sites. The transition between both structures has been studied for doping with Fe (Fig. 11). At increasing temperature the local field decreases continously without a coexistence of split and unsplit components in the spectrum, and disappears far below the Neel temperature of about 400 K [30]. Thus the transition at increasing temperature can be described in the easiest way as a turning of the staggered magnetization of the two planes neighboring the Cu(1) layer from parallel to antiparallel orientation with an intermediate canted spin structure.

The reason for the change of the spin structure is still unclear. According to our measurements a magnetic effect can be excluded since also the nonmagnetic ions Al and Ga show the same influence. One explanation may be that the very weak antiferromagnetic interaction in the chain Cu(2)–O–Cu(1)–O–Cu(2) is modified by a trivalent ion on the Cu(1) site into a stronger ferromagnetic one. Since the interaction within the Cu(2) planes is much stronger, a small number of ferromagnetic links can turn the staggered magnetization in the whole structure. In the case of the very low doping by 0.2 % Fe (Fig. 11) the ferromagnetic interaction is not strong enough and the canted state with a lower local field persists down to 1.2 K.

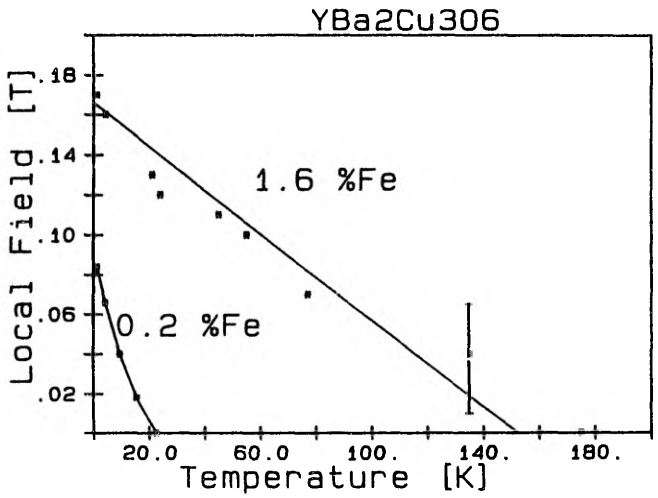

Fig. 11: Temperature dependence of the Zeeman splitting in $YBa_2(Cu_{1-x}Fe_x)_3O_6$ for x = 0.016 and 0.002.

The unsplit lines in pure AF YBCO and GdBCO with x > 6.0 (Fig. 2) show that the oxygen in the chain sites and the neighboring Cu(1) ions do not change the magnetic structure. The situation of NbBCO, however, is still unclear. In this case we have found only one sample with x = 6.0 showing the "normal" unsplit Cu(1) spectrum, whereas four other samples revealed the split spectrum like the Fe doped samples and thus confirm the result from neutron diffraction of the different ground-state of NdBCO [33]. As it seems to be possible that, depending on the conditions of preparation, Nd partly replaces the Ba ions, this may be another way to introduce ferromagnetic couplings into the YBCO structure. In any case, however, the small local field at the Cu(1) sites proves that the expectation value of the magnetic

moments at Cu(1) is extremely small in contrast to the value of about 0.4 μ_B deduced from the neutron spectra [32]. Assuming an hyperfine coupling constant of 10 T/μ_B and the full field found at Cu(1) as an on–site hyperfine field, the upper limit of a static magnetic moment at Cu(1) would be only 0.02 μ_B.

11. Summary

We have discussed the change of the magnetic state of the Cu(2) ions and of the arrangement of the oxygen ions in the Cu(1) plane in YBCOx when the oxygen concentration x increases from 6 to 7. The maim information comes from the fact, that Cu(1) ions with different oxygen concentration can be distinguished by the EFG values generated by the surrounding ions. The second source of information is the NQR signal of the Cu(2) sites which is influenced by the oxygen ions in the Cu(1) plane, too. In our measurements at 4.2 K and 1.2 K the NMR and NQR resonance of Cu(2) can be observed only in samples with $x > 6.5$ i.e.in samples where T_c is in the region of the 60 K plateau or higher.

For the $3d^9$ state of the Cu^{2+} ions at the Cu(2) sites a magnetic moment is expected. This moment is evident in the antiferromagnetic state at low x [14]. A fluctuating magnetic moment with strong antiferromagnetic correlations is assumed generally to explain the temperature dependence of the spin–lattice relaxation rate of the Cu(2) sites of samples in the 60K plateau and at larger x [20]. When the Cu(2) signal disappears in samples with lower Tc this must be due to the slowing down of the magnetic fluctuations, but without freezing in of the Cu(2) spins in a spin–glas or antiferromagnetic state. This is proved by the narrow linewidth of the NQR lines of Cu(1) in all samples which reveal the superconductivity. Frozen spins are detected by the broadening of the Cu(1) line only in samples which do not become superconducting. The development of the antiferromagnetically ordered state with defects is evident from the broadened AFNMR spectrum of the Cu(2) sublattice at about $x = 6.3$ [17]. The NQR and AFNMR spectra become narrow near $x = 6.0$ without a change of the hyperfine field at the Cu(2) sites. This means that introducing a small amount of oxygen into the Cu(1) plane distorts only the magnetic order in the Cu(2) plane without changing the localized magnetic moment.

The NQR lines of all configurations of the Cu(1) sites reveal no magnetic splitting and prove that the time average of the magnetic moment of the Cu(1) sites is zero at any oxygen concentration. A small local magnetic field is induced at the Cu(1) sites, however, in antiferromagnetic samples doped with some trivalent ions like Fe, Al, or Gd which modify the stacking sequence of the antiferromagnetically ordered Cu(2) planes at low temperature [7].

The dependence of the relative intensities of the different configurations of the Cu(1) ions on the oxygen concentration x proves a non–random distribution of the oxygen ions on the chain sites and the existence of the ortho–II structure near $x = 6.5$ with alternatively filled and empty chains. In the region of the 60 K plateau the average length of these chains is about 10 to 13 oxygen ions per chain. At higher x the coexistance of the ortho–II with the ortho–I structure containing only filled chains is the best description of our results. At low x superconductivity disappears when the chain length is below 6 and no extended domains of the ortho–II structure exist.

12. Acknowledgement

We are indebted to many colleagues who supplied the samples used for this investigation, especially to A. Janossy and L. Bottyan, Budapest, G. Krabbes, Dresden, and M. Buchgeister, Bonn. Financial support by the BMFT through the DAAD is acknowledged. I.H. likes to thank Prof. Zinn for the hospitality he received at the KFA.

13. References

1. R.J. Cava, A.W. Hewat, E.A. Hewat, B. Batlogg, M. Marezio, K.M. Rabe, J.J. Krajewski, W.F. Peck Jr. and L.W. Rupp Jr., Physica C 165 (1990) 419.
2. H. Claus, S. Yang, A.P. Paulikas, J.W. Downey and B.W. Veal, Physica C 171 (1990) 205.
3. V.V. Serikov, A.M. Bogdanovich, S.V. Verkhovskii, Yu.I. Zhdanov, B.A. Aleksashin, K.N. Mikhalev, V.L. Kozhevnikov, and S.M. Chesnitskii, JETP Lett., 47 (1988) 534.
4. H. Yasuoka, T. Shimizu, T. Imai and S. Sasaki, Hyperfine Int. 49 (1989) 167.
5. A.J. Vega, W.E. Farneth, E.M. McCarron and R.K. Bordia, Phys. Rev. B39 (1989) 2322.
6. H. Lütgemeier, Physica C 153–155 (1988) 95.
7. H. Lütgemeier and I. Heinmaa, Proc. of XXVI Zakopane School on Physics, Zakopane, 1991, eds. J. Stanek and A.T.Pedziwiatr, (World Scientific, 1991, p.264).
8. T.P. Das and E.L. Hahn, Solid State Physics Suppl.1, F. Seitz and D. Turnbull eds., (Academic Press, New York 1958).
9. A. Janossy, A. Rockenbauer, S. Pekker,G. Oszlonyi, G. Faigel and L. Korecz, Physica C 171 (1990) 457, S. Pekker, A. Janossy, and A. Rockenbauer, Physica C 181 (1991) 11.
10. G. Krabbes, W. Bieger, J. Thomas, P. Verges and H. Lütgemeier, Physica C190 (1992), to be published.
11. M. Buchgeister, P. Herzog, S.M. Hosseini, K. Kopitzki and D.Wagener, Physica C178 (1991) 105.
12. M. Mali, D. Brinkmann, L. Pauli, J. Roos and H. Zimmermann, Phys. Lett. A124 (1987) 112.
13. H. Schiefer, M. Mali, J. Roos, H. Zimmermann, D. Brinkmann, S. Rusiecki and E. Kaldis, Physica C 162–164 (1989) 171.
14. P. Mendels and H. Alloul, Physica C 156 (1988) 355; H. Yasuoka, T. Shimizu, Y. Ueda, and K. Kosuge, J.Phys.Soc.Jpn 57 (1988) 2659; Y. Yamada, K. Ishida, Y. Kitaoka, K. Asayama, H. Takagi, H. Iwabuchi, and S. Uchida, J.Phys.Soc.Jpn 57 (1988) 2633.
15. M. Mali, I. Mangelschots, H. Zimmermann and D. Brinkmann, Physica C 175 (1991) 581.
16. B. Rupp, P. Fischer, E. Pörschke, R.R. Arons, and P. Meuffels, Physica C 559 (1988).
17. M. Matsumura, H. Yamagata, Y. Yamada, K. Ishida, Y. Kitaoka, K. Asayama, H. Takagi, H. Iwabuchi, and S. Uchida, J.Phys.Soc.Jpn 57 (1988) 3297; P. Mendels, H. Alloul, J.F. Marucco, J. Arabski, and G. Collin, Physica C 171 (1990) 429.

18. W.W. Warren, Jr., R.E. Walstedt, G.F. Brennert, R.F. Bell, G.P. Espinosa and R.J. Cava, Physica C 162–164 (1989) 179.
19. T. Shimizu, H. Yasuoka, T. Tsuda, K. Koga and Y. Ueda, Bull. Magn. Res. 12 (1990) 39.
20. M. Takigawa, A.P. Reyes, P.C. Hammel, J.D. Thompson, R.H. Heffner, Z. Fisk, and K.C. Ott, Phys.Rev.B 43 (1991) 247.
21. B.W. Veal and A.P. Paulikas, Physica C 194 (1991) 321.
22. J. Zaanen, A.T. Paxton, O. Jepsen and O.K. Andersen, Phys. Rev. Letters, 60 (1988) 2685.
A. Latge, E.V. Anda and J.L. Moran–Lopez, Phys. Rev.B 42 (1990) 4288).
23. M.A. Alario–Franko, C. Chaillout, J.J. Capponi, J. Chenavas and M. Marezio, Physica C 156 (1988) 455.
24. C.F. Poulsen, N.H. Andersen, J.V. Andersen, H. Bohr and O.G. Mouritsen, Nature 349 (1991) 594.
25. G. Ceder, M. Asta and D.de Fontaine, Physica C 177 (1991) 106.
26. Th. Zeiske, R. Sonntag, D. Hohlwein, N.H. Andersen, and Th. Wolf, Nature 353 (1991) 542.
27. R. Sonntag, D. Hohlwein, T. Bröckel, and G. Collin, Phys.Rev.Lett. 66 (1991) 1497.
28. Th. Zeiske, D. Hohlwein, R. Sonntag, F. Kubanek, and G. Collin, Z.Phys. B 11 (1992) 15.
29. P. Burlet, this conference; J. Rossat–Mignod, L.P. Reynault, M.J. Jurgens, C. Vettier, P. Burlet, J.Y. Henry, and G. Lapertot, Physica C162–164 (1989) 1269.
30. R.A. Brand, Ch. Sauer, P.M. Meuffels, Hyperfine Int. 55 (1990) 1229; H. Lütgemeier, Hyperfine Int. 61 (1990) 1051.
31. K. Kumagai, T. Takatsuka and A. Yammaka, JMMM 104–107 (1992) 577.
32. H. Kadowakai, M. Nishi, Y. Yamada, H. Takeya, H. Takei, S.M. Shapiro, and G. Shirane, Phys. Rev. B37 (1988) 7932.
33. W.H. Li, J.W. Lynn, and Z. Fisk, Phys. Rev. B41 (1990) 4098.
34. L. Bottyan, H. Lütgemeier, J. Dengler, S. Pekker, A. Rockenbauer, A. Janossy and D.L. Nagy, Electronic Properties of High–T_c Superconductors, eds. H. Kuzmany, M. Mehring and J. Fink (Springer 1990, p. 230).

III

H. Lütgemeier, I. Heinmaa, and A. V. Egorov,
Study of Oxygen Ordering in HT_c Superconductors by Magnetic Resonance of Different Nuclei, Physica Scripta, **T49**, pp. 137–142 (1993).

Physica Scripta. Vol. T49, 137–142, 1993

Study of Oxygen Ordering in HT_c Superconductors by Magnetic Resonance of Different Nuclei

H. Lütgemeier and I. Heinmaa*

KFA Jülich/Germany

and

A. V. Egorov

Kazan State University Kazan/Russia

Received March 29, 1993; accepted March 31, 1993

Abstract

NMR of ^{169}Tm and NQR/NMR of ^{63}/^{65}Cu was applied to investigate the order of oxygen in the HT_c superconductors of the type $RBa_2Cu_3O_x$. From the spectra of three different lattice sites, one for Tm and two for Cu, it is evident, that three ordered structures exist: tetra for $x = 6.0$, ortho-II for $x = 6.5$ and ortho-I for $x = 7.0$. No other ordered structures could be detected. A coexistence of ortho-I and -II is evident in a wide region between 6.6 and 6.8. The existence of extended domains of ortho-II is essential for the onset of superconductivity. In the tetragonal region below 6.3 we find mainly insulated oxygen ions in the Cu(1) plane; in superconducting samples of the 60 K plateau oxygen is ordered in chains of a mean length of about 12 oxygen ions. In the region of the 90 K plateau the chains become very long and the oxygen vacancies are clustered in empty fragments of chains.

1. Introduction

The best studied family of HT_c superconductors is formed by the 123 compounds of the type $RBa_2Cu_3O_x$. Here R can be Y, Nd, Sm, Eu, Gd, Dy, Ho, Er, Tm or Yb. The Pr compound with the same structure is a semiconducting antiferromagnet for any x, and Ce, Tb and Lu do not form the 123 structure [1]. The general feature is the change from superconductivity to antiferromagnetic order when the oxygen concentration x is changed from 7.0 to 6.0. At $x = 7.0$, T_c increases with the ionic radius of R^{3+} from 92 K for Yb to 95.5 K for Nd [2]. At lower x, however, T_c decreases at increasing radius while the oxygen concentration where the superconductivity disappears increases markedly from 6.4 for Yb and Y to 6.6 for the larger Nd [3]. Correspondingly the plateau of T_c at about 60 K found for the small R ions in the region $6.5 < x < 6.7$ becomes less pronounced at the large (light) R ions and is missing for Nd [3].

Oxygen can be removed only from the O(1) sites in the Cu(1) planes, which in the orthorhombic structure near $x = 7$ form the Cu–O–Cu–chains (Fig. 1). At high temperature and lower x, a transition to the tetragonal structure appears where all oxygen sites in the Cu(1) plane, O(1) and O(5), are occupied at equal probability. The details of the variation of T_c with x depend on the thermal treatment of the samples. For example, the 60 K plateau becomes more clear by annealing at low temperature, and T_c at low x can be increased by annealing at 300 K [4]. Since the cations cannot change their sites at this low temperature, the arrangement of the easier moving oxygen ions must play the important role for T_c.

The magnetic order of Cu is limited to the Cu(2) sites in the CuO_2 double layers, this holds for the Pr compound as well as for the other the oxygen depleted compounds [5]. At low temperature also the magnetic moments of the R ions show antiferromagnetic order, even in the superconducting state. For Gd-123 the Neel temperature T_N is 2.2 K independent of x, in most other 123 compounds the ordering temperature is lower [6].

Different methods have been applied to study the positions of oxygen in the 123 compounds. Diffraction of electrons [7], neutrons [8], and X-rays [9] have shown in Y-123 at about $x = 6.5$ a second orthorhombic structure with a doubled lattice parameter in the direction perpendicular to the chains caused by alternating "filled" and "empty" chains. This structure is called ortho-II, the normal at $x = 7$ correspondingly ortho-I.

All diffraction methods depend on the periodicity of the lattice and the information is therefore limited by the coherence length of the structure to be investigated. Complementary, magnetic resonance of local probes can be used to determine the symmetry and local properties at the different lattice sites of the system. Useful local probes are either the electrons of paramagnetic ions or the nuclei of ions forming

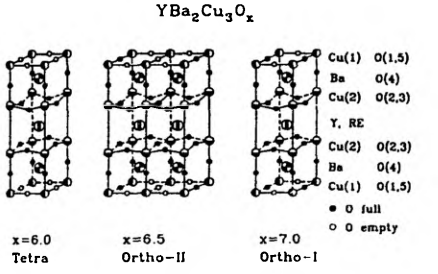

Fig. 1. Structures of $YBa_2Cu_3O_x$ in the 3 phases differing only by the occupation of the O(1) sites in the basal plane, O(5) is always empty. For $x = 0.5$ the 2a superstructure is generated by alternating full and empty Cu(1)–O(1) chains.

* On leave from Institute of Chemical Physics and Biophysics, Tallinn/Estonia

the basic lattice or introduced by doping. For the case of electron spin resonance the concentration of the paramagnetic centers must be very low in order to avoid the spin–spin interaction. Thus only the doping of the Y sites with rare earth ions, mainly Gd^{3+}, has been used to investigate the change of the local structure with oxygen concentration [10]. Fortunately, all elements building up the 123 compounds contain stable isotopes with nuclear spins $I > 0$ which can be used for resonance experiments, nuclear magnetic resonance (NMR) and in the case of $I > 1/2$ nuclear quadrupole resonance (NQR). For some elements the natural abundance of the useful nuclei is too small and the enriched isotopes are needed as for ^{17}O or ^{135}Ba and ^{137}Ba [11]. Systematic investigations of the development of the spectra of 123 compounds with oxygen concentration have been performed for NQR of both Cu isotopes ^{63}Cu and ^{65}Cu at the two Cu sites [12, 13, 14] and for NMR of ^{169}Tm replacing the Y [15]. In this report we will summarize the results obtained for the different local structures obtained from the measurements on these three sites in the 123 compounds.

2. Basic interactions

The basic interactions connecting the local symmetry and the spectral parameters are different in the cases of Tm and Cu. Nuclei with spin $I = 1/2$ like ^{89}Y and ^{169}Tm interact only by their nuclear magnetic moments with the local magnetic field. In the case of Y the spin susceptibility leads to a small Knight shift which has been measured as function of x and temperature [16]. For the rare earth ion Tm^{3+} ($4f^{12}$, $^3H_6$), however, the interaction is strongly enhanced by the $4f$ electrons [15]. For the even number of f electrons the groundstate in the tetragonal or orthorhombic crystal electric field (CEF) is non-degenerate. In a magnetic field the lowest excited states at energies of more than $100\,cm^{-1}$ are mixed with the ground state and induce a strong and anisotropic Van Vlek susceptibility and correspondingly an enhancement of the magnetic field at the nuclear site by more than one order of magnitude. This enhancement is generally described by an effective γ-tensor replacing the γ-value of the bare nucleus, $\gamma/2\pi = 3.54\,MHz/T$. The anisotropy and magnitude of the γ-tensor reflects the symmetry of the CEF at the Tm site and is for that reason sensitive to small changes of the local environment.

The two Cu isotopes ^{63}Cu and ^{65}Cu with $I = 3/2$ interact with the crystal lattice mainly by the nuclear quadrupole moment (eQ) which couples to the electric field gradient (EFG) at the nuclear site. This is determined by the charge distribution in the electron shell of the nucleus under consideration and of the crystal lattice. For the partly filled d-shell of the $3d^9$ state of Cu^{2+} the first part is important and makes the calculation of the EFG difficult. Thus, calculations for the 123 compounds by the local density approximation [17] gives a good agreement with the experiment for the Ba, O, and Cu(1) sites, but errors for the Cu(2) sites by a factor of two. For this reason we do not try to discuss the strength of the quadrupole interaction in the different configurations of the Cu ion. In place of that we use the oxygen concentrations at which a special line in the NQR spectrum is found to determine the EFG for the corresponding oxygen configuration around the Cu ion.

As a traceless tensor the EFG can be described by its largest eigenvalue, eq, and the asymmetry parameter, η[18]. By the quadrupole interaction the degenerate nuclear ground state of the spin $I = 3/2$ is split into the states $|\pm 3/2\rangle$ and $|\pm 1/2\rangle$ with the energy difference $\nu_{NQR} = \nu_Q(1 + \eta^2/3)^{1/2}$ where $\nu_Q = e^2qQ/2h$ is called the quadrupole frequency. The quadrupole interaction can be observed as the "pure quadrupole resonance", NQR, at the frequency ν_{NQR} which for both Cu isotopes is found in the region of 18–32 MHz in the materials considered here. In a magnetic field, the quadrupole interaction induces the "quadrupole splitting" of the NMR line into the transitions $|-3/2\rangle \rightarrow |-1/2\rangle$, $|-1/2\rangle \rightarrow |+1/2\rangle$ and $|+1/2\rangle \rightarrow |+3/2\rangle$ by frequencies of about ν_Q. Since this splitting depends on the direction of the magnetic field with respect to the main axes of the EFG, the NMR spectra of powder samples are broad with singularities for the directions of the main axes of the EFG. The resolution of the NMR spectrum is improved by the use of oriented powder samples where the magnetic field can be applied either parallel or perpendicular to the c-axis of the grains. From the NMR spectra of the oriented samples the directions of the main axes of the EFG tensor can be determined which are important for the assignment of an EFG to the corresponding lattice site.

3. Experimental

The samples used for these experiments were ceramic powder samples supplied by different laboratories. Accordingly the oxygen concentration has been set and determined by different methods which will not be described here. For the Gd-, Tm-, and Nd-samples, prepared at the Institut für Strahlen- und Kernphysik der Universität Bonn, the oxygen concentration was determined from the weight loss after annealing in vacuum [19].

The NQR and NMR spectra have been measured at temperatures 4.2 K and 1.2 K by the normal spin-echo technique with quadrature detection. The NQR spectra of Cu have been recorded by frequency sweep, the NMR spectra of Tm and Cu at fixed frequency by fieldsweep up to 7 T. In all the cases the bandwidth of excitation was much narrower than the sharpest lines. For this reason the spectral density at each frequency was determined from the echo amplitude at optimal excitation. For comparing the intensities at different frequencies the amplitudes were divided by f^2.

4. Tm NMR spectra

The NMR spectra of Tm could be measured up to 40 K. The limit is determined by the fast relaxation induced when the excited CEF levels become populated at higher temperature. From the temperature dependence of the transverse relaxation rate the activation energy of 176 K has been deduced which agrees well with the CEF splitting [15]. The spectra measured at 4.2 K and 68 MHz (Fig. 2) reveal the transition from the tetragonal symmetry at $x = 6.0$ (antiferromagnet) to the orthorhombic phases with three different components of the γ-tensor at $x = 6.5$ ($T_c = 52$ K) and at $x = 7.0$ (91 K). From the measurements with c-axis oriented samples follows that in all cases the smallest component of the γ-tensor (largest field for resonance) γ_z, is in

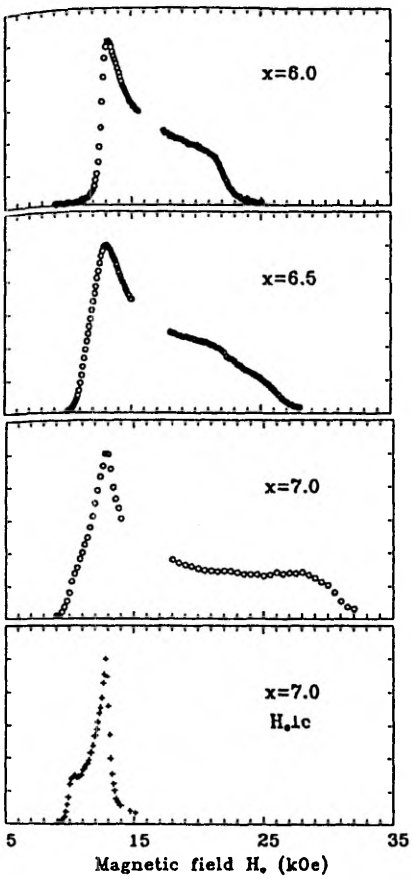

Fig. 2. ^{169}Tm NMR spectra of random and *c*-axis oriented $TmBa_2Cu_3O_x$ powders at 68 MHz, 4.2 K. A part of the field sweep is missing due to the strong resonances of ^{1}H and ^{19}F.

c-direction. The assignment of the *x*- and *y*-components in Table 1 was deduced from estimates of the CEF levels [15]. It is evident that γ_x (perpendicular to the chains) is independent on *x*, whereas γ_y (along the chains) and γ_z increase and decrease, respectively, at increasing *x*. The component most sensitive to a change in the oxygen concentration is γ_z.

The large difference of γ_z between $x = 6.0$ and 7.0 allows to investigate the change of the local structure with high resolution. Spectra measured with the field in *c*-direction for samples with intermediate *x* (Fig. 3) cannot be described as a superposition of the spectra with the γ-values of Table 1, but 5 different values of γ_z are needed. In a fitting procedure it was assumed that the spectra for $x = 6.0$ and 7.0 correspond to a single value of γ_z and are broadened by the not exactly parallel assignment of the *c*-axis of the different grains in the sample. Assuming the same distribution of the deviation from the *c*-axis in all samples, we would determine the relative amount of sites corresponding to 5 different values of γ_z (Table 2). The most simple assumption is to ascribe these to Tm ions for which the 4 nearest O(1) sites in the two Cu(1) planes (Fig. 1) are occupied by 0 to 4 oxygen ions. This idea has been applied at first by Janossy *et al.* [10] to the EPR spectra of Gd^{3+} in YBCO. With this assignment used in Table 2, it is evident that at $x = 6.5$ the configuration with two oxygen neighbours is much more occupied than in a random distribution, a clear indication

Table I. *Components of the γ-tensor in* $TmBa_2Cu_3O_x$ *for the a-, b-, c-axes (x, y, z) at different oxygen concentration x*

x	structure	$\gamma_x/2\pi$ (MHz/T)	$\gamma_y/2\pi$ (MHz/T)	$\gamma_z/2\pi$ (MHz/T)
6.0	tetragonal	53	53	30.5
6.5	ortho-II	53	61	25.6
7.0	ortho-I	53.4	68	22

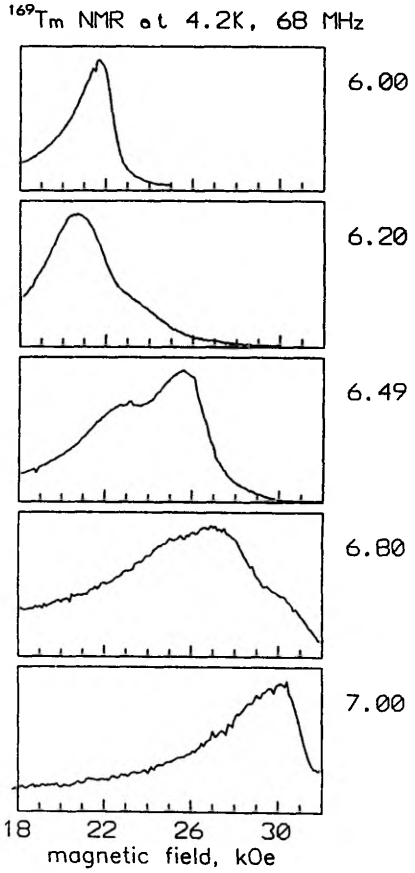

Fig. 3. Tm spectra of aligned $TmBa_2Cu_3O_x$ powders with the magnetic field along the c-axes. The T_c values for different *x* are given in Table II.

Table II. *Relative intensities of* Tm *sites with different values of* γ_x *corresponding to m oxygen neighbours on the 4 nearest* O(1) *sites*

Sample							
		$\gamma_x/2\pi$(MHz/T)	22.0	23	25.6	28	30.5
x	T_c(K)	m	4	3	2	1	0
7.0	91		1.0				
6.8	82		0.2	0.5	0.3		
6.5	52				0.86	0.14	
6.2	—					0.27	0.73
6.0	—						1.0

for an ordered structure at this concentration. For $x = 6.8$ in contrast, the centers with 2, 3, and 4 oxygen neighbours appear with similar probability indicating a random distribution of the oxygen holes. This assignment of the Tm spectra is compatible with the formation of the filled and empty oxygen chains, but other ordering schemes can lead to the same result.

5. Cu spectra

Natural Cu is a mixture of the two isotopes with $I = 3/2$: ^{63}Cu (69%, $\gamma/2\pi = 11.285$ MHz/T, $eQ = 0.209$ barns) and ^{65}Cu (31%, $\gamma/2\pi = 12.089$ MHz/T, $eQ = 0.195$ barns). Thus the Cu NQR lines can be identified by pairs of lines with the frequency ratio determined by the ratio of the quadrupole moments. In the NMR spectra the influence of γ and eQ shifts the satellites of both isotopes in a different way. By proper choice of the field and frequency we could separate the lines of the isotopes in the case where the contributions of both overlap in the NQR spectrum (Fig. 4). Since Cu ions occupy the planar (Cu(2)) and the chain (Cu(1)) sites, it is important to distinguish the spectra of both. One method is to use the different relaxation properties of both sites, if Y^{3+} is replaced by the magnetic Gd^{3+} ion [20]. The magnetic dipole interaction with the near Cu(2) sites suppresses the resonance as long as the Gd spins are fluctuating above their ordering temperature of 2.2 K, and only the more distant Cu(1) sites are visible in the spectrum. At lower temperature, 1.2 K, the Gd spins are ordered and the contributions of both sites are mixed in the spectrum [14].

5.1. *EFG of the Cu(2) sites*

The satellite transitions in the NMR spectrum of Cu(2) in Y-123 measured with the magnetic field applied perpendicular to the c-axis (Fig. 5) show the typical development of the EFG at oxygen concentration x decreasing from 7.0 to 6.5. In the region between 7.0 and 6.7 a continuous broadening of the EFG appears connected with a shift of the center to lower values of the resonance field which means for this satellite a decreasing EFG. At x further reduced to about 6.6 the spectrum splits into two lines of equal intensity. Here the Cu(2) sites are separated in two groups of equal amount and different charge distribution, a clear indication for the existence of the ortho-II phase. The line at the larger field nearly agrees with the line for $x = 7.0$ and is for this reason assigned to Cu(2) neighbouring the full chain, then the other line with lower EFG corresponds to the Cu(2) sites attached to an empty chain. In all spectra observed so far, we have found nearly the same intensity of both lines. This means that a periodic sequence of full and empty chains exists only with equal numbers of both. At larger x ortho-II must

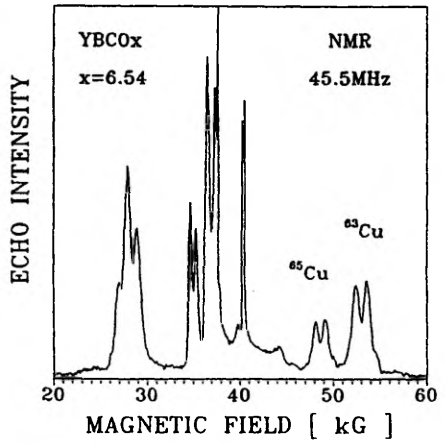

Fig. 4. NMR spectrum of ^{63}Cu and ^{65}Cu in an aligned powder of $YBa_2Cu_3O_{6.54}$ ($T_c = 56$ K) at 45.5 MHz and 4.2 K with the field applied perpendicular to the c-axis.

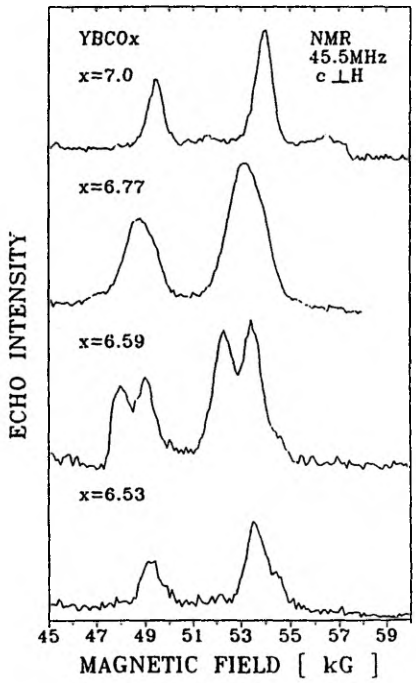

Fig. 5. The high-field satellites in the Cu NMR spectrum of $YBa_2Cu_3O_x$ with the field perpendicular to the c-axes. The T_c values for decreasing oxygen concentration x are 92 K, 61 K, 56 K and 35 K, respectively.

coexist with the ortho-I phase as is shown very clear in a spectrum for $x = 6.63$ published by Takigava *et al.* [21].

In the spectrum for $x = 6.53$ (Fig. 5) no signal from the Cu(2) sites appears. The remaining weak signal arises from the Cu(1) sites as will be discussed below. The Cu(2) NMR and NQR signals disappear for all samples showing superconductivity only below 50 K. At lower x no Cu(2) signal can be detected until at $x < 6.3$, in the antiferromagnetic state of the Cu(2) planes, the NMR spectrum in the hyperfine field appears in the region of 90 MHz from which a much smaller EFG is deduced [22]. The absence of any NQR signal at 4.2 K from the Cu(2) sites in samples with T_c below 50 K can be explained only by extremely fast relaxation which might be induced by a slowing down of antiferromagnetic fluctuations in the exchange correlated electron spin system of the Cu(2) planes.

5.2. *NQR lines of Cu(1)*

Due to the relaxation by the magnetic moments of the Gd^{3+} ions, the NQR spectra observed in Gd-123 at 4.2 K (Fig. 6) represent only the Cu(1) sites. Pure NQR lines without any splitting by a local static magnetic field are found in the full region $6.0 < x < 7.0$, indicating that magnetic order or frozen spins do not exist at the Cu(1) sites for any x. The development of the spectra with oxygen concentration is the same for the Y-, Gd- and Tm-compounds and reveals three pairs of $^{63/65}$Cu NQR lines appearing at different x: The pair at 22 MHz (for the more abundant isotope ^{63}Cu) near $x = 7$ broadens quickly at decreasing x and must be ascribed to the ions $Cu(1)_4$ with four oxygen neighbours, two on the O(1) positions in the chain and the two on the apical sites. At x near $x = 6$ another narrow pair appears at 30 MHz corresponding to the ions $Cu(1)_2$ in the empty chain with only the two apical oxygen neighbours. This line shifts in the region $6.3 < x < 6.6$ in two steps of about 0.7 MHz to higher frequency. Normally samples in this region show the three lines of $Cu(1)_2$, A, B, C, together with different intensities (Fig. 7). They form the hardly resolved NMR spectrum for $x = 6.53$ (Fig. 5) where the Cu(2) signal has disappeared. A third pair is found only for intermediate x between 6.1 and 6.9. We ascribe this line (24 MHz) with an extremely stable position at changing x to the threefold coordinated $Cu(1)_3$, the neighbour of an insulated oxygen ion or more generally the Cu ion terminating a chain.

We have determined the relative intensities, I_2, I_3, and I_4 of the different pairs in the spectra, from which the mean number n of oxygen ions in the chains could be calculated according to the relation $n = 1 + 2I_4/I_3$. Up to $x = 6.2$, I_4 remains zero indicating mainly insulated oxygen sites in the tetragonal structure. An increase of n appears at the onset of superconductivity above 6.3 (Fig. 4) with saturation at about $n = 12$ for samples in the region of the 60 K plateau. At further increasing x, I_3 decreases quickly. The last signal with intensity corresponding to n larger than 50 was detected in a Tm sample at $x = 6.85$. For this concentration, a random distribution on all O(1) sites would lead to a mean chain length of about 8. The line of $Cu(1)_2$ could be followed up to $x = 6.90$ which means that at this high oxygen concentration the defects in the chains are mainly clustered forming pieces of empty chains.

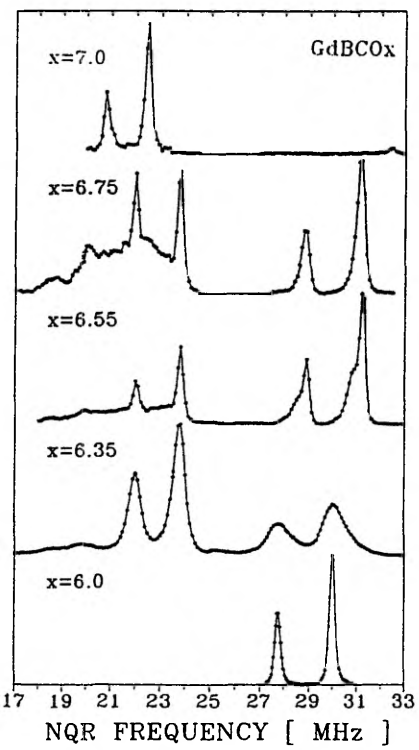

Fig. 6. NQR of the Cu(1) sites in $GdBa_2Cu_3O_x$ at 4.2 K. The T_c values are 92 K for $x = 6.99$, 58 K for $x = 6.75$ and 50 K for $x = 6.55$, the other samples are not superconducting.

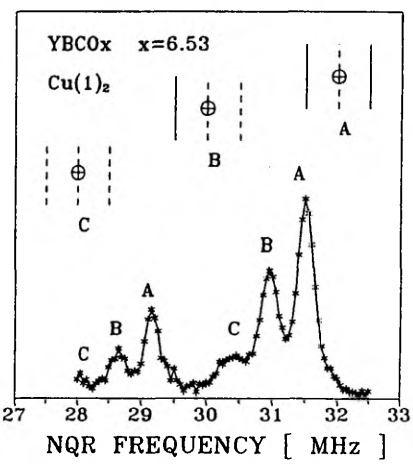

Fig. 7. ^{63}Cu (right) and ^{65}Cu (left) NQR spectrum of Cu(1) sites with twofold oxygen coordination in $YBa_2Cu_3O_{6.53}$ ($T_c = 35$ K). The lines labeled with A, B, C correspond to Cu(1) in empty chains between two full, one full and one empty, and two empty chains, respectively.

From the three components of $Cu(1)_2$, only the line A at the highest frequency of 31.5 MHz appears at $x > 6.6$. As observed already by Serikov *et al.* [23], samples with an onset of superconductivity contain at least a weak A component and the maximum intensity shifts from C to A when T_c increases with x to the 60 K plateau. These facts can be easily described if we assume that the line A belongs to $Cu(1)_2$ in empty chains between two filled chains as neighbours, as in the case of the ortho-II phase. The lines B and C correspond to those empty chains with one or both neighbour chains empty, respectively. With this assignment we arrive at a simple condition for the onset of superconductivity: S.C. is possible only if extended clusters of ortho-II exist. The 60 K plateau is reached when the domains of lower x have disappeared completely.

6. Conclusion

The change of oxygen concentation x in the Cu(1) plane of the 123 compounds affects the other places in a different way. We have studied the influence of x at both Cu sites and at the Tm site. Located in the center between 8 Cu(2) sites, all Tm sites are expected to be equivalent in the three phases tetra, ortho-II, and ortho-I. We have found indeed single γ-tensors in all three cases. At intermediate oxygen concentration a co-existence of these phases must lead to a superposition of the corresponding spectra with the appropriate intensities. Since the main shift with x is found in the c-component (Table 1) this superposition should be most evident in the spectra with the field in c direction (Fig. 3). We have found, however, intermediate values of γ_c which must be ascribed to configurations where only one of the 4 nearest oxygen chains is empty. These configurations are also evident in the EPR spectra of Gd doped Y-123 [10].

Each Cu(2) site is the neighbour of one single chain where two next nearest oxygen neighbours can be removed. Between $x = 7.0$ and 6.7, oxygen is removed randomly as is evident from the increasing width and shift of the spectra to lower values of the EFG (Fig. 5). At further reduction the appearance of the ortho-II lines together with the broadened ortho-I line [21] proves the coexistence of both phases. Other ordered phases between ortho-I and ortho-II with a different sequence of filled and empty chains would produce different Cu(2) spectra and can be excluded in our samples. It is possible, however, that by annealing at low temperature ordered structures like a sequence of one empty and two full chains can be generated which might be detected in the NQR spectra.

The Cu(1) sites are the nearest to the removable oxygen sites and allow the most detailed conclusions. It is evident that already at small oxygen deficit, $x = 6.9$, most vacancies are agglomerated in pieces of empty chains. In the 60 K plateau, these empty chains stay separated by filled chains in a random manner until the ordered arrangement of the ortho-II phase is formed. T_c drops below 60 K when empty chains appear as direct neighbours. In the region of the plateau the average length of the filled chains is rather short with about 12 oxygen ions per chain and decreases fast at lower x. Below 6.3 mainly insulated oxygen ions form the tetragonal structure.

All these results hold for the 123 compounds of Y, Gd, and Tm; a small shift of the line positions is related to the radii of the R^{3+} ions. Also for the larger Nd ion on the Y site the spectra for 6.0 and 7.0 agree with those for the smaller R ions [24], at intermediate oxygen concentration, however, first measurements show NQR lines which do not fit into the scheme described above and give an indication of another arrangement of the oxygen ions. This fits with the fact that the 60 K plateau is missing [3] and that the ortho-II structure could be detected only with difficulty by electron diffraction [3]. Further investigations are needed to clarify the arrangement of oxygen in this system.

Acknowledgements

We are indebted to colleagues from many institutes who supplied us with samples needed for this investigation, especially to S. M. Hosseini and D. Wagener, Bonn for the Gd, Tm and Nd containing 123 compounds of well defined oxygen concentration. I. H. and A. V. E. like to express their thanks for the financial support by the Bundesminister für Forschung und Technologie given by the DAAD and to Prof. W. Zinn for the hospitality they received at the KFA Jülich.

References

1. Tamhane, A. S. *et al.*, Mater. Lett. **14**, 185 (1992); Markandeyulu, G. *et al.*, Phys. Rev. **B47**, 1123 (1993).
2. Büchner, B., Calliess, U., Jostarndt, H. D., Schlabitz, W. and Wohlleben, D., Sol. State Comm. **73**, 357 (1990).
3. Buchgeister, M., Thesis Universitaet Bonn (1991); Krekels, T. *et al.*, Physica **C196**, 363 (1992).
4. Claus, H., Yang, S., Paulikas, A. P., Downey, J. W. and Veal, B. W., Physica **C171**, 205 (1990).
5. Lütgemeier, H., JMMM **90&91**, 633 (1990); Lütgemeier, H. and Heinmaa, I., in: "Condensed Matter by Nuclear Studies" Proc. of XXVI Zakopane School on Physics. 1991, p. 264. (Edited by J. Stanek and A. T. Pedziwiatr) (World Scientific 1991).
6. Lee, B. W. *et al.* Phys. Rev. **B37**, 2368 (1988).
7. Cava, R. J. *et al.*, Physica **C165**, 419 (1990).
8. Zeiske, Th., Sonntag, R., Hohlwein, D., Andersen, N. H. and Wolf, Th., Nature **353**, 542 (1991).
9. Zeiske, Th., Hohlwein, D., Sonntag, R., Kubanek, F. and Wolf, Th., Physica **C194**, 1 (1992); Simon, A., Trübenbach, K. and Bormann, H., J. Solid State Chem. to be published.
10. Pekker, S., Janossy, A. and Rockenbauer, A., Physica **C181**, 11 (1991); Rockenbauer, A., Janossy, A., Korecz, L. and Pekker, S., J. Mag. Res. **97**, 540 (1992).
11. Yakubowskii, A., Egorov, A. and Lütgemeier, H., Appl. Mag. Res. **3**, 665 (1992).
12. Vega, A. J., Farneth, W. E., McCarron, E. M. and Bordia, R. K., Phys. Rev. **B39**, 2322 (1989).
13. Yasuoka, H., Shimizu, T., Imai, T. and Sasaki, S., Hyperfine Int. **49**, 167 (1989).
14. Heinmaa, I., Lütgemeier, H., Pekker, S., Krabbes, G. and Buchgeister, M., Appl. Mag. Res. **3**, 689 (1992); Lütgemeier, H. and Heinmaa, I in: "Phase Separation in Cuprate Superconductors" Proc. of the Erice Workshop 1992, p. 243 (Edited by K. A. Mueller and G. Benedek) (World Scientific 1993).
15. Bakharev, O. N. *et al.*, Appl. Mag. Res. **3**, 613 (1992); Egorov, A. V., Lütgemeier, H., Wagener, D., Dooglav, A. V. and Teplov, M. A., Sol. State Comm. **83**, 111 (1962).
16. Alloul, H., Ohno, T. and Mendels, P., Phys. Rev. Lett. **63**, 1700 (1989).
17. Schwarz, K., Ambrosch-Draxl, C. and Blaha, P., Phys. Rev. **B42**, 2051 (1990).
18. Das, T. P. and Hahn, E. L., Solid State Physics Suppl. **1**, (Edited by F. Seitz and D. Turnbull) (Academic Press 1958).
19. Buchgeister, M. *et al.*, in: "High Temperature Superconductors - Physics and Materials Science" NATO ASI Series **E181**, 319 (1990).
20. Lütgemeier, H., Physica **C153–155**, 95 (1988).
21. Takigawa, M. *et al.*, Phys. Rev. **B43**, 247 (1991).
22. Mendels, P., Alloul, H., Marucco, J. F., Arabski, J. and Collin, G., Physica **C171**, 429 (1990).
23. Serikov, V. V. *et al.*, JETP. Lett. **47**, 534 (1988).
24. Rajarajan, A. K., Gupta, L. J. and Vijayaraghavan, R., Physica **C193**, 413 (1992).

IV

H. Lütgemeier, I. Heinmaa, D. Wagener, and S. M. Hosseini,
Superconductivity Versus Oxygen Concentration in 123 Compounds: Influence of RE Ionic Radii Studied by Cu NQR,
in: Phase Separation in Cuprate Superconductors,
Proceedings of the second international workshop on "Phase Separation in Cuprate Superconductors" September 4–10, 1993, Cottbus, Germany,
eds. E. Sigmund and K. A. Müller, Springer-Verlag, Berlin, 1994, pp. 225–235.

Superconductivity Versus Oxygen Concentration in 123 Compounds: Influence of RE Ionic Radii Studied by Cu NQR

H. Luetgemeier[1], I. Heinmaa[2], D. Wagener[3], and S.M. Hosseini[3]

[1] Institut f. Festkoerperforschung Juelich GmbH, 52428 Juelich
[2] Institute of Chemical Physics and Biophysics EE0100, Tallinn/Estonia
[3] Institut fuer Strahlen- und Kernphysik der Universitaet Bonn

Summary. The NQR spectra of Cu in 123 compounds $REBa_2Cu_3O_x$ containing either the large RE ion Nd or the smaller ones Gd, Y, or Tm are investigated at 4.2 and 1.2 K for different oxygen content x. In our powder samples of Tm123 we find a maximum of T_c at $x = 6.92$ but the sharpest lines are at $x = 7.0$, indicating that no phase separation exists at 7.0. For the larger Nd ion the maximum of $T_c$is obtained for 7.0 and T_c decreases fast at reduced x. Different schemes of oxygen ordering in the two types of 123 compounds are derived from the NQR spectra: whereas the oxygen defects in the Cu-O chains are distributed randomly in Nd123, the holes cluster in the compounds with the small RE ions and form extended pieces of empty chains surrounded by full chains, and near $x = 6.5$ the ortho-II structure. Correspondingly the mean length n of the full chain fragments depends in a different way on x in both types of 123 compounds. A unique dependence of T_c on n, however, is found with $n = 5$ oxygen for the onset of superconductivity.

1. Introduction

In the high-T_c superconductor $YBa_2Cu_3O_x$ (Y123) the orthorhombic structure ortho-I at oxygen concentration x near 7.0 with T_c of about 90 K is formed since only half of the oxygen sites in the Cu(1) layer is occupied. The occupied sites, designed as O(1), form the Cu-O-Cu chains along the b axis whereas the O(5) sites along the a axis remain empty. At $x = 6.4$ a transition to the tetragonal structure occurs with random occupation of both sites. The arrangement of the oxygen ions in the Cu(1) layer at $x < 7$ has an important influence on the superconducting transition in this compound and the related ones obtained when Y is replaced by rare earth ions. The plateau of T_c at 60 K for Y123 is connected with the ordered ortho-II structure at x near 6.5, characterized by doubling of the unit cell in a-direction due to alternating oxygen full and empty chains. Since the dependence of T_c on x is different for large and small ions on the Y site [1, 2], it must be expected that the oxygen arrangement changes with the ionic radii.

We have investigated previously this arrangement for Gd123 and Y123 by using the Cu nuclei as local probes in the nuclear quadrupole resonance (NQR) [3]. The NQR frequency is determined by the electric field gradient (EFG) of the charge distribution at the nuclear site. Since the intensity of the resonance line is proportional to the number of nuclei in corresponding sites,

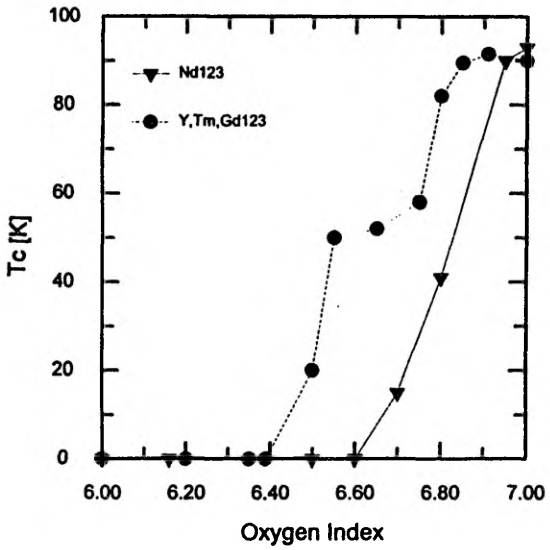

Fig. 2.1. Dependence of T_c on the oxygen content in the 123 samples containing either Nd or Gd, Y, Tm.

one can study the distribution of different copper sites created by various oxygen arrangements. Here we have applied the copper NQR to Nd123 with the aim to compare the oxygen arrangement in the compound with RE of large ionic radius to that in the compounds with small RE (Y-, Gd-, and Tm123). A special effort was made in order to follow the structural changes in Tm123 in the region of the 90 K plateau.

2. T_c versus x for different RE in $REBa_2Cu_3O_x$

In the series of the the superconducting 123 compounds $REBa_2Cu_3O_x$ (RE123), the critical temperature T_c obtains its largest value of 95 K for the largest ion Nd^{3+} [4]. The two plateaus in the depence of T_c on x are best developed for the smaller ions like Gd^{3+}, Y^{3+}, Tm^{3+} etc. [1, 2] (Fig. 2.1). For Nd the 60 K plateau is missing completely and T_c decreases very fast at reduced x and disappears already at $x < 6.7$. Electron diffraction has proved the missing of the 60 plateau in Nd123 to be connected with the absence of the ordered ortho-II structure [2]. In contrast to the fast decay of T_c with x for Nd123, the small RE ions reveal a weak maximum of T_c at x slightly reduced to about 6.9 [5, 6, 7], as shown for the case of Tm in Fig. 2.2. This maximum is generally taken as an indication for the transition from the underdoped region at low x to the slightly overdoped at $x = 7$. Up to now it is not clear if the maximum of T_c is connected also with a structural transition [6, 7].

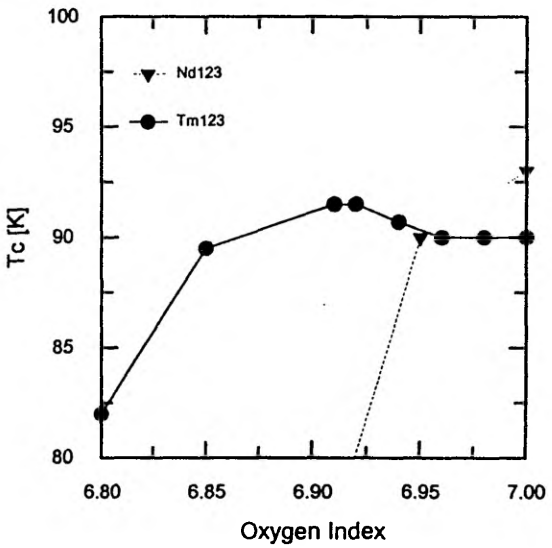

Fig. 2.2. T_c versus oxygen content for Tm123 and Nd123 in the region of the maximum of T_c.

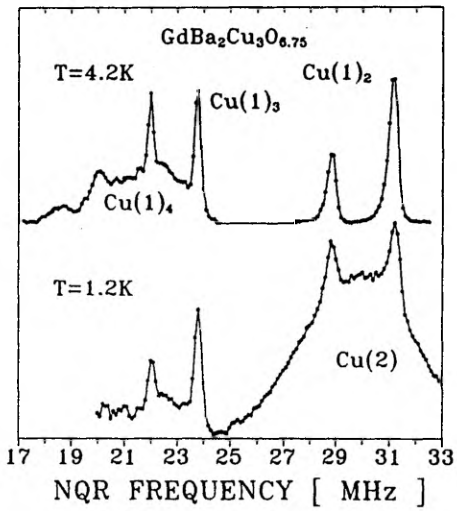

Fig. 3.1. NQR spectra of Cu in Gd123 with $x = 6.75$ with the doublets for the isotopes ^{63}Cu (higher intensity and frequency) and ^{65}Cu (lower). At 4.2 K the broad signal from Cu(2) sites seen at 1.2 K is suppressed by fast relaxation due to the fluctuations of the Gd 4f spins above the Neel temperature at 2.2 K.

3. Cu NQR lines in different configurations

The NQR spectra of Cu have been discussed in detail for RE = Y and Gd [3]. Since the EFG determining the NQR frequencies depends on the charge dis-

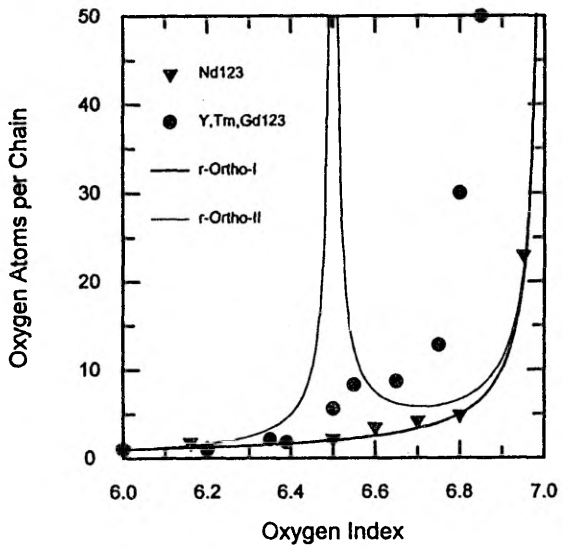

Fig. 3.2. Mean number n of oxygen ions in the Cu-O-Cu chains versus oxygen content in the different 123 compounds. Model calculations are shown for random dilution of the ortho-I structure and for random dilution for $x < 6.5$ and random filling for $x > 6.5$ of the ortho-II structure.

tribution at the lattice site under inspection, one pair of NQR lines for the two isotopes is expected for each configuration of Cu. Three components in the spectra could be ascribed to Cu(1) sites with 2, 3, or 4 oxygen neighbors $Cu(1)_2$, $Cu(1)_3$ and $Cu(1)_4$, respectively (Fig. 3.1). $Cu(1)_4$ is the only NQR line of the Cu(1) sites in the ortho-I structure at $x = 7.0$ whereas $Cu(1)_2$ appears in the tetragonal antiferromagnetic state at $x = 6.0$. In the pure ortho-II structure the same amount of $Cu(1)_2$ and $Cu(1)_4$ is to be expected. $Cu(1)_2$ appears in the same frequency region as the Cu(2) NQR line but can be distinguished by the longer transversal relaxation time at 4.2 and 1.2 K when magnetic RE ions like Gd are used in the place of Y [3]. The NQR line of $Cu(1)_3$ corresponds to the terminal Cu ion of a Cu-O chain and can be especially the Cu(1) ion neighboring a single oxygen ion at low x or a single oxygen defect at high x. This line is observed nearly in the full region $6.0 < x < 7.0$. From the relative intensities I_2, I_3, and I_4 of the three components we have concluded on the mean number n of oxygen atoms in the Cu-O chains given by the relation

$$n = 1 + 2I_4/I_3 \tag{3.1}$$

From a large number of samples with RE = Y or Gd [3] the sytemetic variation of n with x has been found (Fig. 3.2): n increases with x at the onset of superconductivity at 6.3 and $n > 5$ holds in all superconducting samples. In the region of the 60 K plateau n stays constant at about 8 and

increases only at $x > 6.8$ where I_3 decreases quickly. The relative intensities can be discussed also in another way. Normally $Cu(1)_2$ is ascribed to the monovalent state, whereas $Cu(1)_3$ and $Cu(1)_4$ are assumed to be divalent. This means that I_2 corresponds to the monovalent component of the Cu(1) layer which has been determined by X ray absorption spectroscopy (XAS) [8]. The dependence on x of the resonance of the Cu(2) ions in the double layers is quite different [3]. In the antiferromagnetic state for $x < 6.3$ the spins localized at the Cu(2) ions induce the hyperfine field at the nuclei which is observed by antiferromagnetic NMR at frequencies much higher than the NQR frequencies. With increasing x this line disappears at about $x = 6.3$ [9]. The resonance of the Cu(2) sites appears again as NQR at $x > 6.6$. In the region $6.3 < x < 6.6$ no nuclear resonance of Cu(2), neither NMR nor NQR, is observed at 4.2 K, probably due to strong relaxation by the slow fluctuations of the electronic spins localized at the Cu(2) sites. For x at about 6.6 the characteristic NQR spectrum of Cu(2) in the ortho-II structure is identified by two slightly different NQR frequencies corresponding to the Cu(2) sites attached to either a full or empty chain. At larger x a broad line from a highly distorted ortho-I structure is superimposed on the spectrum. With x approaching 7.0 this line becomes the single sharp line of the pure ortho-I structure.

4. Experimental details

In the following we describe experiments with a series of Tm123 samples prepared with small steps for $x > 6.9$ of only 0.02 and a series of Nd123. All samples were polycrystalline powders prepared by the technique as described previously [1, 2]. The NQR spectra have been recorded by standard spin-echo technique at 1.2 and 4.2 K in the region from 18 to 35 MHz. By measuring the spectra with short (30 μs) and long (150 μs) delay time between both rf. pulses, the fast and slowly relaxing contributions of Cu(2) and Cu(1), respectively, were separated. In the comparison of the intensities at different frequencies these were normalized by f^2. T_c was determined from the DC susceptibility at 10 Oe measured by a SQUID magnetometer.

5. Results

5.1 NQR of Tm123

The spectra of Tm123 show the same evolution with x as those observed previously with the Y and Gd compounds [3]. In the region of high x the systematic variation of T_c with x (Fig. 2.2) and of the spectra (Fig. 5.1) confirms the high accuracy of determining differences in the oxygen concentration. The absolute values of x, however, may be affected with larger errors.

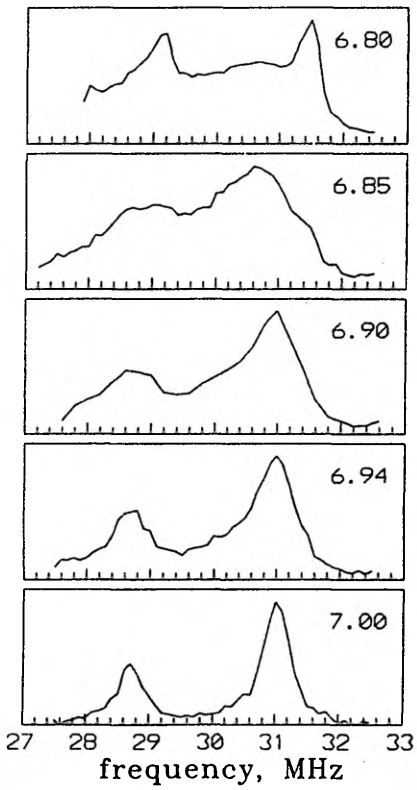

Fig. 5.1. NQR spectra of Cu in Tm 123 in the frequency range of the Cu(2) signal for large x. The narrow peaks for $x = 6.8$ correspond to $Cu(1)_2$ and can be detected up to 6.90.

A clear maximum of T is found at $x = 6.92$ which is 1.5 K above the value for 7.0. In the NQR spectra of the Cu(2) sites we find the narrowest line for $x = 7.0$ and a systematic broadening when x is reduced to 6.8, without any special feature in the region of the T_c maximum at $x = 6.92$. In the spectra observed at short delay time (Fig. 5.1), the $Cu(1)_2$ signal is evident the first time at $x = 6.85$ as a narrow shoulder, but a weak $Cu(1)_2$ line could be detected even at $x = 6.90$. This line is the main line of $Cu(1)_2$ in the ortho-II structure and corresponds to a piece of an empty chain between filled chains [3]. The $Cu(1)_3$ line, in contrast, is absent already for $x > 6.85$. This means the oxygen defects are not isolated but clustered into empty fragments containing at least 4 vacant sites. It is difficult to estimate the mean length of the Cu-O chains in the limit of high x, but $n > 50$ holds for $x = 6.85$ (Fig. 3.2).

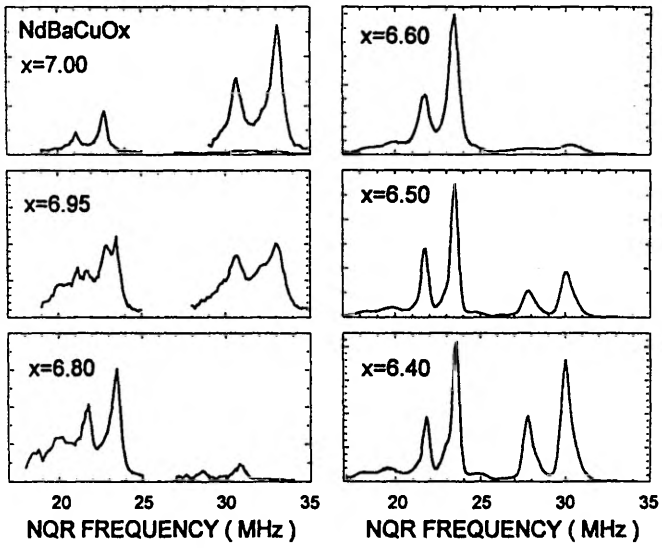

Fig. 5.2. NQR spectra of Nd123 at different x at 1.2 K. From the relaxation rate it is evident that for $x < 6.8$ no signal of Cu(2) is detected and for $x > 6.8$ no signal from $Cu(1)_2$.

5.2 NQR of Nd123

In the Nd123 samples T_c is reduced very fast at decreasing x (Fig. 2.1) and superconductivity disappears already at $x = 6.6$. Due to the low antiferromagnetic ordering temperature of about 1 K for the Nd spins, the Cu(2) NQR signal reveals strong relaxation and can be observed only at a very short delay time (Fig. 5.2). This fast relaxing signal disappears already for $x = 6.8$ in a sample with $T_c = 40$ K, that is the same region of T_c where for Gd123 and Y123 no Cu(2) signal can be observed [3]. For the Cu(1) signals the lines corresponding to the three different configurations can be distinguished. It is evident that the intensity of the line of $Cu(1)_3$ at 23.6 MHz is the largest in the region of x between 6.8 and 6.4. Correspondingly the mean length of chains decreases very fast at decreasing x (Fig. 3.2) with $n = 5$ at $x = 6.8$ for the sample with $T_c = 40$ K.

6. Discussion

The different n vs. x dependence for Nd and the smaller RE ions reflect different schemes of removing oxygen. If the oxygen are distributed randomly over all O(1) sites of the ortho-I structure, the dependence $n = 1 + 1/(7 - x)$ results. As can be seen in Fig. 3.2 this relation, indicated as r-ortho-I (random

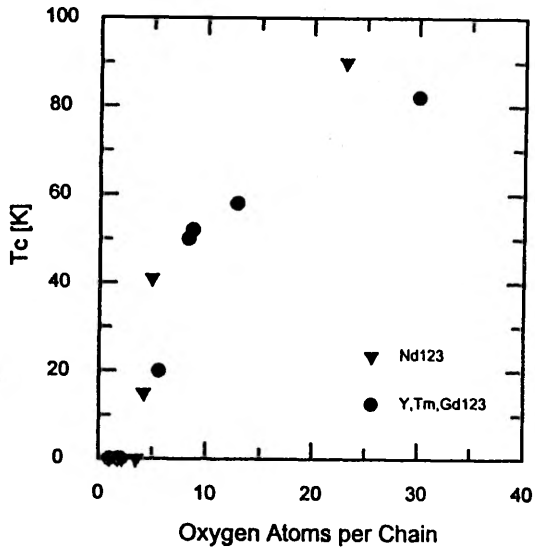

Fig. 6.1. Dependence of T_c on the mean number n of oxygen ions in the Cu-O-Cu chains in the different 123 compounds with the onset of superconductivity for $n = 5$.

dilution of ortho-I) holds for the case of Nd123. Since no correlation exists between the oxygen vacancies the ortho-II structure cannot develop.

The other simple oxygen ordering scheme is based on the ortho-II structure where at $x > 6.5$ the oxygen ions are removed only from every other chain leaving the remaining ones complete. Only at further reduction below 6.5, oxygen is removed randomly also from the remaining chains. This leads to a dependence of $n(x)$ with infinite chain length at 6.5 and a deep minimum at $x = 6.7$ as indicated by the curve r-ortho-II in Fig. 3.2. It is evident that $n(x)$ for Y, Gd, and Tm follows this dependence rather well for $x < 6.5$, but remains constant at about 10 for $6.5 < x < 6.7$ where it starts to increase again. As we pointed out before [3] this behavior must be ascribed to the coexistence of domains of ortho-I and ortho-II. A surprising result of the comparison of the two types of 123 compounds is that the onset of superconductivity appears in both cases of ortho-I (Nd) or ortho-II (Gd,Y,Tm) at the same n of about 5 as indicated in the dependence of $T_c(n)$ in Fig. 6.1. This confirms the idea that a minimal length of the Cu-O chains is needed for doping holes into the Cu(2) layers.

The difference of both types of 123 compounds can also be seen from the relative numbers of the twofold coordinated Cu(1) ions, I_2, corresponding to the amount of monovalent Cu ions (Fig. 6.2). Three limiting cases can be considered. If all oxygen ions are arranged in chains of "infinite" length which means $I_3 \ll I_2$, a linear decay $I_2 = (7-x)$ would result as is seen for the case of Gd, Y, Tm for $x > 6.5$. For $x < 6.5$ and for Nd the dependence of I_2 on

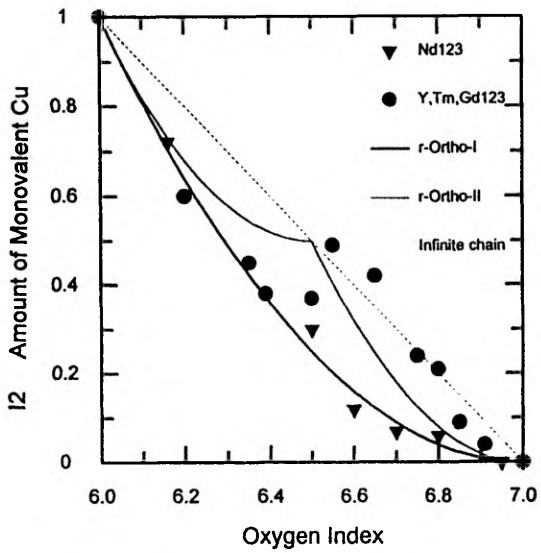

Fig. 6.2. Relative intensity I_2 of twofold coordinated Cu(1) corresponding to the amount of monovalent Cu versus oxygen content x. The curves indicate different models for oxygen order: random dilution of the ortho-I structure, random dilution and filling of the ortho-II structure, and ordering of the oxygen ions in chains of infinite length.

x follows much better the dependence expected for the case of the random dilution of the ortho-I structure leading to the relation $I_2 = (7-x)^2$. For the random filling of ortho-II values between these limiting cases are expected.

Our results for the amount of monovalent Cu(1) can be compared with the data deduced from XAS for Y123 [8]. Good agreement is found for the region $x < 6.3$ where the oxygen ions remain separated, but a clear difference appears for $x > 6.6$. Here Tolentino et al. find only a small amount of monovalent Cu corresponding to a random distribution of the oxygen defects whereas our experiments for the small RE ions show the strong tendency of the oxygen defects to cluster in empty fragments of the chains and to form monovalent Cu(1).

There remains the open question which parameters are responsible for the different behavior of the large and small RE ions. On the one hand it is possible that by the increased lattice parameters for Nd123 the interaction energies between the oxygen ions in the Cu(1) plane are modified leading to different ordering schemes. On the other hand it might be possible that the larger Nd ions can replace some Ba sites. In any case it is evident that the formation of the ortho-II structure is suppressed in the case of Nd123 and that already at high x the length of the filled chains becomes so short that the superconductivity is suppressed.

The investigation of polycrystalline samples of Y123 [6, 9] and of single crystals [7] has revealed anomalies in the lattice parameters and the pressure dependence of T_c in the region of the T_c maximum at x near 6.9. From this and from two steps found in the temperature dependence of the magnetic shielding at high x it has been concluded that the system consists of two phases for x above the maximum of T_c. The NQR spectra of our Tm123 samples show the narrowest lines of the Cu(2) sites for the largest oxygen concentration and a continuous broadening at decreasing x as expected when the number of lattice defects in an ordered structure increases. The NQR spectra of Cu(1) show that the maximum of T_c appears at the oxygen concentration where the NQR line of Cu(1) in empty chain fragments appears for the first time, which means the formation of small domains of the ortho-II structure within the ortho-I structure. Thus the anomalies at the maximum of T_c are probably connected with the coexistence of the ortho-I and ortho-II phases but not with another phase at higher oxygen concentration.
All results presented here are based on the fact that all the Cu(1) sites can be observed by NQR which means that the expectation value of the magnetic moment disappears for times longer than 10^{-12} s. This holds especially also for the $Cu(1)_3$ configuration at the chain ends. In many models the chain ends are assumed to be paramagnetic and to be the reason for the reduced T_c by pair breaking. Our results show that at least most of these sites do not carry a stable magnetic moment.

7. Conclusion

The NQR spectra of Cu in the oxygen depleted 123 compounds allow a direct determination of the relative amounts of the Cu(1) sites with two, three or four oxygen neighbors. From these it is evident that the arrangement of the oxygen defects depends on the radii of the RE ions on the Y sites. For the large ion of Nd the oxygen vacancies show no tendency to cluster. Correspondingly only short pieces of Cu-O-Cu chains exist already at slightly reduced oxygen content x which leads to the fast decay of T_c. For the smaller ions like Gd, Y, Tm we have found a strong clustering of the defects in fragments of empty chains which keeps the mean length of the filled chains large and leads to the ortho-II structure with alternating full and empty chains near $x = 6.5$. In spite of this different arrangement of the defects we found a unique dependence of T_c on the mean length of the filled chains with the onset of superconductivity at 5 oxygen ions per chain.

Acknowledgement. We are indebted to C. Osthoever, KFA Juelich, and E. Bruecher, MPI FKF Stuttgart for the measurement of the susceptibility. Financial support by the BMFT given through the DAAD for the stay of I.H. at the KFA Juelich is thankfully acknowledged. I.H. likes to thank Prof. Zinn for the hospitality he received in his institute.

References

1. Buchgeister, M., Thesis Universitaet Bonn (1991).
2. Krekels, T. et al., Physica C196 (1992) 363.
3. Luetgemeier, H. and Heinmaa, I. in "Phase Separation in Cuprate Superconductors", Proc. of the Erice Workshop 1992, p. 243. K.A. Mueller and G. Benedek eds., (World Scientific 1993) Heinmaa I. et al., Appl. Mag. Res. 3 (1992) 689.
4. Buechner, B. et al., Sol. State Comm. 73 (1990) 357.
5. Graf, T., Triscone, G. and Mueller, J, J. Less-Common Met. 159 (1990) 349.
6. Rusiecki S. et al., J. Less-Common Met. 164-165 (1990) 31.
7. Claus, H. et al., Physica C200 (1992) 271.
8. Tolentino, H. et al., Physica C192 (1992) 115.
9. Mendels, P., Alloul, H., Marucco, J.F., Arabski, J. and G. Collin, Physica C171 (1990) 429.

V

H. Lütgemeier, S. Schmenn, and I. Heinmaa,
A microscopic Model for the different Tc(x) dependence in $REBa_2Cu_3O_{6+x}$ HT_c —
Superconductors containing different RE-ions,
J. Low Temp. Phys. **105**, pp. 693–698 (1996).

Journal of Low Temperature Physics, Vol. 105, Nos. 3/4, 1996

A microscopic Model for the different $T_c(x)$ dependence in $REBa_2Cu_3O_{6+x}$ HT_c - Superconductors containing different RE-ions

H. Lütgemeier, S. Schmenn, and I. Heinmaa*
IFF, Forschungszentrum Jülich, D-52425 Jülich
** Inst. of Chem. Physics and Biophysics, Tallinn, Estonia*

Replacing Y in $YBa_2Cu_3O_{6+x}$ by the larger ions Nd or La increases the critical oxygen content for the transition from antiferromagnetic to superconducting behavior from x=0.4 to 0.6. From the analysis of the NQR spectra of the Cu(1) sites at different x follows a change of the interaction in the oxygen pairs connected by a Cu(1) ion from attractive for Y to repulsive for La.

1. INTRODUCTION

In the cuprates of the type $REBa_2Cu_3O_{6+x}$, $0 \le x \le 1$, the 123 compounds, RE can be either Y, La, or most of the rare earth ions. With the exception of the special case of Pr123, all are superconducting for high oxygen content x. The transition from the antiferromagnetic order at low x to the superconducting behavior, however, is shifted from x about 0.4 for Y123 to above 0.6 for the compounds with the larger ions Nd and La (Fig. 1),

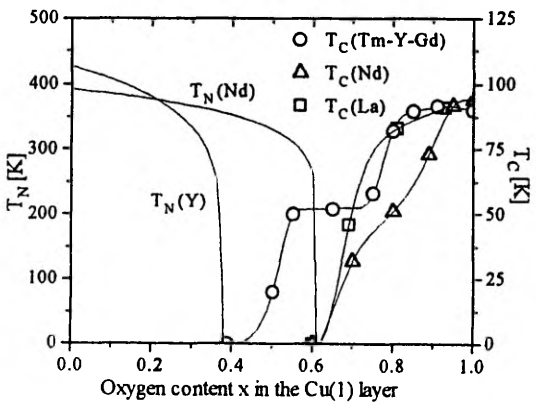

Fig. 1:
T_N in Y123 and Nd123 and and T_C inY,Tm,Gd123, Nd123 and La123 versus x /1/.

as has been shown by μSR and NMR for the antiferromagnetic range /1/ and by susceptibility measurements for the superconductivity /2/. Since the same shift is found for the Nd and La ions, it cannot be explained by hybridization effects of the partially filled 4f shell. The reason must be the structural differences by the larger radii of the ions replacing Y, which mainly increase the lattice parameters a and b and the distance of the Cu(2) layers while the orthorhombicity (a-b)/(a+b) decreases from 0.84% for Y to 0.5% for La /3, 4/. In the oxygen depleted Y123 the order of the oxygen in the Cu(1) plane is important for the superconducting transition temperature. So the differences connected with the RE ionic radii may also be caused by a different arrangement of the oxygen ions induced by the increasing distances in the Cu(1) layer.

Diffraction studies have shown the ortho-I structure for all 123 compounds at full oxygen loading near x=1 /3/. In this structure the oxygen occupies in the Cu(1) layer only half of the possible sites, O(1), forming the Cu(1)-O chains in the b direction and leaving the O(5) sites empty. For lower x the oxygen is removed from the Cu(1) layer. This may lead either to a disordered arrangement, to superstructures or to a phase separation into oxygen rich and oxygen poor domains. Among different proposed superstructures the ortho-II with alternating 'full' and 'empty' chains could be clearly identified by X-ray diffraction in single crystals /5/ of Y123. The '60K plateau' of T_C at x about 0.6 in the 123 compounds containing small RE ions is generally ascribed to this superstructure. The increasing T_C at low temperature annealing of samples with low x indicates the increasing perfection of this structure. Another superstructure with only insulated oxygen ions in the Cu(1) layer has been found in an Y123 single crystal at x=0.35 /6/.

In this communication we discuss the distribution of the oxygen in the Cu(1) layers investigated by nuclear quadrupole resonance (NQR) at 4.2 K in 123 compounds of small RE ions, Tm, Y, Gd (r=0.0994 to 0.1053 nm), medium, Nd (r=0.1109 nm), and of the largest ion, La (r= 0.1160 nm). All samples were powders prepared by the ceramic route and loaded from x=0.0 by absorbing a known amount of oxygen. For La123 the maximum value obtained at an oxygen pressure of 1000 Torr was x=0.93 /1/.

2. EXPERIMENTAL RESULTS

The NQR of Cu is especially useful to investigate the nearest neighbor configuration of the Cu(1) sites /7/ since the NQR frequency is determined by the electric field gradient (EFG) at the nuclear site. The EFG depends besides on other contributions like valency etc. on the number and position

of the oxygen neighbors of the ion under inspection. No reliable calculation of the EFG for the different Cu sites in the 123 compounds has been possible up to now. But three configurations of the Cu(1) site could be identified from the dependence of the NQR spectra on x. They are denoted corresponding to the number of oxygen nearest neighbors including the apex sites by Cu(1)-2, the site in the completely empty Cu(1) layer, Cu(1)-3, the two Cu(1) neighbors of a single oxygen ion or more generally the ends of a (Cu-O)n-Cu chain of length n, and Cu(1)-4, the planar fourfold coordinated site within a chain.

The NQR frequencies and linewidths of these three configurations change only little with the overall oxygen content of the samples. All three lines shift contineously with the RE radius increasing for Cu(1)-4 and decreasing for the other two lines /1/. In La123 the NQR frequencies agree for Cu(1)-4 and Cu(1)-3 which makes the clear separation difficult. No other configurations which would correspond to the simultaneous occupation of the O(1) and the O(5) neighbor sites of a given Cu(1) ion have been identified in the NQR spectra of Cu(1).

For comparing the relative intensities of the three lines (I2, I3, I4) which are proportional to the number of Cu nuclei in the corresponding configurations, the observed spectra were normalized by ν^2 corresponding to the frequency dependence on the NQR intensity, and the separated lines were integrated. I3 and I4 are connected with x by the relation $x = I3/2 + I4$. The data discussed here are only from samples where the difference between this value of x and the nominal concentration was below 0.1.

The dependence of the relative intensity I3 on the oxygen content for the compounds with different ionic radii is the most characteristic and is compared in Fig. 2 with three simple models. It is evident that in all the three systems the configuration Cu(1)-3 is present in contrast to early claims from crystal chemistry that in the Cu(1) layer only either 'full' or 'empty' chains should be allowed /8/. The change of the NQR spectra with the RE ionic radius is most evident for x near 0.5, where the intensity of the Cu(1)-2 lines decreases from 37% in Gd123 to 13% for La123 /1/.

For all three systems the dependence for $x \leq 0.4$ can be well described by a random distribution of the oxygen ions on all sites of the Cu(1) layer with the condition that the 90° configuration of two direct oxygen neighbors of a Cu(1) ion is forbidden as in the ortho-I stucture. This model leads to the relations:

$$I2 = (1-x)^2 \qquad I3 = 2x(1-x) \qquad I4 = x^2 \,. \tag{1}$$

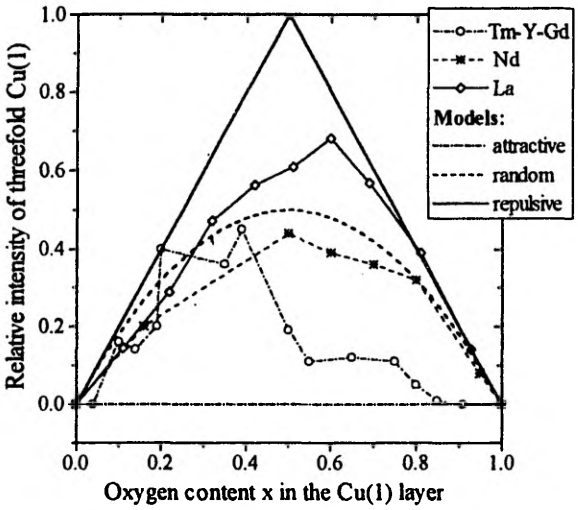

Fig. 2:
The relative abundance versus x of Cu(1)-3 in the 123 compounds with small (Tm, Y, Gd), medium (Nd), and large (La) RE ions.

For $x \geq 0.4$, however, the three systems become extremely different. For Nd123 the model (1) is still the best approximation for all values of x. For the small RE ions the assumption that all oxygen ions order in chains of infinite length, leading to

$$I2 = 1-x \qquad I3 = 0 \qquad I4 = x \tag{2}$$

gives the better description of the data. La123 with the high intensity I3, in contrast, can be best described by a model where pairs of oxygen vacancies or ions are forbidden for $x > 0.5$ or $x < 0.5$, respectively:

$$I2 = 0 \qquad I3 = 2(1-x) \qquad I4 = 2x-1 \qquad \text{for } x > 0.5,$$
$$I2 = 1-2x \qquad I3 = 2x \qquad I4 = 0 \qquad \text{for } x < 0.5. \tag{3}$$

From the relative intensities the mean value of the chain length n can be determined according to the relation

$$n = 1 + 2I4/I3. \tag{4}$$

The results presented in Fig.3 show the large differences in the dependence of the chain length on the ionic radii. Only in the compounds with small RE ions, chains with a length of about $n = 8$ are formed at low oxygen content x near 0.5. In this case the plateau of n reflects directly the plateau of T_C (Fig.1). In the Nd and La compounds a chain length of this size is obtained only for $x > 0.8$, but for all the compounds the transition from antiferromagnetic to superconducting behavior appears at the same mean chain length of about of 3 to 5 oxygen ions.

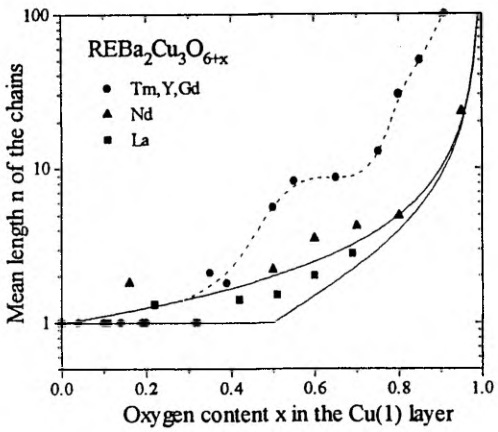

Fig. 3:
The mean length of the CuO chains versus x for the different RE123 compounds, the dashed line serves as a guide to the eye, the full lines represent the models of eq. 1 and 3 for Nd and La.

3. DISCUSSION

The experimental data confirm the models which claim that a minimal length of the Cu-O chains is necessary for doping holes to the $Cu(2)O_2$ layers which destroys the antiferromagnetic order and induces metallic and superconducting behavior. The formation of the chains in the Cu(1) layers of the Y123 is generally described by the phenomenological ASYNNNI (asymmetric next-nearest-neighbor Ising) model /9/. In this lattice gas model three basic interactions between pairs of oxygen ions are introduced. V_1 is the strong electrostatic repulsion of nearest oxygen pairs adjacent to a common Cu ion in a 90° configuration and explains the ordering of the oxygen in chains at $x=1$ in all the 123 compounds. The second neighbor interactions are different depending upon wether the interaction is mediated by a Cu ion, V_2 (in-chain interaction), or not, V_3 (ions in neighboring chains). V_3 is repulsive from the same reason as V_1, but weaker corresponding to the larger distance. For V_2 the situation is not so clear, but the relation $V_2<0<V_3<V_1$ can explain the formation of the ortho-II structure in $YBa_2Cu_3O_{6+x}$ with the sequence of full and empty chains at $x=0.5$. As pointed out by D. de Fontaine, this model with interaction parameters independent on x is symmetric in the number of oxygen ions and vacancies and leads to the separation into full and empty chains at low x as well as at high x /9/.

In contrast the x dependence of I3 in Fig.2 shows the tendency to form 'full' and 'empty' chain fragments with large contributions of I4 and I2 only in the compounds with the small RE ions and at $x>0.4$. This means

that V_2 is attractive only in this case. So it must be stated that the ASYNNNI model with fixed parameters V_1, V_2, and V_3 cannot describe the general situation of the RE123 compounds. At least V_2 is different in the semiconducting and the metallic states and depends in a critical way on the lattice parameters. At the increase e.g. of the b-axis from 0.388 nm for Y123 to 0.391 nm for Nd123 and to 0.394 nm for La123 changes V_2 from attractive through indifferent to repulsive.

Different proposals have been given to explain the missing attractive interaction in $YBa_2Cu_3O_{6+x}$ at $x \leq 0.4$ most evident in the ordered structure with only single oxygens found for YBCO with $x=0.35$ /6/ and similar ones found by electron microscopy. Aligia et al. /10/ have considered screened Coulomb repulsion for all three interactions with the screening length changing on the transition from the semiconductiong to the metallic state. De Fontaine et al. /11/ claim V_2 independend of x and the structures with single oxygens to be metastable due to slow kinetics. Uimin and coworkers /12/ consider the electronic state of a finite chain fragment in dependence on the length and the number of holes. By this they arrive at a sign of V_2 changing with the length of the chains and also depending on the size of the unit cell. So this model may be appropiate to describe the ordering of oxygen in the 123 compounds containing small or large RE ions.

REFERENCES

1. H. Lütgemeier et al., to be published
2. T. B. Lindemer et al., Physica **C231,** (1994), 80
3. M. Guillaume et al., J. Phys. Condens. Matter **6,** (1994), 7963
4. T. B. Lindemer et al., Physica **C216,** (1993), 99
5. Th. Zeiske et al., Physica **C194,** (1992), 1 and
   A. Simon et al., J. Solid State Chem. **106,** (1993), 128
6. Th. Zeiske et al., Z. Phys. **B6,** (1992), 11
7. I. Heinmaa et al., Appl. Magn. Res. **3,** (1992), 687 and
   H. Lütgemeier et al., in 'Phase Separation in Cuprate Superconductors'
   E. Sigmund and K. A. Müller eds., Springer (1994), p. 225
8. B. Raveau et al., Physica **C153-155,** (1988), 3
9. D. de Fontaine et al., Europhys. Letters **19,** (1992), 229
10. A. A. Aligia et al., Solid State Comm. **87,** (1993), 363 and
    A. A. Aligia, Europhys. Letters **26,** (1994), 153
11. M. de Fontaine, Europhys. Letters **26,** (1994,) 155
12. P. Gawiec et al., Phys. Rev. **B53,** (1996), 5580 and
    D. R. Grempel et al., to be published (LT-21, Prague)

VI

H. Lütgemeier, S. Schmenn, P. Meuffels, O. Storz, R. Schöllhorn, Ch. Niedemayer,
I. Heinmaa, Yu. Baikov,
A different type of oxygen order in $REBa_2Cu_3O_{6+x}$ HT_c superconductors
with different RE ionic radii,
Physica C **267**, pp. 191–203 (1996).

ELSEVIER

Physica C 267 (1996) 191–203

PHYSICA C

A different type of oxygen order in RE $Ba_2Cu_3O_{(6+x)}$ HT_c superconductors with different RE ionic radii

H. Lütgemeier *[,a], S. Schmenn [a], P. Meuffels [a], O. Storz [b], R. Schöllhorn [b], Ch. Niedermayer [c], I. Heinmaa [d], Yu. Baikov [e]

[a] *KFA Forschungszentrum, Jülich, IFF, Germany*
[b] *Technical University of Berlin, Berlin, Germany*
[c] *University of Konstanz, Konstanz, Germany*
[d] *Institute of Chemistry, Physics and Biophysics, Tallinn, Estonia*
[e] *Joffee Institute, St. Petersburg, Russia*

Received 13 May 1996

Abstract

Using the copper Nuclear Quadrupole Resonance (NQR) spectra of RE $Ba_2Cu_3O_{6+x}$ (RE123, RE = Y, Nd, La, $0 \le x \le 1$) we have determined the relative intensities of the resonance lines belonging to the Cu(1) sites in the Y123 structure type with two, three and four nearest neighbor oxygens as a function of the oxygen concentration x. The different intensity distribution for different RE shows that, unlike the case in Y123, where the oxygen ions in the basal plane order preferentially into long chain fragments leading to the formation of the ortho-II structure at $0.5 < x < 0.6$, the ordering in Nd123 can be described by the model where the chain fragments are formed by random occupation of the oxygen sites along the fragment direction. In La123 oxygen ions below $x = 0.5$ and oxygen vacancies above this value tend to be single, forming near $x = 0.5$, most probably, the "herringbone" structure. Due to different oxygen order, the Nd123 and La123 become superconducting only at high oxygen contents, $x \ge 0.6$, whereas at lower x the systems show the antiferromagnetic order in the Cu(2) planes, detected by the zero field nuclear magnetic resonance spectra of the Cu(2) sites and by muon spin rotation experiments.

1. Introduction

The 123 compounds of the type RE $Ba_2Cu_3O_{(6+x)}$ (RE123), $0 \le x \le 1$, where RE can be either Y or La or one of most of the rare earth ions, show at increasing oxygen content the transition from a semiconducting antiferromagnet with ordered Cu spins in the Cu(2) layers to superconductivity in the same layers. It is generally accepted that the holes needed to obtain the metallic behavior of the Cu(2) layers are doped from the Cu(1) layers with the oxygen content x. The increase of the RE ionic radii from the smallest Yb with $r = 0.0985$ nm in eightfold coordination by oxygen [1] to Nd ($r = 0.1109$ nm) results in an increase of the maximal T_c found for x near 1.0 [2,3] and to an increase of the minimal oxygen concentration needed for the onset of superconductivity from about $x = 0.4$ to 0.6 [4–7]. At the same time the plateau of T_c at about 60 K in the compounds with the small RE ions is replaced at

* Corresponding author. Fax: +49 2461 612 016; e-mail: h.luetgemeier@kfa-juelich.de.

PII S0921-4534(96)00380-2

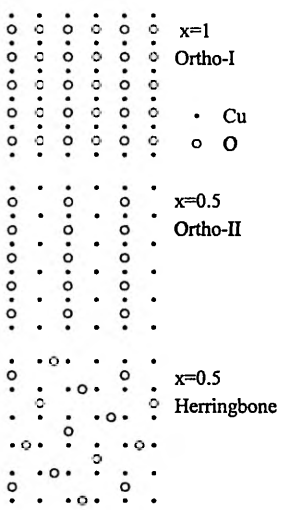

Fig. 1. Oxygen superstructures in the Cu(1) plane of the 123 compounds at $x = 1$ and $x = 0.5$.

larger r by a mainly continuous increase of T_c with the oxygen content. The 123 compound containing the larger Pr does not become superconducting at all, but with RE = La ($r = 0.1160$ nm) a superconducting 123 compound with T_c above 90 K exists again [8–13].

For Y123 two ordered arrangements of the oxygen in the Cu(1) layer corresponding to the two plateaus of T_c are known, ortho-I for x near 1.0 where the oxygen ions form chains in the b-direction with all O(1) sites occupied and the O(5) sites empty, and ortho-II at x near 0.5 where every second chain remains empty (Fig. 1). Especially in the range of the ortho-II structure, T_c depends on the perfection of the oxygen order: Samples quenched from temperatures above 200°C generally reveal lower T_c than samples carefully annealed at lower temperature, and even keeping the samples at room temperature for a longer period leads to an increase of T_c [14]. Thus the change of the $T_c(x)$ behavior at increasing ionic radii may also be connected with differences in the order of oxygen. Indeed, the electron diffraction pattern corresponding to ortho-II could not be detected in Nd123 [7]. At $x = 0.5$ other ordered superstructures can be constructed [15]. Among these the "herringbone structure" with only single oxygen ions has been found by X-ray diffraction in a single crystal of Y123 at $x = 0.35$ [16], a result which could not be confirmed in a later experiment [17].

Nuclear quadrupole resonance (NQR) of copper is a valuable tool to investigate the ordering of oxygen in the Cu(1) layer since according to the number of oxygen nearest neighbors three configurations of the Cu(1) ion can be distinguished by their different NQR frequencies [18,19]. Cu(1)-2 with only the two oxygen neighbors at the apex sites and Cu(1)-4 with both chain sites occupied are the configurations of the stoichiometric compounds at $x = 0$ and $x = 1$, respectively. Cu(1)-3 ions appear either as the neighbors of single oxygen ions in the tetragonal structure near $x = 0$ or of oxygen vacancies in the orthorhombic structure or as the terminating Cu ions of Cu–O chains. Due to the different charge distribution, the electric field gradient (EFG) determining the NQR frequency of the Cu(1) sites is different for the three configurations. Thus the relative intensities of the corresponding NQR lines allow conclusions about the distribution of the oxygen ions in the Cu(1) layer.

In contrast to the limits of superconducting behavior, the range of the antiferromagnetic order in the Cu(2) layers has not yet been reported so far for other RE ions but Y. A simple method to observe the antiferromagnetic order of the Cu ions is the nuclear magnetic resonance of Cu in the antiferromagnetic state (AFNMR). The hyperfine field in the magnetically ordered state of Cu induces a splitting of the nuclear levels which can be observed without an external magnetic field as a NMR spectrum split by the quadrupole interaction. Thus the observation of an AFNMR spectrum in the range between 60 and 110 MHz with a quadrupole splitting of about 10 MHz is a clear indication of the magnetically ordered system of Cu(2) spins. At increasing temperature or at the approach to the x values of disappearing antiferromagnetic order, this signal is lost, most probably by the onset of fast relaxation of the Cu spins [20]. Due to the short time needed to detect the Larmor precession of a muon in the local field, the spin rotation of muons (MuSR) is distorted much less by relaxation and the Néel temperature and the

x value for disappearing antiferromagnetic order can be determined more accurately by this method [21]. Other methods to determine the Néel temperature use the line broadening of the Y NMR in the antiferromagnetic state [22] and the appearing of the magnetic reflections in neutron diffraction [23–26].

In this communication we discuss the connection of oxygen content and oxygen order with the superconducting transition temperature and antiferromagnetic order of the Cu(2) ions in RE123 compounds containing RE ions with different ionic radii. Besides the NQR data for RE = Y, Gd and Nd published already [18,19,27] we present new values for RE = La and the results obtained by MuSR and AFNMR in the Nd123 compounds.

2. Experimental details

2.1. Preparation of La123

The preparation of the RE123 compounds with large RE ions and especially with La is difficult since the large ions can replace the Ba ions forming $La_{(1+z)}Ba_{(2-z)}Cu_3O_{(6+x)}$ and $BaCuO_2$. Refinement of the neutron diffraction patterns has indicated that Ba can occupy the La sites [3] and La the Ba sites [9], in both cases T_c was highly reduced. A large amount of La on the Ba sites suppresses the superconductivity, though the limits of z are still unclear. Lindemer et al. [12] show a maximum of T_c at $z = 0.15$ and $T_c > 30$ K up to $z = 0.4$. According to the results of different groups [8–11] it is essential for minimizing z, to perform all sintering steps above 900°C under a low oxygen partial pressure and to load with oxygen only at temperatures below the tetragonal to orthorhombic transition temperature [10]. We found, however, that a first calcination in oxygen or air is required to achieve a complete reaction of the starting material. The La123 samples used here were prepared from dried and sieved La_2O_3, $BaCO_3$ and CuO powders in stoichiometric amounts (La:Ba:Cu = 1:2:3). The La_2O_3 had to be pretreated because it is hygroscopic [8]. It was fired in air at 900°C for 12 h, rapidly cooled to room temperature and weighed immediately. An intimate mixture of the starting materials was calcined at 920°C for 24 h in a dried oxygen flow, then the gas supply was switched to nitrogen and the sintering continued in the N_2 flow for another 12 h at 920°C before slowly cooling down to room temperature at a rate of 2 K/min. The prereacted material was reground, pressed into pellets and the calcination process in O_2 and N_2 was repeated, this time at 950°C, with all other parameters left unchanged. In the following sintering steps no more oxygen was used, the processes were completely run in a dried N_2 flow. After regrinding new pellets were pressed, heated to 200°C, held there for 2 h to ensure removal of residual moisture and air, then sintered at 920°C for 24 h and finally cooled down to room temperature at a rate of 2 K/min. This procedure was repeated several times with intermediate grindings and pressing of new pellets between each step. After each sintering step the samples were chequed by X-ray diffraction. The process was stopped after 4 cycles when the tetragonal splitting and the width of the reflections did no more change. No impurity phases, especially no $BaCuO_2$, could be identified. EDX analysis showed for the La content $1 + z = 1.05$ (5). The oxygen content of the samples after cooling under N_2 was determined by iodometric titration as $6 + x = 6.09(1)$.

For the preparation of La123 samples with different x the initial pellets with a total mass of about 10 g were divided into 10 pieces and have been treated without grinding. The first step was vacuum treatment at 10^{-6} Torr and 690°C for 4 hours. The weight loss after this treatment agreed with the oxygen content $x = 0.09$ determined for the starting material by titration. This confirms our experience from other 123 compounds that by this treatment only all oxygen from the Cu(1) layer is removed and $0 < x \leq 0.02$ is obtained. We must consider, however, that this holds only in the case that all Ba sites are occupied by divalent ions. In the case of partly replacing Ba by La in $La_{(1+z)}Ba_{(2-z)}Cu_3O_{(6+x)}$ we must expect a larger oxygen content x corresponding to $z/2 < x < 1 + z/2$ [11] which cannot be detected by titration or by measuring weight or pressure differences as used here.

For loading with oxygen a calibrated volume of 103 cm^3 was used and the amount of oxygen absorbed was determined from the pressure difference and the increase of the weight. For $x < 0.6$ all oxygen was absorbed at 200–400°C. To avoid

nonuniform distribution, the samples were heated to 700°C and then cooled at a rate of 10°K/min. After this procedure the oxygen pressure was below 0.1 Torr. For $x \geq 0.6$ pressures above the equilibrium values are required due to slow kinetics. At the maximum pressure of 1000 Torr we obtained $x = 0.93$. The oxygen content determined from the changes of weight and pressure agreed within ± 0.01. For the high oxygen content the equilibrium pressure was found to be larger than in Y123 at the same temperature by about one order of magnitude.

The reproducibility of the oxygen content within one series of samples prepared from the same starting material has been found to be better than $\Delta x < \pm 0.02$ [27]. But a much larger systematic shift up to $\Delta x = \pm 0.1$ may exist between different materials, e.g. by a different amount of impurity phases. For this reason differences in the oxygen concentration for the orthorhombic to tetragonal transition of Nd123 and La123 (Fig. 2) and of the onset of superconductivity (Fig. 3) cannot be discussed on the basis of the present data.

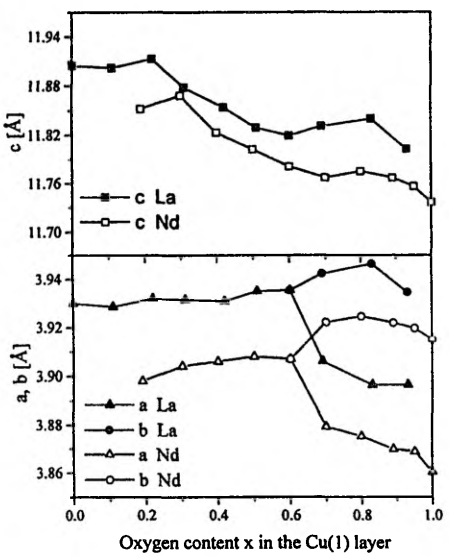

Fig. 2. Lattice parameters of the Nd123 and La123 samples investigated.

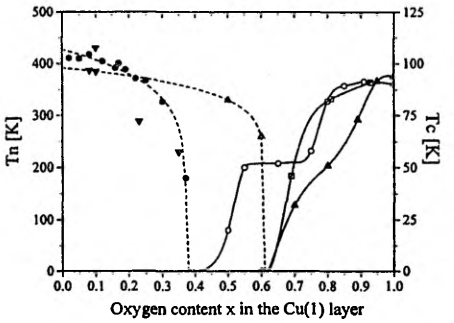

Fig. 3. Transition temperatures T_n to AF order (left scale and full symbols) and T_c to superconductivity (right scale and open symbols) versus oxygen content. Left scale: circles Y123 from Y NMR [22], at $x = 0.37$ from neutron diffraction [23], up triangles Nd123, our data from MuSR, down triangles data from neutron diffraction [24–26]. Right scale: T_c from DC susceptibility (1% of the diamagnetic signal at 2 mT), circles Y, Gd and Tm 123 compounds, triangles Nd123, squares La123. All lines serve only as guide to the eye.

2.2. Sample characterization

The lattice parameters of the Nd123 and La123 samples have been determined by standard powder X-ray diffraction (Fig. 2). In both cases the transition tetragonal-orthorhombic appears at about $x = 0.6$. Different from the compounds with the smaller RE ions, $c/3 = b$ holds in the full orthorhombic range. The values obtained for $x = 0.93$ well agree with data reported for stoichiometric material with the highest x and the lowest amount of La on Ba sites [8,11]. The superconducting transition has been determined from the DC susceptibility at 2 mT. For La123 with $x = 0.93$, the highest oxygen content obtained, the onset, diamagnetism is seen at 92 K, 1% of the diamagnetic signal at the conditions of shielding and Meissner effect appears at 91 K. These values are slightly below the values of 95 K claimed for stoichiometric La123 [10,13] but agree with those by Lindemer et al. [12] who find the maximal T_c of 95 K only at a slight excess of La by about $z = 0.15$. The variation of T_c (determined by 1% of the diamagnetic signal) with decreasing oxygen content x (Fig. 3) shows for the La123 a slower decay than for Nd123. The La123 sample with $x = 0.81$ ($T_c = 83$ K)

reveals a very broad transition range starting at 90 K. Similar results have been found for samples with La excess $z = 0.08$ [9]. In both cases the reason may be a not completely homogeneous distribution of the oxygen. In Nd123 and La123 T_c disappears between $x = 0.7$ and 0.6 just in the range of the structural transition from orthorhombic to tetragonal symmetry.

2.3. NQR and AFNMR measurements

The NQR and AFNMR spectra have been measured at temperatures of 4.2 or 1.2 K by the standard spin-echo-technique by stepwise sweeping the frequency and tuning the resonance circuit for each step. The r.f. amplitude of the pulses was choosen to obtain the maximum echo intensity at a duration of about 5 μs for the 180° pulse. Since under these conditions the bandwidth of excitation is below the linewidth of all components in the spectrum, the echo hight normalized by the square of the exciting frequency is proportional to the number of nuclei at resonance. Due to the two isotopes ^{63}Cu (69%) and ^{65}Cu (31%) with spin 3/2, the NQR spectrum consists for each Cu site of a doublet with frequencies differing by about 8%, corresponding to the ratio of the nuclear quadrupole moments, and the higher frequency for the more abundant ^{63}Cu. In the AFNMR spectra the central transition for ^{65}Cu appears at the higher frequency, since the magnetic moment of this isotope is the larger one. In the following we always mention only the resonance frequencies of the more abundant ^{63}Cu isotope.

At high oxygen content, the NQR signals from the Cu(2) sites and from Cu(1)-2 overlap in the frequency range 27–32 MHz. In the Gd123 and also in Nd123 the signals from both sites could be separated due to the fast relaxation induced to the Cu(2) nuclei by the fluctuating magnetic moments of the RE ions [18,19] which influences the more distant Cu(1) nuclei only weakly. From these experiments it is also evident that at decreasing x the NQR lines of the Cu(2) sites broaden quickly and disappear in the samples with T_c below 60 K whereas the sharp Cu(1)-2 signal corresponding to pieces of "empty chains" increases in intensity.

The NQR spectrum for La123 with the largest oxygen content 6.93 obtained at our conditions of preparation with oxygen pressure up to 1000 Torr

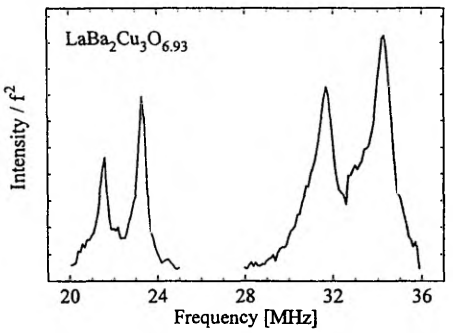

Fig. 4. NQR spectrum of La123 with $x = 0.93$.

(Fig. 4), with the Cu(2) lines between 30 and 36 MHz is very similar to a spectrum published recently for a sample prepared at 760 Torr [13,28] for which an oxygen content of about 7.0 was claimed. The linewidth agrees with the Cu(2) signal of slightly oxygen deficient Nd123 [27]. Also the Cu(1) NQR spectrum between 20 and 24 MHz contains besides the narrow lines of the Cu(1)-4 other components due to defects. At decreasing x the Cu(2) signal broadens further and disappears at $x = 0.7$ where another line at lower frequency appears. In analogy with the Nd123 [27] we ascribe these broad and narrow high frequency components of the NQR spectrum to Cu(2) and Cu(1)-2, respectively.

The NQR frequencies obtained for the three configurations of Cu(1) are presented for different RE ions in Fig. 5. The Cu(1)-3 site plays a special role since its frequency for a fixed RE ion does not depend on x, that means on the configuration in the more distant neighbor shells. The frequency of Cu(1)-2 shifts from the value at $x = 0$ in a narrow range of x near 0.5 either under broadening or in two steps in the case of the small RE ions [18] by about 1.5 MHz to higher frequency. The line of Cu(1)-4 broadens at $x < 0.8$. Nevertheless it is possible for Y and Gd 123 [18] and for Nd123 [27] to determine the relative intensities I_2, I_3, and I_4 corresponding to the abundance of the three configurations. In La123 the lines of Cu(1)-3 and Cu(1)-4 overlap and it is not possible to separate the corresponding intensities unambiguously for x above 0.5. At lower x, a weak Cu(1)-4 signal can be detected

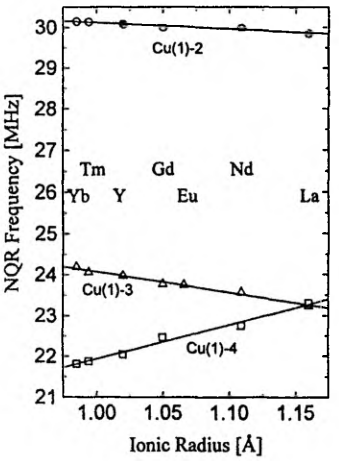

Fig. 5. RE123: NQR frequencies of Cu(1)-2, Cu(1)-3 and Cu(1)-4 at different radii of the RE ions.

around 20 MHz and as a broad background under the Cu(1)-3 signal. So we use for La123 at $x > 0.5$ only the relative intensity I_2 of the Cu(1)-2 configuration. When all three intensities can be determined the oxygen content of the Cu(1) plane is given by

$$x = I_4 + I_3/2, \quad (1)$$

which allows one to control the correctness of the data. In the results presented the deviation of the concentration determined from the intensities by Eq. (1) differed from the nominal ones by less than 0.1. When only I_2 is known as for La123, I_3 and I_4 can be estimated from x and I_2.

The evaluation of the NQR data relies on the assumption, that all Cu(1) sites are visible for NQR. This means that no signal is lost by magnetic interactions with localized static or slowly fluctuating magnetic moments with correlation times below 10^{-8} s. In the antiferromagnetic state normally the AF-I structure is established where the local field at the Cu(1) sites is completely canceled [19,29], but by doping with Fe, Al and other trivalent ions on the Cu(1) sites a transition to the AF-II structure with a different stacking sequence of the antiferromagnetic Cu(2) layers appears at low temperature [19,26]. This structure becomes evident in the NQR spectrum of the Cu(1)-2 sites by a splitting due to a small local field of about 0.2 T. The same AF-II structure appears in most Nd123 single crystals [24,25] probably induced by Al impurities. But also most nominally pure Nd123 and La123 powder samples reveal at oxygen content x below 0.1 the AF-II splitting in the NQR spectra. This transition to AF-II may be induced by a small amount of Nd or La ions on the Ba sites and disappears if the oxygen content is above $x = 0.1$. All the samples discussed here were in the AF-I state without splitting of the Cu(1)-2 line. The unsplit NQR line of the Cu(1)-3 site in the antiferromagnetic and the superconducting states of all 123 compounds proves that also this configuration does not carry a localized magnetic moment. Any localized magnetic moment would induce a strong magnetic hyperfine field which in its paramagnetic state would suppress the NQR signal by fast relaxation and in the ordered state would shift the resonance out of the range of the NQR frequencies.

2.4. Muon spin rotation measurements

The MuSR experiments were performed at the low momentum beam of the Paul Scherrer Institut/Switzerland in zero external field. Polarized positive muons with an energy of 4 MeV are implanted into the samples. The decay positrons preferently emitted in the muon spin direction are registered by detectors in the forward and backward

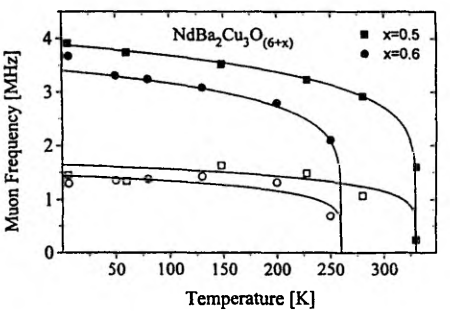

Fig. 6. Nd123: Temperature dependence of the muon Larmor frequencies.

directions relatively to the polarisation of the incident beam. Muons trapped at a site with a static local magnetic field perform a Larmor precession leading to an oscillating decay function of the polarization.

We have measured for two of the Nd123 samples with oxygen content $x = 0.5$ and 0.6 the decay functions of the muon polarization for temperatures up to 330 K. In both cases an oscillatory decay of the polarization gives clear evidence of the antiferromagnetic order in Nd123 up to the oxygen content $x = 0.6$. For both samples the decay of the polarization can be fitted with two components of similar intensity but different Larmor frequencies of 3.9 and 1.45 MHz for $x = 0.5$ and 3.7 and 1.3 MHz for $x = 0.6$ at 6 K. The temperature dependence (Fig. 6) was approximated by the relation

$$\nu = \nu_0((T_n - T)/T_n)^{\beta}, \tag{2}$$

with $\beta = 0.16$ which we used to determine the values for the Néel temperature of 330 K for $x = 0.5$ and 260 K for $x = 0.6$ presented in Fig. 3.

3. Results

3.1. NQR intensities

The differences of the NQR spectra at increasing ionic radius r of the RE ions are most evident at x about 0.5 where only half of the oxygen sites in the chains are occupied (Fig. 7). The intensity at the highest frequency corresponding to Cu(1)-2 sites decreases whereas the intensity of Cu(1)-3 increases. This means that the portion of oxygen ions clustered in "full chains" decreases when the radius of the RE ion increases. This tendency is evident in the dependence of the three components I_2, I_3, and I_4 on x for the different ionic radii (Fig. 8) which will be compared with three limiting cases for the arrangement of the oxygen ions in the Cu(1) plane. A complete ordering of the oxygen into the long chains leaving the remaining part empty would lead to

$$I_2 = 1 - x, \qquad I_3 = 0, \qquad I_4 = x. \tag{3a}$$

Completely random distribution of the oxygen on all allowed oxygen sites of the orthorhombic structure gives

$$I_2 = (1 - x)^2, \qquad I_3 = 2x(1 - x), \qquad I_4 = x^2. \tag{3b}$$

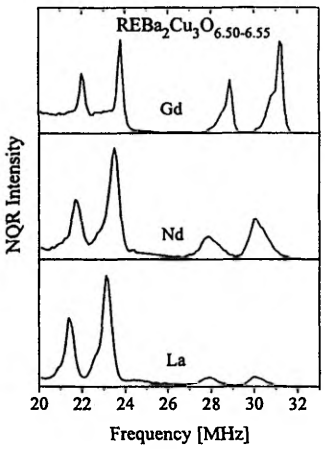

Fig. 7. NQR spectra of of the Cu(1) sites in Gd123, Nd123 and La123 with x near 0.5.

A repulsive interaction keeping the number of nearest oxygen neighbors in a chain as low as possible leads to

$$I_2 = 1 - 2x, \qquad I_3 = 2x, \qquad I_4 = 0, \quad \text{for } x < 0.5, \tag{3c}$$

$$I_2 = 0, \qquad I_3 = 2 - 2x, \qquad I_4 = -1 + 2x, \quad \text{for } x > 0.5.$$

In Fig. 8 we compare the experimental results with the model (3b) of a random distribution. Evidently the data for Nd123 are in the best way approximated by this model. For the smaller RE ions this model cannot describe the intensities since the number of Cu(1)-3 sites is too small for $x > 0.4$ indicating the tendency to form long chain fragments which are either occupied or empty. The opposite situation is presented in the case of La123 where I_2 disappears already for $x \geq 0.6$. Here the number of vacancies clustered in empty chains is much smaller than expected in the random case and is approximated by the model (3c) of a repulsive interaction. The state of only single oxygen ions in the Cu(1) layer at $x = 0.5$ can be obtained by two superstructures from which the "herringbone" structure (Fig. 1) should be the one with the lower energy [15]. A difference of the oxygen order in Y123 and Nd123 with Nd123 repre-

senting the disordered limit has also been derived from the optical reflectivity of single crystals [30].

3.2. Length of copper–oxygen chains

In no spectrum of the Cu(1) sites in the 123 compounds studied we could identify a signal which might be attributed to a Cu ion with oxygen nearest neighbors forming an angle of 90°. If we neglect such configurations which might exist in the twinnng bounderies of the orthorhombic structure, all oxygen

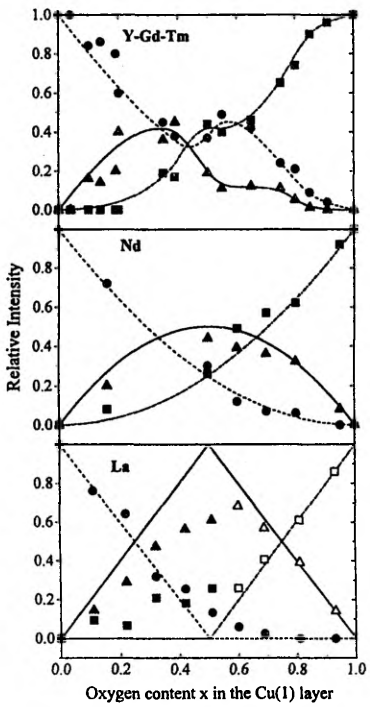

Fig. 8. Relative NQR intensities of the three Cu(1) configurations in the 123 compounds with different RE: circles I_2, triangles I_3, squares I_4. Full symbols determined directly, open symbols (for La123) calculated from I_2 and x according to Eq. (2); top: small RE ions, the lines are only a guide to the eye; middle: Nd, lines according to the model (3b) for random distribution of oxygen; bottom: La, lines from model (3c), repulsive interaction.

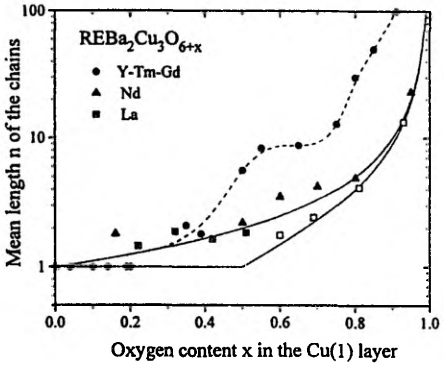

Fig. 9. Mean length of the $(Cu–O)_n$ chains versus oxygen content for different RE ions, the dashed line (Y123) is only a guide to the eye, the full lines represent Eqs. (5a) and (5b) for Nd123 and La123, respectively.

ions are arranged in fragments of the type $(Cu\text{-}O)_n\text{-}Cu$ with an average length n given by

$$n = 1 + 2I_4/I_3. \tag{4}$$

From Fig. 8 it follows that this average chain length depends in a quite different way on the oxygen content for the three RE ions considered (Fig. 9): the plateau character of the T_c versus x dependence in Y123 is exactly reproduced in the dependence $n(x)$. For Nd123 a continuous decay of $n(x)$ as of $T_c(x)$ is evident which is well described by the relation from Eq. (3b)

$$n = 1/(1-x) \tag{5a}$$

In La123 reliable values of n cannot be determined in the superconducting range since the frequencies of Cu(1)-3 and Cu(1)-4 are not separated. From the model (3c) it follows

$$n = x/(1-x) \quad \text{for } x > 0.5;$$

$$n = 1 \quad \text{for } x < 0.5, \tag{5b}$$

which within the accuracy of the experimental data cannot be distinguished from (5a). The comparison of Figs. 3 and 9 shows as the condition for the onset of superconductivity the development of $(Cu\text{-}O)_n\text{-}Cu$ chain fragments with a mean length of about $n = 4$.

3.3. The antiferromagnetic state

For the Y123 the breakdown of the antiferromagnetic order and the onset of the superconductivity appear at the same oxygen concentration, neither an overlap of the two states nor a gap between both could seriously be detected (Fig. 3). We have investigated if the same situation is also found for the systems with the larger RE radii. The AFNMR spectra of the Cu(2) sites could be detected up $x = 0.5$ for Nd123 and La123 (Fig. 10). The spectra can be analyzed as in the Y123 by a symmetric EFG along the c-axis and a perpendicular hyperfine field. At $x = 0.6$ only a weak AFNMR signal is left as for the limiting value 0.3 in Y123 [20]. In spite of the strong change of the oxygen concentration in the Cu(1) layer, the hyperfine field and the quadrupole splitting representing the ordered magnetic moment and the charge distribution at the Cu(2) sites are nearly constant in the full range of antiferromagnetic order (Fig. 11). The decay of the hyperfine field at increasing RE radii continues the linear relation for the smaller RE ions [31]. The large range of antiferromagnetic order in the Nd123 proved by the hyperfine field existing up to $x = 0.6$ is in contrast to data for T_n in some single crystals determined from different groups by neutron diffraction [24–26] which indicate a similar behavior as for Y123 with a limit of the antiferromagnetic order at $x = 0.4$ (Fig. 3). The result from the AFNMR is confirmed by the MuSR experiments (Fig. 6) which show for $x = 0.6$ the Neel temperature still as high as 290 K. The two values of the local field seen by the muons in the Nd123 with x near 0.5 agree with results found in other antiferromagnetic 123 compounds, where the antiferromagnetism of the Cu(2) layers is induced either by oxygen depletion [21], hydrogen loading [32] or replacing the Y by Pr [33]. The frequencies near about 4 and 2 MHz are generally ascribed to muons trapped either at the apical or chain oxygen ions. In Y123 with $x = 0$ only the line at 4 MHz is found, but with higher oxygen content the second broad component appears. In the Nd123 with the higher oxygen content the well resolved second line confirmes the assignment of this line to traps near the chain oxygen sites.

According to the AFNMR and MuSR experiments the range of the antiferromagnetic order in Nd123 and La123 is extended to oxygen contents in the chains above 0.6. Thus the loss of magnetic order and the appearing of superconductivity in Nd123 and La123 take place in the range $0.6 < x < 0.7$. This is

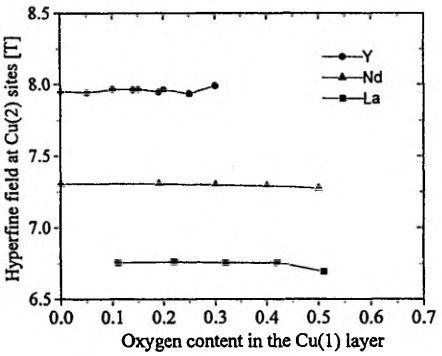

Fig. 11. Hyperfine field at the Cu(2) sites in the antiferromagnetic range of the RE123 compounds versus oxygen content x.

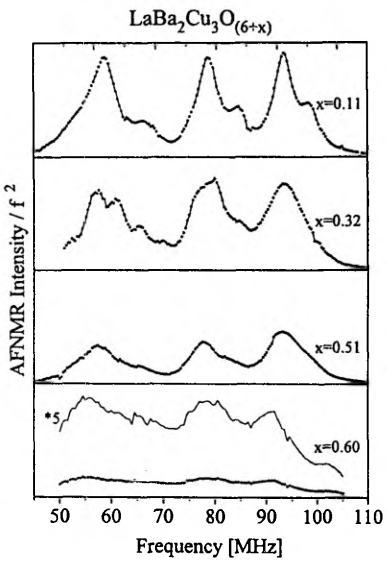

Fig. 10. AFNMR spectra of the Cu(2) sites in La123 for different x.

the range where the mean length of filled chain fragments in both compounds increases to values above $n = 3$. A somewhat higher value of n for the transition holds in Y123 where by the formation of ortho-II structure the growing of the chains starts already at $x = 0.4$. This means that both transitions, breakdown of the magnetic order and the onset of superconductivity are determined by one mechanism which is connected with the length of the filled chain fragments.

4. Discussion

Most models applied to describe the doping of the $Cu(2)O_2$ planes assume that CuO chain fragments in the Cu(1) layer of a minimal length or ortho-I clusters of a minimal size are needed to transfer holes to the planes [34–36]. The results presented here indicate that the three systems with very different oxygen arrangement show the transition from antiferromagnetic to superconducting behavior if the average chain length exceeds 3–5 oxygen ions. Theoretical calculations of the minimum fragment lengths for an effective charge transfer yield 2 or 4 oxygens depending on the relative position of the chain and the plane energy bands [34]. These values seem to be in accordance with our results. For determining the number of holes inducing the transition and the connection between T_c and the number of holes, the distribution function of the chain length would be needed. This distribution may be very different in the three cases considered but cannot be deduced from the NQR results, since only the nearest neighbor Cu–O configurations can be distinguished. So it is rather surprising that a correlation between T_c and n has been found for the RE123 compounds forming the ortho-II structure and Nd123 with the random distribution of the oxygen ions [27]: After the onset of superconductivity at n about 4, $T_c = 60$ K is obtained at n about 8 and 90 K at about 20. Our data for La123 reveal lower values of n for the same T_c. This is a strong indication that the distribution of chain length is different in this case.

The reason for the different type of oxygen order at $x < 1$ in Y123, Nd123, and La123 leading to the different $n(x)$ must be found in a different interaction energy of the oxygen ions in the Cu(1) layer. The most simple lattice gas model describing the ortho-II structure of the Y123 was proposed by de Fontaine et al. [37]. It needs three pair potentials, V_1 for nearest oxygen neighbor pairs, V_2 for next nearest pairs connected by a Cu ion, and V_3 for those without Cu in between, with the condition $V_2 < 0 < V_3 < V_1$. The strong repulsive interaction V_1 of two oxygen ions connected by a Cu(1) ion at 90° prevents the occupation of the oxygen sites at 90° and leads to the formation of the ortho-I structure near $x = 1$. The clustering of oxygen defects and oxygen ions to long chain fragments is induced by the attractive potential V_2, and the alternating sequence of filled and empty chains follows from the weak repulsive V_3.

Cluster variation calculation of the O-Cu-O chain lengths by Tournau et al. [38] showed, that the values observed by NQR in Y123 and Gd123 [18] can be well reproduced if the intrachain attractive interaction V_2 was reduced by 30% in comparison to that obtained from the first principle calculations [39]. The different order of the oxygen in the Nd123 and La123 cases, where the mean value of the fragment length is close to the random oxygen distribution or even less, can be taken as clear evidence, that the effective interaction V_2 changes from attractive to repulsive at increasing radii of the RE ion. This repulsive interaction should increase the chemical potential of the oxygen. Thus the much higher oxygen pressure (compared with Y123) needed for loading the La123 to high oxygen content is also a clear indication for the loss of the attractive interaction energy of oxygen neighbors linked by a Cu(1) ion.

Oxygen ordering in the case of repulsive (Coulombic) interaction V_2 was handled within the lattice gas model by Aligia et al. [15]. Here the chain formation is possible due to the screening of the Coulombic interaction in the metallic phase. In this model a number of oxygen superstructures at different $x < 0.5$ was predicted. Unfortunately, solely from the NQR data it is not possible to decide whether the single oxygens in the basal plane of La123 are disordered or organized into the superstructures. For $x = 0.5$ two alternative structures of single oxygen arrangements can be constructed. As mentioned above, one is the "herringbone" structure and the other can be formed by removing every second

oxygen from the perfect ortho-I structure. In the latter case an orthorhombic symmetry should be expected. According to the X-ray data for $x = 0.51$ sample, the structure is not orthorhombic, therefore we believe that here the oxygens are ordered into the "herringbone" structure. The superstructures proposed for $x > 0.5/15/$yield quite different chain length distributions, e.g. the structure for $x = 2/3$ has one half of the oxygens in long chains whereas the other half of oxygens are organized into stacks of perpendicularly oriented single oxygen chain fragments between the long chains. Thus the number of oxygens in long chains is even larger than in the case for random distribution. Similar types of superstructures containing long chains together with single oxygens at higher oxygen concentration may be the reason why the T_c values for La123 at given x are higher than that for Nd123 (Fig. 3) although the average chain length is lower. A large number of long chains together with single oxygen fragments would explain our result and the finding by Lindemer et al. [9] that T_c in La123 in contrast to Nd123 stays at about 90 K down to $x = 0.8$.

The attractive interaction V_2 of oxygen ions connected by Cu in Y123 is the reason why the transition to the metallic and superconducting state appears already at low oxygen content. On the other hand, this attractive interaction seems to exist only in the metallic state. Below $x = 0.5$ the number of chain ends, I_3, increases to the value of the random distribution of the oxygen ions as in the case of Nd123. This fits well with the detection of the "herringbone" structure mentioned above in a single crystal of Y123 with $x = 0.35$ by X-ray diffraction [16].

In the phase diagram of all the 123 compounds investigated here, the sharp transition from antiferromagnetism to superconductivity is quite different from the case of doping the antiferromagnetic Y123 by Ca in $Y_{(1-y)}Ca_yBa_2Cu_3O_6$ where the doping level needed for superconductivity ($y = 0.17$) is about twice the value for destroying the antiferromagnetic order [37]. The difference must come from the different sources of the holes: whereas each Ca ion induces one hole into the Cu(2) layers, at oxygen doping only those oxygen ions agglomerated in the filled chain fragments are effective. When the oxygen content once reaches the limit for forming these fragments the number of holes increases as an avalanche and induces the transition between the antiferromagnetic and superconducting states in the narrow range of oxygen content observed for all RE ions.

5. Conclusion

From the viewpoint of crystal chemistry it is often claimed that for the Cu(1) ions in the $REBa_2Cu_3O_{(6+x)}$ compounds only the twofold or planar fourfold coordinations should be allowed [41]. A consequence of this assumption is the model of a separation into "full" and "empty" chains in the Cu(1) plane for partly oxygen depleted compounds ($0 < x < 1$), an arrangement that is found experimentally in the ortho-II structure of Y123. The NQR spectra discussed here, however, give clear evidence that the relative portion of threefold Cu(1) is systematically increased in the compounds with the large RE ions Nd and La.

In the case of small RE ions like Y or Gd the Cu(1)-3 configuration may be considered as a defect either due to extra oxygen ions near $x = 0$ in the tetragonal structure or due to oxygen deficienty in the ortho-I and ortho-II structures near $x = 1$ and $x = 0.5$, respectively. The high concentration of Cu(1)-3 for $x < 0.5$ (Fig. 8), however, is much better described by a random distribution of the oxygen on all possible oxygen sites in the Cu(1) plane with the restriction that nearest oxygen-oxygen pairs are forbidden [simultaneous occupation of O(1) and O(5) sites next to the same Cu(1)].

On the other hand, the NQR spectra of Nd123 and La123 show that here Cu(1)-3 is the most probable configuration near $x = 0.5$. In the case of La123 up to 70% of all Cu(1) ions reveal the threefold coordination which is even more than the value of 50% expected for a random distribution at $x = 0.5$ and as found for Nd123. Thus there must exist an interaction between the oxygen ions in the chains which changes from attractive to repulsive with increasing Cu-Cu distance determined by the radius of the RE ion. The attractive interaction in the compounds with small RE ions leads to the formation of the $(Cu(1)–O)_n$ chains with an average length of $n = 5$ already at an oxygen content of about $x = 0.4$. These chain

fragments are assumed to induce the "critical" number of holes into the Cu(2) layers that is required for the transition from the antiferromagnetic to the superconducting state. In Nd123 and La123 without the attractive interaction the level of doping needed for this transition is reached only at the higher oxygen content of $x = 0.7$.

Acknowledgement

We like to express our thanks to H.J. Bierfeld, IFF, for his help at the oxygen loading of the samples and Ch. Freiburg, ZCH, for the X-ray analysis. I. Heinmaa and Yu. Baikov are indebted to the DAAD for financial support during their stay in Jülich. O. Storz and R. Schöllhorn acknowledge support by the BMFT.

References

[1] R.D. Shannon, Acta Cryst. A 32 (1976) 751.
[2] B. Büchner, U. Calließ, H.D. Jostarndt, W. Schlabitz and D. Wohlleben, Solid State Commun. 73 (1990) 357.
[3] M. Guillaume, P. Allenspach, W. Henggeler, J. Mesot, B. Roessli, U. Staub, P. Fischer, A. Furrer and V. Trounov, J. Phys. Condens. Matter 6 (1994) 7963;
M. Guillaume, P. Allenspach, J. Mesot, B. Roessli, U. Staub, P. Fischer and A. Furrer, Z. Phys. B 90 (1993) 13.
[4] B.W. Veal, A.P. Paulikas, J.W. Downey, H. Claus, K. Vandervoort, G. Tomlins, H. Shi, M. Jenssen and L. Morss, Physica C 162–164 (1989) 97.
[5] H. Shaked, B.W. Veal, J. Faber, R.L. Hittermann, U. Balachandran, G. Tomlins, H. Shi, L. Morss and A.P. Paulikas, Phys. Rev. B 41 (1990) 4173.
[6] M. Buchgeister, Thesis Universität Bonn (1991).
[7] T. Krekels, H. Zou, G. Van Tendeloo, D. Wagener, M. Buchgeister, S.M. Hosseini and P. Herzog, Physica C 196 (1992) 363.
[8] T. Wada, N. Suzuki, T. Maeda, A. Maeda, S. Uchida, K. Uchinokura and S. Tanaka, Appl. Phys. Lett. 52 (1988) 1989.
[9] M. Izumi, T. Yabe, T. Wada, A. Maeda, K. Uchinokura, S. Tanaka and H. Asano. Phys. Rev. B 40 (1989) 6771.
[10] S.G. Brass and H.M. Ghandehari, Appl. Phys. A 48 (1989) 401.
[11] T.B. Lindemer, E.D. Specht, C.S. MacDougall, G.M. Taylor and S.L. Pye, Physica C 216 (1993) 99.
[12] T.B. Lindemer, B.C. Chakoumakos, E.D. Specht, R.K. Williams and Y.J. Chen, Physica C 231 (1994) 80.
[13] K. Otzschi, A. Hayashi and Y. Ueda Physica C 235–240 (1994) 839.
[14] H. Claus, S. Yang, A.P. Paulikas, J.W. Downey and B.W. Veal, Physica C 171 (1990) 205.
[15] A.A. Aligia, J. Garcés and H. Bonadeo, Physica C 190 (1992) 234.
[16] Th. Zeiske, D. Hohlwein, R. Sonntag, F. Kubanek and G. Collin, Z. Phys. B 86 (1992) 11.
[17] F. Yakhou, V. Plakhty, G. Uimin, P. Burlet, B. Kviatkovsky, J.Y. Henry, J.P. Lauriat, E. Elkaim and E. Ressouche, Solid State Commun. 94 (1995) 695.
[18] I. Heinmaa, H. Lütgemeier, S. Pekker, G. Krabbes and M. Buchgeister Appl. Magn. Resonance 3 (1992) 689.
[19] H. Lütgemeier and I. Heinmaa in: Phase Separation in Cuprate Superconductors, eds. K.A. Müller and G. Benedek (World Scientific, Singapore, 1993) p. 243.
[20] P. Mendels, H. Alloul, J.F. Marucco, J. Arabski and G. Collin, Physica C 171 (1990) 429.
[21] N. Nishida and H. Miyatake, Hyperfine Interactions 63 (1990) 183
[22] H. Alloul, T. Ohno, H. Casalta, J.F. Marucco, P. Mendels, J. Arabski and G. Collin, Physica C 171 (1990) 419.
[23] J. Rossat-Mignot, L.P. Regnault, C. Vettier, P. Burlet, J.Y. Henry and G. Lapertot, Physica B 169 (1991) 58.
[24] A.H. Moudden, G. Shirane, J.M. Tranquada, R.J. Birgeneau, Y. Endoh, K. Yamada, Y. Hidaka and T. Murakami, Phys. Rev. B 38 (1988) 8720.
[25] W.H. Li, J.W. Lynn and Z. Fisk, Phys. Rev. B 41 (1990) 4098.
[26] E. Brecht, W.W. Schmahl, H. Fuess, H. Casalta, P. Schleger, B. Lebech, N.H. Andersen and Th. Wolf, Phys. Rev. B 52 (1995) 9601.
[27] H. Lütgemeier, I. Heinmaa, D. Wagener and S.M. Hosseini, in: Phase Separation in Cuprate Superconductors, eds. E. Sigmund and K.A. Müller (Springer, Berlin, 1994) p. 225.
[28] A. Goto, H. Yasuoka, K. Otzschi and Y. Ueda, J. Phys. Soc. Japan 64 (1995) 367.
[29] H. Casalta, P. Schleger, E. Brecht, W. Montfrooij, N.H. Andersen, B. Lebech, W.W. Schmahl, F. Fuess, Ruixing Liang, W.N. Hardy and Th. Wolf, Phys. Rev. B 50 (1994) 9688.
[30] K. Widder, D. Berner, H.P. Geserich, W. Widder and H.F. Braun, Physica C 251 (1995) 274.
[31] K. Kumagai, T. Takatsuka and A. Yamanaka, JMMM 104 (1992) 577.
[32] Ch. Niedermayer, H. Glückler, R. Simon, A. Golnik, M. Rauer, E. Rechnagel, A. Weidinger, J.I. Budnick, W. Paulus and R. Schöllhorn, Phys. Rev. B 40 (1989) 11386.
[33] T.M. Riseman, J.H. Brewer, E.J. Ansaldo, P.M. Grant, M.E. Lopez-Morales and B.M. Sternlieb, Hyperfine Interactions 63 (1990) 249.
[34] J. Zaanen, A.T. Paxton, O. Jepsen and O.K. Andersen, Phys. Rev. Lett. 60 (1988) 2685.
[35] G. Uimin and J. Rossat-Mignot, Physica C 199 (1992) 251.

[36] H.F. Poulsen, N.H. Andersen, J.V. Andersen, H. Bohr and O.G. Mouritsen, Nature 349 (1991) 594.
[37] D. de Fontaine, L.T. Wille and S.C. Moss, Phys. Rev. B 36 (1987) 5709.
[38] E.E. Tournau, S. Lapinskas, A. Rosengren and V.M. Matic, Phys. Rev. B 49 (1994) 15952.
[39] P.E. Sterne and L.T. Wille, Physica C 162–164 (1989) 223.
[40] H. Casalta, H. Alloul, and J.F. Marucco, Physica C 204 (1993) 331.
[41] B. Raveau, C. Michel, M. Hervieu and D. Groult, Crystal Chemistry of High-T_c Superconducting Copper Oxides (Springer, Berlin, 1991).

VII

R. Stern, I. Heinmaa, H. Lütgemeier, M. Mali, J. Roos, and D. Brinkmann,
^{63,65}Cu NQR Studies in Oxygen Deficient $Y_2Ba_4Cu_7O_{15-x}$ ($0 \leq x \leq 0.6$),
Physica C **235–240**, 1655–1656 (1994).

Physica C 235–240 (1994) 1655–1656
North-Holland

PHYSICA C

^{63,65}Cu NQR Studies in Oxygen Deficient $Y_2Ba_4Cu_7O_{15-x}$ ($0 \leq x \leq 0.6$)

R. Stern[a,b], I. Heinmaa[b,c], H. Lütgemeier[c], M. Mali[a], J. Roos[a] and D. Brinkmann[a]

[a]Physik-Institut, Universität Zürich, CH-8057 Zürich, Switzerland

[b]Institute of Chemical Physics and Biophysics, EE-0001 Tallinn, Estonia

[c]IFF, Forschungszentrum Jülich, D-52425 Jülich, Germany

We report the low temperature copper nuclear quadrupole resonance (NQR) measurements in oxygen deficient $Y_2Ba_4Cu_7O_{15-x}$ (247) superconductors with x varying between 0 and 0.6. Through oxygen removal the NQR lines broaden and shift, displaying a decrease of charge-carrier concentration. The shift of double chain line with x monitors the charge transfer between the building blocks of 247.

The $Y_2Ba_4Cu_7O_{15-x}$ (247) [1] consists of alternating $YBa_2Cu_3O_{7-x}$ (123) and $YBa_2Cu_4O_8$ (124) blocks with single and double CuO chains, respectively. Its structure contains double–planes formed by two inequivalent CuO_2 planes of differing doping levels [2]. Similar to $YBa_2Cu_3O_{7-x}$ the depletion of oxygen from the single chains reduces T_c, whose variation with oxygen content, however, is linear without the $YBa_2Cu_3O_{7-x}$–typical plateau. To understand this difference we decided to study oxygen deficient samples ($0 \leq x \leq 0.6$) by copper nuclear quadrupole resonance (NQR). This method is able to distinguish all four copper sites [2] and is thus suitable to monitor the effect of missing oxygen in each block separately.

The 247 samples (Table 1) were prepared by the solid state reaction technique, described in [3]. X-ray diffraction and TEM show a pure 247 phase without impurity phases within a detection limit of less than 0.5% by volume. The absolute oxygen content of samples was either measured by reducing samples in hydrogen or estimated from the determined lattice parameters [4].

The NQR spectra have been measured at 1.2 K by the spin–echo technique sweeping the spectrometer frequency ν. To compare the intensities at different frequencies the echo amplitudes were divided by ν^2.

The two copper isotopes ^{63}Cu and ^{65}Cu have both spin $\frac{3}{2}$ and a single NQR frequency

$$^{63,65}\nu_Q = \frac{e\,^{63,65}Q\,V_{zz}}{2h}\sqrt{1+\frac{1}{3}\eta^2}\,, \qquad (1)$$

where V_{zz} is the major eigenvalue of the electric field gradient (EFG) tensor and η its asymmetry parameter. The EFG tensor depends sensitively on the charge distribution.

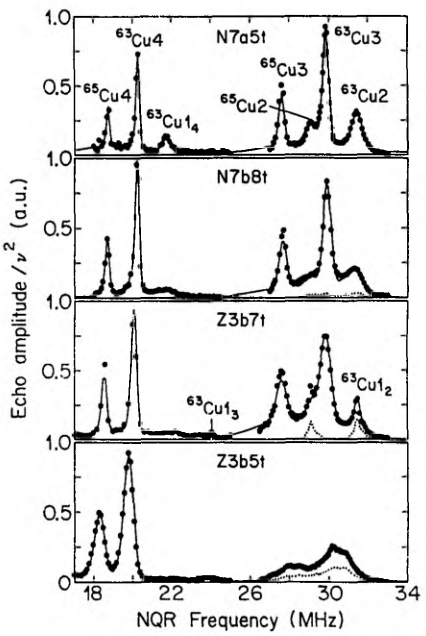

Figure 1. The experimental data points with fitted curves. Dashed lines show results using longer echo times.

The four ^{63,65}Cu NQR spectra are presented on Fig. 1. In both samples with T_c >90 K, all four

SSDI 0921-4534(94)01394-2

Table 1
The lattice parameters, transition onset, oxygen content and ^{63}Cu NQR frequencies of $Y_2Ba_4Cu_7O_{15-x}$ samples used in this study. The assignment of lines is discussed in details in Ref. [2].

Sample	Lattice parameters			T_c [K]	x	NQR frequency [MHz]				
	a [A]	b [Å]	c [Å]			$Cu1_2$	$Cu1_4$	$Cu2$	$Cu3$	$Cu4$
N7a5t	3.830	3.877	50.58	94.0	−0.04(4)	-	21.71(3)	31.44(3)	29.84(2)	20.26(1)
Z15b1t	3.834	3.879	50.61	92.8	−0.10(8)	-	21.65(3)	31.39(3)	29.84(2)	20.22(2)
N7b8t	3.833	3.878	50.59	84.8	0.05(8)	-	21.41(5)	31.25(4)	29.90(4)	20.23(2)
Z3b7t	3.838	3.877	50.64	68.6	0.24(4)	31.47(3)	-	-	29.84(4)	20.06(2)
Z3b5t	3.846	3.872	50.78	42.0	0.61(4)	30.66(4)	-	-	-	19.80(2)

^{63}Cu lines are well resolved and do practically not differ in frequency (Table 1). One of the critical parameters displaying the sample quality, is the NQR linewidth, narrow lines indicate high order at respective lattice sites.

Oxygen removal broadens the lines, in particular the line of the four oxygen coordinated single chain copper ($Cu1_4$) which disappears already at $x \simeq 0.2$. This line, the 123 block's plane line ($Cu2$) and the double chain line ($Cu4$) shift to lower frequencies, displaying at respective sites a decreasing V_{zz} or η (Eq.(1)). To distinguish between the two possibilities a separate measurement of η on oriented 247 crystallites would be neccessary. However, since η's of chain (and plane) copper do practically not differ in $YBa_2Cu_3O_7$ and $YBa_2Cu_4O_8$ we assume that η's of the shifting lines remain constant, and the observed shift results from a decreasing V_{zz}. The decrease cannot arise from the changes of lattice parameters alone, because in this case also the 124 block's plane line ($Cu3$) has to shift for the same amount, which it does not. Therefore we interpret the shifts of $Cu4$, $Cu2$ and $Cu1_4$ lines with decreasing oxygen content as arising from charge-carrier depletion at these sites. The fact that also the most stable $Cu4$ is involved in this process supports the idea of double chains in 247 as acting as a donator of charge-carriers for the 123 block [5].

At $x \simeq 0.25$ from the original lines only the two 124 block lines remain, appart of some possible remnants of $Cu2$ under the $Cu3$ line. On the other side new $Cu1$ lines appear, that can be identified as such by their longer spin-spin relaxation time. In the detailed study [6] different $Cu1$ lines in $YBa_2Cu_3O_{7-x}$ are interpreted, and it is natural to use the same interpretation for 247. In both compounds with $x \simeq 0.25$ a well-defined $Cu1_2$ line at $\sim$ 31.5 MHz arises, which with increasing x broadens and shifts to lower frequency, reaching by $x \simeq 0.6 \sim$ 30.7 MHz. In $YBa_2Cu_3O_{7-x}$ the first (second) frequency belongs to the two-coordinated coppers ($Cu1_2$) in the empty single chains placed between two filled (empty) chains as neighbors. There is still a third $Cu1$ line at 24 MHz, ascribed to the Cu ion terminating a chain, $Cu1_3$. This line is in 247 much weaker than in $YBa_2Cu_3O_{7-x}$, which may indicate a smaller number of terminating $Cu1_3$ or, others to say, longer chain-fragments.

The dissapearance of plane copper lines from NQR spectra at large x may be due to the strong oxygen disorder or due to for a superconductor impropable copper antiferromagnetic ordering.

Our results confirm the suitability of NQR to monitor the effects of oxygen deficiency in cuprate superconductors. For a more detailed and systematic study additional samples with intermediate x are neccessary.

We thank the group of Prof. J. Muller (Université de Genève) for preparing the 247 materials.

REFERENCES

1. J. Karpinski and E. Kaldis, Nature **331**, 242 (1988).
2. R. Stern *et al.*, Phys. Rev. **B50**, in press.
3. J.-Y. Genoud *et al.*, Physica **C192**, 137 (1992).
4. J.-Y. Genoud *et al.*, Physica **C177**, 315 (1991).
5. R. P. Gupta and M. Gupta, Phys. Rev. **B48**, 16 068 (1993).
6. H. Lütgemeier *et al.*, Physica Scripta **T49**, 137 (1993).

VIII

H. Lütgemeier and I. Heinmaa,
Investigation of the Antiferromagnetic Order in the 123 Compounds $REBa_2Cu_3O_y$ by NQR and NMR,
in: Condensed matter studies by nuclear methods,
Proceedings of XXVI Zakopane School on Physics, Zakopane, Poland 13–21 April 1991.
eds. J. Stanek and A. T. Pedziwiatr, World Scientific, Singapore, 1991, pp. 264–276.

INVESTIGATION OF THE ANTIFERROMAGNETIC ORDER IN THE 123 COMPOUNDS $REBa_2Cu_3O_y$ by NQR AND NMR

H. Lütgemeier and I. Heinmaa* IFF, Forschungszentrum Jülich, D–5170 Jülich

*Permanent address: Institut of Chemical Physics and Biophysics, Tallinn 200001, Estonia

ABSTRACT

The NMR and NQR spectra of Cu in the 123 compounds $YBa_2Cu_3O_y$ and related ones containing rare earth metals in the place of Y are discussed. Antiferromagnetic order in the Cu(2) sites exists in the Y and rare earth compounds at reduced oxygen concentration y but in the Pr compounds at any y. In both cases the Cu(1) sites do not carry a static magnetic moment. The EFG at the Cu(1) sites is not influenced by the replacement of Y by Pr, but reduced at the Cu(2) sites. At low oxygen concentration the hyperfine field at the Cu(2) sites of Pr123 reveals a field distribution which may be the indication of a modulated structure.

1. INTRODUCTION

The application of nuclear magnetic resonance, NMR, in the research of superconductors has a long tradition[1)]. The NMR experiments performed with the classical superconductors have confirmed the BCS type pairing in simple metals like Al and the existance of a flux line lattice in type II superconductors. In these applications the interaction of the nuclear magnetic moment with the conduction electrons and the static local field allows to determine the change of the spin susceptibility at T_c from the change of the Knight shift, and the field distribution in the mixed state from the NMR line shape. Furthermore, the behavior of the spin–lattice relaxation rate at the transition from the normal to the supercondcuting state contains information about this state since the spin–paired electrons contribute no longer to the relaxation. The most important features of a BCS superconductor with an isotropic gap are the Hebel Slichter peak of the relaxation rate just below T_c due to the piling up of the density of states when the gap opens, and the Arrhenius type decrease at lower temperature.

In HT_c superconductors (HTSC), the situation is more complicated since

most useful nuclei in these compounds have a spin $I > 1/2$ and carry a large electric quadrupole moment. Thus the quadrupole interaction is important in these systems and leads to complicated NMR spectra, at least for polycrystalline samples. From the quadrupole interaction structural information is obtained concerning the electric field gradient (EFG) at the different lattice sites. Furthermore the pure nuclear quadrupole resonance (NQR) spectra of most nuclei can be observed without an external magnetic field and allow an easy measurement of the spin–lattice relaxation.

A special feature of the HTSC is their relation to magnetic order of either Cu^{2+} or rare earth (RE) ions. Whereas the coexistence of superconductivity with antiferromagnetic (AF) order of the RE ions is well established, the coexistence with ordered Cu moments is still a matter of controversy. The influence of these magnetic moments and the type of the magnetic order can be studied by nuclear resonance, too.

In the following, some examples will be presented from our work at Jülich for the study of structural and magnetic properties of the HTSC and related compounds. We limit ourselves to the 123 compounds $YBa_2Cu_3O_y$ (Y123) and compounds with RE in the place of Y. A special emphasis will be given to some new results for the nonsuperconducting Pr123 compounds[2]. For all experiments polycrystalline powder samples have been used and measured by standard spin–echo technique mostly at 4.2 K.

2. Cu RESONANCE IN Y123

In $YBa_2Cu_3O_y$ all ions have been detected by NMR or NQR. Y is the only nucleus without a quadrupole moment since the spin is $I = 1/2$. Therefore this nucleus shows pure magnetic interaction and the narrow lines have allowed a detailed investigation of the Knight–shift and spin–lattice relaxation rate as function of the oxygen concentration and temperature[3].

The two Cu isotopes with $I = 3/2$ show strong quadrupole effects on both Cu sites (fig. 1). The small difference of the quadrupole moments of both Cu isotopes is the reason for the doublets in the Cu NQR spectra with the intensity ratio 2:1 and the frequency ratio 1:0.92. Since only one NQR transition 3/2, 1/2 exists for $I = 3/2$, the full EFG tensor with the largest component V_{zz} and the asymmetry parameter η ($0 \leq \eta \leq 1$) can be determined only from the spectrum in an external magnetic field. The field–sweep spectra of grain oriented powder

samples[4] and of small single crystals[5] with either $y < 6.3$ or $y > 6.8$ show an EFG of axial symmetry around the c–axis for the doublets at the higher frequency, and a nonsymmetric EFG for the low frequency doublets. Nevertheless the assignment of these lines to the Cu sites in the lattice is quite different.

At high oxygen concentration the line at 31.5 MHz for ^{63}Cu corresponds to the Cu(2) sites (CuO_2 planes) and that at 22 MHz with $\eta = 1$ to the Cu(1) sites (CuO chains). This assignment follows from the intensity ratio of the lines and from the fact that an EFG with symmetry axis in c direction can be expected only for the Cu(2) sites. This assignment follows also from the influence of the magnetic moments of rare earth ions replacing Y (see below).

At low oxygen concentration the situation is different. Here the 123 compounds show antiferromagnetic order with localized magnetic moments at the Cu(2) ions[6]. The zero–field spectrum of the Cu(2) sites is in this case an antiferromagnetic NMR spectrum in the region 70–110 MHz determined by an hyperfine field of 7.95 T [7] and an EFG with the symmetry axis perpendicular to the hyperfine field (fig. 2). The NQR doublets observed at lower frequency (fig. 1) correspond only to the Cu(1) sites: the line at 30.2 MHz with the symmetric EFG to those with twofold oxygen coordination, and that at 24 MHz with $\eta = 0.3$ [8] to those with three oxygen neighbours. The pure NQR spectra observed for the two–, three–, or fourfold coordinated Cu(1) sites prove that these do not carry a static magnetic moment even in the antiferromagnetic state. If magnetic moments exist at these sites, their correlation time must be shorter than 10^{-10}s. Otherwise either a static splitting or a loss of the signal by fast relaxation would appear.

3. MAGNETIC STRUCTURE OF $YBa_2Cu_3O_6$

In the antiferromagnetic state the order must be of a type that the dipolar field of the electronic moments localized at the Cu(2) sites cancel at the Cu(1) sites. This holds for the structure deduced from neutron diffraction[6] which is described by a wave vector (1/2,1/2,1) with no doubling of the unit cell in c–direction (fig.3a). In this structure the stacking sequence along the c–axis is + o – + o – where + and – describe the spin directions of the Cu(2) sites and o the zero spin at Cu(1). A different sequence is found in samples containing a small amount of Fe (about 1%) at the Cu(1) sites[9]. Here a Zeeman splitting of the NQR line by a local field of about 0.16 T is found (fig.4) which is equal to the dipolar field in a magnetic structure described by the wave vector (1/2,1/2,1/2)

or the stacking + o + − o − (fig.3b) and magnetic moments of 0.67 μ_B at the Cu(2) sites.

At higher temperature the splitting decreases continuously (fig.5) indicating a continuous transition from structure B to A via a noncollinear canted structure (fig.6). The low–temperature structure depends clearly on the concentration x of the Fe impurities in $YBa_2(Cu_{1-x}Fe_x)_3O_6$ (fig.7). The splitting saturates at $x > 1\%$ indicating that this small amount is sufficient to change the structure completely. This is a consequence of the strong in–plane antiferromagnetic exchange interaction of the Cu(2) ions and the weak one between the planes. An extra ferromagnetic coupling between the planes induced by the impurities at Cu(1) sites will turn the staggered magnetization of the whole planes. At increasing oxygen concentration y the extra coupling is reduced. Thus a sample with $x = 0.2\%$ Fe showed the transition from A to B[10] at $y = 6.0$, but not at $y = 6.15$.

At first we had assumed that the reason for the extra coupling was the magnetic moment of the Fe ions at the Cu(1) sites which are in a frustrated situation in the high temperature structure. This is evident from ^{57}Fe Mössbauer studies which reveal the appearance of the hyperfine field for one component of the spectrum in the transition region from structure A to B [10], whereas the hyperfine field of the second component follows the staggered magnetization of the Cu(2) planes with $T_N = 420$ K. Further experiments, however, showed that doping with Al or Ga which mainly occupy the Cu(1) sites, results in the same effect as Fe, whereas doping with Ni (preferrently at the Cu(2) sites) has no influence on the NQR spectra. This means that the extra coupling is an effect of the different valency state of the 3+–ions at the Cu(1) site and not of the magnetic moment[11].

In contrast to our result that in the pure 123 compounds with Y, Gd or Nd only the structure A exists above 1.2 K, a change of the magnetic structure above 10 K has been found by neutron diffraction in different single crystals of Y123 and Nd123 [12,13]. Since many single crystals contain a large amount of Al from the flux, we assume that this transition is not a property of the pure 123 compounds but induced by Al. In contrast to the structure A, the symmetry of B allows a magnetic moment at the Cu(1) sites. The results of the different neutron scattering experiments is quite different ranging from below 0.1 [12] to 0.4 μ_B [13]. Our results, however, prove that the magnetic moment at the Cu(1) site is smaller

than 0.03 μ_B, if the normal hyperfine coupling constant of Cu, 12 T/μ_B, is assumed.

4. INFLUENCE OF RE IONS

Besides the magnetic Cu ions, a second magnetic sublattice exists if Y is replaced by rare earth ions. For Nd and the heavier rare earth metals this happens without a distortion of the lattice structure and the superconducting properties. The magnetic moments of the RE ions show at low temperature a transition to antiferromagnetic order and a coexistence of antiferromagnetism and superconductivity. For Gd123 the Neel temperature is 2.23 K. The magnetic order of Gd does not influence the NQR frequencies 22.5 and 32.35 MHz of Cu(1) and Cu(2), respectively. This means that the dipolar field of the RE ions is completely canceled at the Cu sites by symmetry. The fluctuating components of the Gd spins, however, introduce strong longitudinal and transverse relaxation processes especially at the Cu(2) sites which are located nearest to the Gd sites (fig.8). Above T_N the transverse relaxation rate of the Cu(2) sites is increased by an order of magnitude compared with the values of Cu(1) and reveals a maximum at T_N. Below T_N the rate decreases since the Gd spins are fixed. At the same temperature the relaxation behavior changes from Lorentzian above T_N to more Gaussian like below T_N. But even at the lowest temperature of our experiment, 1.2 K, the longitudinal and transverse relaxation rates are increased at the Cu(2) sites compared with the Cu(1) sites and prove strong fluctuations in the Gd spin system.

At low oxygen concentration the two magnetic systems of the RE ions and the Cu(2) ions coexist without a strong interaction. The situation at the Cu(1) sites is not changed by the replacement of Y by Gd or Nd and no magnetic moment is found at these sites. For the Cu(2) sites, the zero field NMR spectra found below the Neel temperature of the Gd reveal an hyperfine field of 7.68 T which is reduced by 0.3 T compared with Y123.

5. Cu RESONANCE IN Pr123 COMPOUNDS

The lightest RE metal which can build up the 123 structure is Pr. In contrast to the other RE ions, Pr suppresses the metallic behaviour and the

transition to superconductivity already at full oxygen loading, if more than 50% of the Y is replaced. At the same Pr content AF order of Cu has been observed by Mössbauer effect of Fe at Cu sites[14] and by muon spin relaxation[15]. The reason for the suppression of the superconductivity by Pr in contrast to the heavier RE ions is an open question. The larger ionic radius can lead to pair breaking by the stronger overlap of the 4f states with the electron states in the CuO_2 planes. Another reason may be that Pr enters the lattice as Pr^{4+} and fills up the holes responsible for the metallic behaviour. This model is supported by the similarity of the phase diagrams of the systems $Y_{1-x}Pr_xBa_2Cu_3O_7$ and $YBa_2Cu_3O_{7-x}$.

We have investigated the Cu resonance in a series of Pr123 samples of oxygen concentration between $x = 6.0$ and 7.0 prepared by the ceramic technique in different laboratories. All these samples reveal at 4.2 K NQR lines in the region between 18 and 32 MHz which are much broader than the lines in Y123 and do not allow to separate the lines of the two Cu isotopes. This means a broad distribution of the EFG values and indicates a much lower crystal perfection in this system. Nevertheless the comparison of the NMR spectra at field–sweep (fig.9) and the NQR spectra (fig.10) allows conclusions about the EFG. At high oxygen concentration ($x = 6.9$) there is only one NQR line at 22 MHz (for ^{63}Cu) with a nonsymmetric EFG ($\eta = 1$) as seen from the NMR spectrum. At lower oxygen concentration two other lines at 24 MHz with nonsymmetric EFG and at 30 MHz with symmetric EFG appear from which only the 30 MHz line remains at $x = 6.0$. These are just the frequencies found in Y123 for the Cu(1) sites with four, three and two oxygen neighbours. Thus the EFG at the Cu(1) sites is not influenced by replacing of Y by Pr.

No signals corresponding to the Cu(2) sites could be detected at 4.2 K. At 1.2 K, however, broad zero–field lines are found for each oxygen concentration in the frequency region above 60 MHz (fig.10), which must be ascribed to NMR lines of Cu in a hyperfine field and proves that the Cu(2) sites carry a stable magnetic moment as in the case of Cu(2) in $YBa_2Cu_3O_6$. Reyes et al.[16] present the NMR spectra of $PrBa_2Cu_3O_7$ for temperatures between 285 and 300 K with the line of the Cu(2) sites. This line disappears at 285 K indicating a well defined Neel temperature.

The shape of the zero–field spectra of Cu(2) for high oxygen concentration differs for the samples measured up to now [2] and must be connected with the crystal perfection. Similar to our spectrum for the sample with the narrowest line

(fig.10), the zero field spectrum by Reyes et al. shows no resolved quadrupole splitting but is shifted to lower frequency by 5 MHz. Thus it is impossible to obtain a reliable fit of these spectra and to determine the quadrupole coupling. In any case, however, the EFG of the Cu(2) sites in Pr123 with high oxygen concentration is smaller than in YBCO for any oxygen concentration, and the hyperfine field is definitely smaller, 6.7(3) T, compared with 7.95 T in antiferromagnetic YBCO.

At lower oxygen concentration, x = 6.0 and 6.3, the Cu(2) site spectra reveal an unexpected shape with two well defined maxima at 80 and 95 MHz (Fig.10) which coincide with the values of the hyperfine field in Pr123 for x = 7 and Y123 for x = 6, respectively. The distance of the maxima is too large to be explained as lines of the two Cu isotopes, since the nuclear magnetic dipole and electric quadrupole moments of both isotopes differ at most by about 8%. Therefore the line shape reflects a distribution of the hyperfine fields which is an indication of a modulated magnetic structure. As in the case of x = 7 the spectra for low x do not show any quadrupole splitting proving again a smaller EFG at the Cu(2) sites than in Y123.

Thus we must conclude that the EFG at the Cu(2) sites is strongly reduced if Y is replaced by Pr, whereas it stays constant at the Cu(1) sites. This result is different from our earlier conclusion [2] where due to the broader linewidth in the first available samples a similar EFG also for the Cu(2) sites was assumed in YBCO and PrBCO. The reduced EFG means that the charge distribution in the Cu(2) planes is changed by the substitution and supports the model of different valency states of Y and Pr as the reason for the suppression of the superconductivity in Pr123. The magnetic structures of Pr123 and Y123 are similar in the fact that the Cu(1) sites do not carry a stable magnetic moment. The broad distribution of the hyperfine fields at Cu(2), however, indicates different types of magnetic order in these planes.

A last conclusion can be made on the magnetic order of the Pr ions in these compounds. Specific heat measurements [14] and neutron diffraction [17] reveal antiferromagnetic order of the Pr sublattice at about 17 K for x = 7. Moessbauer effect of Gd in Pr123 doped with Gd shows the same Neel temperature for x = 7, but only 7.5 K for x = 6 [18]. The intensity of the zero–field NMR spectra of the Cu(2) sites decreases very fast at increasing temperature above 2 K and disappears at about 3 K by fast transverse relaxation, whereas the Cu(1) site inten-

sity reveals only the normal decrease corresponding to the Curie law. This means that even in the ordered state the magnetic fluctuations of the Pr sublattice are very strong, a feature found also in the Moessbauer spectra of Gd in Pr123 [18], where the hyperfine field increases down to the lowest temperature.

ACKNOWLEDGEMENT

We are indebted to many colleagues who supplied the samples used for this research. Special thanks are due to B. Maple for the new Pr123 samples with oxygen concentration 6.9 and 6.0, to R. Dupree for Y123 samples doped with Al, Gd and V and to H. Buchgeister and F.M. Hosseini for the Gd123 samples. I. Heinmaa thanks Prof. Zinn for the hospitality he received at the IFF of the KFA Jülich, and the DAAD for financial support.

REFERENCES

1. MacLaughlin, D.E., Solid State Physics 31, edited by F. Seitz and D. Turnbull (Academic Press, New York 1977).
2. Lütgemeier, H., JMMM 90&91, 633 (1990).
3. Alloul, H., et al., Phys. Rev. Lett. 63, 1700 (1989).
4. Lütgemeier, H., Physica C153–155, 95 (1988); Lütgemeier, H. et al., Physica C153–155, 731 (1988).
5. Pennington, C.H. et al., Phys. Rev. B37, 7944 (1988).
6. Burlet, P. et al., Physica C153–155, 1115 (1988).
7. Mendels, P. and Alloul, H., Physica C156, 355 (1988).
8. Heinmaa, I. and Lütgemeier, H., to be published.
9. Lütgemeier, H. et al., Physica C162–164, 1367 (1989).
10. Brand, R. et al., Hyp. Inter. 22, 1229 (1990).
11. Bottyan, L. and Lütgemeier, H., to be published.
12. Kadowaki, H. et al., Phys. Rev. B37, 7932 (1988).
13. Li, W.H., Lynn, J.W., and Fisk, Z., Phys. Rev. B41, 4098 (1990).
14. Felner, I. et al., Phys. Rev. B40, 6739 (1989).
15. Cooke, D.W. et al., Phys. Rev. B41, 4801 (1990).
16. Reyes, A.P. et al., Phys. Rev. B42, 2688 (1990).
17. Li, W.H. et al., Phys. Rev. B40, 5300 (1989).
18. Wortmann, G. and Felner, I., Solid State Comm. 75, 981 (1990).

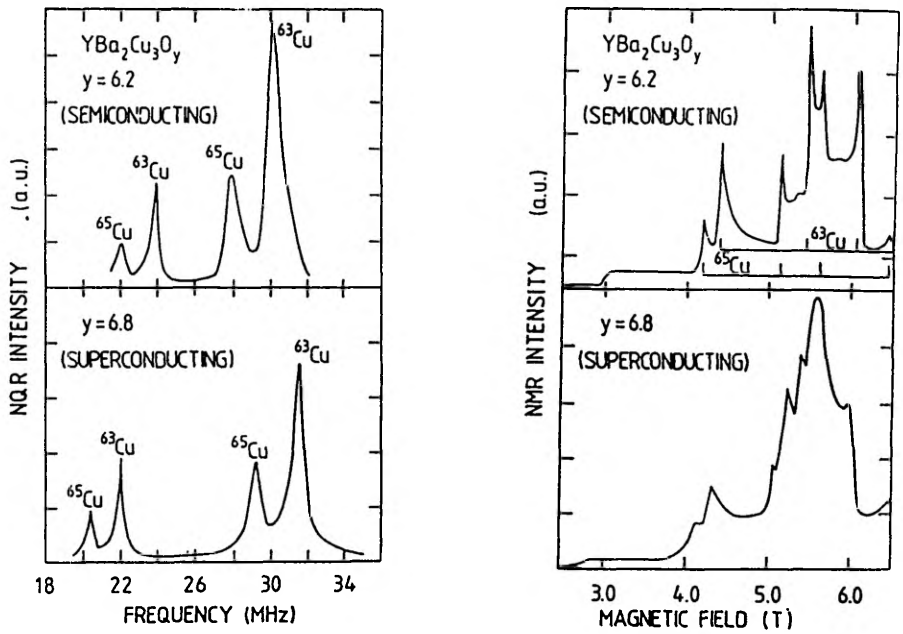

Fig. 1: NQR spectra (left) and NMR spectra at 64 MHz (right) of antiferromagnetic and of superconducting $YBa_2Cu_3O_y$ at 4.2 K.

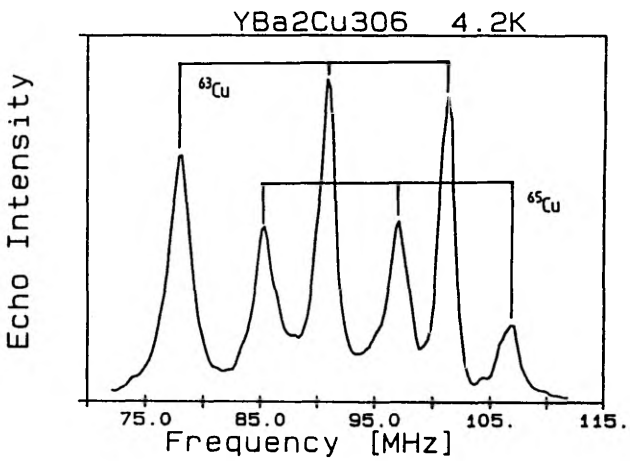

Fig. 2: Antiferromagnetic zero–field spectrum of Cu(2) in $YBa_2Cu_3O_6$ at 4.2 K.

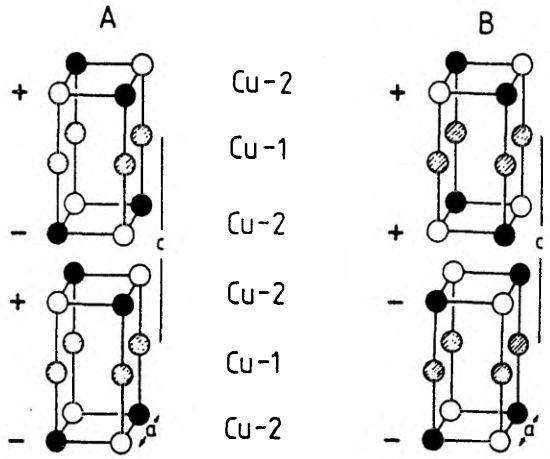

Fig. 3: The two different AF structures of Cu in 123 compounds with different stacking sequence of the magnetic Cu(2) sites.
A: structure of pure samples without a local field at Cu(1). .
B: structure in samples containing Fe impurities with a dipolar field at Cu(1).

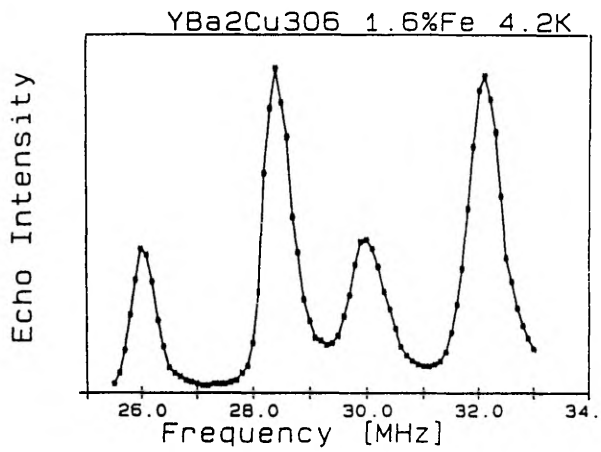

Fig. 4: NQR spectrum of the Cu(1) sites in $YBa_2(Cu_{.984}Fe_{.016})_3O_6$ at 4.2 K showing the dipolar splitting by a field of 0.16 T.

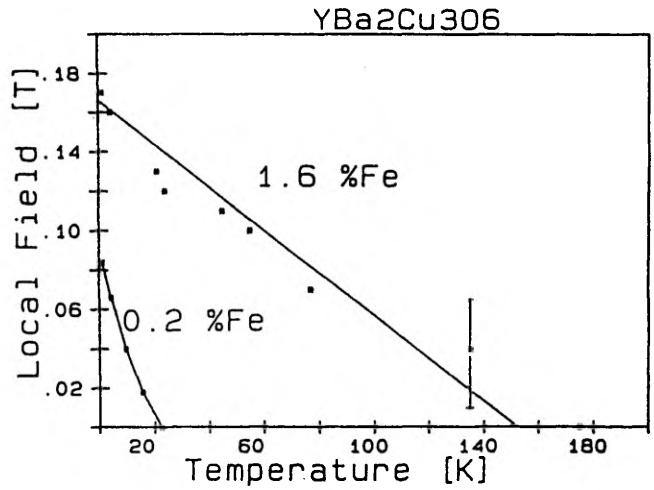

Fig. 5: Temperature dependence of the dipolar splitting in $YBa_2(Cu_{1-x}Fe_x)O_6$ for x = 0.002 and 0.016.

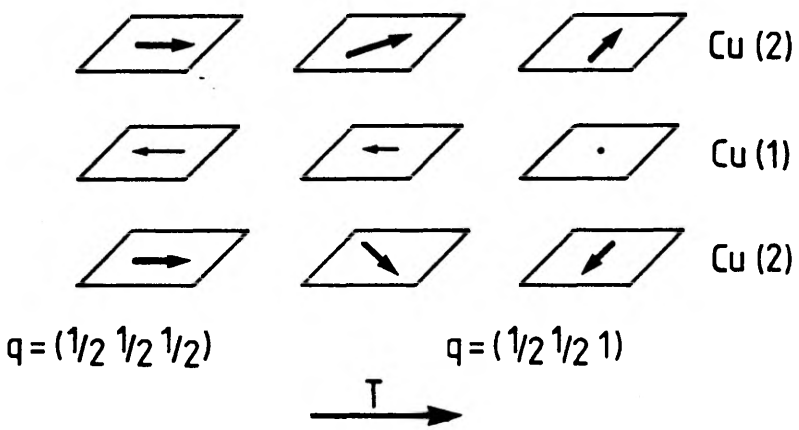

Fig. 6: Model for the continuous transition between the high– and low temperature structures with the intermediate canted spin–structure. The bold arrows indicate the staggered magnetization in the Cu(2) planes, the weak arrows the dipolar field at the Cu(1) sites.

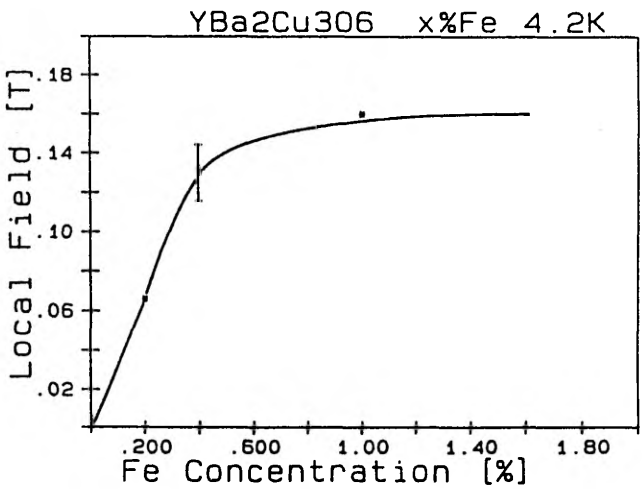

Fig. 7: The dipolar field at the Cu(1) site at low temperature as function of the iron concentration x.

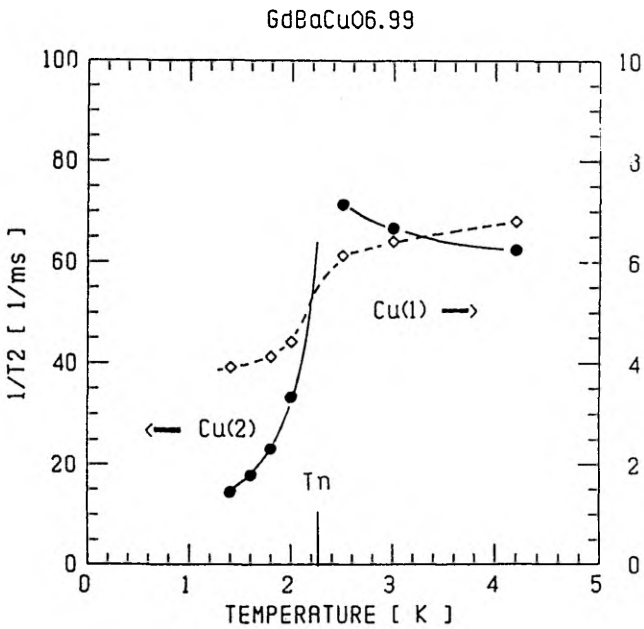

Fig. 8: Temperature dependence of the transverse relaxation rate, $1/T_2$, of Cu(2) sites (solid left scale) and Cu(1) sites (dashed, right scale) in $GdBa_2Cu_3O_7$. The lines are only guides to the eye.

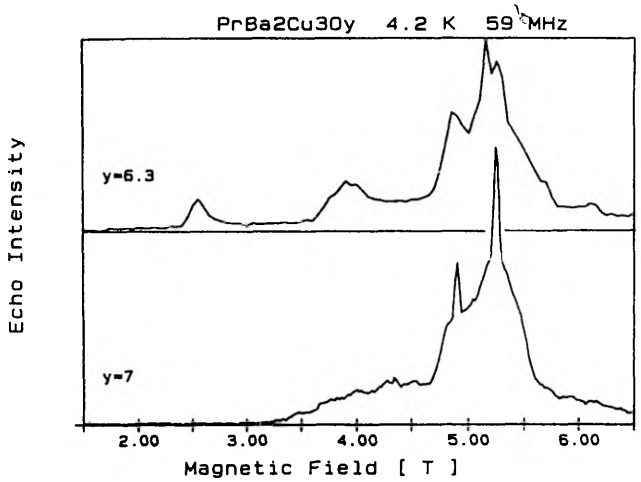

Fig. 9: NMR powder spectra of Cu in $PrBa_2Cu_3O_y$ at 4.2 K and 59 MHz. y = 7.0: Spectrum of both Cu isotopes in a non–symmetric EFG ($\eta = 1$). y = 6.3: A symmetric EFG leads to the 3/2, 1/2 satellite at 3.9 T, the central transition is mixed with the spectrum of a different site with non–symmetric EFG.

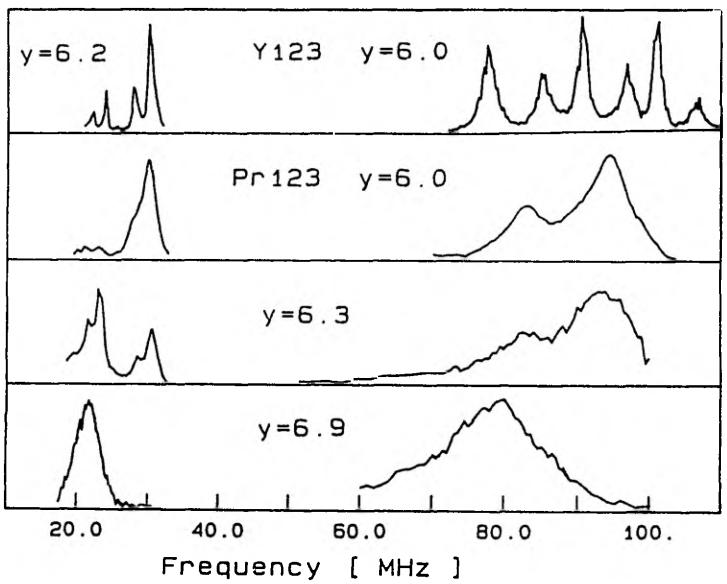

Fig.10: Zero–field spectra of antiferromagnetic 123 compounds at 4.2 K (low frequency part) or 1.2 K (high frequency part).

E. Lippmaa, E. Joon, I. Heinmaa, V. Miidel, A. Miller, and R. Stern,
Radio-Spectroscopic Studies of Magnetic Properties
of High Temperature Superconductors,
Z. Naturforsch., **45a**, 401–404 (1990).

Radio-Spectroscopic Studies of Magnetic Properties of High Temperature Superconductors *

E. Lippmaa, E. Joon, I. Heinmaa, V. Miidel, A. Miller, and R. Stern

Institute of Chemical Physics and Biophysics, Estonian Academy of Sciences, Tallinn, Estonia

Z. Naturforsch. 45a, 401–404 (1990); received August 26, 1989

We have performed ^{17}O and ^{63}Cu NMR measurements in $YBa_2Cu_3O_{7-\delta}$ ($\delta \approx 0.15$) oriented powder samples at CuO_2 plane sites Cu(2) and O(2, 3) in the temperature range 10–300 K. The temperature dependent Knight shift $K(T)$ and spin lattice relaxation rate $T_1^{-1}-(T)$ of O(2, 3) yield $K^2 T_1 T = \text{const}$ in accordance with the presence of free carriers at plane oxygen sites. A sharp decrease of T_1^{-1} of Cu(2) below 120 K is associated with the opening of a gap in the spectrum of antiferromagnetic spin fluctuations of localized copper $3d^9$ electrons. The comparison of different temperature dependences of spin densities at the Cu and O sites shows the presence of two nearly independent spin systems. A close similarity of $YBa_2Cu_3O_{7-\delta}$ with heavy fermion superconductors is discussed.

Introduction

The electronic states at the Fermi energy (ε_F) play a very important role in studies of the nature and mechanism of high temperature superconductivity (HTSC). According to the data of photoelectron spectroscopy [1], the conductivity band consists predominantly of the 2p states of oxygen, and the 3d states of copper are localized and do not exceed ε_F. On the other hand, copper NMR data show that at $T < T_c$ the components of the magnetic hyperfine shift of copper in the CuO_2 plane site Cu(2) (K_{aa} and K_{bb}) decrease by half while K_{cc} remains constant [2], and the spin-lattice relaxation rate T_1^{-1} of Cu(2) decreases without enhancement below T_c by 2 to 3 orders of magnitude [3, 4]. This has been attributed to opening of the superconducting gap in the spectrum of electronic states of copper.

Oxygen ^{17}O NMR provided new results [5, 6]:

1) The relaxation rate T_1^{-1} of oxygen O(2, 3) in the plane sites was found to show enhancement just below T_c, as expected for usual singlet S-wave superconductivity [7].

2) At $T > T_c$, oxygen $T_1^{-1}(T)$ follows the usual Korringa law $T_1^{-1} \propto T$, in accordance with the existence of free carriers at oxygen orbitals [1].

For correct interpretation of the copper NMR results, parallel measurements of ^{17}O and ^{63}Cu NMR shift and relaxation data using the same sample are essential.

Experimental

The pellet of $YBa_2Cu_3O_{7-\delta}$ was prepared with standard methods. The gas exchange process consisted of removal of ^{16}O from the initial sample and exposing a pellet to $^{17,18}O$ gas (22 atom% of ^{17}O, 63 atom% of ^{18}O) at 500 °C during 5 days. The weight increase of the initial pellet (1.7%) suggests a nearly complete exchange of ^{16}O in all oxygen positions of the lattice. The pellet was crushed into fine powder with the grain size less than 2 μm, mixed with epoxy, and the mixture was hardened in 11.7 T magnetic field during 12 hours. Thus we got a solid sample where the $YBa_2Cu_3O_{7-\delta}$ ($\delta \approx 0.15$) microcrystals were oriented with the crystal axis c aligned in one direction. The onset temperature of the superconducting transition in zero field T_c^0 was 91 K. The NMR measurements were performed in the 8.5 T field of a Bruker CXP-360 FT spectrometer. The spin-lattice relaxation times T_1 were calculated from the recovery of the magnetization after a train of saturating pulses. The magnetic shift of Cu(2) was measured from the resonance frequency of solid copper iodide CuI and the magnetic shift of ^{17}O from that of H_2O.

* Presented at the Xth International Symposium on Nuclear Quadrupole Resonance Spectroscopy, Takayama, Japan, August 22–26, 1989.

Reprint requests to Prof. E. Lippmaa, Institute of Physics and Biophysics, Estonien Academy of Sciences, Tallinn/Estland.

0932-0784 / 90 / 0300-0401 $ 01.30/0. – Please order a reprint rather than making your own copy.

Results

The NMR spectrum of the central $(1/2 \leftrightarrow -1/2)$ transition of ^{63}Cu in the Cu(2) site shows the line with the full width at half height FWHH = 70 kHz ($c \parallel H$) and the magnetic shift $K_{cc} = 1.27\%$ at $T = 295$ K, in excellent agreement with the data measured in $YBa_2Cu_3O_7$ single crystal [8, 9]. With decreasing temperature the linewidth increases to FWHH = 100 kHz at $T = 100$ K, but the magnetic shift remains constant with an accuracy of 0.01% in the $T_c < T < 295$ K range. The transverse components of the magnetic shift K_{aa}, $K_{bb} = K_\perp = 0.6\%$ in the $120 < T < 295$ K range begin to decrease at $T < 120$ K and reach the value $K_\perp \simeq 0.2\%$ at $T \leq 40$ K. The temperature dependence of T_1^{-1} of Cu(2) at the orientation $c \perp H$ is presented in Figure 1. Over the whole temperature range, except the $T = 200$ to 220 K region, the magnetization recovery function was established to be

$$M(\infty) - M(0) = A\,e^{-\tau/T_1} + B\,e^{-6\tau/T_1}, \qquad (1)$$

corresponding to a wholly magnetic relaxation mechanism of the quadrupolar $I = 3/2$ nuclei [10]. The nearly constant relaxation rate T_1^{-1} in the $120 < T < 295$ K range with an anomaly between 200 to 220 K closely follows the data for the $YBa_2Cu_3O_7$ single crystal [11]. A sharp decrease of T_1^{-1} begins below $T^* \simeq 120$ K, some 40 K higher than the transition temperature into the superconducting state at $T_c^\perp = 81$ K in the magnetic field used. Between $40 < T < 120$ K the relaxation rate $T_1^{-1} \propto T^\alpha$ ($\alpha = 3$ to 4). There is a certain instability of T_1^{-1} at $T = 100$ K, but no anomaly in the vicinity of $T = T_c^\perp$ was found.

The NMR spectrum at 295 K of the central transition of ^{17}O consists of three lines (see Fig. 2), denoted by α, β, and γ. As the spectrum recorded in the $c \parallel H$ orientation should not contain any broadening due to the anisotropy of the quadrupolar and magnetic shift interactions, the intensity ratio 4:2:1 of the lines α, β, and γ, respectively, corresponds to the already established [12, 13] assignment. Therefore the line α corresponds to oxygens in the CuO_2 plane sites O(2, 3), β to the oxygen bridging the CuO planes and chains O(4), and the smeared line γ to the oxygen in the CuO chains, O(1). According to the measured values of the quadrupolar interaction parameters, the frequency shift due to the second order quadrupolar interaction ($c \parallel H$) is less than 0.01%. Therefore we ignore the quadrupolar contribution to the shift and attribute the frequency shift to the Knight shift component in

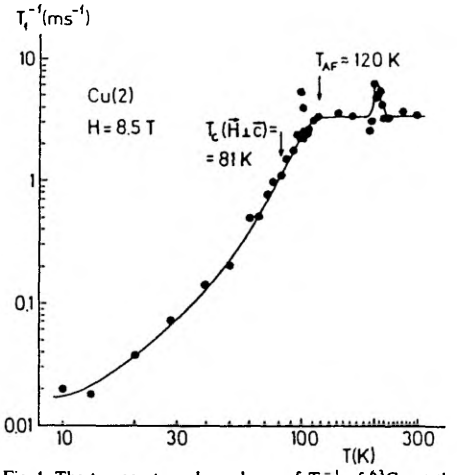

Fig. 1. The temperature dependence of T_1^{-1} of ^{63}Cu at the Cu(2) site, orientation is $c \perp H$.

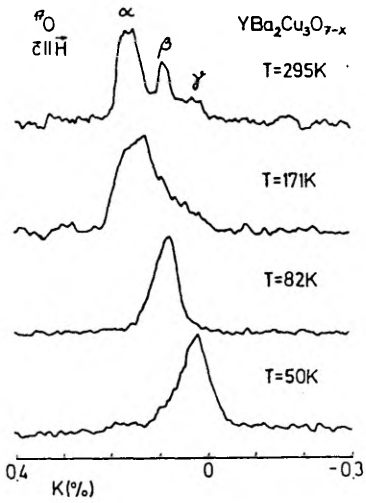

Fig. 2. The temperature dependence of the ^{17}O NMR spectrum at the orientation $c \parallel H$. We have assigned the α-oxygen to O(2, 3) sites, the β line to the bridge oxygen O(4) and the γ line to the chain oxygen O(1).

the c axis direction. The Knight shift of O(4) oxygens $K \simeq 0.095\%$ does not depend on temperature in the $120 < T < 295$ K range. At $T < 120$ K the overlapping of lines α and β makes the separation of lines impossible. The inhomogeneously broadened line of

O(2, 3) shows a remarkable temperature dependence (Figs. 2 and 3). The Knight shift of the maximum of the line, K_M, decreases with the decreasing of temperature from $K_M \simeq 0.16\%$ at 295 K to $K_M \cong 0.08\%$ at $T_c'' = 75$ K. At temperatures between $90 < T < 200$ K, $K_M \propto T^{0.6}$. The high frequency shoulder at the O(2, 3) line exhibits a constant value of $K_0 \simeq 0.18\%$ between $120 < T < 295$ K. At $T < 120$ K the line of O(2, 3) narrows and the Knight shift of the whole line decreases rapidly to zero in the superconducting state. The temperature dependence of the relaxation rate T_1^{-1} measured at the frequency of K_M is shown in Figure 4. At all temperatures the magnetization recovery was approximated by the function

$$M(\infty) - M(\tau) = A\, e^{-\tau/T_1} + B\, e^{-6\tau/T_1} + C\, e^{-15\tau/T_1}, \quad (2)$$

as expected for a purely magnetic relaxation mechanism for quadrupolar nuclei with spin $I = 5/2$ [10]. The temperature dependence of the relaxation rate can be described by the function $T_1^{-1}(T) \propto T^{\alpha}$ ($\alpha = 2$ to 3) and shows no maximum below T_c'', in contrast with the opening of a BCS-like gap at the Fermi energy.

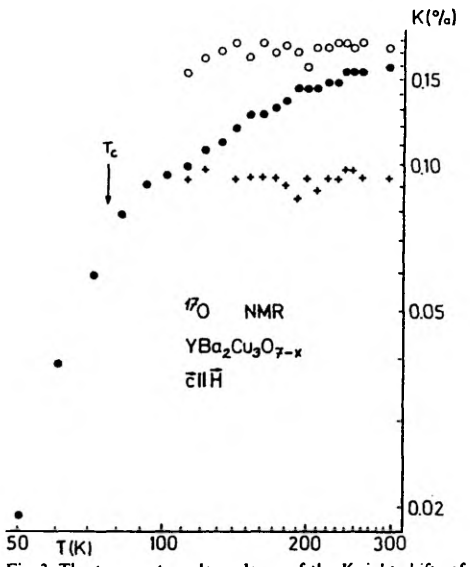

Fig. 3. The temperature dependence of the Knight shifts of ^{17}O in the O(4) site (+) and in the O(2, 3) sites (o: the high frequency edge, K_0; •: the maximum of the line, K_M).

Discussion

Inhomogeneous broadening of the O(2, 3) line shows a distribution of spin densities at the O(2, 3) sites which can be caused, as was proposed in [13], by the presence of oxygen deficient clusters of $YBa_2Cu_3O_{6.7}$ type in our sample. The temperature dependence of the Knight shift $K_M \propto T^{0.6}$ is in accordance with the temperature dependence of the density of states in the case of a linear temperature dependence of the concentration of carriers within a closed Fermi surface. According to the Korringa relation for free carriers, $K^2 T_1 T$ is constant. In our case, the K_M temperature dependence yields $T_1^{-1} \propto T^{2.2}$ in rough agreement with the dependence shown in Figure 4. Therefore we can conclude that the data of ^{17}O NMR correspond to the case of free carriers at O(2, 3) orbitals.

The sharp decrease of the relaxation rate T_1^{-1} of copper in the Cu(2) site was already reported for $YBa_2Cu_3O_{6.7}$ [14] below $T^* \simeq 100$ K $> T_c$. We believe that the temperature T^* cannot be attributed to the opening of the superconductivity gap. Most probably the gap is opening at $T = T^*$ in the spectrum of copper antiferromagnetic fluctuations, because the main relaxation mechanism of Cu(2) is due to the quantum mechanical fluctuations of localized 3d^9

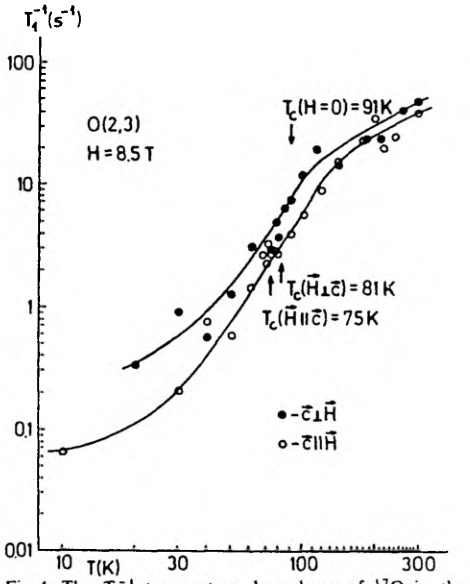

Fig. 4. The T_1^{-1} temperature dependence of ^{17}O in the O(2, 3) site, measured at K_M.

electrons [8]. This circumstance underlines the close similarity of the phenomenon of HTSC to the superconductivity in heavy fermion compounds (e.g. $CeCu_2Si_2$), where at $T^* > T_c$ the correlation gap opens and in the superconducting phase the nuclear spin-lattice relaxation rate T_1^{-1} follows the T^3 law [15]. In the absence of the correlation gap the superconductivity does not occur in these systems [16]. Taken together, all this means a magnetic mechanism of high temperature superconductivity in doped CuO_2 layers.

[1] H. Katayama-Yoshida, T. Takahashi, H. Matsuyama, Y. Okabe, Y. Kitaoka, K. Ishida, K. Asayama, H. Fujimoto, and H. Inokuchi, Int. J. Modern Phys. **B 1,** 1273 (1988).
[2] M. Takigawa, P. C. Hammel, R. H. Heffner, Z. Fisk, J. L. Smith, and R. B. Schwarz, Phys. Rev. B **39,** 300 (1989).
[3] M. Mali, D. Brinkmann, L. Pauli, J. Roos, H. Zimmermann, and Hulliger, J. Phys. Lett. **A 124,** 112 (1987).
[4] T. Imai, T. Shimizu, T. Tsuda, H. Yasuoka, T. Takabatake, Y. Nakazawa, and M. Ishikawa, J. Phys. Soc. Japan **57,** 1771 (1988).
[5] K. Ishida, Y. Kitaoka, K. Asayama, H. Katayama-Yoshida, Y. Okabe, and T. Takahashi, J. Phys. Soc. Japan **57,** 2897 (1988).
[6] P. Wzietek, D. Köngeter, P. Auban, D. Jérome, J. P. Contures, B. Dubois, and Ph. Odier, Europhys. Lett. **8,** 363 (1989).
[7] The latest result of P. C. Hammel, M. Takigawa, R. H. Heffner, Z. Fisk, and K. C. Ott, Phys. Rev. Lett., in press, show no enhancement of T_1^{-1} below T_c for the O(2, 3) site.
[8] C. H. Pennington, D. J. Durand, C. P. Slichter, J. P. Rice, E. D. Bukowski, and D. M. Ginsberg, Phys. Rev. **B 39,** 274 (1989); ibidem. 2902 (1989).
[9] I. A. Heinmaa, A. M. Vainrub, J. O. Past, V. O. Miidel, A. V. Miller, I. F. Štšegolev, and G. A. Jemeltšenko, Pis'ma v JETP **48,** 171 (1988).
[10] A. Narath, Phys. Rev. **162,** 320 (1967).
[11] A. V. Miller, A. M. Vainrub, I. A. Heinmaa, A. V. Reinhold, E. T. Lippmaa, and I. F. Štšegolev, Pis'ma v JETP **49,** 211 (1989).
[12] C. Coretsopoulos, H. C. Lee, E. Ramli, L. Reven, T. B. Rauchfuss, and E. Oldfield, Phys. Rev. B **39,** 781 (1989).
[13] M. Horvatić, Y. Berthier, P. Butand, Y. Kitaoka, P. Segransan, C. Berthier, H. Katayama-Yoshida, Y. Okabe, and T. Takahashi, Physica C, submitted.
[14] W. W. Warren, Jr., R. E. Walstedt, G. F. Brennert, R. J. Cava, R. Tycko, R. F. Bell, and G. Dabbagh, Phys. Rev. Lett. **62,** 1193 (1989).
[15] Y. Kitaoka, K. Ueda, T. Kohara, and K. Asayama, Solid State Commun. **51,** 461 (1984).
[16] F. Steglich, in: Theory of heavy fermions and valence fluctuations (T. Kasuya and T. Saso, eds.), Springer-Verlag, Berlin 1985.

CURRICULUM VITAE

IVO HEINMAA

Date and place of birth:	December, 11 1953, Vändra, Estonia
Citizenship:	Estonia
Family status:	Married, three daughters
Address:	Institute of Chemical Physics and Biophysics, Akadeemia 23, 12614 Tallinn, Estonia
Fax:	+372 6 398 393
Phone:	+372 6 398 350
E-mail:	ivo@kbfi.ee

Education

1961–1972	Viru-Jaagupi Secondary School, Vajangu 8-Year School, Tamsalu Secondary School
1972–1977	Tartu University, Department of Physics and Chemistry. Received diploma in physics and electronics.

Employment

1977–1980	Junior Research Associate, Institute of Cybernetics, Tallinn, Estonia.
1980–Present	Junior Research Associate, Research Associate, Institute of Chemical Physics and Biophysics, Tallinn, Estonia.
1990, 1991, 1993, 1995	Guest Scientist, Institut für Festkörperforschung; Forschungszentrum Jülich, Germany.

Scientific work

Main topics of research:	Methods of solid state NMR, NMR studies of conducting materials (organic conductors and superconductors, conducting polymers, high temperature superconductors).
Number of publications:	37

CURRICULUM VITAE

IVO HEINMAA

Sünniaeg ja koht:	11. detsember 1953, Vändra
Kodakondsus:	Eesti
Perekonnaseis:	abielus, kolm tütart
Aadress:	Keemilise ja Bioloogilise Füüsika Instituut, Akadeemia tee 23, 12614 Tallinn, Eesti
Faks:	26 398 393
Telefon:	26 398 350
E-post:	ivo@kbfi.ee

Hariduskäik

1961–1972	Viru-Jaagupi Keskkool, Vajangu 8-kl Kool, Tamsalu Keskkool
1972–1977	Tartu Ülikooli füüsika-keemiateaduskond, füüsik-elektroonik

Teenistuskäik

1977–1980	Küberneetika Instituudi füüsika sektori nooremteadur
alates 1980	Keemilise ja Bioloogilise Füüsika Instituudi teadur
1990, 1991, 1993, 1995	Jülichi Teaduskeskuse Tahke Keha Füüsika Instituudi (Institut für Festkörperforschung, Forschungszentrum Jülich) külalisteadur

Teadustegevus

Peamised töösuunad:	Tahke keha tuumamagnetresonants, mitmesuguste materjalide, sh. orgaanilised ülijuhid, elektrit juhtivad polümeerid, kõrgtemperatuursed ülijuhid, struktuuri ja omaduste uurimine raadiospektroskoopia meetoditega.
Publikatsioonide arv:	37

DISSERTATIONES PHYSICAE UNIVERSITATIS TARTUENSIS

1. Andrus Ausmees. XUV-induced electron emission and electron-phonon interaction in alkali halides. Tartu, 1991.
2. Heiki Sõnajalg. Shaping and recalling of light pulses by optical elements based on spectral hole burning. Tartu, 1991.
3. Sergei Savihhin. Ultrafast dynamics of F-centers and bound excitons from picosecond spectroscopy data. Tartu, 1991.
4. Ergo Nõmmiste. Leelishalogeniidide röntgenelektronemissioon kiiritamisel footonitega energiaga 70–140 eV. Tartu, 1991.
5. Margus Rätsep. Spectral gratings and their relaxation in some low-temperature impurity-doped glasses and chrystals. Tartu, 1991.
6. Tõnu Pullerits. Primary energy transfer in photosynthesis. Model calculations. Tartu, 1991.
7. Olev Saks. Attoampri diapasoonis voolude mõõtmise füüsikalised alused. Tartu, 1991.
8. Andres Virro. AlGaAsSb/GaSb heterostructure injection lasers. Tartu, 1991.
9. Hans Korge. Investigation of negative point discharge in pure nitrogen at atmospheric pressure. Tartu, 1992.
10. Jüri Maksimov. Nonlinear generation of laser VUV radiation for high-resolution spectroscopy. Tartu, 1992.
11. Mark Aizengendler. Photostimulated transformation of aggregate defects and spectral hole burning in a neutron-irradiated sapphire. Tartu, 1992.
12. Hele Siimon. Atomic layer molecular beam epitaxy of A^2B^6 compounds described on the basis of kinetic equations model. Tartu, 1992.
13. Tõnu Reinot. The kinetics of polariton luminescence, energy transfer and relaxation in anthracene. Tartu, 1992.
14. Toomas Rõõm. Paramagnetic H^{2-} and F^+ centers in CaO crystals: spectra, relaxation and recombination luminescence. Tallinn, 1993.
15. Erko Jalviste. Laser spectroscopy of some jet-cooled organic molecules. Tartu, 1993.
16. Alvo Aabloo. Studies of crystalline celluloses using potential energy calculations. Tartu, 1994.
17. Peeter Paris. Initiation of corona pulses. Tartu, 1994.
18. Павел Рубин. Локальные дефектиые состояния в CuO_2 плоскостях высокотемпературиых сверхпроводников. Тарту, 1994.
19. Olavi Ollikainen. Applications of persistent spectral hole burning in ultrafast optical neural networks, time-resolved spectroscopy and holographic interferometry. Tartu, 1996.

20. Ülo Mets. Methodological aspects of fluorescence correlation spectroscopy. Tartu, 1996.
21. Mikhail Danilkin. Interaction of intrinsic and impurity defects in CaS:Eu luminophors. Tartu, 1997.
22. Ирина Кудрявцева. Создание и стабилизация дефектов в кристаллах KBr, KCl, RbCl при облучеиии ВУФ-радиацией. Тарту, 1997.
23. Andres Osvet. Photochromic properties of radiation-induced defects in diamond. Tartu, 1998.
24. Jüri Örd. Classical and quantum aspects of geodesic multiplication. Tartu, 1998.
25. Priit Sarv. High resolution solid-state NMR studies of zeolites. Tartu, 1998.
26. Сергей Долгов. Электронные возбуждения и дефектообразоваиие в некоторых оксидах металлов. Тарту, 1998.
27. Kaupo Kukli. Atomic layer deposition of artificially structured dielectric materials. Tartu, 1999.

ISSN 1406–0647
ISBN 9985–56–410–3